Investigation into the stability of WEE1 kinase in plants

Gemma S. Cook

PhD thesis

Cardiff University and

The University of Worcester

February 2012

DECLARATION

This work has not been submitted in substance for any other degree or award at this or any other university or place of learning, nor is being submitted concurrently in candidature for any degree or other award.

Signed …… (candidate) Date ……..

STATEMENT 1

This thesis is being submitted in partial fulfillment of the requirements for the degree of PhD

Signed …… (candidate) Date ……..

STATEMENT 2

This thesis is the result of my own independent work/investigation, except where otherwise stated.

Other sources are acknowledged by explicit references. The views expressed are my own.

Signed …… (candidate) Date ……..

STATEMENT 3

I hereby give consent for my thesis, if accepted, to be available for photocopying and for inter-library loan, and for the title and summary to be made available to outside organisations.

Signed …… (candidate) Date ……..

STATEMENT 4: PREVIOUSLY APPROVED BAR ON ACCESS

I hereby give consent for my thesis, if accepted, to be available for photocopying and for inter-library loans **after expiry of a bar on access previously approved by the Academic Standards & Quality Committee.**

Signed …… (candidate) Date ……..

ABSTRACT

Phosphoregulation is essential for the control of cell division. In yeasts and animals, premature entry into mitosis is prevented by the inhibitory phosphorylation of CDK by WEE1 kinase. WEE1 homologues have been identified in several species of higher plant, including *Arabidopsis* and tobacco. However, while WEE1 function has been confirmed in the DNA replication checkpoint in higher plants, a role for the protein in the G2/M transition during an unperturbed plant cell cycle is yet to be identified. To address this issue, the further characterisation of *Arabidopsis* WEE1 was completed, particularly focussing on the localisation and stability of the protein. A GFP-*Arath*;WEE1 construct under the 35S promoter was transformed into both *Arabidopsis* plants and the tobacco BY-2 cell line, and a nuclear localisation of the protein at interphase was confirmed. Additionally, the study of WEE1 subcellular localisation in different cell cycle phases revealed that the protein was absent during metaphase. Interestingly, levels of WEE1 degradation varied in different *Arabidopsis* root tissues, and the protein was absent in lateral root primordia. The proteasome inhibitor MG132 was used to demonstrate that *Arath*;WEE1 is degraded via the 26S proteasome pathway, as in yeasts and animals. Bimolecular fluorescence complementation confirmed an interaction between *Arath*;WEE1 and the F-box protein *Arath*;SKIP1 *in vivo,* which may target *Arath*;WEE1 for degradation. Tobacco BY-2 cells were stably co-transformed with BiFC constructs to facilitate the study of any changes in this interaction during the cell cycle. There was again no evidence of the interaction during metaphase, but a return of the signal during anaphase and telophase. The root phenotype of an *Arath*;SKIP1 knockdown line suggested that this F-box protein may target *Arath*;WEE1 for degradation early in development, but this requires confirmation. The work presented in this thesis describes, to my knowledge, the first investigation into the stability of *Arath*;WEE1 protein.

ABBREVIATIONS

AD	transcriptional activator domain
ANOVA	analysis of variance
APC	anaphase promoting complex
Arath	*Arabidopsis thaliana*
ATM	ataxia telangiectasia-mutated
ATR	Rad3-related
BiFC	bimolecular fluorescence complementation
BPB	bromophenol blue
CAK	cyclin activating kinase
CAKAK	CAK activating kinase
CDK	cyclin dependent kinase
CIAP	calf intestine alkaline phosphatase
Cip/Kip	CDK inhibitory protein
CKI	CDK inhibitor
D-box	destruction box
DBD	DNA-binding domain
DIC	differential interference contrast
dNTP	deoxyribonucleotide triphosphates
DP	dimerization protein
DUB	deubiquitylating enzyme
E1	ubiquitin-activating enzyme

E2	ubiquitin-conjugating enzyme
E3	ubiquitin ligase
FRET	fluorescence resonance energy transfer
gDNA	genomic DNA
GFP	green fluorescent protein
GST	glutathione S-transferase
H2B	histone 2B
HU	hydroxyurea
ICK	interactors with/inhibitors of CDK
K29/K48/K63	lysine residues
Kan	kanamycin
KO	knockout
KRP	kip-related protein
M	mitosis
Mik1	mitotic inhibitory kinase
mc-BiFC	multicolour bimolecular fluorescence complementation
MPF	mitosis promoting factor
NAA	1-Naphthaleneacetic acid
Nicta	*Nicotiana tabacum*
ORF	open reading frame
PCR	polymerase chain reaction
pSPYCE	split YFP C-terminal fragment expression vector

pSPYNE	split YFP N-terminal fragment expression vector
RFP	red fluorescent protein
ROS	reactive oxygen species
RT-PCR	reverse transcriptase PCR
S	DNA synthesis phase
SCF	SKP-CULLIN-F-box
SDW	sterile distilled water
SE	standard error
SKIP1	SKP1 interacting protein
Solly	*Solanum lycopersicum*
SMR	SIAMESE-related
SUMO	small-ubiquitin modifier
T^{14}	threonine 14 residue of CDK
T^{167}	threonine 167 residue of CDK
Ub	ubiquitin
UV	ultraviolet
WT	wild type
Y^{15}	tyrosine 15 residue of CDK
Y2H	yeast two-hybrid
YFP	yellow fluorescent protein

ACKNOWLEDGEMENTS

This work was funded by Cardiff University and The University of Worcester.

Firstly, I would like to thank my supervisors at Cardiff University, Dr. Dennis Francis and Dr. Hilary Rogers, and my supervisor at the University of Worcester, Dr. Rob Herbert, for their invaluable support and advice over the past 3.5 years.

My thanks also go to all my colleagues in the lab, especially Dr. Faezah Mohd Salleh and Dr. Julie Hunt, for help with experiments, but also for providing light relief and giggles. Dr. Natasha Spadafora (now University of Calabria) created the GFP-*Arath*;WEE1 construct. I thank Mike O'Reilly and Joan Hubbard for technical support. My thanks go to everybody in Prof. Jim Murray's lab for advice and loan of equipment, and provision of the H2B-YFP seeds. Jorg Kudla's lab provided the BiFC vectors.

I would like to thank Dr. Tony Hayes and Marc Isaacs in the BIOSI Confocal Microscopy Unit, and Dr. John Runions and Dr. Katja Graumann (Oxford Brookes University) for confocal imaging, and further assistance and advice. I would also like to thank Katja for providing the RFP-*Arath*;SUN1 seeds.

Thank you to my little sister, Tamsin, and step-dad, Col, for trying to understand what I've been doing, and always being on the end of the phone. And an especially huge thank you to Col (and Trebs) for putting up with me over the past few months, I'll be out of your hair soon! To my friends, the Lemons, thank you for always being there for me and always having fun times lined up so I always had something to look forward to; here's to even funner times ahead! And I would like to thank my friends back home for understanding my absence over the last few years, and especially over the last few months, I'll make up for it soon!

My biggest thanks go to my wonderful fiancé, Dr. Nick Puts. Thank you for always being there for me and sharing in the trials and triumphs of the PhD over the last three years. There's no way I would have got through the toughest times without your support. I can't wait to come and join you in America! And I guess I have a wedding to organise now, no rest for the wicked!

Finally, I would like to dedicate this PhD thesis to my mummy, Elizabeth; sorely missed. I wish she could have been here to see me finish, but I know she's proud of me.

CONTENTS

1. INTRODUCTION

The cell cycle is the mechanism by which living cells proliferate. It consists of four distinct phases: mitosis (M), during which the cell divides; G1, the first period of cell growth; DNA synthesis (S), during which the cell's DNA is replicated, and G2, the second period of cell growth. Non-proliferative cells often occupy a fifth stage, G0, or stationary phase, in which the cells are arrested in G1 (Drebot et al., 1987; Figure 1.1). Cells can also arrest in G2 phase.

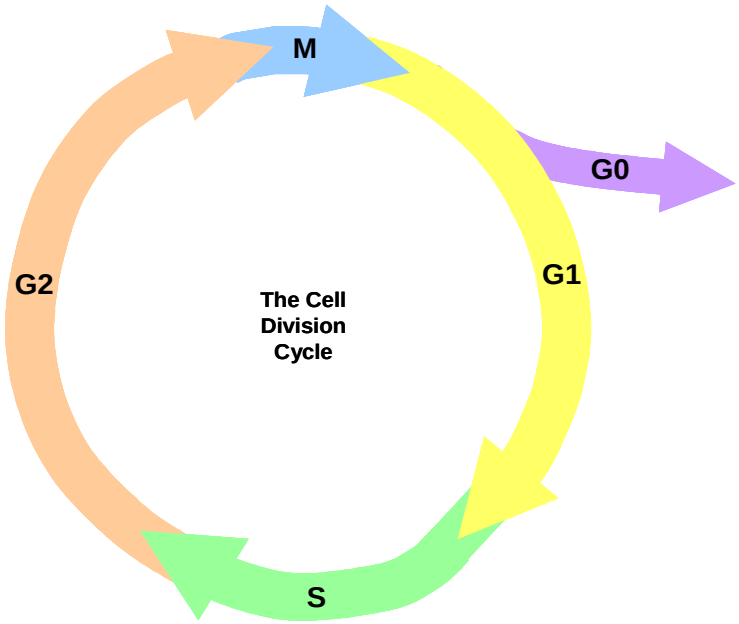

Figure1.1 Schematic diagram showing the eukaryotic cell cycle, consisting of several phases including mitosis (M), during which the cell divides; G1 phase, the first period of cell growth; DNA synthesis (S), during which the cell's DNA is replicated; and G2 phase, the second period of cell growth. Also represented is G0, or stationary phase, which is often occupied by non-proliferating cells.

Many aspects of cell division are remarkably well conserved in all eukaryotes including yeasts, animals and plants. Due to the importance of timing in the cell cycle, phosphoregulatory mechanisms are in place to ensure that DNA synthesis and cell division progress smoothly. These mechanisms, or transition points, are sometimes wrongly referred to as checkpoints. Checkpoints are defined as operational when a step "B" depends on a step "A", unless a loss-of-function mutant can relieve the dependence (Hartwell and Weinert, 1989). In other words, the checkpoint is a hurdle which needs to be overcome before a cell is competent for the transition. Most commonly for experimental data on checkpoints, cells are exposed to hydroxyurea, which induces the DNA replication checkpoint, or ionizing radiation (mimicked by zeocin), which induces the DNA damage checkpoint (described below

in section 1.5). Two phosphoregulatory mechanisms are those at the transition from G1 to S-phase and at the transition from G2 to M-phase. Another level of control is also imposed by the varying stability of the proteins involved in these processes, and their timely degradation is highly regulated.

1.1 CYCLIN-DEPENDENT KINASES

The phosphoregulation of proteins involved in the cell cycle transitions is controlled by cyclin-dependent kinases (CDKs), all of which require the binding of a non-catalytic cyclin for their enzymatic activity. There are several categories of CDK, although not all are involved in the regulation of the cell cycle (reviewed by Morgan, 1997). Both the G1/S and G2/M transitions in fission yeast (*Schizosaccharomyces pombe*) are regulated primarily by Cdc2 (Nurse, 1990). Cdc2 is well conserved in eukaryotes (Table 1.1), including *Saccharomyces cerevisiae* (termed CDC28; Nasmyth and Reed, 1980), Drosophila (Jimenez et al., 1990), humans (CDK1 & CDK2; Lee and Nurse, 1987) and plants (CDKAs & CDKBs; Ferreira et al., 1991).

Table 1.1 Summary of CDKs and cyclins important at the cell cycle transitions in different organisms

		S. cerevisiae	***S. pombe***	**Human**	**Plants**
G2/M	***CDKs***	CDC28	Cdc2	CDK1	CDKA/CDKB
	Cyclins	CLB1-3	Cdc13, Cig1, Cig2	B/A	A, B, D
G1/S	***CDKs***	CDC28	Cdc2	CDK1, 2, 4, 5	CDKA
	Cyclins	CLN1-3	Puc1, Mcs2	A, D/E, D2, D3	6 D-types

To be capable of catalytic activity several levels of control are exerted onto these CDKs – cyclin-binding alone is not always sufficient for enzyme activity. The CDK must be phosphorylated on the threonine ($T^{160/161/167}$) residue, near to the C-terminus of the protein's polypeptide chain (Gould et al., 1991), which increases the stability

of the interaction with the cyclin protein. Phosphorylation of $T^{160/161/167}$ is implemented by CDK activating kinase (CAK; Figure 1.2) which was first isolated in *Xenopus* oocyte extracts and found to be a CDK itself (Solomon et al., 1992). The isolation of human CAK (CDK7) led to the discovery of the cyclin partner of CAK, a previously undescribed cyclin protein designated as cyclin H (Fisher and Morgan, 1994; Makela et al., 1994). In addition, the CDK7-cyclinH complex can contain a MAT1 subunit, a RING-finger protein which is thought to stabilise the complex (Devault et al., 1995; Fisher et al., 1995; Tassan et al., 1995) and may also be responsible for substrate recognition (Yankulov and Bentley, 1997). CAKs have also been identified in both *S. pombe* and *S. cerevisiae* (reviewed by Draetta, 1997; Table 1.2). As well as their cell cycle function, CAKs also have a role in the control of transcription (reviewed by Nigg, 1996). Being CDKs, the CAKs also require phosphorylation on a T-loop threonine residue for their catalytic activity. While it is possible that this occurs via a positive feedback loop involving the CDK2-cyclinA complex, it is more likely that CAK activating kinases (CAKAKs) are responsible. One CAKAK, Csk1, which is able to regulate the activity of Mcs6-Mcs2, has been isolated in *S. pombe* (Hermand et al., 1998, 2001). To be catalytic, the CDK also needs to be dephosphorylated at the tyrosine 15 (Y^{15}; and, in mammals, also the threonine 14 (T^{14})) residue near to the N-terminus of the molecule (described in Section 1.4.2).

Table 1.2 Summary of CAKs and cyclins in different organisms (adapted from Draetta, 1997).

	S. cerevisiae	***S. pombe***	**Human**	**Plants**
CAKs	CAK1 (unrelated to CDK7)	Mcs6	CDK7	CDKDs
Cyclins		Mcs2	H	H

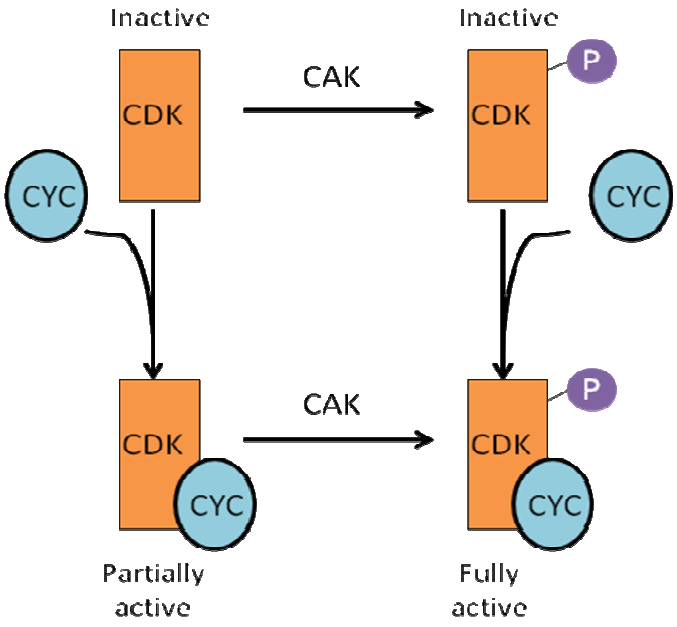

Figure 1.2 The change in CDK enzyme activity with changes in cycling-binding and phosphorylation on $T^{160/161/167}$ by CAK. The CDK-cyclin complex can be partially active without $T^{160/161/167}$ phosphorylation, but is only fully active after $T^{160/161/167}$ phosphorylation (diagram adapted from Draetta, 1997).

1.1.1 PLANT CDKs

In plants, at least 152 CDKs have been identified from 41 different species (reviewed by Dudits et al., 2007). However, the mechanisms regulating the cell cycle are less well known, and although these mechanisms are generally well conserved with yeasts and animals, there are some important differences. In *Arabidopsis thaliana* two classes of CDK, A, encoded by a Cdc2 homologue, and B, unique to plants, show peaks of activity around the stage of the G2/M transition (Ferreira et al., 1991; Joubes et al., 2000; Porceddu et al., 2001). CDKAs and CDKBs are distinguished by differences in their amino acid sequences in the cyclin-binding domain – CDKAs are characterised by the presence of the PSTAIRE motif, whilst in CDKBs this is altered to PPT(A/T)LRE. The A-type CDK is able to complement the *cdc2*$^{-}$ and *cdc28* mutants in fission yeast and budding yeast respectively, whereas the B-type CDKs do not complement the yeast mutants (Imajuku et al., 1992). In *A. thaliana*, *CDKB* transcripts accumulate in cells at the G2/M transition, whereas *CDKA* is consistently expressed throughout the cell cycle (Menges and Murray, 2002; Menges et al., 2005). Similarly, in *Nicotiana tabacum* BY-2 cells, CDKA kinase activity peaks from S-phase until the G2/M transition, while CDKB kinase activity peaks in late G2, suggesting that CDKA has a role in many stages of the cell cycle, while CDKB

is only active at the transition between G2 and mitosis (Porceddu et al., 2001; Sorrell et al., 2001). Five additional classes of CDKs (C-G) have been identified in plants (Table 1.3).

Table 1.3 Summary of CDKs and cyclins in higher plants, including function in the cell cycle and putative function outside of the cell cycle where appropriate (adapted from Francis, 2007, 2009).

	Family Members	**Cell cycle phase or *putative function outside of the cell cycle***
CDKs		
A	;1	G1/S + G2/M
B	1;1, 1;2	G2/M
	2;1, 2;2	G2
C	;1	*Regulation of RNA polymerase II*
D	;1, ;2, ;3	CAK
E		?
F		CAKAK
G		?
Cyclins		
A	1;1, 1;2, 2;1, 2;2, 2;3, 2;4, 3;1, 3;2, 3;3, 3;4	G1/S (G2/M)
B	1;1, 1;2, 1;3, 1;4, 2;1, 2;2, 2;3, 2;4, 3;1	G2 or G2/M
D	1;1, 2;1, 3;1, 3;2, 3;3, 5;1, 6;1, 7;1	G0/G1/S
	4;1, 4;2	G2/M

The threonine residues in the T-loops of CDKs are generally conserved between animals and plants, except in the C-type CDKs, and require phosphorylation by a CAK for their catalytic activity (Harashima et al., 2007; Figure 1.3). The plant D-

type CDKs are homologous to the human CAK, CDK7 (Joubes et al., 2000). Three D-type CDKs have been identified in *Arabidopsis*: CDKD;1, CDKD;2 and CDKD;3, originally named CAK3At, CAK4At and CAK2At respectively (Shimotohno et al., 2003). Cyclin H has also been discovered in *Arabidopsis* and interacts with CDKD;2 and CDKD;3 to form active CAK complexes, which, like CAKs in other organisms, have a role in transcription as well as cell cycle regulation (Shimotohno et al., 2004, 2006; Figure 1.3).

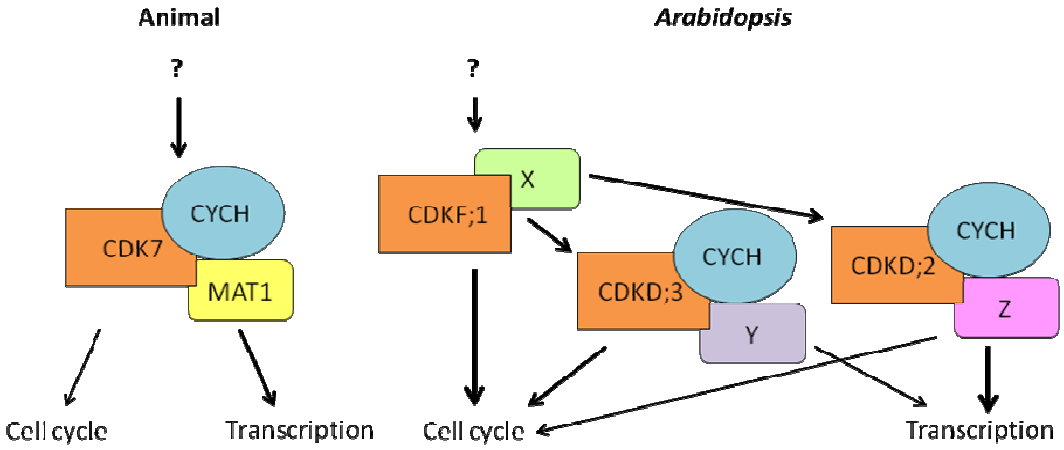

Figure1.3 Comparison between animal and *Arabidopsis* CAK pathways. CDKF;1 phosphorylates and activates CDKD;2 and ;3 in *Arabidopsis*, whereas no CAKAK has been identified in animals. In *Arabidopsis*, CDKF;1 forms a complex with unknown subunit (X) but not with cyclin H (CYCH), while CDKD;2 and ;3 form complexes with cyclin H and other unknown subunit(s) (diagram adapted from (Shimotohno and Umeda, 2007).

Arath;CDKF;1 (originally named CAK1At; Umeda et al., 1998) is able to phosphorylate and activate CDKA;1, but has no direct role in transcription (Shimotohno et al., 2004, 2006), and is also dispensable for CDKA;1 activation (Takatsuka et al., 2009; Figure 1.3). CDKF;1 is also a CAKAK with the ability to phosphorylate conserved serine and threonine residues in the T-loops of both CDKD;2 and CDKD;3 (Shimotohno et al., 2004). However, CDKF;1 does not interact with cyclin H, indicating that it may be a cyclin-independent CAK (Shimotohno et al., 2004).

1.2 CYCLINS

As described in section 1.1, as well as phosphoregulation, CDKs require the binding of a cyclin subunit for their catalytic activity. Cyclins were first discovered in sea urchin oocytes due to the pattern of their expression which clearly oscillates during the cell cycle. Mitotic cyclins increase in concentration throughout interphase, peaking at the G2/M transition and disappearing before telophase (Evans et al., 1983). As for the CDKs, cyclin nomenclature varies depending on the organism in question. In *S. cerevisiae* there are three CLN proteins which are important at the G1/S-phase transition, while three CLB proteins are active at the G2/M transition. In animals, various CDKs are activated by A-, D- and E-type cyclins at the G1/S-phase transition, while CDK1 forms a complex with A- and B-type cyclins at the G2/M-phase transition (Table 1.1). Different CDK-cyclin complexes are responsible for the initiation of different stages of the cell cycle (Table 1.1; reviewed by Pines, 1995).

Cyclins contain a sequence of 100 amino acids called the cyclin box which is able to bind to the T^{167} residue of CDK (Kobayashi et al., 1992). They also contain a "destruction box" which is subject to rapid degradation through ubiquitination prior to and during early anaphase by the anaphase promotion complex, an ubiquitin E3 ligase (Glotzer et al., 1991; Hershko et al., 1991; see Section 1.6). The G1 cyclins, ie. the CLN proteins of budding yeast and the animal D- and E-type cyclins, additionally contain PEST sequences, rich in proline, glutamate/aspartate and serine/threnonine, which are markers of unstable proteins (Tyers et al., 1992).

1.2.1 PLANT CYCLINS

In animals the cyclins are grouped into 13 classes, A-L and T. In plants, over 100 cyclin homologues have been identified, which can be grouped into classes according to their animal homologues (reviewed by Nieuwland et al., 2007). In Arabidopsis there are 50 cyclins which fall into 9 classes including A-D, H, P and (T), three of which, A, B and D, are well characterised in the cell cycle (reviewed by Dewitte and Murray, 2003). The H-type cyclins form complexes with CAKs (Shimotohno et al., 2004, 2006; see Section 1.1).

The plant A-type cyclins can be subdivided into three classes: CYCA1, CYCA2 and CYCA3 (Chaubet-Gigot, 2000; Renaudin et al., 1996). The expression of the A-type cyclins commences close to the beginning of S-phase, prior to the expression of B-type cyclins (Fuerst et al., 1996; Ito et al., 1997; Kouchi et al., 1995; Meskiene et al., 1995; Reichheld et al., 1996; Setiady et al., 1995). The different subclasses of A-type cyclins may have different biological functions, implied by the timing of their expression during the cell cycle in the tobacco BY-2 cell line. While the two A3-type cyclins were maximally expressed at the G1/S-phase transition, the A1-type was up-regulated in the middle of S-phase (Reichheld et al., 1996). Interestingly, the A2-type cyclin was found to peak in expression in more than one phase, once in the middle of S-phase then decreasing to a basal level prior to its maximal expression at the G2/M-phase transition (Roudier et al., 2000).

The plant B-type cyclins are expressed later in the cell cycle than the A-types. They can be categorised into three subclasses: CYCB1, CYCB2 and CYCB3 (Vandepoele et al., 2002). Functionally, the B-type cyclins are involved in the transition from G2-phase into mitosis (Qin et al., 1996; Schnittger et al., 2002). This is reflected by the pattern of expression of B-type cyclins, with transcripts generally absent during S-phase before rising during G2 to peak in late G2 and early in mitosis, followed by a rapid decrease in expression as mitosis progresses (Hirt et al., 1992; Menges and Murray, 2002; Qin et al., 1996; Trehin et al., 1997).

The plant D-type cyclins are important at the transition from G1 to S-phase, and were isolated by their ability to complement mutant G1 cyclins in yeast (Dahl et al., 1995; Soni et al., 1995). Ten D-type cyclins have been identified in *Arabidopsis*, which can be classified into seven separate subclasses, with three D3-types, two D4-types and one member of every other subclass (Vandepoele et al., 2002). Several structural features of the D-type cyclins, in addition to the cyclin box, are conserved with their mammalian counterparts, including putative PEST sequences (the markers of unstable proteins), and the RB-interaction motif. Both CYCD2;1 and CYCD3;1 bind the RB-protein, which is important at the G1/S-phase transition, *in vitro* (Ach et al., 1997; Huntley et al., 1998; see Section 1.4.1). Another indicator of the importance of the D-type cyclins at G1/S is the competence of CYCD2;1 and CYCD3;1 to bind and activate CDKA;1, which is expressed throughout the cell

cycle, but not CDKB1;1, expressed at the G2/M transition only (Healy et al., 2001). An interesting feature of the plant D-type cyclins is their ability to respond to environmental signals. The expression of both CYCD2;1 and CYCD3;1 is dependent upon the availability of sucrose (Riou-Khamlichi et al., 2000) and the kinase activity of both drops when sucrose is removed from the plant growth medium (Healy et al., 2001). The D-type cyclins also respond to hormonal signals, especially cytokinin, the application of which causes a rapid super-induction of CYCD3;1 (Riou-Khamlichi et al., 1999; Soni et al., 1995).

1.3 CDK INHIBITORS

As well as regulation by phosphorylation, negative regulation is also exerted upon CDKs by cyclin dependent kinase inhibitors (CKIs). In budding yeast, SIC1 is an inhibitor of cyclin-CDK complexes at the G1/S-phase transition (Mendenhall, 1993; Schwob et al., 1994), while FAR1 induces cell cycle arrest at G1/S in response to pheromones (Peter and Herskowitz, 1994). In mammalian cells two classes of CDK inhibitor have been identified. The INK4 proteins specifically inhibit CDK4 and CDK6 by preventing the formation of an active complex with D-type cyclins (Serrano et al., 1993). CIP (CDK inhibitory proteins) and KIP proteins bind to a wider range of CDKs (reviewed by Besson et al., 2008; Sherr and Roberts, 1999). Four INK4 proteins have been identified in mammalian cells (Hannon and Beach, 1994; Guan et al., 1994; Hirai et al., 1995; Chan et al., 1995), all of which contain ankyrin repeats, necessary for protein-protein interactions (Serrano et al., 1993). The INK4 proteins are maximally expressed during S-phase, and inhibit G1/S cyclin-CDK complexes (Hirai et al., 1995; Chan et al., 1995).

The CIPs and KIPs have a conserved N-terminal domain which mediates their binding with cyclin-CDK complexes, however the remainder of the sequence is different in each inhibitor, suggesting they have distinct roles. CIPs and KIPs mainly control the transition from G1 to S-phase, exerting weaker inhibition on CDK1-cyclinB complexes at the G2 to M-phase transition. A human CIP protein, CDI1 was found to interact with *S. cerevisiae* CDC28, and human and Drosophila Cdc2s by a yeast two-hybrid screen, and interestingly shares a degree of sequence similarity

with both *S. pombe* and human Cdc25 phosphatases (Gyuris et al., 1993). $p21^{CIP1}$, $p27^{KIP1}$ and $p57^{KIP2}$ interact with and inhibit cyclinA-CDK2, cyclinE-CDK2, cyclinD1-CDK4 and cyclinD2-CDK4 (Harper et al., 1993; Xiong et al., 1993; Polyak et al., 1994a; Polyak et al., 1994b; Toyoshima and Hunter, 1994; Lee et al., 1995; Matsuoka et al., 1995). Additionally $p27^{KIP1}$ and $p57^{KIP2}$ both have a weak inhibitory effect on the mitotic cyclinB-Cdc2 complex (Toyoshima and Hunter, 1994; Lee et al., 1995; Matsuoka et al., 1995). The CKIs are in turn regulated via phosphorylations and protein-protein interactions (reviewed by Besson et al., 2008).

1.3.1 PLANT CDK INHIBITORS

Seven CKIs have been identified in *Arabidopsis*: ICK1 and ICK2 (interactors with, or inhibitors of, CDK) and KRPs 3-7 (Kip-related proteins), all of which share limited homology with mammalian CIPs and KIPs (Wang et al., 1997; De Veylder et al., 2001; Lui et al., 2000). The C-terminal domain of the plant ICKs and KRPs is conserved and similar to the mammalian N-terminal domain which is important for their binding with cyclin-CDK complexes. In plants this conserved domain is equally required for the interaction of ICK1 with CDKA;1 and CYCD3;1 (Wang et al., 1998), and consequently for its function as a CDK inhibitor (Zhou et al., 2003). The ICKs and KRPs are differentially expressed in different *Arabidopsis* tissues which implies varying roles for these proteins (Ormenese et al., 2004). They are also differentially expressed during the cell cycle. KRPs 3 and 4 peaked during S-phase and KRP6 peaked at the G1/S-phase transition, while ICK1 and 2 peaked during G2 (Menges et al., 2005; De Veylder et al., 2001). The fact that ICK proteins are able to block the cell cycle at the G2/M transition, but allow the progression of S-phase, often leads to endoreduplication (Lui et al., 2000; Zhou et al., 2002; Weinl et al., 2005). Also in support of their varying roles in the cell cycle, the ICKs and KRPs display different patterns of interaction with CDKs and cyclins. ICK1 and 2 and KRP3 and 4 are able to interact with CDKA, while KRP6 and 7 do not (Zhou et al., 2002). Interestingly, none of the ICKs or KRPs bind B-type CDKs (Lui et al., 2000). All of the plant ICKs and KRPs interact with D-type cyclins (Jasinski et al., 2002; Zhou et al., 2003).

A second class of CDK inhibitors, the SIAMESE(SIM)-related proteins (SMRs), have been discovered in plants. SMR proteins are localised to the nucleus and contain a motif found in the ICKs/KRPs, as well as a cyclin-binding motif (Churchman et al., 2006). SMRs are expressed throughout the *Arabidopsis* plant, and are able to interact with CDKA;1, and D-type cyclins including CYCD2;1, CYCD3;2 and CYCD4;1 (Churchman et al., 2006). While the trichomes of wild type *Arabidopsis* are unicellular, with a high DNA content of approximately 16C-32C, recessive *sim* mutants produce multicellular trichomes with each cell containing a nucleus with a low ploidy level (Churchman et al., 2006). Taken together, these results suggest that SMRs inhibit mitotic progression, allowing cells to switch to the endocycle in trichomes by inhibiting the activity of CYCD-CDKA;1 complexes (Churchman et al., 2006).

In light of the activity of these proteins, and the apparent redundancy of *Arath*;WEE1 in a normal cell cycle (see Section 1.4.2.3), a recent theory postulates that the G2/M transition could be controlled by the phosphorylation of ICK2/KRP2 by CDKB, which would then dissociate from CDKA, enabling cell cycle progression (Boudolf et al., 2006). However, this would still require the dephosphorylation of CDKA, and the phosphorylation of ICK2/KRP2 primarily by CDKB, as both CDKA and CDKB phosphorylate these proteins to a similar degree *in vitro* (Verkest et al., 2005).

1.4 CELL CYCLE TRANSITIONS

1.4.1 G1/S

The transition of cells from G1 into S-phase is ultimately regulated by the phosphorylation status of the RB-protein and, in mammalian cells, RB-related proteins p107 and p130. In its dephosphorylated form, during G1, RB sequesters and inactivates the E2F family of transcription factors, preventing the expression of genes required for entry into S-phase. The hyperphosphorylation of RB by cyclin-CDK complexes is required for the release and activation of E2F, and the subsequent entry of cells into S-phase (reviewed by Neganov and Lako, 2008).

In mammalian cells, there are six members of the E2F family, each of which is able to heterodimerise with the DNA-binding proteins DP1 and DP2, resulting in a possible twelve different DNA-binding transcriptional regulators (Cam and Dynlacht, 2003). The E2Fs can be further divided into two classes: activators (1, 2 and 3) and repressors (4 and 5) of transcription; while E2F6 lacks functional cyclin- and RB-binding and the trans-activation domains, so is considered an independent member (Trimarchi et al., 1998). RB is the main binding partner of the activator E2Fs, while the RB-like protein, p130, binds the repressor E2Fs (with the exception of E2F4, which preferentially binds the alternative RB-like protein p107; Frolov and Dyson, 2004).

In mammalian cells, the complexes required for the G1 to S-phase transition are cyclinD-CDK4/6 and cyclinE-CDK2. D-type cyclin expression can be induced by mitogenic growth factors. CyclinD-CDK4/6 activity occurs in mid- to late-G1, prior to that of cyclinE-CDK2. As well as the direct hyperphosphorylation of RB, cyclinD-CDK4/6 complexes may regulate the progression of S-phase indirectly by the sequestration of CIPs/KIPs. A balance exists between the CIPs/KIPs acting on the cyclinD and cyclinE complexes. When the expression of cyclinD is increased by mitogenic factors, $p27^{KIP1}$ is redistributed from cyclinE complexes to the new cyclinD complexes, releasing cyclinE-CDK2 (Sherr and Roberts, 1995, 1999). The binding of CIP/KIP also stabilises the cyclinD-CDK4/6 complex and leads to its transport into the nucleus (Cheng et al., 1999). The expression of cyclinE, and also CDC25A, is sufficient to induce the restriction point, a critical point in late G1 after which the cell is committed to undergo DNA replication and is no longer sensitive to growth factors (Pardee, 1974). CDC25A promotes S-phase entry by dephosphorylating and activating the cyclinE-CDK2 complex (Blomberg and Hoffmann, 1999).

1.4.1.1 G1/S in Plants

The mechanisms of the G1/S-phase transition in plants are generally well conserved with those of mammalian cells. Hence, in plants, a negative regulation of E2F transcription occurs through its tight binding to the RB protein. As described in section 1.2.1, plant D-type cyclins are induced in response to sucrose and hormone

signalling, providing a mechanism for control of the cell cycle in response to external conditions (Riou-Khamlichi et al., 1999, 2000). Rising levels of the D-type cyclins, late in G1, form complexes with CDKA, which in turn hyperphosphorylate the RB protein (Boniotti and Guttierrez, 2001) allowing E2F to activate the transcription of S-phase genes, including *CDC6* (de Jager et al., 2001) and *MCM(s)* (Stevens et al., 2002). *CYCD3;1* transcription is also activated by E2F activity, providing a positive feedback loop for the inactivation of RB. However, transcription of E2Fc, which lacks a transactivation domain, leads to negative feedback by the competitive inhibition of E2F. In total, nearly 6000 genes in *Arabidopsis* have been identified as containing E2F-binding sites, one-third of which are cell cycle genes (Ramirez-Parra et al., 2003).

One RB and several RB-related proteins have been identified in plants (Grafi et al., 1996; Xie et al., 1996), while three E2F genes (a, b and c; Ramirez-Parra et al., 1999; Sekine et al., 1999) and two DP genes (a and b; Magyar et al., 2000; Ramirez-Parra et al., 2000) have been discovered. At least three more E2F-like genes have been discovered in *Arabidopsis*, however these are less well characterised and may not require the association of DP for their function (Ramirez-Parra et al., 2007). Interestingly, no E-type cyclins have been identified in plants which may explain, at least in part, the relatively increased number of D-type cyclins compared to mammalian cells.

1.4.2 G2/M

1.4.2.1 CDKs/cyclins

Two cyclin subclasses are primarily involved in the transition from G2-phase into mitosis in mammalian cells, the A-types and B-types, and of these the B-types are the most important at this stage. Cyclin A is primarily expressed shortly after cyclin E, binding to CDK2 to regulate S-phase entry, but also interacts with CDK1 in G2 and mitosis. Cyclin B also binds CDK1, and was originally identified as the maturation or mitosis promoting factor (MPF) in meiotic *Xenopus* oocytes (Masui and Markert, 1971; Dunphy et al., 1988; Gautier et al., 1988; Murray et al., 1989).

The activity of cyclinB-CDK1 is strongly regulated by several mechanisms in order to maintain the timing of mitotic entry.

In human cells, cyclin B transcription begins late in S-phase (Pines and Hunter, 1989; Piaggio et al., 1995). During G2, the cyclinB-CDK1 complex is phosphorylated on the threonine 14 (T^{14}) and tyrosine 15 (Y^{15}) residues, inhibiting its activity. Fission yeast Cdc2 is phosphorylated on Y^{15} only (Gould and Nurse, 1989). The phosphorylation of Y^{15} inhibits CDK activity by interfering with phosphate transfer to any bound substrate, due to the residue's situation in the ATP-binding site (Atherton-Fessler et al., 1993), while the phosphorylation of T^{14} interferes with ATP-binding (Endicott et al., 1994). This inhibitory phosphorylation of the cyclinB-CDK1 complex is important to prevent premature entry of the cell into mitosis. It is controlled by the WEE1 family of protein kinases (Lundgren et al., 1991; Parker and Piwnica-Worms, 1992; see Section 1.4.2.3). At the onset of mitosis, WEE1 activity is countered by the phosphatase, CDC25 (Russell and Nurse, 1986; see Section 1.4.2.2).

In animals, another level of regulation is imposed on the cyclinB-CDK1 complex by inhibitory proteins. While these are less evident than at the G1/S-phase transition, $p21^{CIP1}$ may have a role in the regulation of G2/M (Dulic et al., 1998; Medema et al., 1998; Niculescu et al., 1998). The induction of $p21^{CIP1}$ led to the accumulation of cells in G2-phase as well as G1, and the inhibition of cyclin B-associated kinase activity as well as that of cyclins A and E (Medema et al., 1998; Smits et al., 2000).

In plants, both A- and B-type CDKs are important for entry into mitosis. While CDKA;1 activity peaks at both the G1/S and G2/M transitions in *Arabidopsis*, CDKB1;1 kinase activity displays a single peak at G2/M (Joubes et al., 2000). Similarly, in tobacco BY-2 cell culture CDKA kinase activity is evident from S-phase to G2/M, while the kinase activity of CDKB peaks late in G2 (Porceddu et al., 2001; Sorrell et al., 2001). As in mammalian cells, the A- and B-type cyclins are primarily thought to be responsible for the G2/M transition in plants, with cyclin B expression occurring from G2 up to mitosis. However the D-type cyclin CYCD4;1, which is expressed throughout the cell cycle, was also found to bind CDKB2;1 in a yeast two-hybrid screen (Kono et al., 2003) and may form an active kinase complex

(Sorrell et al., 1999). So, at G2/M in plants there are potentially three important classes of cyclin-CDK complex: cyclinA-CDKA, cyclinB-CDKB and cyclinD4-CDKB (Sorrell et al., 2001; Kono et al., 2003).

1.4.2.2 CDC25

Y^{15} of Cdc2 is dephosphorylated by Cdc25 phosphatase in *S. pombe* (Nurse, 1990). In mammalian cells, the CDC25 family members are phosphatases with dual-specificity for both T^{14} and Y^{15} of CDK1 (Dunphy and Kumagai, 1991; Gautier et al., 1991; Millar et al., 1991; Strausfeld et al., 1991; Lee et al., 1992; Sebastian et al., 1993). This dephosphorylation occurs late in G2-phase, and results in the onset of mitosis via the induction of cyclinB-CDK1 kinase activity. A positive feedback loop is affected by the phosphorylation of CDC25C by cyclinB-CDK1, which further activates CDC25C (Hoffmann et al., 1993; Izumi et al., 1993).

There are three members of the mammalian CDC25 family, A, B and C, with specificity for different cyclin-CDK complexes. CDC25A dephosphorylates the cyclinA-CDK2 and cyclinE-CDK2 complexes, promoting entry into S-phase (Jinno et al., 1994; see Section 1.4.1). Both CDC25B and CDC25C function in the transition from G2-phase to mitosis. It is thought that CDC25B regulates the nucleation of the centrosomal microtubules (Gabrielli et al., 1996). As previously mentioned, CDC25C is responsible for the dephosphorylation and activation of cyclinB-CDK1 at the G2/M transition (Russell and Nurse, 1986).

CDC25 phosphatase may also be responsible for the dephosphorylation of the T^{14} and Y^{15} residues of CDKs in higher plants. Phosphatase activity during prophase has been demonstrated in *Nicotiana plumbaginifolia* cells in which mitosis was induced via the application of cytokinins (Zhang et al., 2005). The expression of *S. pombe Cdc25* in tobacco BY-2 cells led to a short G2-phase and premature division at a small cell size, as well as premature activation of CDKB, but not CDKA (Orchard et al., 2005). However, in higher plants *CDC25* lacks a regulatory domain (Landrieu et al., 2004) and is poorly expressed in all tissues (Sorrell et al., 2005). Despite this, the *Arabidopsis* CDC25 protein can dephosphorylate *Arabidopsis* CDKs (Landrieu et al., 2004), and is also able to induce a typical short cell length when expressed in fission yeast (Sorrell et al., 2005).

The cytokinin plant growth regulatory group is required for the G2/M transition in tobacco (John et al., 1993). Given that either cytokinin treatment or expression of *Spcdc25* was able to dephosphorylate plant CDK it has been hypothesised that a cytokinin signalling cascade culminates in CDC25 (Zhang et al., 1996, 2005). Additionally, the expression of *Spcdc25* in tobacco BY-2 cells may inhibit the production of cytokinins (Orchard et al., 2005). Conversely, it has been postulated that the plant cell cycle may have lost the requirement for CDC25 altogether, evolving CDKBs instead (Boudolf et al., 2006), however this theory lacks evidence.

1.4.2.3 WEE1

As mentioned in Section 1.4.2.1, in fission yeast the inhibitory phosphorylation of the Y^{15} residue of the cyclinB-Cdc2 complex is regulated by the Wee1/Mik1 (mitotic inhibitory kinase) family of protein kinases (Den Haese et al., 1995). The budding yeast homologue of WEE1, SWE1, phosphorylates T^{19} of CDC28 (Booher et al., 1993; Sia et al., 1996). In mammals, WEE1 is also responsible for the phosphorylation of Y^{15} (Featherstone and Russell 1991; Lundgren et al., 1991; Parker and Piwnica-Worms, 1992), while a further WEE1-related kinase, MYT1, is able to phosphorylate both T^{14} and Y^{15}, but with a preference for T^{14} (Mueller et al., 1995). Although WEE1 is nuclear (Baldin and Ducommun, 1995; Heald et al., 1993), MYT1 localises to the membranes of the endoplasmic reticulum and Golgi apparatus (Liu et al., 1997), possibly allowing for the inhibition of distinct subpopulations of cyclinB-CDK2 complex prior to mitosis.

In humans, the kinase activity of WEE1 is relatively high during interphase, dropping in mitosis (McGowan and Russell, 1995). In interphase, in human cells, WEE1 is found in the nucleus whilst CDC25 is sequestered in the cytoplasm. At this stage WEE1 is associated with a 14-3-3 protein, protecting it from deactivation by hyperphosphorylation (Morgan, 2007). At the G2/M transition these proteins reverse positions so that CDC25 is present in the nucleus and WEE1 in the cytoplasm (Baldin and Ducommun, 1995; Figure 1.4). During G2, the T-loop of CDK1 containing T^{167} physically protects Y^{15} from dephosphorylation by CDC25, even if it is able to enter the nucleus. At G2/M the arrangement of the T-loop suddenly alters, probably due to the phosphorylation of T^{167} and subsequent binding of cyclin.

Consequently, CDC25 is able to out-compete WEE1, dephosphorylating the Y^{15} of CDK1 and allowing progression into mitosis (reviewed by Draetta, 1994; Figure 1.4). This may be regulated by the accumulation of cyclin during interphase. Additionally, the deactivation of WEE1 at mitosis is concomitant with its hyperphosphorylation (Tang et al., 1993). This inhibitory phosphorylation has been attributed to Nim1 in fission yeast (Parker et al., 1993; Wu and Russell, 1993), however Nim1 homologues have not been identified in any other organism. In fact, in *Xenopus* this hyperphosphorylation is attributed to cyclinB-CDK1 activity (Watanabe et al., 2005). Following hyperphosphorylation, WEE1 is degraded via the 26S proteasome pathway (see Sections 1.6 and 5.1).

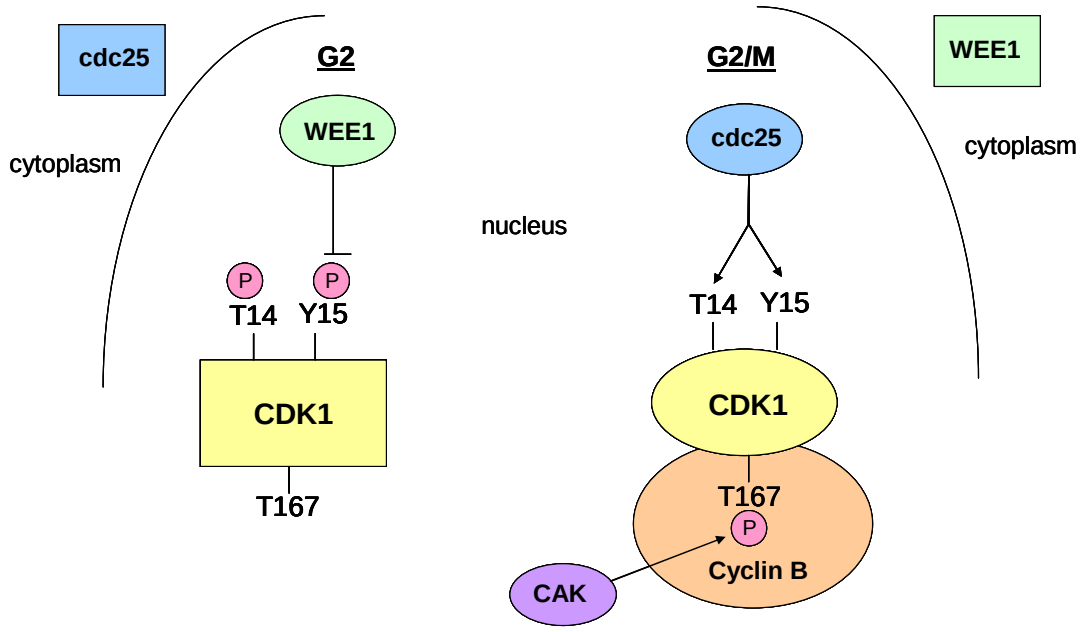

Figure 1.4 Schematic diagram showing some of the important proteins at the G2/M transition of the mammalian cell cycle. At G2, threonine 14 (T14) and tyrosine 15 (Y15) of CDK1 are phosphorylated (P; Y15 by WEE1) and T167 is dephosphorylated, inhibiting the activity of CDK1 and transition into mitosis. During G2, CDC25 is sequestered in the cytoplasm. At the G2/M transition, WEE1 and CDC25 are reversed, with WEE1 being sequestered in the cytoplasm and CDC25 dephosphorylating T14 and Y15. Cyclin activating kinase (CAK) phosphorylates T167, allowing the binding of cyclin B and progression into mitosis. ○= active protein. □=inactive protein. (Diagram adapted from Francis, 2007)

Homologues to *WEE1* have been discovered in several higher plants including maize (*Zea mays*; Sun et al., 1999), tomato (*Solanum lycopersicum*; Gonzalez et al., 2004), rice (*Oryza sativa*; Guo et al., 2007) and *Arabidopsis* (Sorrell et al., 2002). *Arath;WEE1* is found on chromosome 1 of the *Arabidopsis* genome, in a single copy

which encodes approximately 500 amino acids (Sorrell et al., 2002). The strongest expression of *Arath;WEE1* is seen in tissues with high rates of cell division, and is not observed in non-cycling tissues such as mature leaves, suggesting a role for this protein in the cell cycle (Sorrell et al., 2002). Furthermore, in both tobacco BY-2 and *Arabidopsis* cell culture, *WEE1* expression peaks in late S-phase (Gonzalez et al., 2004; Menges et al., 2005), while protein levels of *Nicta*;WEE1 peak early in G2 (Lentz Grønlund, 2007). Interestingly, *Nicta*;WEE1 kinase activity is highest early in S-phase, dropping consistently during S and G2 to its lowest level in mitosis (Lentz Grønlund, 2007). A role for *Arath*;WEE1 in S-phase under conditions of replication stress was recently proposed (Cools et al., 2011). However, a role in the inhibition of the G2/M transition under normal conditions, similar to the function of yeast and mammalian WEE1 (described above), has not been confirmed in higher plants.

The *Arath*;WEE1 protein consists of 500 amino acids and contains a serine/threonine kinase domain at the C-terminal. This includes an ATP-binding region signature from isoleucine at position 255 to lysine at position 278 and a serine/threonine protein kinase signature from isoleucine at position 368 to isoleucine at position 380. In *Arabidopsis*, WEE1 is able to physically interact with CDKA;1 but not with B-type CDKs (De Schutter et al., 2007; Boruc et al., 2010). Interestingly, in *Arabidopsis* the system of phosphorylation is differentially regulated between CDKs – *Arath*;WEE1 is able to phosphorylate CDKA;1 at Y^{15}, but phosphorylates CDKD;1,CDKD;2 and CDKD;3 at $Y^{23/24}$ *in vitro* (Shimotohno et al., 2006), probably reflecting the different roles of these CDKs in the cell cycle. It has recently been discovered that the control of the cell cycle in plants is not actually dependent on sudden changes in the phosphorylation status of CDKA;1 (Dissmeyer et al., 2009), leading to further questions regarding the role of WEE1 in plants.

In *S. pombe* Wee1 shows functional redundancy due to Mik1 (Lundgren et al., 1991), and to MYT1 in mammalian cells (Mueller et al., 1995). In *Arabidopsis*, although the presence of both Mik1 and MYT1 is not apparent, *Arath;*WEE1 knockouts grow relatively normally (De Schutter et al., 2007), which again may demonstrate functional redundancy to other kinases. Alternatively, higher plants may not require WEE1 for the inhibition of the G2/M transition under normal growth conditions. As previously mentioned in Section 1.3.1, a recent theory postulates that

the G2/M transition could be controlled via the regulation of CDK inhibitors, by the inhibitory phosphorylation of these proteins by CDKB. This would lead to the dissociation of ICK2/KRP2 from, enabling cell cycle progression (Boudolf et al., 2006). However, evidence is also lacking for this proposal.

One role for higher plant WEE1 which has been demonstrated is in endoreduplication, the repeated expansion in ploidy level of plant cells via repeated S-phase, which is important for cell expansion. In tomato plants, the downregulation of *Solly*;*WEE1* expression led to a decreased plant and fruit size phenotype. Although little effect was observed on mitosis, there was a decrease in Y^{15} phosphorylation of CDKA, leading to increased kinase activity and decreased endoreduplication (Gonzalez et al., 2007). High expression levels of *Zeama*;*WEE1* were also observed in maize tissue undergoing endoreduplication (Sun et al., 1999). However, this function for WEE1 may be species specific, as no change in ploidy level could be detected in *Arath*;*WEE1* T-DNA insertion mutants compared to wild type (De Schutter et al., 2007).

As described at the beginning of this chapter, the DNA damage and replication checkpoints are signal transduction pathways which ensure that cells containing damaged DNA or perturbed replication forks are not able to proceed through the cell cycle transitions. One mechanism for this is via the maintenance of the inhibitory phosphorylation of CDKs, which can be achieved by stabilising WEE1 activity (see Section 1.5). *Arath*;*WEE1* T-DNA insertion mutants were hypersensitive to hydroxyurea, which depletes cellular deoxyribonucleotide triphosphates (dNTPs) required for DNA synthesis, leading to the conclusion that *Arath;*WEE1 is mainly involved in the DNA replication checkpoint in those cells which are exposed to stress (De Schutter et al., 2007). The possibility remains that WEE1 also has a role in the unperturbed cell cycle in higher plants, and investigations into the function of WEE1 in plants are the focus of this thesis.

1.4.3 MITOSIS

The cyclinB-CDK1 complex triggers mitosis by phosphorylating a wide range of proteins required for mitotic progression (Nurse, 1990), including protein kinases such as Aurora and Polo, and hundreds of additional phosphoproteins (Dephoure et al., 2008; Errico et al., 2010; Holt et al., 2009). This leads to the re-organisation of the cell structures, such as the network of microtubules and actin microfilaments, and the nuclear lamina.

At mitosis, the sister chromatids of the chromosomes replicated during S-phase separate and divide into two new daughter cells. During prophase, when the chromosomes condense, the two chromatids of each chromosome are joined together by cohesin, a multiprotein complex which is produced and attached to the chromatids during telophase of the previous mitosis (Nurse, 1990). At metaphase, the chromosomes align on the mitotic spindle. Rather than attaching directly to DNA, the microtubules are connected by kinetochore complexes to the DNA of the centromere (Connelly and Hieter, 1996). The attachment of kinetochore complexes to the mitotic spindle is regulated by Aurora kinases (reviewed by Bischoff and Plowman, 1999). Also at metaphase, the anaphase promoting complex (APC) is activated by the cyclinB-CDK1 complex which has the dual effect of targeting both securin and cyclin B for degradation via the 26S proteasome (see Section 2.6). The destruction of securin allows separase activity, which in turn destroys cohesin, allowing the sister chromatids to part, triggering anaphase (Funabiki et al., 1996; Ciosk et al., 1998; Nasmyth, 2001). The degradation of cyclin B leads to the deactivation of CDK1 and consequently exit from mitosis and the onset of cytokinesis (Pines, 1995).

1.4.3.1 Mitosis in Plants

In plants, the mechanisms of mitotic progression are well conserved with those of animals, described above (reviewed by Francis, 2007). Homologues of separase, Aurora kinases, APC components and the 26S proteasomes have all been identified in plants, as well as the cyclinB-CDKA/B complexes. *Arath*;AURORAS localise to the spindle microtubules and centromeres, and are exclusively expressed in proliferative tissues, supporting a role in kinetochore regulation (Demidov et al.,

2005). Cytokinesis, however, is very different in plants compared to higher animals due to the need to construct a new cell wall (reviewed by Staehelin and Hepler, 1996; Francis, 2007).

1.5 DNA DAMAGE AND REPLICATION CHECKPOINTS

As previously mentioned, cell cycle checkpoints are regulatory pathways which ensure that events such as DNA replication and chromosome segregration are completed correctly prior to the onset of the subsequent cell cycle stage. These pathways are able to respond to DNA damage or stalled replication forks by arresting the cell cycle in G1-, S- or G2-phase and, in the case of the DNA damage checkpoint, inducing the transcription of DNA repair genes (Hartwell and Weinert, 1989). Mammalian cells are also able to respond by apoptosis (programmed cell death).

DNA damage and replication checkpoints are less well conserved between organisms than the general cell cycle mechanisms described above. The budding and fission yeast checkpoint pathways have been the most comprehensively studied to date (reviewed by Elledge, 1996; Weinert, 1998), however the mechanisms in other organisms are being uncovered. Generally, checkpoint genes fall into three categories: sensors, which recognise the DNA damage or perturbation of DNA replication; and signal transducers, which mediate the response via phosphoregulation of the third class, the target proteins. For cells arresting in G2, phosphorylation of the Y^{15} residue of Cdc2/CDK1 is the target of the DNA damage pathway in fission yeast and mammals (Kharbanda et al., 1994; O'Connell et al., 1997; Rhind et al., 1997).

ATM (ataxia telangiectasia-mutated) and ATR (Rad3-related) are kinases active in the DNA repair and replication checkpoints, respectively, acting as the sensors in mammalian cells (Hoekstra, 1997; Figure 1.5). CHK1 is the signal transducer in these pathways, phosphorylated by ATM and ATR (Walworth et al., 1993). CHK1 is able to phosphorylate both WEE1 (O'Connell et al., 1997) and CDC25C (Sanchez et al., 1997), which in turn inhibits cyclins A and B from binding to CDK1,

preventing mitosis (Figure 1.3). The phosphorylated WEE1 and CDC25 kinases are protected from dephosphorylation by 14-3-3 proteins (Lee et al., 2001; Zeng and Piwnica-Worms, 1999). PLK1, an upstream activator of CDC25C, may also have a role in the mammalian DNA damage checkpoint, by the inhibition of both CDC25C and the APC (Smits et al., 2000). A second important signal transducer in the mammalian DNA damage checkpoint pathway is CDS1 (reviewed by Rhind and Russell, 2000). In mammals, p53 is also a target of both CHK1 in the DNA replication checkpoint pathway and CDS1 in the DNA damage pathway (Chehab et al., 1999; Hirao et al., 2000; Shieh et al., 2000). P53 is able to induce the CDK inhibitor $p21^{CIP1}$ in response to DNA damage, preventing the onset of S-phase (Deng et al., 1995).

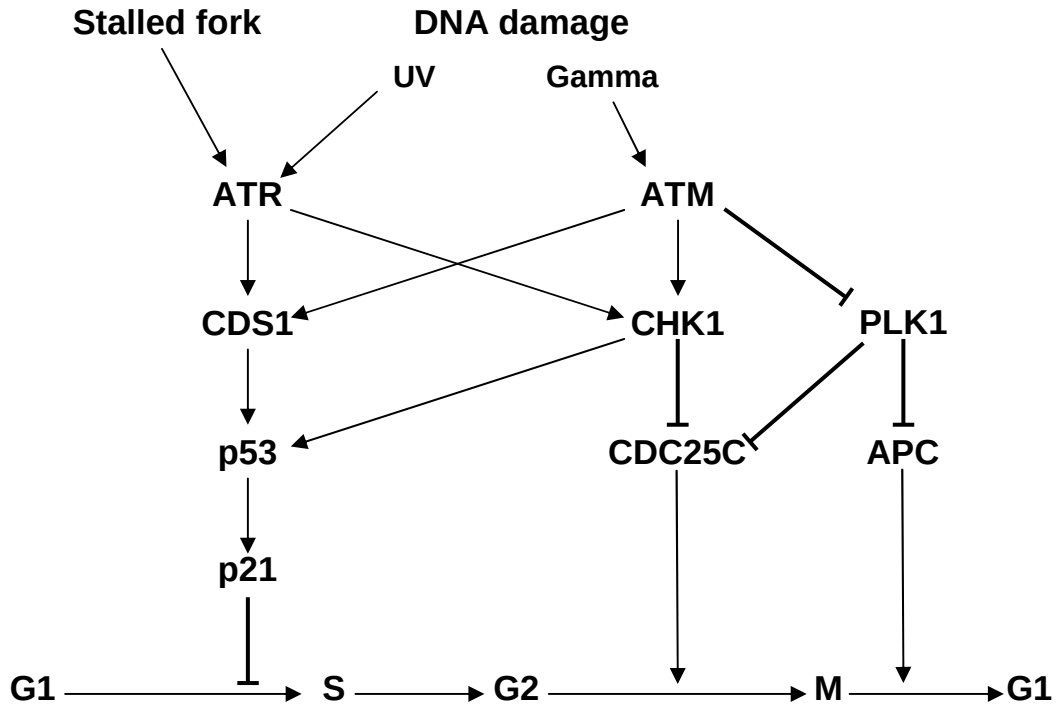

Figure 1.5 The DNA damage and DNA replication (stalled fork) checkpoint in mammalian cells (adapted from Rhind and Russell, 2000 and Smits and Medema, 2001).

1.5.1 PLANT DNA DAMAGE AND REPLICATION CHECKPOINTS

Homologues to ATM and ATR have been identified in plants (Garcia et al., 2003; Culligan et al., 2004), however the checkpoint mechanisms are yet to be fully resolved (reviewed by Cools and De Veylder, 2009; Figure 1.6). Homologues to

CHK1 or CHK2 have not been discovered in plants, although CIPK proteins, implicated in the response to environmental stress, share characteristics with CHK1. However, WEE1 is a major regulator of the response to DNA stress in plants, responding to both ATM and ATR phosphorylation by increased *Arath;WEE1* transcription (De Schutter et al., 2007). Interestingly, *Arath*;WEE1 was found to be required for the arrest of cells in S-phase in response to DNA replication stress, and was able to protect against premature vascular differentiation in the root (Cools et al., 2011). WEE1 has also been implicated in the DNA damage response to ROS in *Arabidopsis* (Vanderauwera et al., 2011). In addition, *Arath*;WEE1 interacts with a 14-3-3 protein, GF14ω, *in vivo*, an interaction which is likely to stabilise the WEE1 protein by preventing its dephosphorylation, as observed in animal cells (Lentz Grønlund et al., 2009).

While there is no evidence for a link between DNA damage and KRPs, plant CDK inhibitors may have a role to play in the response to DNA stress. A second class of CDK inhibitor, SIAMESE-related (SMR) proteins, has been identified in plants (Peres et al., 2007), the transcription of which is strongly up-regulated by DNA stress, in an ATM-dependent manner (Culligan et al., 2006). Interestingly, DNA stress can also lead to the upregulation of CYCB1;1 in plants, also dependent upon ATM (Culligan et al., 2006; Ricaud et al., 2007; Chen et al., 2003). This may provide a mechanism for preventing entry of all cells into the endocycle upon DNA stress, allowing for the re-activation of division following the completion of DNA repair (Cools and De Veylder, 2009). These discoveries provide a basis for the characterisation of cell cycle-linked DNA damage and repair checkpoints in higher plants.

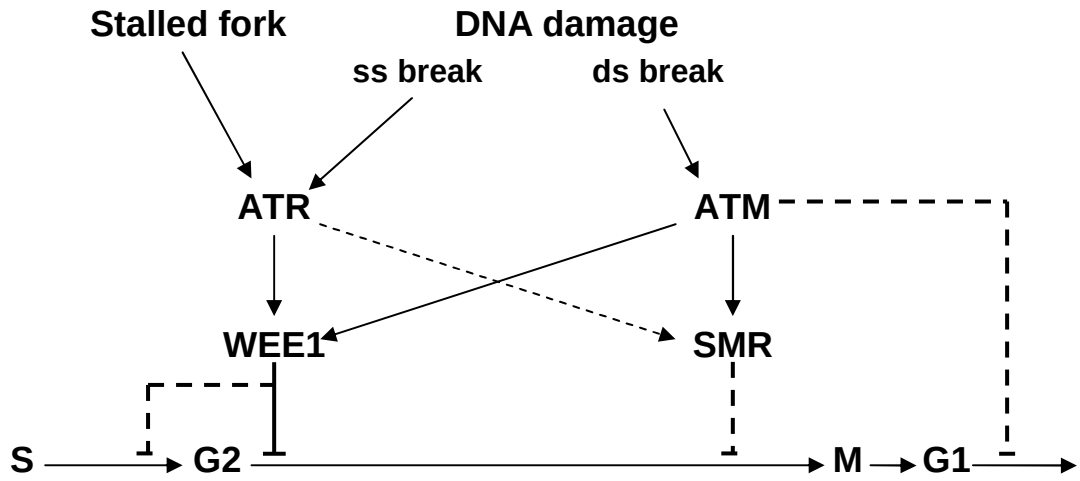

Figure 1.6 The DNA damage and DNA replication (stalled fork) checkpoint in plant cells (adapted from Cools and De Veylder, 2009).

1.6 UBIQUITIN-MEDIATED DEGRADATION IN THE CELL CYCLE

Many of the key cell cycle and DNA damage response events, described above, rely on phosphoregulatory mechanisms to ensure the smooth progression of the pathway. Another level of regulation is imposed by the physical availability of the relevant proteins, which is regulated in part by their timely expression and control of subcellular localisation, but is also controlled by their timely degradation. The most widely studied and probably most important method of proteolysis in eukaryotes is the ubiquitin/26S proteasome pathway. This mechanism is widely conserved among eukaryotes, and proteolysis of plant proteins is frequently achieved via the ubiquitin/26S proteasome pathway (reviewed by Sullivan et al., 2003).

The ubiquitin protein consists of 76 amino acids and attaches to a lysine residue in the protein targeted for degradation via its C-terminus. This is achieved by a cascade of three different enzymes (reviewed by Sullivan et al., 2003; Vierstra, 2003; Figure 1.7). Firstly, a generic ubiquitin-activating enzyme (E1) attaches to ubiquitin and transfers it to an ubiquitin-conjugating enzyme (E2). The third enzyme, ubiquitin ligase (E3) mediates ubiquitin transfer from the E2 to a lysine residue of the target protein. An intermediate complex consisting of the E3, E2 and the target protein may form. The E3 ligase provides the specificity for the degradation of the target protein.

Subsequently, more ubiquitins may be added to form a chain on the target protein, with different types of chain dictating the fate of the protein. Generally the chain forms on the K48 residue of the target protein, targeting it for degradation via the 26S proteasome, however the K29 and K63 residues can also be ubiquitinated which can have a role in protein trafficking, DNA repair and the regulation of both transcription and translation (Aguilar and Wendland, 2003; Conaway et al., 2002; Weissmann, 2001).

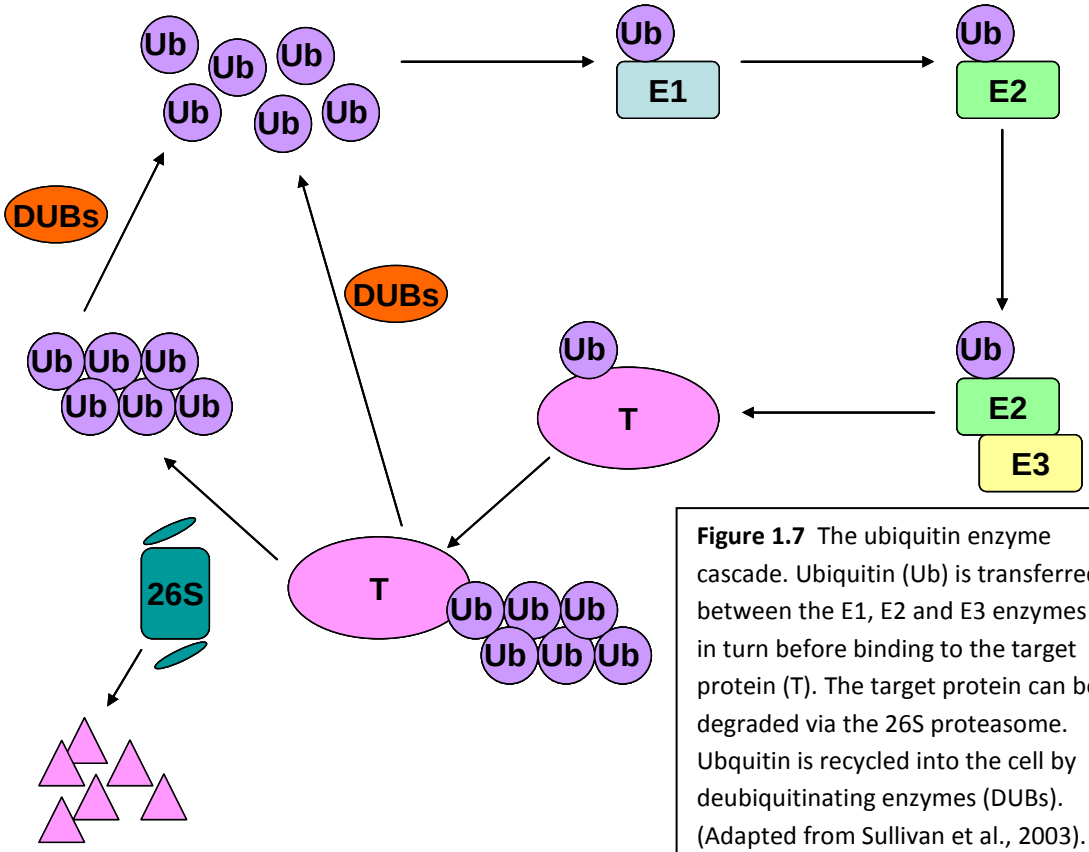

Figure 1.7 The ubiquitin enzyme cascade. Ubiquitin (Ub) is transferred between the E1, E2 and E3 enzymes in turn before binding to the target protein (T). The target protein can be degraded via the 26S proteasome. Ubquitin is recycled into the cell by deubiquitinating enzymes (DUBs). (Adapted from Sullivan et al., 2003).

The 26S proteasome is a large protein complex (approximately 700kDa) formed of two subcomplexes, the 20S core protease and the 19S regulatory particle (Glickman, 2000; Voges et al., 1999). The 20S complex contains the catalytic domain, and consists of a hollow cylinder. The 19S complex binds the 20S complex at one or both ends and consists of both a lid and a base complex containing ATPases. Polyubiquitinated proteins are recognised by the 19S complex and fed through the base, which probably acts as a "reverse chaperone" by both unfolding the protein and transferring it to the 20S complex (Ferrell et al., 2000). Five types of protease activity act on the protein within the 20S complex, producing short peptides which

are deubiquitinated by deubiquitinating enzymes and recycled by the cell (Vierstra, 1996; Wilkinson, 2000). The 26S proteasome in plants is well conserved with that of yeasts and animals (Fu et al., 1999; Smalle et al., 2002).

Over 1400 genes for either constituents of or interactors with the 26S proteasome pathway have been identified in *Arabidopsis*, of which 90% encode E3 ligase subunits (reviewed by Moon et al., 2004; Vierstra, 2003). As mentioned above, the specificity of the ubiquitin/26S proteasome pathway is conferred via the E3 ligases. Several types of E3 ligase have been identified in eukaryotes, however two complex E3 ligases are mostly important for cell cycle progression in budding yeast and mammalian cells: the anaphase-promoting complex and the SCF complex (King et al., 1995; Feldman et al., 1997; Skowyra et al., 1997). Although these were in the past considered to be active in completely separate pathways, there is some evidence for their collaboration in the cell cycle. SCF^{TOME1} is the complex responsible for the degradation of WEE1 (Ayad et al., 2003). In *Xenopus*, the F-box protein TOME1 is a target of APC^{CDH1}, which removes SCF^{TOME1} activity during G1, allowing WEE1 activity and preventing premature onset of mitosis (Ayad et al., 2003). Another F-box protein, SKP2, is also targeted for degradation by APC^{CDH1} (Bashir et al., 2004; Wei et al., 2004), demonstrating a further link between these E3 ligases.

1.6.1 ANAPHASE-PROMOTING COMPLEX

The APC is mainly important for the progression of and exit from mitosis. It is a large protein complex, consisting of 11 subunits in mammalian cells (Peters, 2002) and 13 in yeasts (Yoon et al., 2002). At minimum, the APC consists of the APC2 protein and the RING-finger protein APC11, which interact both with each other and with E2 enzymes. Additionally the APC must be activated by an activating protein, either CDC20 or CDH1, which are thought to confer different substrate specificities to the complex, allowing for phase-specific degradation of proteins (reviewed by Peters, 2002; Castro et al., 2005).

Activation of the APC occurs early in mitosis via both cyclinB-CDK1 phosphorylation and the association of its activator, CDC20. As described in section

1.4.3, APC^{CDC20} is required for the degradation of securin which allows separase activity and consequently the onset of anaphase (Uhlmann et al., 2000; Yanagida, 2000). While CDC20 is the APC activator required for the degradation of securin, APC^{CDH1} has been identified as the complex responsible for the maintenance of APC activity until the end of G1-phase (Nasmyth, 2001; Zur and Brandeis, 2001). It is thought that CDH1 has a wider substrate specificity than CDC20 (Zur and Brandeis, 2002), with targets including the AURORA kinases (Crane et al., 2004) and CDC25A (Donzelli et al., 2002).

The degradation of mitotic cyclins by APC has been widely studied. The B-type cyclins contain a motif of nine residues in the N-terminus (RxxLxxIxN) known as the destruction or "D" box (Glotzer et al., 1991), deletion of which inhibits cyclin degradation (Brandeis and Hunt, 1996; Yamano et al., 1998). A-type cyclins also contain a "D"-box, but are degraded earlier in the cell cycle than the B-type cyclins, for example animal cyclin A is degraded at prometaphase (Whitfield et al., 1990; den Elzen and Pines, 2001; Geley et al., 2001). CyclinB1 proteolysis is initiated during metaphase and continues throughout mitosis and into G1 (Clute and Pines, 1999). This is regulated first by APC^{CDC20} then by APC^{CDH1}. A wide range of processes vital for mitotic progression and exit are initiated by the degradation of cyclinB and the consequent deactivation of CDK1, including sister chromatid separation, the disassembly of the mitotic spindle, decondensation of chromosomes and nuclear envelope formation (Murray et al., 1989; Luca et al., 1991; Gallant and Nigg, 1992; Holloway et al., 1993; Surana et al., 1993). Additionally the proteolysis of the B-type cyclins is absolutely required for exit from mitosis in a wide variety of organisms including *Xenopus*, sea urchin, *Drosophila*, humans and both budding and fission yeasts. The inhibition of cyclinB degradation leads to the continued activity of CDK and arrest of cells in mitosis (Murray et al., 1989; Holloway et al., 1993; Rimmington et al., 1994; Sigrist et al., 1995; Gallant and Nigg, 1992; Surana et al., 1993; Yamano et al., 1996).

1.6.1.1 Plant APC

Homologues to APC subunits have been identified in plants, all in a single copy except the *CDC27* homologue, of which there are two copies in *Arabidopsis*, A and

B/HOBBIT (Capron et al., 2003). This may imply that there are two different APC complexes present in plants, APC^{CDC27A} and $APC^{CDC27B/HOBBIT}$, with distinct roles in the cell cycle (Genschik and Criqui, 2007). There are also multiple homologues to the APC activating proteins in plants, with six homologues to CDC20 and three to CDH1 (termed CCS52 in plants) in *Arabidopsis*. Although no homologues to securin have been identified in plants, the treatment of tobacco BY-2 cells with the proteasome inhibitor MG132 during prophase prevents the onset of anaphase, indicating that a similar mechanism for anaphase initiation does exist in plants (Genschik et al., 1998).

The majority of plant cyclins contain a "D"-box (Renaudin et al., 1998), although some do not (Vandepoele et al., 2002). Plant B-type cyclins are also subjected to ubiquitin-mediated degradation at metaphase, for example *Zeama*;CYCB1;2 and *Nicta*;CYCB1;1 are both degraded in a cell cycle dependent manner (Mews et al., 1997; Criqui et al., 2000, 2001). Similarly to other organisms, the degradation of B-type cyclins is absolutely required for mitotic exit. The inhibition of cyclin B1 degradation in tobacco BY-2 cell culture led to cells which progressed normally through prophase and metaphase, but were arrested in anaphase, leading to a mitotic catastrophe and reiterating the importance of the timing of cyclin destruction (Weingartner et al., 2004). Similarly to animal cells, plant A-type cyclins are degraded earlier in the cell cycle than the B-types, with *Nicta*;CYCA3;1 never being detected at mitosis (Criqui et al., 2001).

1.6.2 SCF COMPLEX

The SCF E3 ligase complex consists of four subunits. SKP1 and CULLIN provide the structural backbone, while RBX is a ring finger protein which binds the E2 enzyme. Finally an F-box protein, which binds to SKP1, provides specificity to the target protein (Skowyra et al., 1997; Zheng et al., 2002; Deshaies et al., 1999; Figure 1.8). The SCF complex is involved in several aspects of the cell cycle. In yeast, both SKP1 and CDC53 (CULLIN) are required for entry into S-phase (Schwob et al., 1994; Bai et al., 1996). SKP1 has also been implicated in the G2/M-phase transition (Bai et al., 1996; Connelly and Hieter, 1996).

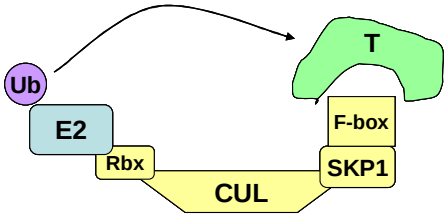

Figure 1.8 Schematic diagram representing the SCF protein complex, an ubiquitin E3 ligase. The E3 ligase consists of RBX; CULLIN (CUL) and SKP1; and F-box, which provides specificity for the target protein (T) through protein-protein interaction motifs in its C-terminus. The complex functions to transfer ubiquitin (Ub) from the E2 ligase to the target protein as part of the ubiquitin/26S protein degradation pathway. (Diagram adapted from Sullivan et al., 2003)

Frequently, the degradation of proteins via SCF requires their phosphorylation (Hershko and Ciechanover, 1998; Jackson et al., 2000), which in the case of cell cycle regulators is usually by a cyclin-CDK complex. In budding yeast, the cyclin-CDK phosphorylation-dependent degradation of SIC1 by SCF^{CDC4} is required for progression into S-phase (Schwob et al., 1994; Nash et al., 2001). In animals, the regulators of the G1/S-phase transition, RB and E2F, are both targeted for ubiquitin-mediated degradation. The RING-finger protein MDM2 regulates RB stability (Sdek et al., 2005), while the RBR protein, p130, and E2F-1 degradation involves the SCF^{SKP2} complex, and is phosphorylation-dependent (Tedesco et al., 2002; Marti et al., 1999). The degradation of $p27^{KIP1}$ is also dependent upon phosphorylation of a conserved threonine residue by cyclinE-CDK2 (Sheaff et al., 1997), and may also involve the SCF^{SKP2} (Carrano et al., 1999; Montagnoli et al., 1999; Sutterlluty et al., 1999; Tsvetkov et al., 1999).

1.6.2.1 Plant SCF

Homologues to both CULLIN and SKP1 have been identified in *Arabidopsis* (*Arath*;CUL and *Arath*;ASK respectively; Yan et al., 2000; Deshaies 1999; Farras et al., 2001; Shen et al., 2002). Additionally F-box proteins are present in all plant cells (reviewed by Wang et al., 2004). All F-box proteins contain a conserved sequence near their N-terminus of approximately 40 amino acids, known as the F-box, which is thought to interact with SKP1, joining the F-box protein to the rest of the complex. The specificity for the target protein is provided by protein-protein interaction sequences in the C-terminus of the F-box protein (Wang et al., 2004). The F-box protein superfamily is one of the largest in plants with 694 potential genes identified in *Arabidopsis* (Gagne et al., 2002). The vast number of different F-box proteins in

Arabidopsis provides the potential for the formation of many different SCF complexes, each specific to a different protein or group of proteins. F-box proteins in plants are central to the regulation of many key processes, including auxin signalling (SCF^{TIR1}; Gray et al., 2001), pathogen resistance, senescence, circadian rhythms, lateral branching and self-incompatibility (reviewed by Vierstra, 2003).

The degradation of cell cycle proteins via SCF in plants also often relies upon their phosphorylation by a cyclin-CDK complex. In *Arabidopsis*, the degradation of KRP2 is dependent on phosphorylation by CDK (Verkest et al., 2005), however the E3 ligase responsible for this degradation is unknown. Notably, two proteins similar to the animal SKP2 F-box protein have been identified in *Arabidopsis* (del Pozo et al., 2002), so it is possible that one of these is responsible for KRP2 degradation. SCF^{SKP2A} has been identified as being responsible for the CDK-phosphorylation-dependent degradation of E2Fc in plants (del Pozo et al., 2002).

1.7 EXPERIMENTAL AIMS

Currently, much less is known about the cell cycle in plants in comparison with yeast and mammalian systems. Especially of interest is the controversy regarding WEE1's role, and whether it truly does not have a function in an unperturbed cell cycle in higher plants, and only functions in response to the DNA replication and repair checkpoints. In an attempt to answer this question the further characterisation of higher plant WEE1 was completed. In particular, the aims of the work presented in this thesis were to examine:

1. the subcellular and tissue-specific localisation and stability of *Arath*;WEE1 during the cell cycle;
2. the changes in the subcellular localisation of *Arath*;WEE1 during its interactions with other proteins during the cell cycle;
3. the effect of perturbing one of *Arath*;WEE1's interactors, SKIP1, an F-box protein which may be involved in the degradation of WEE1 protein.

2. GENERAL MATERIALS AND METHODS

All standard chemicals were sourced from Sigma-Aldrich, Poole, UK unless otherwise specified.

TABLE 2.1 BUFFERS AND MEDIA

LB medium	10 g/L tryptone, 5 g/L yeast extract and 10 g/L sodium chloride dissolved in water, pH7 For plates: 0.8% Difco agar, granulated (BD, Oxford, UK)
BY2 medium	4.3 g/L Murashige & Skoog basal salts (Duchefa Biochemie, NL), 30 g/L sucrose, 0.1 g/L myoinositol, 0.2 g/L potassium hydrophosphate, 0.2 mg/L 2,4-Dichlorophenoxyacetic acid (prepared in 20 mM sodium hydroxide (NaOH)) and 1 µg/L thiamine hydrochloride dissolved in water, pH5.7 For plates: 0.8% Difco agar, granulated (BD, Oxford, UK)
MS medium	4.708 g/L Murashige & Skoog basal salts (Duchefa Biochemie, NL), 10 g/L sucrose, pH5.7 For plates: 0.8% Difco agar, granulated (BD, Oxford, UK)
Hoechst stain	1% 10 mg/mL Hoechst stain (Bisbenzimide Ca), 2% Triton X-100
Bromophenol blue (BPB) dye	10 mM Tris-HCl (pH8), 1 mM EDTA, 50% glycerol, bromophenol blue
50X Tris-Acetate-EDTA buffer	2 M Tris base, 1 M glacial acetic acid, 50 mM EDTA (pH8.0) diluted in water
Edward's extraction buffer (Edwards et al., 1991)	0.5% SDS, 250 mM NaCl, 100 mM Tris-HCl pH8.0, 25 mM EDTA
TE buffer	10 mM Tris-HCl pH8.0, 0.1 mM EDTA
Lysis buffer -	50 mM Tris-HCl pH7.5, 75 mM NaCl, 15 mM EGTA, 15 mM $MgCl_2$, 60 mM β-Glycerophosphate, 0.1% Tween-20
25x PI	One protease inhibitor tablet (Roche, UK) dissolved in 2 mL distilled water
50X PPI	50mM Sodium fluoride, 10mM Sodium vanidate, 100mM Sodium pyrophosphate
Lysis buffer +	94% lysis buffer -, 4% 25x PI, 2% PPI, 1.05mM DTT

SDS-PAGE separation buffer	1.875 M Tris-HCl pH7.5, 0.25% SDS
SDS-PAGE stacking buffer	1 M Tris-HCl pH6.8, 0.5% SDS
5x loading buffer (proteins)	250 mM Tris-HCl pH6.8, 10% SDS, 30% glycerol, 0.5 M dithiothreitol (DTT), 0.02% bromophenol blue
10x SDS running buffer	1 g/L SDS, 3.03 g/L Tris base, 14.4 g/L glycine
Coomassie Brilliant blue stain	2.5 g/L Coomassie Brilliant Blue R-250 dye, 45% ethanol, 10% acetic acid
Coomassie de-staining solution	45% ethanol, 10% acetic acid
Blotting buffer	20% methanol, 0.01% SDS, 14.4 g/L glycine, 8.08 g/L Tris base
Basic buffer	20 mM Tris-HCl pH7.5, 150 mM NaCl, 0.05% Tween-20, 1% Triton X-100
Blocking solution	5% milk powder dissolved in basic buffer

TABLE 2.2 ANTIBIOTIC SELECTION

CONSTRUCT	PLANT	ANTIBIOTIC			
		In planta	Concentration	In bacteria	Concentration
kanSPYCE-AtWEE1	Tobacco BY-2	Kanamycin	50 µg/mL	Kanamycin	50 µg/mL
pGFP-AtWEE1-N	Tobacco BY-2 + Arabidopsis	Kanamycin	50 µg/mL		
pSPYNE-AtSKIP1	Arabidopsis	Hygromycin	20 µg/mL		

For antibiotic selection relevant to stable transformation of bimolecular fluorescence complementation refer to section 4.2.1.

TABLE 2.3 PRIMERS

TARGET	PRIMERS	SEQUENCE (5'-3')	Tm (°C)	FRAGMENT SIZE (bp)
pGFP-*Arath*; WEE1-N	GFPEND1F	AGCTCAAGGGCATCGATTT	55	~900
	P62R	CACCTCATCTGTGTC	46	
Arath; WEE1	AtWEE1F	AGCTTGTCAGCTTTGCCT	55	229
	AtWEE1R	CGTGCATCCCTCCTTCTTCTACT	55	
pSPYCE-*Arath*;WEE1	P81F	GCTAATCAAACAGAGAGGAC	55	1000
	HATAGR	AGCGTAATCTGGAACATCGTAT	55	
pSPYCE-*Arath*;WEE1	P38F	TGGTGATTATGCATCAGATAGC	53	500
	HATAGR	AGCGTAATCTGGAACATCGTAT	55	
pSPYNE-*Arath*;SKIP1	FBOXF	ATGGCGCGCCATGGAAGAAGACGGGTCTG	55	900
	CMYCR	AGATCCTCCTCAGAAATCAACT	55	
pSPYNE-*Arath*;GSTF9	GST9F	ATGGCGCGCCATGGTGCTAAAGGTGTAC	66	700
	CMYCR	AGATCCTCCTCAGAAATCAACT	55	
pSPYNE-BZIP63	BZIP63F	GAGTGAGCTAGAGACACAAGT	54	450
	CMYCR	AGATCCTCCTCAGAAATCAACT	55	
18s rRNA	PUV2	TTCCATGCTAATGTATTCAGAG	55	459
	PUV4	ATGGTGGTGACGGGTGAC	55	
Arath; SKIP1	FBOXF	ATGGCGCGCCATGGAAGAAGACGGGTCTG	55	900
	FBOXR	TCCCCCCGGGGATTCTCATGGCTTGTATGTC	67	
SKIP1-KO: WT	promF	ATTACCGAACACAAAGAACC	51	377
	exon1R	CTATCGGCTGCGTAAGA	51	
SKIP1-KO: Insertion	GABI LB	ATATTGACCATCATACTCATTGC	51	277
	exon1R	CTATCGGCTGCGTAAGA	51	
mRFP-*Arath*;SUN1	35S332	CCAGCTATCTGTCACTTCATC	53	~1000
	AtSUN1R2	TAGTCGCTGCCGCCGTATTA	58	

2.1 TOBACCO BY-2 CULTURE

2.1.1 WILD TYPE BY-2 CULTURE

Tobacco BY-2 culture medium was prepared as described (Table 2.1). The WT BY-2 cells were cultured under sterile conditions by adding 7 day old culture (3 mL) to BY-2 culture medium (95 mL) in a 300 ml conical flask, and sealed using two layers of foil. They were grown at 27°C in darkness at 130 rpm in a Gallenkamp Cooled Orbital Shaker. The cells were subcultured using the above method every 7 days to maintain the cell line.

2.1.2 BY-2 TRANSFORMATION

Stable transformation of BY-2 cells was achieved using a method modified from An (1985). *A.tumefaciens* LBA4404 containing the appropriate construct was plated from glycerol stocks (see section 2.2.3) onto LB agar plates in the presence of rifampicin (100 μg/mL) and grown at 30°C for 3 days. They were then subcultured onto a fresh LB-rifampicin (100 μg/mL)-kanamycin (50 μg/mL) agar plate and grown at 30°C for 2 days (these cell lines were maintained by subculturing onto fresh agar plates every 7 days). Overnight cultures of the appropriate *Agrobacterium* cultures were established, inoculating from the 2 day old colonies into LB medium (7 mL) and 2 mM magnesium sulphate in 50 mL conical flasks and cultured overnight at 30°C and 100 rpm in a Gallenkamp Cooled Orbital Shaker. Five mL of each culture was subsequently transferred to a 15 mL centrifuge tube, centrifuged at 2000 rpm in a MSE Centaur 2 centrifuge for 5 minutes, the supernatant removed and discarded, and the pellet resuspended in 5 mL BY-2 medium.

A three day old BY-2 culture was diluted to 50% using fresh BY-2 medium. Ten mL aliquots of this 50% BY-2 culture containing 100 μM of freshly added acetosyringone were co-cultivated with 1 mL of overnight *Agrobacterium* culture (transformed with the appropriate construct) in 50 mL conical flasks, sealed using aluminium foil and incubated at 27°C, 130 rpm in a Gallenkamp Cooled Orbital Shaker in darkness for 48 hours.

BY-2 cells were washed by transferring the cells into a 50 mL centrifuge tube and bringing to 50 mL with BY-2 medium followed by centrifugation for 5 minutes at 3000 rpm in a MSE Centaur 2 centrifuge, and the supernatant was removed. Fresh medium was added up to 50 mL, mixed and centrifuged as above, before the supernatant was removed and this step repeated once. The final pellet was resuspended in 10 mL of BY-2 medium containing either 500 μg/mL carbenicillin (for vectors under kanamycin selection) or 250 μg/mL timentin (for vectors under hygromycin selection). Aliquots of 2.5 mL were plated onto plates of BY-2 medium containing either carbenicillin or timentin as above, and appropriate antibiotic selection. Plates were sealed with autoclave tape, wrapped in foil and incubated at 27°C in the dark. Antibiotic resistant calli were isolated after 2-4 weeks.

Transformants appeared as yellow calli on a background of dead white cells. Each individual callus was considered as an independent clone and grown for a further two weeks on fresh plates until it reached an area of approximately 2 cm^2. Half of each callus was then transferred to a fresh plate of BY-2 medium containing appropriate selection, and a tiny piece of callus (approximately 0.05 cm^2) placed into 8 mL BY-2 medium containing appropriate selection in a sterile 25 mL conical flask and incubated at 27°C, 130 rpm in a Gallenkamp Cooled Orbital Shaker until the culture reached stationary phase (approximately 1.5-2 weeks). The culture was subcultured at seven or fourteen day intervals by transferring 250 µL of 7 or 14 day old culture to 8 mL BY-2 medium containing either carbenicillin or timentin as above, and appropriate antibiotic selection.

2.1.3 SYNCHRONISATION OF TOBACCO BY-2 CELL LINES

For synchronisation of cell division in tobacco BY-2 cells, 1 mL of the appropriate cell line was subcultured into 30 mL of BY-2 medium containing appropriate antibiotics in a 100 mL flask, and subcultured at 7- or 14-day intervals until the cultures were stable at this size. For the synchrony, 5 mL of cells were subcultured into 25 mL of medium with 30 µL of aphidicolin (5 mg/mL to a final concentration of 5 µg/mL) to block the G1/S-phase transition and to arrest any cell that was in S-phase during exposure to aphidicolin, and returned to 27°C, 130 rpm in a Gallenkamp Cooled Orbital Shaker for 24 hours. After 24 hours the cells were washed with culture medium to release them from G1 and S-phase arrest. The contents of the flask were transferred to a 50 mL centrifuge tube and centrifuged at 800 rpm for 30-60 s in an MSE Centaur 2 centrifuge. The supernatant was carefully removed and the cells resuspended in 50 mL BY-2 medium by gentle agitation, being careful not to damage the cells. The centrifugation and resuspension steps were repeated 5 times in a period of 15 minutes. After the final centrifugation, cells were resuspended in 30 mL BY-2 medium, returned to a sterile 100 mL flask and returned to 27°C, 130 rpm in a Gallenkamp Cooled Orbital Shaker. Cell samples were taken as described in section 2.1.4.

2.1.4 MEASUREMENTS OF CELL DENSITY, MITOTIC INDEX AND MITOTIC CELL SIZE

BY-2 cell density was measured using a Pye Unicam SP8-400 UV-Vis spectrophotometer at 600 nm. The mitotic index was calculated by adding dilute Hoechst stain (1 μL; Table 2.1) to 20 μL of cells on a microscope slide. These were mixed, a coverslip applied gently and the cells viewed under an Olympus BH-2 light microscope using a x20 objective, an ultraviolet light and a 420 nm barrier filter. Cells (300) were scored and images of each mitotic cell captured using a Fujifilm Fujix HC-300Z digital camera and the pictures obtained using Fujifilm Photograb 300Z 2.0 software. Duration of cell cycle phase was calculated according to Nachtwey and Cameron (1968; see Appendix I). Mitotic cell area was calculated using SigmaScan Pro 5 software.

2.1.5 MONITORING GFP/YFP FLUORESCENCE

To prepare slides, 20 μL of culture was taken using a sterile cut-off pipette tip, taking well dispersed cells which looked like normal subculture, and avoiding large masses. This was pipetted onto a slide and spread out a little, before a coverslip was applied. For counter-staining with Hoechst, a 1/100 dilution of stain (Table 2.1) was prepared in 2% Triton X-100 and applied to cells on a microscope slide as described in section 2.1.4. The cells were observed under an Olympus BX61 light microscope under a x20 objective, using ultraviolet light (at a wavelength of 510 nm) to find cells positive for GFP/YFP fluorescence. The cells were photographed using a SIS F-view B&W digital camera and the pictures obtained using AnalySIS imaging software. The photographs were coloured using IrfanView imaging software. Alternatively, the cells were observed as above but under a Zeiss Imager M1 AX10 microscope, photographed using a Zeiss Axiocam Mrc5 camera and images obtained using Zeiss Axiocam imaging software.

2.1.6 CLONING OF TRANSGENIC BY-2 LINES

A recently described protocol (Nocarova and Fischer, 2009) was used in an attempt to clone cells which were successfully stably transformed. Transgenic BY-2 culture was diluted with BY-2 medium in a ratio of 1:3, and separately wild type BY-2 culture was also diluted with BY-2 medium in a ratio of 1:3. The diluted cultures were mixed gently in a ratio of 1:1000 transgenic:WT. A sterile glass rod was used to spread 750 µL of the culture onto each of 4 plates of BY-2 medium containing appropriate selection. The plates were sealed using autoclave tape, wrapped in foil and incubated at 27°C for 2 weeks. The resulting calli were screened for homogenous expression of fluorescence using a Leica MZ 16F fluorescence dissecting microscope. Homogenous calli were cultured into liquid and maintained as described in section 2.1.2.

2.2 *AGROBACTERIUM* PREPARATION

2.2.1 *AGROBACTERIUM* COMPETENT CELLS

LBA4404 glycerol stock (5 µL) was inoculated into 10 mL LB medium with 100 µg/mL rifampicin and incubated at 30°C, 100 rpm, overnight in a Gallenkamp Cooled Orbital Shaker. This culture (3 mL) was used to inoculate 100 mL of LB medium (no selection) in a 300 mL conical flask and incubated at 30°C, 100 rpm in a Gallenkamp Cooled Orbital Shaker to an optical density of 0.6 at 600 nm. The culture was then divided into 25 mL aliquots and centrifuged at 3000 g at 4°C for 10 minutes. The pellets were resuspended together in 1mL of ice-cold 20 mM $CaCl_2$ and divided into 100 µL aliquots in pre-cooled Eppendorf tubes. These were frozen in liquid nitrogen and stored at −80°C.

2.2.2 *AGROBACTERIUM* TRANSFORMATION

DNA samples in a volume of up to 10 μl (0.2 μg/μL) were added to separate aliquots of competent *Agrobacterium* cells that had been thawed on ice, and mixed. The cells were then frozen in liquid nitrogen and thawed for 5 minutes at 37°C. LB medium (1 mL) was added and the *Agrobacterium* was incubated for 4 hours at 30°C at 100 rpm in a Gallenkamp Cooled Orbital Shaker. The cells were then centrifuged at 13000 rpm in an Eppendorf MiniSpin® microcentrifuge for 30 seconds, all supernatant removed, and resuspended in LB medium (100 μL). The cells were spread onto LB agar plates in the presence of the antibiotic rifampicin (200 μg/mL). The plates were then incubated at 30°C for 3 days and monitored for the appearance of *Agrobacterium* colonies.

2.2.3 GLYCEROL STOCKS

Liquid cultures were set up by inoculating colonies of each bacterial transformant into growth tubes containing LB (3 mL) and appropriate antibiotics. These were grown shaking overnight at 30°C for *Agrobacterium* and 37°C for *E. coli*. Glycerol stocks of the cultures were made by pipetting 1.5 mL of each cell culture into 1.5 mL Eppendorf tubes and centrifuging in an Eppendorf MiniSpin® microcentrifuge for 3 minutes at 8000 rpm. The resulting bacterial pellets were each resuspended in 4:1 LB medium: sterile glycerol (500 μL), mixed thoroughly and stored at -80°C.

2.3 *ARABIDOPSIS* LINES

2.3.1 TRANSFORMATION OF *ARABIDOPSIS*

Arabidopsis plants were transformed using the floral dip method (Clough and Bent, 1998). *Agrobacteria* EHA105 containing the appropriate construct were streaked out onto an LB agar plate containing 100 μg/mL rifampicin and 50 μg/mL kanamycin and grown for 2 days at 30°C. A single colony was picked and inoculated into 10 mL of LB medium containing 100 μg/mL rifampicin and 50 μg/mL kanamycin and grown overnight at 30°C, 100 rpm in a Gallenkamp Cooled Orbital Shaker. This

starter culture was added to 500 mL LB medium containing 100 μg/mL rifampicin and 50 μg/mL kanamycin and grown at 30°C, 100 rpm in a Gallenkamp Cooled Orbital Shaker, for 16-18 hours. The culture was centrifuged at 5500g for 20 minutes at room temperature and the supernatant removed and discarded. Bacteria were gently resuspended in a solution of 5% sucrose and 0.05% Silwett L-77® (GE Silicones, USA) and transferred to a bowl. Flowering *Arabidopsis* plants grown in domed pots were dipped into the bacterial suspension for approximately 10 seconds with agitation. The plants were covered with black plastic overnight to retain humidity and then grown under 18 hours light and 6 hours dark for 3-4 weeks. Once siliques had developed the plants were allowed to dry out and harvested when the siliques had turned yellow, but before they began to shatter.

2.3.2 SELECTION OF *ARABIDOPSIS* PRIMARY TRANSGENIC LINES

Arabidopsis plants were transformed using the floral dip method (Clough and Bent, 1998; as described in section 2.3.1) and seed collected and stored. Transgenic lines were then selected from the background of untransformed seed as follows. Seed (100 mg) was weighed and placed in a 50 mL Falcon tube. In sterile conditions in a laminar flow cabinet the seeds were first treated with 70% ethanol solution (30 mL) for 10 minutes, shaking to mix. The ethanol solution was carefully removed by pipetting and the seeds treated with sterilising solution (30 mL of 20% sodium hypochlorite, 0.05% Tween-20) for 10 minutes, shaking to mix. The sterilising solution was carefully removed by pipetting and the seeds washed with sterile distilled water (30 mL) four times for 5 minutes, shaking to mix. The seeds were divided between fifteen separate pre-warmed Falcon tubes, 2 mL to each tube. Once the seeds had settled the water was removed. A sterile solution of 0.8% Difco agar, granulated (5 mL; at 45°C; BD, Oxford, UK) was added to each tube and immediately poured onto plates of MS medium (Table 2.1) containing appropriate antibiotic selection (see Table 2.2). Plates were then sealed using micropore tape and the seeds were stratified at 4°C for 48 hours to ensure uniform germination before being moved to a growth chamber at 21°C. Seedlings were grown under 18 hours light and 6 hours dark for two to three weeks. The majority of untransformed

seedlings yellowed and died, whereas transformed seedlings remained green (Figure 2.1). These were carefully removed from the agar with forceps and transplanted into compost which was kept damp while the seedlings adapted from the agar to the soil. After the plants had flowered and siliques had developed, the plants were allowed to dry out before seeds were harvested. Siliques were stored in envelopes for 2 weeks and allowed to dry out completely before seeds were collected and stored in Eppendorf tubes.

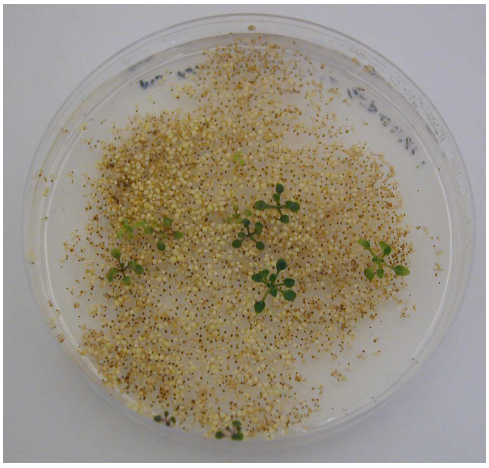

Figure 2.1 An example of selected transgenic seedlings on a background of dead, yellow, non-transgenic seedlings

2.3.3 STERILISATION AND SOWING OF *ARABIDOPSIS* SEEDS

Seeds were transferred to a clean Eppendorf tube. In sterile conditions, in a laminar flow cabinet, dilute bleach solution (10% sodium hypochlorite; 1 mL) was pipetted onto the seeds and mixed thoroughly before being left to stand for 2-5 minutes. The bleach solution was carefully removed by pipetting leaving approximately 50-100 µL. Ethanol mix (70% ethanol, 10% sodium hypochlorite; 1 mL) was added and mixed thoroughly before being left to stand for 2-5 minutes. The ethanol mix was carefully removed by pipetting leaving approximately 50-100 µL. Sterile distilled water (1 mL) was added and mixed thoroughly, and left to stand until the seeds had settled to the bottom of the tube. The water was then carefully removed by pipetting leaving approximately 50-100 µL, and sterile distilled water (1 mL) added as before. The water was left in the tube and, using a sterile pipette, seeds were transferred to an MS agar plate (Table 2.1) containing appropriate selection if required (see Table 2.2). Single seeds were sown approximately 1 cm apart, with 5-50 seeds to each

plate. Plates were sealed with cling film and cold treated at 4°C for 24 hours before being moved to a growth incubator at 21°C and grown under 18 hours light and 6 hours dark, with the plates in a horizontal or vertical position as appropriate.

2.3.4 CROSSING *ARABIDOPSIS* LINES

Arabidopsis seeds were surface sterilised as described in section 2.3.3 and sown in 9 cm diameter pots, which were then germinated and grown at 21°C and under 18 hours light and 6 hours dark for approximately 6 weeks. A branch was selected on the female parent plant which was strong with well-filled siliques, and the mature flowers and siliques were removed. Under a dissecting microscope, a mature unopened bud was selected in which the anthers had not yet dehisced and fine forceps used to carefully open the petals and remove all anthers, leaving the mature stigma and petals intact. If there was any sign of pollen the flower was discarded and a fresh unopened bud selected. The plants were then returned to 21°C for 48 hours and then the stigmas checked to ensure they were still healthy and unpollinated. A branch was selected on the male parent plant with healthy, well-filled siliques. A flower which had recently fully opened was selected and removed from the plant. The flower was grasped with fine forceps to allow the flower to splay out displaying the anthers, which were then examined under the dissecting microscope. Good anthers had sticky, yellow pollen – young smooth anthers and old anthers with dry, orange pollen were discarded and a new flower selected. The anthers of the male flower were touched to the end of the previously prepared stigma of the female flower, attaching as much pollen as possible to the hairs of the stigma. The pollinated stigma was labelled appropriately. After 1-2 weeks, once the silique had filled and yellowed it was removed and allowed to dry fully before the seeds were collected. The seeds were sown as described in section 2.3.3 and DNA extracted and tested for each construct by PCR as described in sections 2.4.1 and 2.4.2.

2.3.5 PHENOTYPING OF TRANSGENIC *ARABIDOPSIS* LINES

For phenotyping of transgenic lines of *Arabidopsis*, seeds were sown as described in section 2.3.3. Five seeds were sown on each plate in a vertical line approximately 1 cm apart at one end of the petri dish. Plates were allowed to dry and sealed using micropore tape after sowing and the seeds cold-treated at 4°C for 3 days prior to incubation. Plates were incubated in a vertical position to ensure the growth of the roots along instead of through the agar. After germination, primary root length was measured daily. For measurement of number of lateral roots and primordia, seedlings were fixed by the application of 3:1 absolute ethanol: glacial acetic acid. This was pipetted over the seedlings in the plates and the plates stored at 4°C prior to analysis. Fixed seedlings were mounted on a microscope slide in water and viewed under an Olympus BH-2 microscope at 10x magnification. The number of lateral roots and lateral root primordia were counted and recorded.

2.3.6 MONITORING GFP/RFP FLUORESCENCE

To prepare slides, a drop of water was applied to a microscope slide, the seedling was carefully removed from the agar using forceps and applied to the water, and an extra drop of water applied to the root until covered. The roots were observed under an Olympus BX61 light microscope under a x20 objective, using ultraviolet light (at a wavelength of 510 nm) to find cells positive for GFP/RFP fluorescence.

2.3.7 PROPIDIUM IODIDE STAINING AND CONFOCAL IMAGING OF *ARABIDOPSIS* SEEDLINGS

GFP-*Arath*;WEE1 localisation was observed using a Leica TCS SP2 AOBS spectral confocal microscope. Seeds from the appropriate line were sown (as described in section 2.3.3) and grown vertically for 5 days (as described in section 2.3.5). Cell walls were counter-stained using propidium iodide as follows. Propidium iodide stock solution and dilutions were prepared using tapwater. A 20 µL drop of 25-35 µg/mL propidium iodide solution was applied to a microscope slide. The seedling was carefully removed from the agar using forceps, the aerial parts removed, and the

roots immediately placed into the drop of propidium iodide solution. Another 20 μL drop of propidium iodide solution was added and a coverslip carefully applied, not squashing the seedling. The seedlings were viewed using the confocal microscope. GFP fluorescence was excited using a 488nm argon ion laser line and detected between 500 and 550 nm. Propidium iodide fluorescence was excited using a 543 nm helium neon ion laser line and detected between 600 and 650 nm. Images were captured using Leica confocal software and exported to TIF format. Fluorescence was quantified using Image J software.

2.4 DNA

2.4.1 DNA EXTRACTION FROM CALLUS/LEAF DISCS

DNA extraction was achieved using the method from Edwards et al., 1991. Material was ground in liquid nitrogen in a pre-cooled sterile pestle and mortar (callus) or in an Eppendorf tube using a sterile Eppendorf grinder (leaf discs). Sterile extraction buffer (200 μL; Table 2.1) was added to the homogenate in the pestle and mortar or Eppendorf tube, allowed to thaw and transferred to a 1.5 mL Eppendorf tube. The sample was centrifuged in an Eppendorf MiniSpin® microcentrifuge at 13000 rpm for 5 minutes. 150 μL of the supernatant was added to an equal volume of isopropanol in a fresh sterile Eppendorf tube, mixed well and incubated on ice for 5 minutes. The sample was then centrifuged in an Eppendorf MiniSpin® microcentrifuge at 13000 rpm for 10 minutes before carefully removing and discarding the supernatant, being sure not to disturb the pellet. The pellet was air-dried at 60°C for 5-10 minutes to aid solution in TE (100 μL; Table 2.1). The DNA was checked by using 1 μL in a PCR reaction.

2.4.2 PCR

For each sample, 1 μL of DNA template was added to a PCR mix of 5x Green GoTaq Flexi buffer (5 μL; Promega, Southampton, UK), 25 mM magnesium chloride (1.5 μL), 0.5 μL of each appropriate primer (10 μM; see Table 2.3), 10 mM

dNTPs (0.5 μL; Promega, Southampton, UK) and finally GoTaq DNA polymerase (0.125 μL; Promega, Southampton,UK). Sterile distilled water was added to bring the sample to 25 μL. Sterile distilled water (1 μL) was used in the place of DNA template as a negative control. The samples were amplified using the following PCR cycle: 2 minutes at 95°C; 40 cycles of 1 minute at 95°C, 1 minute at Tm°C and 1 minute at 72°C; 7 minutes at 72°C, using either a PTC-100 (MJ Research, Inc, Quebec, Canada) or GeneAmp PCR system 2700 (Applied Biosystems, Warrington, UK) PCR machine. The PCR products were separated on a 1% agarose gel, adding 3 μL of Bromophenol blue to each sample (BPB; see table 2.1), prepared as described in section 2.4.3.

2.4.3 AGAROSE GEL ELECTROPHORESIS OF DNA

The DNA was checked using a 1% agarose gel, prepared by adding multi-purpose agarose (5 g; Bioline, London, UK) to 1x Tris-acetate-EDTA (TAE) buffer (Table 2.1). This was then heated to dissolve the agarose and cooled to approximately 60°C, before adding ethidium bromide (1 μg/mL). This was swirled to mix, poured into a tray and a comb inserted to form wells. The gel was then left to set for 30 minutes, at which point the surface of the gel was flooded with 1x TAE buffer and the comb removed. Each DNA sample was pipetted into a separate well, and the gel was electrophoresed at 50-100v for approximately 1 hour. The gel was photographed using Syngene GeneSnap software.

2.5 RNA

2.5.1 RNA EXTRACTION

For the extraction of RNA approximately 200 mg of material was sampled and frozen in liquid nitrogen, which was then not allowed to thaw. Sterile equipment was used for RNA extraction as it is susceptible to contamination by RNases. Samples were placed into a pestle and mortar with liquid nitrogen and ground to a fine dust. In a fume hood, 1 mL Tri reagent was added and grinding resumed to

form a homogenous paste. Equal amounts of paste were transferred to two sterile 1.5 mL Eppendorf tubes, vortexed and allowed to stand at room temperature for 5 minutes. The samples were then centrifuged at 12000 rpm for 10 minutes at 4°C in a cooled Beckman Coulter Allegre™ 21R, rotor F2402H centrifuge and the clear supernatants transferred to fresh 1.5 mL Eppendorf tubes. Chloroform (200 µL) was added to each tube, vortexed for 15 seconds and left to stand at room temperature for 5 minutes. The samples were then centrifuged at 12000 rpm for 15 minutes at 4°C in a cooled Beckman Coulter Allegre™ 21R, rotor F2402H centrifuge and the aqueous top layers transferred to fresh 1.5 mL Eppendorf tubes. Isopropanol (500 µL) was added to each tube, mixed and left to stand at room temperature for 10 minutes. The samples were then centrifuged at 12000 rpm for 10 minutes at 4°C in a cooled Beckman Coulter Allegre™ 21R, rotor F2402H centrifuge and the supernatants removed and discarded, without disturbing the pellets. Ethanol (75%, 1 mL) was added to each tube and vortexed for 15 seconds. The samples were then centrifuged at 12000 rpm for 10 minutes at 4°C in a cooled Beckman Coulter Allegre™ 21R, rotor F2402H centrifuge, and the supernatants removed and discarded. The pellets were then allowed to dry in air for 10-30 minutes in a laminar air flow cabinet before being dissolved together in a total of 50 µL of sterile water. The quality of RNA was assessed by agarose gel electrophoresis (see section 2.4.3) after soaking the tank, tray and comb of the electrophoresis equipment in 0.1 M NaOH for 10 minutes and rinsing them in distilled water prior to use to eliminate possible contamination by RNases. The concentration of RNA was analysed using a ThermoScientific NanoDrop 1000 UV-Vis Spectrophotometer. RNA was stored at -80°C. RNA was used for cDNA synthesis and subsequently semi-quantitative RT-PCR (as described below in sections 2.5.2 and 2.5.3).

2.5.2 REVERSE TRANSCRIPTASE PCR

2.5.2.1 cDNA SYNTHESIS

Extracts of RNA were used to produce cDNA. The RNA extracts were first treated with DNase to remove residual DNA. DNA-free DNase1 10x buffer (2µL) and rDNase1 (1 µL; Ambion/Applied Biosystems, Warrington, UK) were added to RNA

(2 μg), made up to 20 μL with sterile distilled water, mixed and incubated at 37°C for 30 minutes. DNase Inactivation Reagent (Ambion/Applied Biosystems, Warrington, UK) was resuspended by flicking/vortexing and 2 μL was added to the RNA samples to terminate the reaction. The samples were then incubated at room temperature for 2 minutes, mixing occasionally to redisperse the DNase Inactivation Reagent. The samples were centrifuged at 10000g for 90 s and the RNA carefully transferred to fresh tubes. Oligo(dT) 15 primer (1 μL; 500 μg/mL; Promega, Southampton, UK) was added to DNase-treated RNA extract (19 μL) and incubated at 70°C for 10 minutes before being cooled at 0°C for 10 minutes. 5x M-MLV RNase H^- reaction buffer (6 μL; Promega, Southampton, UK), 0.1M DTT (2 μL) and 10 mM dNTPs (1 μL; Promega, Southampton, UK) were added and incubated at 42°C for 2 minutes. M-MLV RNase H^- Reverse Transcriptase (1 μL; Promega, Southampton, UK) was added and incubated at 42°C for 50 minutes then at 70°C for 15 minutes, producing single stranded DNA. To check that cDNA synthesis was successful, 1 μL was used in a PCR reaction (as previously described) using primers directed against 18S rRNA (see Table 2.3). DNase-treated RNA (1 μL) was also included as a negative control to ensure that all genomic DNA was indeed removed.

2.5.2.2 SEMI-QUANTITATIVE RT-PCR

Primers against 18S rRNA were also used to compare the amount of cDNA in the samples, as it was unrelated to the gene of interest. It was assumed that rRNA expression was constant so the expression of other genes was compared to the expression of rRNA. This methodology has been published (Price et al., 2008) and has provided reliable and acceptable results for a range of experimental systems in the Cardiff lab. For semi-quantitative RT-PCR, cycle number must be limited to ensure that PCR products are analysed after a number of cycles that ensures linear amplification across a range of concentrations. Cycle numbers were tested using dilutions of a mix of cDNA. A mix of cDNA was made using an equal volume from each cDNA sample. 50% and 25% dilutions were made from this mix. PCR was run at a low cycle number using 1 μL of each mix/dilution and the products quantified using Syngene Gene Tools software. Product amount was plotted against dilution and if a straight line formed it was assumed that the cycle number was optimised for detecting differences in the amount of cDNA template. cDNA samples were

normalised by setting up a PCR reaction using 1 μL of each sample with 18S rRNA primers. Each dilution was also run alongside to ensure linear amplification, limiting the cycle number to that previously calculated. PCR products were quantified as previously described and, if dilutions were linear, a ratio of the samples was taken. This was repeated three times to enable calculation of the mean and standard error of the three ratios. This was then repeated using PCR primers for the gene of interest. A mix of cDNA samples was used to calculate the optimum cycle number for these primers, and the PCR run on the separate cDNA samples. This was repeated in triplicate to enable calculation of the mean and standard error of expression levels. To calculate the differences in expression levels of the target gene between samples the results were multiplied by the ratio obtained using the 18S rRNA PCR in order to normalise for differences in cDNA amount.

2.6 PROTEIN

2.6.1 PROTEIN EXTRACTION

10 day old *Arabidopsis* seedlings were frozen in liquid nitrogen and stored at -80°C prior to protein extraction. Plant material (1 g) was ground to a fine powder with liquid nitrogen in a pre-cooled sterile pestle and mortar, transferred to a 50 mL centrifuge tube and lysis buffer + (1mL; Table 2.1) added to the tube, mixed and kept on ice. The sample was homogenised by sonication (Soniprep MSE thin tip, 10 micrometre amplitude) for 40 seconds x4 with 1 minute on ice between each sonication. The sample was transferred to a 1.5 mL Eppendorf tube and centrifuged in pre-cooled Beckman Coulter Allegre™ 21R, rotor F2402H, at 14000 rpm for 30 minutes at 4°C. The supernatant was transferred to a fresh tube, frozen in liquid nitrogen, and stored at -80°C.

2.6.2 BRADFORD ASSAY

The Bradford Assay was used to determine protein concentrations. BSA standards of 0, 0.125, 0.25, 0.5, 1 and 2 mg/mL were prepared from a stock solution of 2 mg/mL

BSA diluted in lysis buffer +. Each BSA standard and each protein sample were loaded into separate wells of a microtitre plate in duplicate (5 μL). Bradford reagent (250 μL) was added to each well and mixed gently, followed by incubation at room temperature for 5-45 minutes. Absorbance at 570 nm was measured using a Dynex Technologies MRX-TC Revelation Microtiter plate reader and protein concentrations determined using a standard curve obtained from the BSA protein measurements.

2.6.3 SDS-PAGE

To prepare a SDS PAGE gel (Sodium Dodecyl Sulphate Polyacrylamide Gel Electrophoresis) a 12% SDS stacking gel was overlaid onto a 12% SDS separation gel using a BIO-RAD Mini Protean electrophoresis system. Glass plates were cleaned thoroughly with 70% ethanol and allowed to dry before use. To make the 12% separation gel, 40% acrylamide/bis-acrylamide 37:5:1 (3.3 mL; Melford Laboratories Ltd, UK), 2.5x separation buffer (4.4 mL; Table 2.1), distilled water (3.3 mL), 10% ammonium persulfate (APS; 100 μL) and N,N,N',N'-tetramethyl-ethylenediamine (TEMED; 10 μL) were mixed and 3-4 mL pipetted between two glass plates. Distilled water was added to the top of the acrylamide to prevent drying of the gel, and the gel allowed to set for 10-15 minutes. The 12% SDS stacking gel was made by mixing 40% acrylamide (37:5:1; 0.65 mL), stacking buffer (0.66 mL; Table 2.1), 10% APS (30 μL), distilled water (2 mL) and TEMED (5 μL). The water was removed and the stacking gel pipetted between the plates over the separation gel, combs were added and the gel was left to set for approximately 30 minutes. The concentration of acrylamide could be altered to produce a 15% gel.

Protein samples (20 μg in a volume of 10-15 μL) were mixed with 5x loading buffer (3 μL; Table 2.1) and boiled at 100°C for 5 minutes, or 50°C for 10 minutes. Samples were then returned to ice before being centrifuged in an Eppendorf MiniSpin® microcentrifuge at 13000 rpm for 15 seconds. Samples were again returned to ice before being loaded onto the gel and run in SDS running buffer (1x; Table 2.1) at 100V for 20-30 minutes, then 120V for 2-3 hours; or 50V for 1 hour,

then 100V for 2-3 hours. PageRuler™ pre-stained protein marker (10 μL; Fermentas) was used as a marker for protein size.

2.6.4 COOMASSIE STAINING

Proteins were detected by staining the completed SDS-PAGE gel (described in section 2.6.3) with Coomassie Brilliant blue stain (Table 2.1) for 45 minutes. The gel was then de-stained with de-staining solution (Table 2.1) for one hour or until sharp blue bands were visible.

2.6.5 WESTERN BLOTTING

Samples were run out on an SDS gel as previously described (see section 2.6.3). Hybond-P PVDF membrane was pre-wetted in 100% methanol for 30 seconds then rinsed in distilled water for 5 minutes. Six filter papers, two sponges, the SDS gel and the pre-wetted PVDF membrane were soaked in blotting buffer (Table 2.1) for 15 minutes. On the black side of a Mini-Trans Blot© Western Blotting System Cassette (Bio-Rad) the sponge, three filter papers, SDS gel, PVDF membrane, the other three filter papers and the other sponge were layered and sandwiched together in the cassette. The cassette was then placed in a gel tank filled with stirred blotting buffer and an ice cassette, packed with ice and blotted at 100V for one hour.

After blotting, the PVDF membrane was transferred, gel side down, to 1 mL/cm^2 of blocking solution (Table 2.1) and incubated on a shaking platform overnight at 4°C. Blocking solution was discarded and NtWEE1 (3rd bleed) primary antibody (25 μL; fully described by Lentz Grønlund et al., 2009), diluted in fresh blocking solution, was added. The membrane was incubated shaking for 1-2 hours at room temperature. The membrane was then rinsed in basic buffer (Table 2.1) for 20 minutes, followed by fresh basic buffer for 5 minutes x2. Basic buffer was discarded and an anti-rabbit IgG secondary antibody (0.5-5 μL) added, diluted in fresh blocking solution, and the membrane incubated shaking for up to 1 hour at room temperature, before rinsing the membrane as previously described. The membrane was gently blotted in filter paper,

placed on 0.125 mL/cm^2 ECL solution (1:40 reagent A:reagent B; Amersham™ ECL plus Western Blotting Detection System) on a transparent plastic bag, gel side down, and incubated for 5 minutes. ECL reagents were removed by gently blotting with filter paper, the membrane enclosed in the plastic bag and placed in an X-ray cassette, gel side up. Hyperfilm™ ECL (Amersham Biosciences) was placed on top of the membrane and exposed for between 12 seconds and 15 minutes before the film was developed using a Curix 60 developer (Agfa).

2.7 STATISTICAL ANALYSES

Statistical analysis was used to determine the significance of differences in results in the case of quantitative measurements such as *Arabidopsis* phenotyping, measurements of mitotic cell size, and semi-quantitative RT-PCR. Where the means of only two samples were compared a two-sample T-test was used. For the comparison of more than two samples a one-way ANOVA was used to determine overall levels of significance. This was followed by post-hoc testing using the Fisher's LSD test to determine specifically which samples differed significantly from wild type or another sample of interest. Alternatively, the non-parametric Mann-Whitney test was used to compare data sets which deviated significantly from normal distribution. Regression analysis was used to calculate rates of primary root growth. Analysis of covariance was used for the comparison of different rates of primary root growth. The contingency chi-squared test was used to determine significance of associations between samples where frequencies or proportions were used. Significance was thought to be determined if $P \leq 0.05$ in all statistical tests used.

3. THE SUBCELLULAR LOCALISATION OF *ARATH*;WEE1 IS NUCLEAR AT INTERPHASE BUT ALTERS AT MITOSIS

3.1 INTRODUCTION

The localisation and stability of cell cycle proteins is important in the temporal regulation of the cell cycle, physically separating interacting proteins and other components. In mammalian cells Cdc2 is localised to the nucleus and cytoplasm, and localises to the centrosomes at the onset of mitosis (Bailly et al., 1989; Riabowol et al., 1989). The cyclin partner of Cdc2, cyclin B, accumulates in the cytoplasm of interphase cells, localising to the nucleus shortly before the breakdown of the nuclear envelope. Cyclin B then associates with the condensed chromosomes at prophase and metaphase, before being degraded at the transition from metaphase to anaphase (Pines and Hunter, 1991). The physical separation of Cdc2 and cyclin B is likely to be a very important mechanism for controlling the correct timing of cell cycle progression, and it is likely that other cell cycle proteins are also spatially regulated in a cell cycle dependent manner. The physical separation of CDC25 from the Cdc2-cyclinB complex in mammalian cells also appears to be important. Conversely to cyclin B, CDC25 is localised to the nucleus during interphase and early prophase, relocalising to be distributed throughout the cytoplasm just before nuclear envelope breakdown. CDC25 remains distinct from the condensed chromosomes during metaphase and anaphase, reappearing in the nucleus during telophase, after cyclin B has been degraded (Girard et al., 1992).

A recent study has demonstrated the subcellular localisation of many key cell cycle regulators in plants (Boruc et al., 2010a). Proteins of interest were fused to GFP at the C-terminal and stably expressed in tobacco BY-2 cells under the strong constitutive 35S promoter. It was found that, as in mammalian cells, the main cell cycle CDKs localise to both the nucleus and cytoplasm during interphase, altering to localise exclusively to the nucleus or the region vacated by the nuclear membrane at mitosis. The localisation of plant cyclins is variable, for example cyclin A1;1 localises to both the nucleus and cytoplasm during interphase, while the cyclin B1

subfamily localises to the cytoplasm. Also, at interphase, cyclins were unstable, or expressed at low levels. In mitosis, B1-type cyclins were found to associate with the chromosomes until the transition from metaphase to anaphase, a similar mechanism to that seen in mammalian cells (Boruc et al., 2010a). Other studies have also made use of BY-2 cells for expressing fusions of GFP with cell cycle proteins such as CYCB2;2 and CDKB2;1 (Lee et al., 2003), CDKA;1 (Harashima et al., 2007) and CYCB1 (Criqui et al., 2000), demonstrating the suitability of this system for this application.

From a whole tissue perspective it has been demonstrated by RT-PCR that, in *Arabidopsis*, *WEE1* is predominantly expressed in proliferative tissues, including seedlings, flowers and weakly in the stem, but not in the leaves (Sorrell et al., 2002). WEE1-promoter-GUS analysis has shown that at the transcriptional level expression is highest in the shoot apical meristem, vascular tissue and young flowers, but surprisingly not in the root apical meristem or lateral root primordia (De Schutter et al., 2007). More recently a systematic analysis of cell cycle gene expression during *Arabidopsis* development has shown that *WEE1* is strongly expressed in dark-grown seedlings and the xylem of light-grown seedlings, and in the vascular tissues of young and mature roots. Tighter regulation of expression is indicated by patchy expression patterns in parts of the young and mature leaves, shoot apical meristem and young roots (Engler et al., 2009).

At a protein level, in mammalian cells WEE1 is located in the nucleus during interphase, transferring into the cytoplasm at mitosis, specifically to the microtubules (Baldin and Ducommun, 1995). Boruc et al. (2010a) showed that WEE1 also localises to the nucleus during interphase in higher plants, but they did not show the localisation of WEE1 during mitosis. It has also been demonstrated that during interphase *Arath*;WEE1 is able to interact with GF14ω, a 14-3-3 protein which may protect WEE1 from inhibitory phosphorylation as in animal cells; a complex which localises to the nucleus during interphase, and possibly also to the newly formed cell plate at cytokinesis (Lentz Grønlund et al., 2009). *Arath*;WEE1 is also able to interact with several other proteins, all of which localise to the nucleus during interphase (G. Cook, unpublished data; see Chapter 4 and Appendix IV). These results suggest that we should expect WEE1 to be detected in the nucleus at

interphase, possibly altering location to the cytoplasm or cell wall at mitosis. If the subcellular localisation of WEE1 in *Arabidopsis* is cell cycle dependent, this could indicate a role for WEE1 in a normal cell cycle.

The stability of cell cycle regulators is also important in the control of these processes. The best-studied example of this is the sudden degradation of B-type cyclins by the APC at mitosis (Pines, 1995). The degradation of WEE1 protein is required for the onset of mitosis in many organisms, including budding yeast (Kaiser et al., 1998) and *Xenopus* (Michael and Newport, 1998). In tobacco BY-2 cells, WEE1 protein levels peak in S-phase, dropping as the proportion of mitotic cells increases (Lentz Grønlund, 2007), indicating that WEE1 proteolysis may also be necessary for the onset of mitosis in higher plants.

3.1.1 EXPERIMENTAL AIMS

In order to ascertain the dynamics of WEE1 protein in higher plants, the subcellular and tissue-specific localisation and stability of *Arath*;WEE1 during the cell cycle were studied in detail. The following questions were addressed, using a GFP-*Arath*;WEE1 construct as a tool:

1. Is *Arath*;WEE1 degraded during the cell cycle in tobacco BY-2 cells?
2. Is *Arath*;WEE1 degraded during the cell cycle in *Arabidopsis* roots?
3. Does the GFP-*Arath*;WEE1 construct affect root phenotype?
4. What is the subcellular localisation and stability of *Arath*;WEE1 in *Arabidopsis* root tissues?
5. Is *Arath*;WEE1 degraded via the ubiquitin/26S proteasome pathway?

3.2 MATERIALS AND METHODS

3.2.1 CELL SIZE MEASUREMENTS IN *ARABIDOPSIS* ROOTS

Seeds were surface sterilised as described in section 2.3.3. Five seeds were sown on each plate in a vertical line approximately 1 cm apart at one end of the Petri dish. Plates were allowed to dry and sealed using micropore tape, and the seeds cold-treated at 4°C for 3 days prior to incubation. Plates were incubated in a vertical position to ensure the growth of the roots along instead of through the agar. After 7 days growth, forceps were used to carefully remove the seedlings from the surface of the agar. Seedlings were fixed in 8:3:1 chloral hydrate: water: glycerol in 1.5 mL Eppendorf tubes, before being transferred to microscope slides. Slides were prepared by mounting a seedling in a drop of 8:3:1 chloral hydrate fixative on a microscope slide and applying a second drop to ensure the seedling was covered. A coverslip was applied, sealed with transparent nail varnish and left to dry. Slides were stored at room temperature. Roots were observed by DIC under a 40x oil immersion objective using a Zeiss Imager M1 AX10 microscope, photographed using a Zeiss Axiocam Mrc5 camera and the images obtained using Zeiss Axiocam imaging software. Image J software was used for cell size measurements. Cell length and width, and cell number were calculated for each tissue in the meristem (epidermis, cortex and cell lineages destined to become the stele), up to the transition zone.

3.2.2 HOECHST STAINING AND MITOTIC INDEX IN *ARABIDOPSIS* ROOT MERISTEMS

For the Hoechst staining of nuclei in live *Arabidopsis* roots, seeds were surface sterilised as described in section 2.3.3. Five seeds were sown on each plate in a vertical line approximately 1 cm apart at one end of the Petri dish. Plates were allowed to dry and sealed using micropore tape, and the seeds cold-treated at 4°C for 3 days prior to incubation. Plates were incubated in a vertical position to ensure the growth of the roots along instead of through the agar. After 7 days growth, seedlings were carefully removed from the surface of the agar using forceps and placed into 1.5 mL Eppendorf tubes containing a 1/20 dilution of Hoechst stain (Table 2.1),

prepared in 2% Triton X-100, for 30 minutes. Stained seedlings were transferred to a microscope slide and the root meristems separated from the rest of the root using a sharp blade. The meristems were mounted in the Hoechst dilution, a coverslip applied and gently squashed to separate the cells. Cells were scored for mitosis under an Olympus BH-2 light microscope using a x20 objective, an ultraviolet light and a 420 nm barrier filter.

3.2.3 MG132 TREATMENT OF *ARABIDOPSIS* SEEDLINGS

MG132 (an inhibitor of the 26S proteasome) was dissolved in DMSO to create a stock solution (25 mg/mL) and stored at -80°C. Seed was sterilized and sown as described in Section 2.3.3, and plates were incubated in a vertical position to encourage growth over, rather than through, the agar. For confocal imaging, MG132 stock solution (or for the mock-treatment, an equal volume of DMSO) was mixed with liquid MS medium (20 mL; Table 2.1) in a Petri dish (ø 9 cm) to a final concentration of 50 μM. Five day old seedlings were carefully removed from the surface of the agar using forceps and added to either the MG132 or the DMSO solution in the Petri dish, and incubated with light at 21°C for 6 hours, with occasional gentle agitation. After treatment, the seedlings were carefully transferred to fresh liquid MS medium (10 mL; Table 2.1) in a clean Petri dish and used for confocal imaging (see Section 2.3.7).

For protein extraction, MG132 stock solution (or for the mock-treatment, an equal volume of DMSO) was mixed with liquid MS medium (10 mL; Table 2.1) in a 50 mL tube to a final concentration of 50 μM. Ten day old seedlings were carefully removed from the surface of the agar using forceps and added to either the MG132 or the DMSO solution in the tube, and incubated with light at 21°C for 6 hours, with occasional gentle agitation. After treatment, the seedlings were carefully drained of as much liquid as possible using a sieve, blotted on filter paper and frozen in liquid nitrogen prior to storage at -80°C. Protein extractions were performed as described in Section 2.6.

3.3 RESULTS

3.3.1 *ARATH*;WEE1 IS DEGRADED DURING MITOSIS IN TOBACCO BY-2 CELLS

Prior to this work a GFP-*Arath*;WEE1 construct under the 35S promoter was produced via the Gateway cloning system (Invitrogen; N. Spadafora, Cardiff Lab. Unpublished results). To investigate the cell cycle dynamics of WEE1 subcellular localisation the GFP-*Arath*;WEE1 construct was transformed into tobacco BY-2 cells via *Agrobacterium* mediated transformation and a liquid culture obtained from one line (Section 2.1.2). Presence of the transgene was checked by PCR (Section 2.5; Table 2.3). This line was shown to be positive for the GFP-*Arath*;WEE1 fusion and *Arath;*WEE1 (Figure 3.1). The second, larger fragment amplified from the GFP-*Arath*;WEE1 *Arabidopsis* leaf (positive control) using primers specific for *Arath*;WEE1 was representative of endogenous *Arath*;WEE1, complete with introns (Figure 3.1).

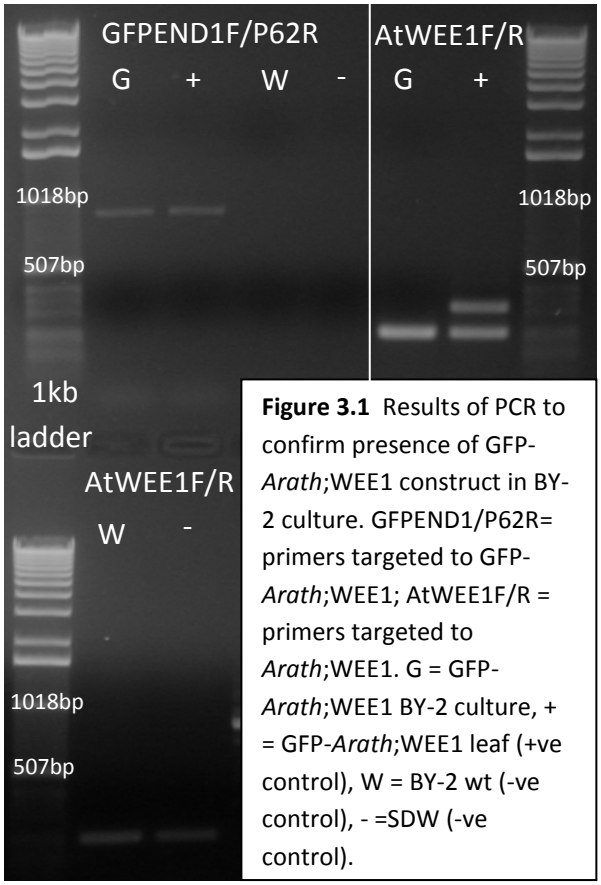

Figure 3.1 Results of PCR to confirm presence of GFP-*Arath*;WEE1 construct in BY-2 culture. GFPEND1/P62R= primers targeted to GFP-*Arath*;WEE1; AtWEE1F/R = primers targeted to *Arath*;WEE1. G = GFP-*Arath*;WEE1 BY-2 culture, + = GFP-*Arath*;WEE1 leaf (+ve control), W = BY-2 wt (-ve control), - =SDW (-ve control).

The GFP-*Arath*;WEE1 BY-2 culture was monitored for growth, mitotic index and mitotic cell size every day over the course of 2 weeks (Section 2.1.4), in order to compare the characteristics of the culture with those of wild type. The GFP-*Arath*;WEE1 culture reached stationary phase after 14 days, as opposed to 7 days for wild type culture (Figure 3.2a). During this time there were two peaks in mitotic index, the first at approximately 10% on day 3 and the second at 6% on days 8 and 9, compared to the one peak at 15% on day 4 in wild type culture (Figure 3.2b). Compared to the mitotic cell size of wild type BY-2 cells, cells from the GFP-*Arath*;WEE1 line were significantly smaller by approximately 26% (Figure 3.2c).

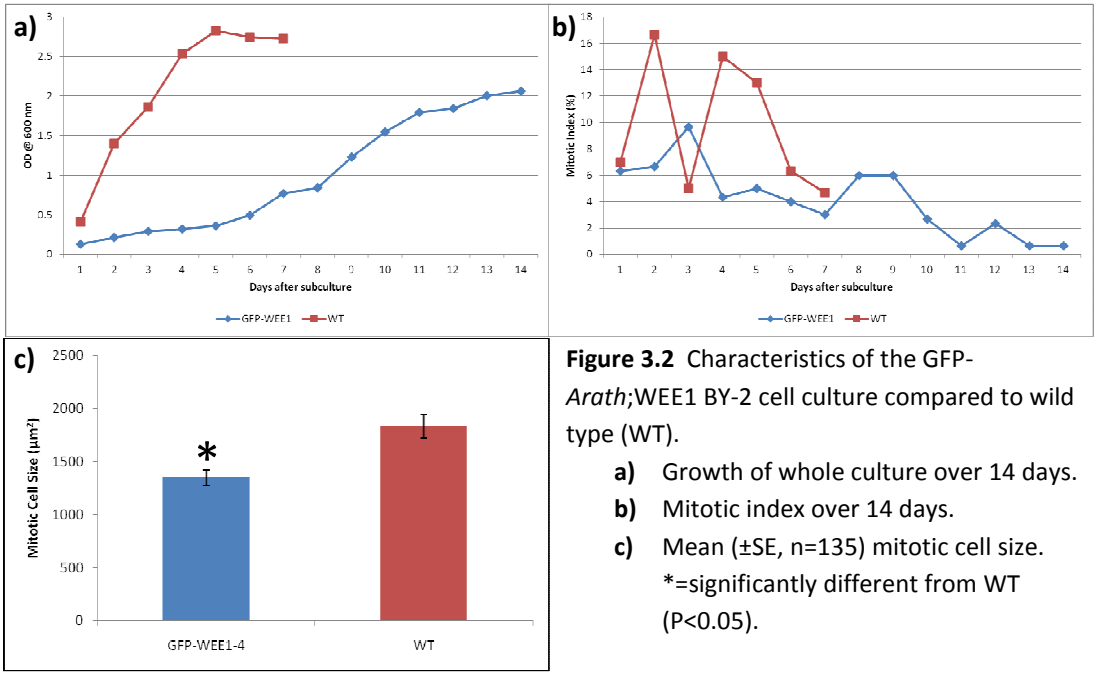

Figure 3.2 Characteristics of the GFP-*Arath*;WEE1 BY-2 cell culture compared to wild type (WT).

- **a)** Growth of whole culture over 14 days.
- **b)** Mitotic index over 14 days.
- **c)** Mean (±SE, n=135) mitotic cell size. *=significantly different from WT ($P<0.05$).

The GFP-*Arath*;WEE1 BY-2 culture was synchronised (Section 2.1.3) and the mitotic index scored (Section 2.1.4). Measurements of mitotic index indicated that the timing of mitosis in both the 35S-GFP and GFP-*Arath*;WEE1 BY-2 lines was similar to wild type, peaking 9 hours after removal of aphidicolin and then again after 22 hours (Figure 3.3), giving a cell cycle duration of 13 hours in total. The duration of each cell cycle phase was also estimated in each line (see Appendix I). The durations of S-phase and mitosis were similar in all three lines, at five hours and one hour, respectively (Figure 3.3). However, G2 appeared shorter in the GFP-*Arath*;WEE1-4 line; only two hours, compared to four and five hours in the wild type and 35S-GFP lines, respectively (Figure 3.3). This shortening of G2-phase in the GFP-*Arath*;WEE1 line was compensated for by a lengthened G1 of 6.5 hours, compared to only three hours in the other two lines (Figure 3.3).

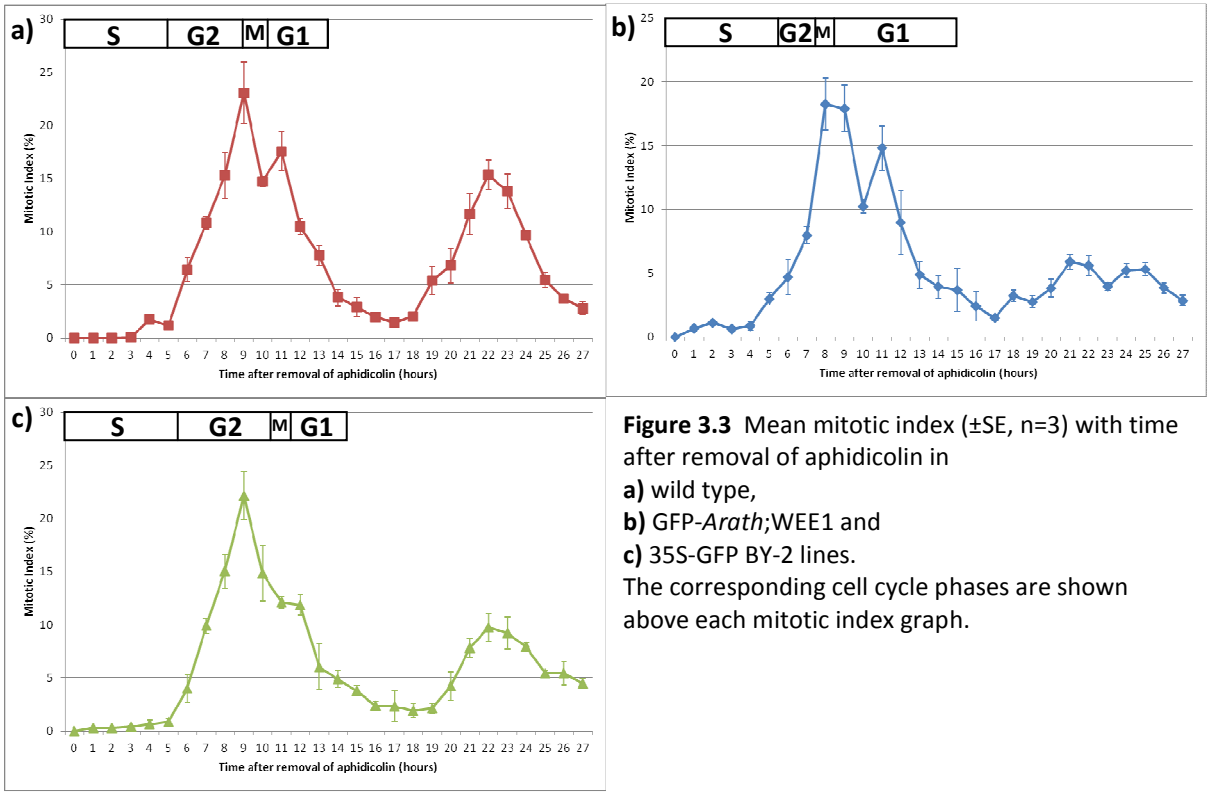

Figure 3.3 Mean mitotic index (±SE, n=3) with time after removal of aphidicolin in
a) wild type,
b) GFP-*Arath*;WEE1 and
c) 35S-GFP BY-2 lines.
The corresponding cell cycle phases are shown above each mitotic index graph.

Measurement of mitotic cell size (Section 2.1.4) indicated that the control 35S-GFP cells were very large, at approximately 6000 μm^2 (Figure 3.4). Conversely, mitotic cells of the GFP-*Arath*;WEE1 line were three-fold smaller than the 35S-GFP cells at approximately 2000 μm^2 (Figure 3.4).

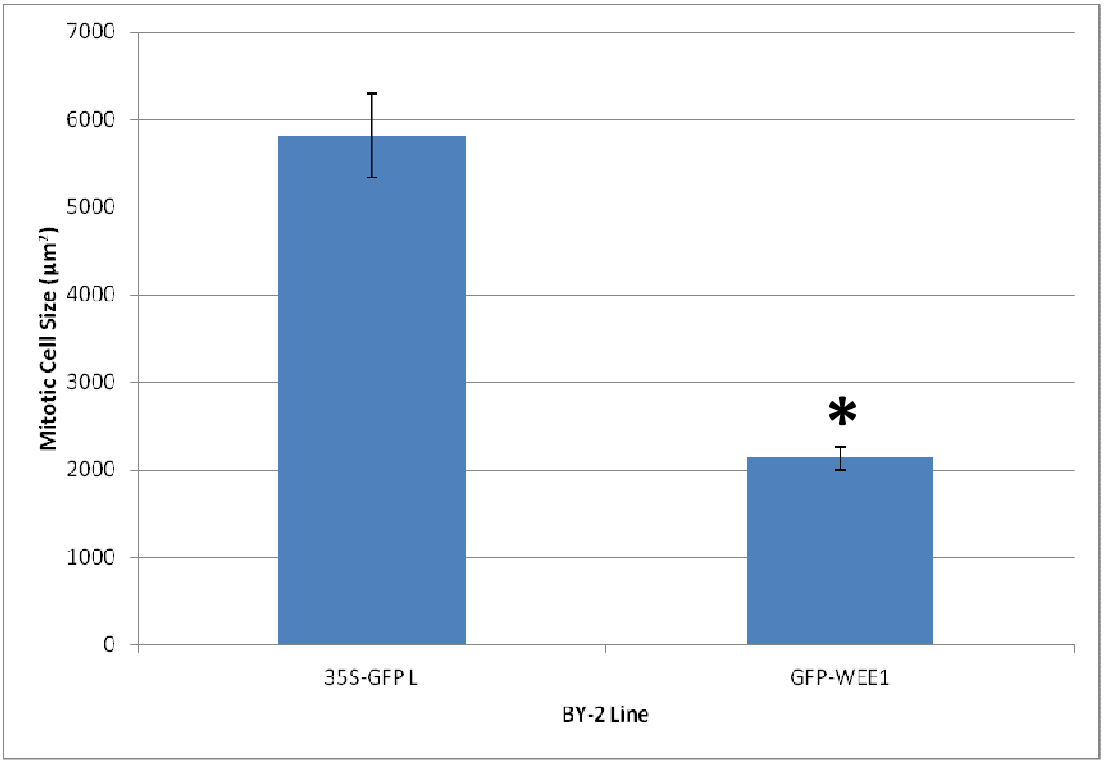

Figure 3.4 Mean mitotic cell size (±SE, n=21-35) in the GFP-*Arath*;WEE1 and 35S-GFP BY-2 lines. * = significantly different from 35S-GFP (P=0.000).

Synchronised GFP-*Arath*;WEE1 BY-2 cells were counter-stained using dilute Hoechst and monitored for GFP signal in each mitotic phase (Section 2.1.5). One-hundred per cent of interphase cells were found to exhibit a GFP-*Arath*;WEE1 signal, however this dropped sharply to only 4% of prophase cells (Figures 3.5 and 3.6). A GFP signal could not be detected in any metaphase cells (Figure 3.5 and 3.6). In anaphase and telophase the proportions of cells exhibiting a GFP signal rose again to 61% and 88% respectively (Figure 3.5 and 3.6). Comparatively, a GFP signal was observed in 100% of 35S-GFP cells, regardless of cell cycle phase (Figure 3.7). Unfortunately counter-staining using Hoechst was not possible in the 35S-GFP line as the addition of Triton X-100 permeabilised the cells causing the dispersal of the unattached GFP (as previously described by Lee et al., 2003).

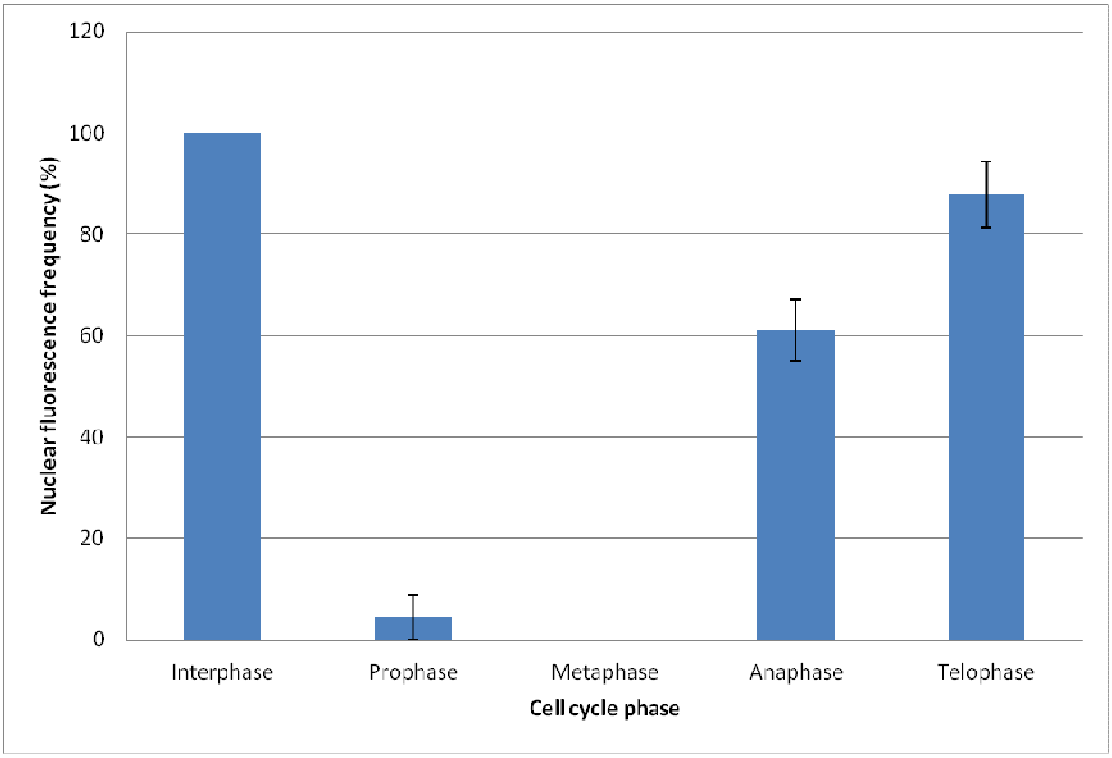

Figure 3.5 Mean nuclear fluorescence frequency (%; ±SE, n=3) in each cell cycle phase in the GFP-*Arath*;WEE1 BY-2 line. Contingency $\chi 2 = 30.031$, df = 6, P =0.000.

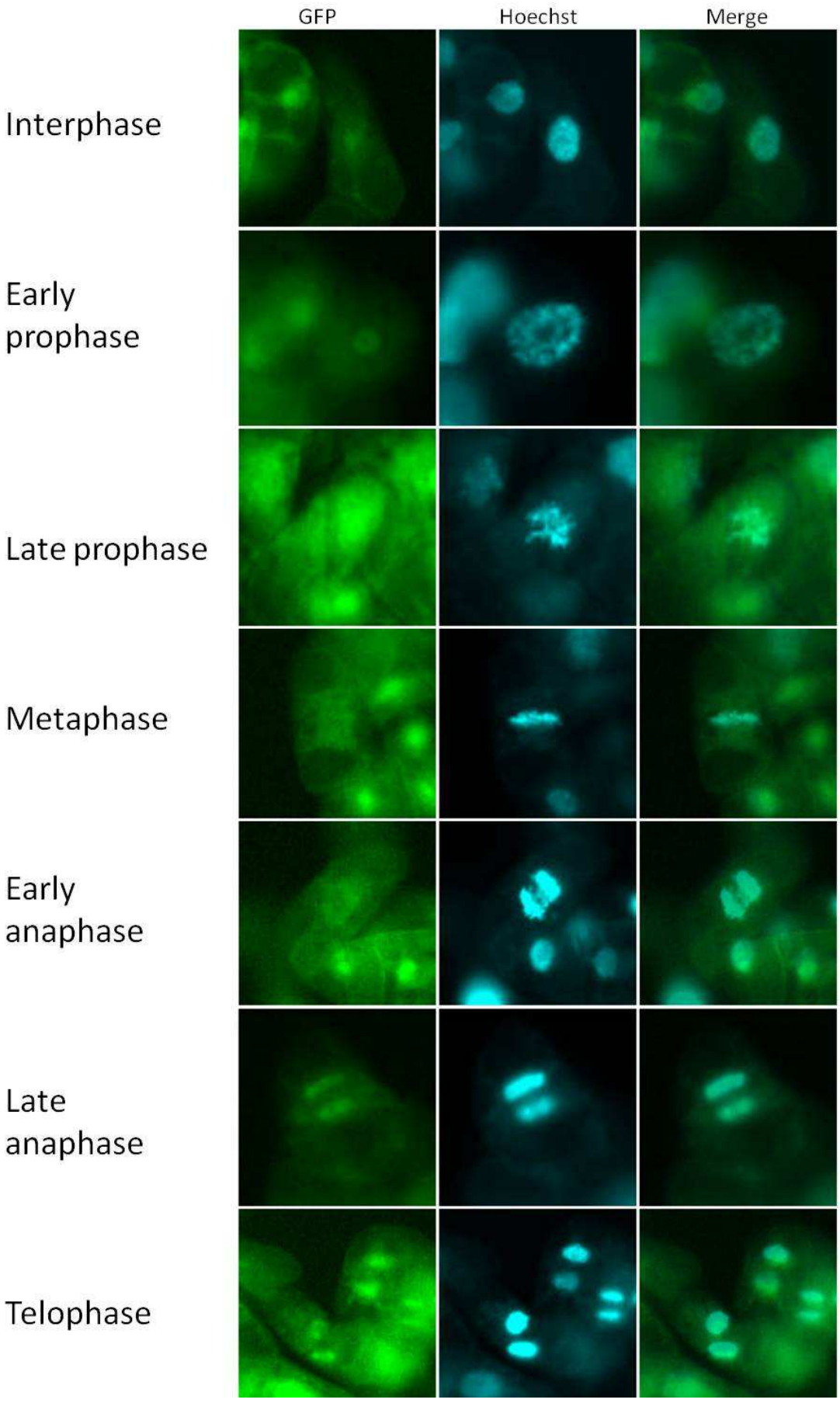

Figure 3.6 GFP-*Arath*;WEE1 expression in each cell cycle phase in synchronised GFP-*Arath*;WEE1 BY-2 cells. Green colouring indicates GFP-*Arath*;WEE1 expression while blue colouring indicates Hoechst nuclear stain.

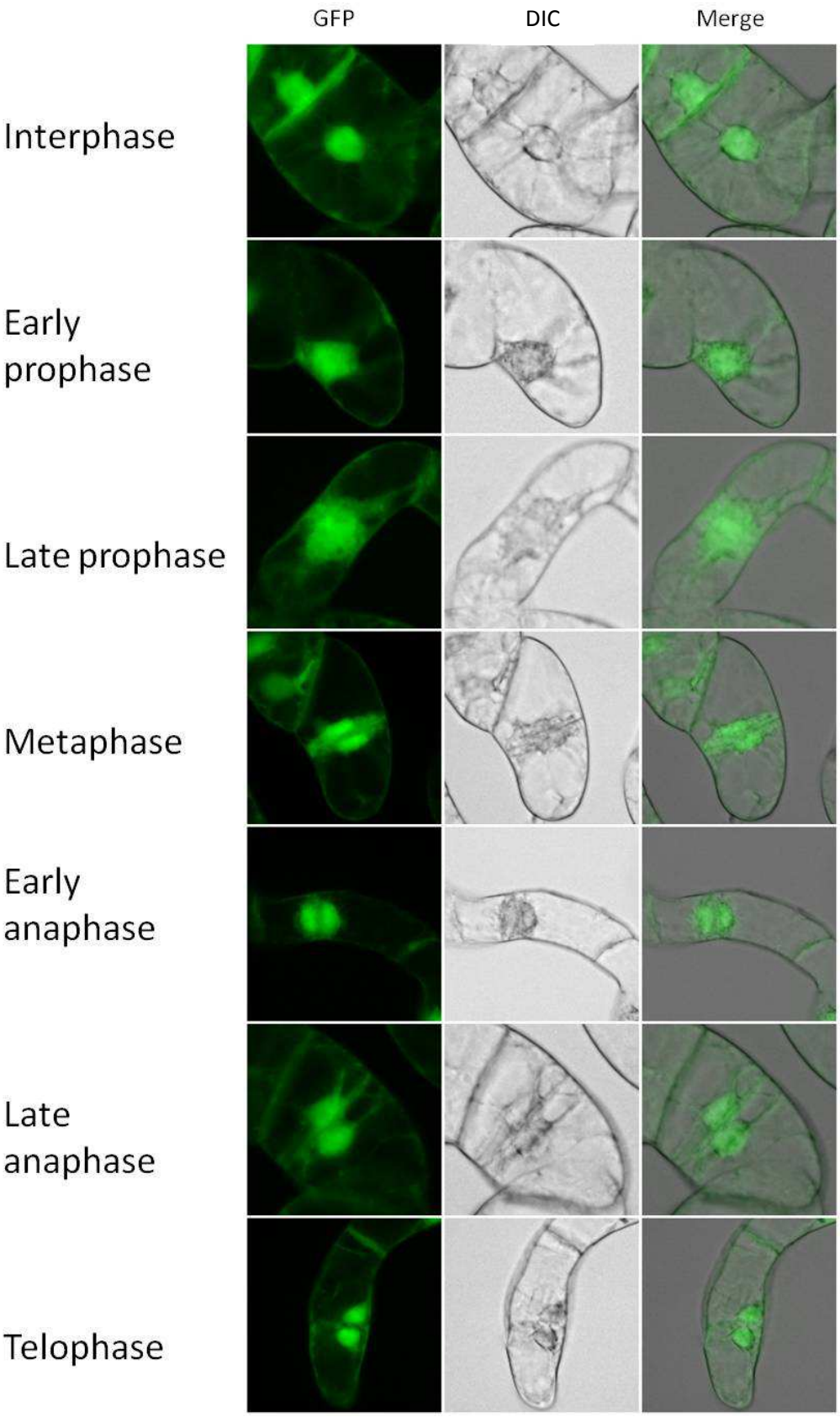

Figure 3.7 35S-GFP expression in each cell cycle phase in synchronised 35S-GFP BY-2 cells. Green colouring indicates 35S-GFP expression.

3.3.2 *ARATH*;WEE1 IS DEGRADED DURING MITOSIS IN *ARABIDOPSIS* ROOT MERISTEM CELLS

Prior to this work the GFP-*Arath*;WEE1 construct was transformed into *Arabidopsis* using the floral dip method (Section 2.3.1; N. Spadafora, Cardiff Lab. Unpublished results). Seed from the transformed plants was collected and stored at room temperature. One independent homozygous line (12) from this transformation was crossed with a line containing RFP-*Arath*;SUN1, a protein which localises to the nuclear envelope, to visualise GFP-*Arath*;WEE1 localisation in mitotic cells in the *Arabidopsis* root meristem more accurately. Seeds from the cross were sown on MS medium, transferred to soil (Section 2.3.3), and the DNA extracted from mature leaf samples (Section 2.4.1). This DNA was tested for the presence of both constructs by PCR (Section 2.4.2, Table 2.3). All 18 plants tested were positive for both constructs. These plants were allowed to self and set seed, and the seed collected for further analysis. Seed from each line was grown on MS medium (Section 2.3.3), with the original GFP-*Arath*;WEE1-12 and RFP-*Arath*;SUN1 lines as controls, and screened for fluorescence (Section 2.3.6). On the high power microscope the original GFP-*Arath*;WEE1-12 line exhibited a weak nuclear green fluorescent signal, while the RFP-*Arath*;SUN1 line exhibited a strong general red fluorescent signal. The majority of the GFP-*Arath*;WEE1 x RFP-*Arath*;SUN1 crossed lines had a weak GFP signal and a strong RFP signal, similar to the original lines. Three lines, 1, 6 and 9, were selected for confocal analysis (Section 2.3.7) as they had a stronger nuclear GFP signal as well as an RFP signal. Good images were obtained from line 1 courtesy of Dr K Grauman (Oxford Brookes University) and show a similar pattern to that seen during mitosis in BY-2 cells. A clear nuclear GFP signal is seen at in interphase, a weaker signal at prophase, no GFP-*Arath*;WEE1 signal visible at metaphase and a strong GFP signal is restored late in telophase/cytokinesis (Figure 3.8).

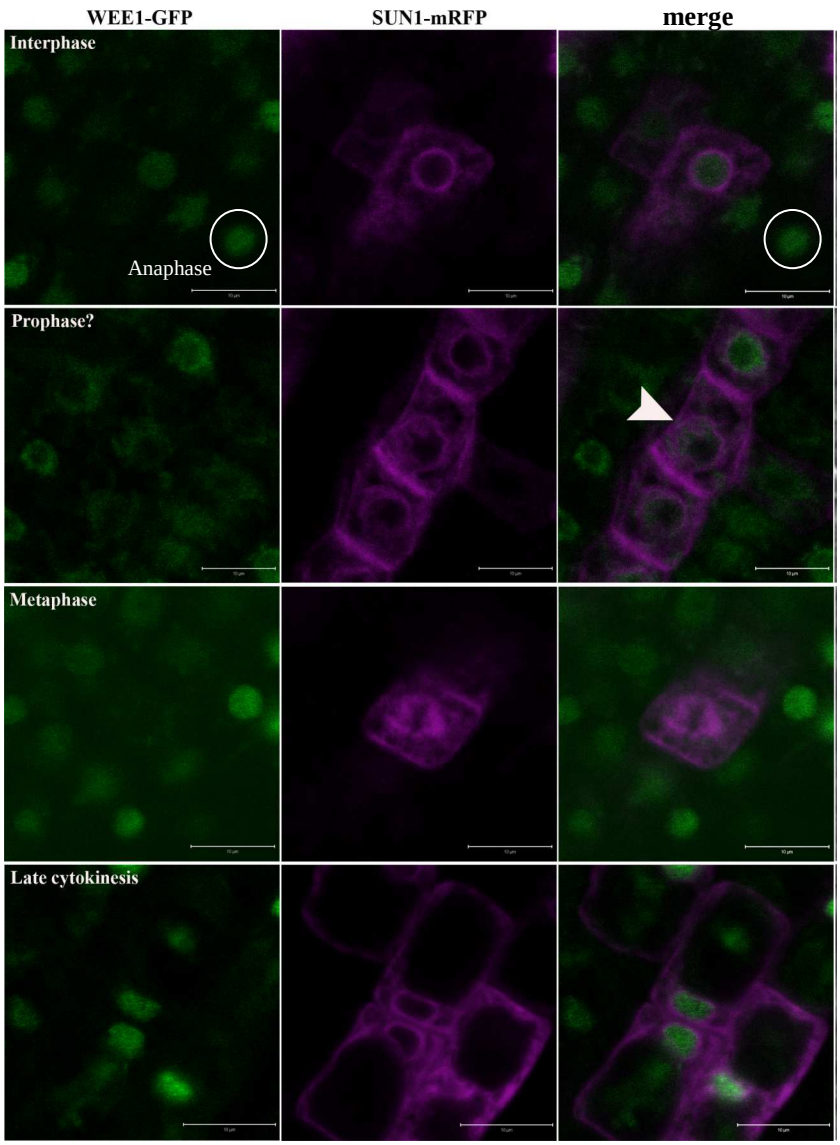

Figure 3.8 GFP-*Arath*;WEE1 and RFP-*Arath*;SUN1 expression in different cell cycle phases in roots of GFP-*Arath*;WEE1/RFP-*Arath*;SUN1 crossed *Arabidopsis* line 1. Green colouring indicates GFP-*Arath*;WEE1 expression while purple colouring indicates RFP-*Arath*;SUN1 expression. (Images by K. Graumann, Oxford Brookes University).

3.3.3 EXPRESSION OF GFP-*ARATH*;WEE1 IN ARABIDOPSIS CAN AFFECT ROOT GROWTH, CELL SIZE AND MITOTIC INDEX

The GFP-*Arath*;WEE1-12 *Arabidopsis* line was tested for over-expression of *Arath*;*WEE1* by semi-quantitative RT-PCR. RNA was extracted from mature leaves of GFP-*Arath*;WEE1-12, the *Arath*;WEE1 over-expressor WEE1-58 and wild type plants, cDNA synthesised and tested for *Arath*;*WEE1* expression using specific primers (Section 2.5; Table 2.3). *Arath*;*WEE1* expression in the GFP-*Arath*;WEE1-12 line was four times that of wild type, but was over-expressed to a lesser extent than in the WEE1-58 line, which was expressing *Arath*;*WEE1* to a level six times that of wild type (Figure 3.9).

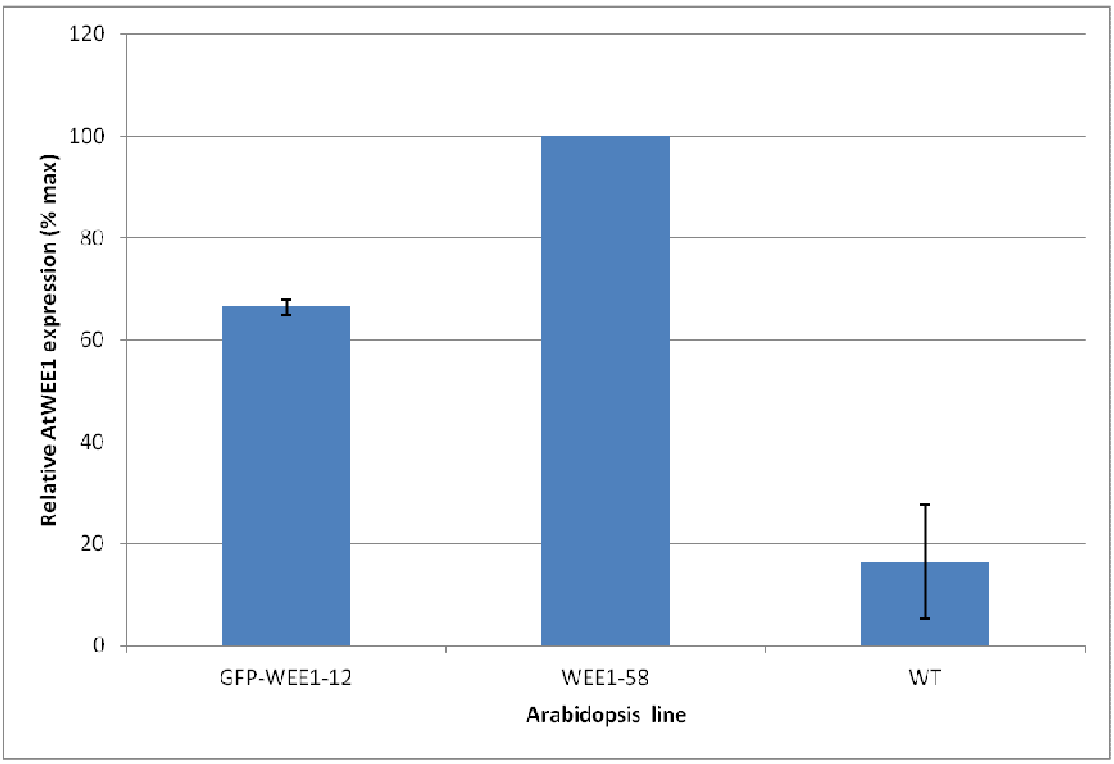

Figure 3.9 Results of semi-quantitative RT-PCR: Mean (±SE, n=3) *Arath*;WEE1 gene expression in the GFP-*Arath*;WEE1-12 transformed line compared to wild type (WT) and the *Arath*;WEE1 over-expressor WEE1-58.

The root phenotype of the GFP-*Arath*;WEE1-12 line was compared to that of wild type and two lines over-expressing *Arath*;*WEE1*: WEE1-58 and WEE1-61 (Section 2.3.5). It was expected that the GFP-*Arath*;WEE1-12 line would display a similar root phenotype to the *Arath*;WEE1 over-expressors. The primary root growth data were analysed by linear regression in order to calculate rates of primary root elongation in each line (Table 3.1). The primary root elongation rates of both WEE1-

58 and WEE1-61 were significantly slower than wild type, at 4 mm per day compared to 5.7 mm per day in wild type (Figure 3.10; Table 3.1). The elongation rate of GFP-*Arath*;WEE1-12 primary roots was also slower than wild type, at 5.3 mm per day, but this was closer to the wild type primary root elongation rate than that of the other over-expressors (Figure 3.10; Table 3.1).

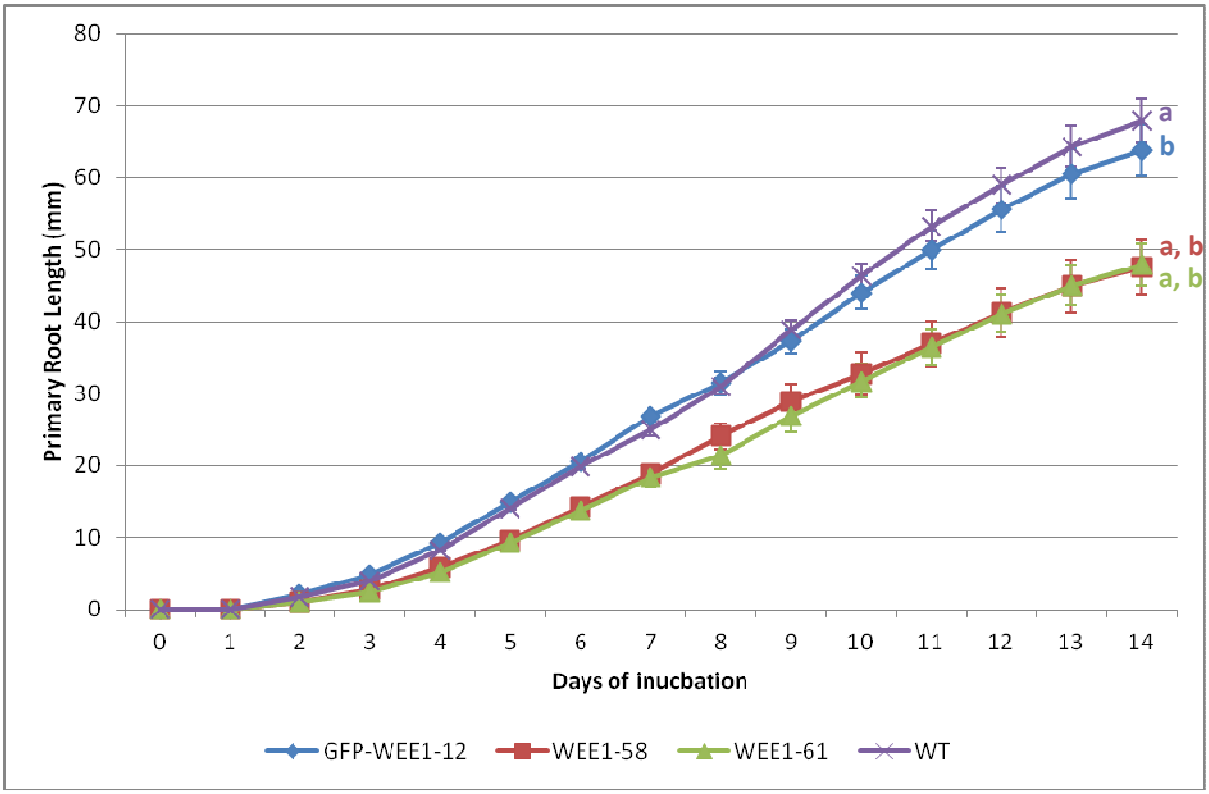

Figure 3.10 Mean primary root length (±SE, n=15-59) over time in the GFP-*Arath*;WEE1-12 line compared to *Arath*;WEE1 over-expressers (WEE1-58 and -61) and wild type (WT) *Arabidopsis*. a, b = significantly different from GFP-*Arath*;WEE1-12, WT respectively (P<0.01).

Table 3.1 Rate of primary root elongation in the GFP-*Arath*;WEE1-12 line compared to *Arath*;WEE1 over-expressors (WEE1-58 and -61) and wild type *Arabidopsis*.

***Arabidopsis* line**	**Linear regression equation (P=0.000)**	**Rate of primary root elongation (mm per day)**
GFP-*Arath*;WEE1-12	y = 5.31x + 9.77	5.31
WEE1-58	y = 4.02x + 8.06	4.02
WEE1-61	y = 4.02x + 8.69	4.02
Wild type	y = 5.73x + 12.00	5.73

After 7 days growth, the WEE1 over-expressors had significantly shorter primary roots than wild type, and WEE1-58 also had significantly fewer lateral roots and primordia (Figure 3.11). However GFP-*Arath*;WEE1-12 primary root length and number of lateral roots were similar to wild type after 7 days (Figure 3.11). After 14 days growth, the WEE1 over-expressing lines both had significantly shorter primary roots and significantly fewer lateral roots than wild type, while the phenotype of the GFP-*Arath*;WEE1-12 line was again similar to wild type (Figure 3.12).

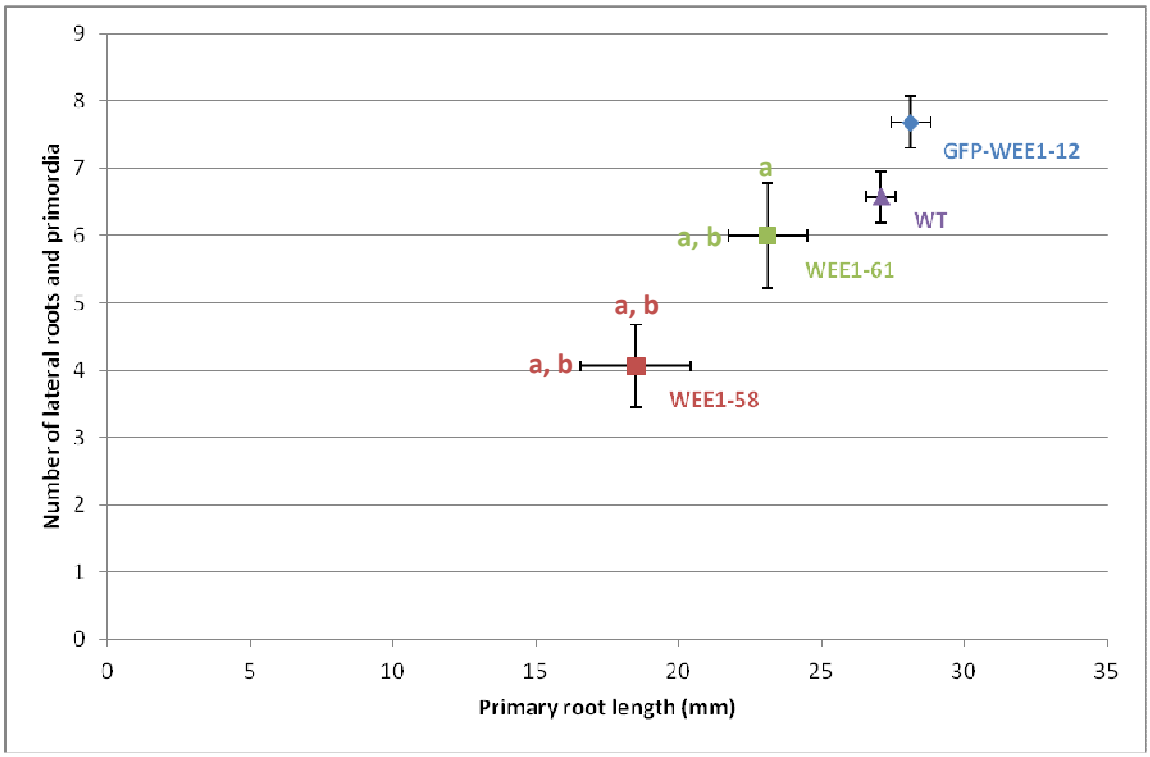

Figure 3.11 Primary root length and number of lateral roots and primordia (±SE, n=9-28) after 7 days growth in the GFP-*Arath*;WEE1-12 line compared to *Arath*;WEE1 over-expressors (WEE1-58 and -61) and wild type (WT) *Arabidopsis*. a, b = significantly different from GFP-WEE1-12, WT respectively ($P<0.05$).

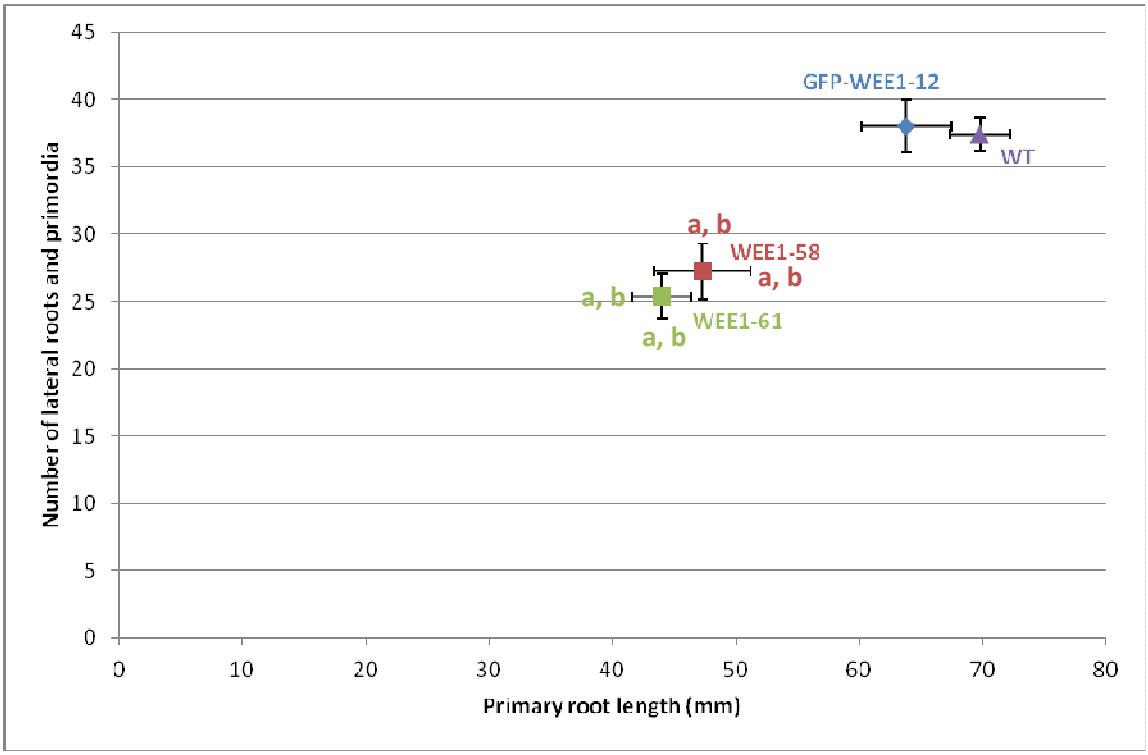

Figure 3.12 Mean primary root length and number of lateral roots and primordia (±SE, n=11-29) after 14 days growth in the GFP-*Arath*;WEE1-12 line compared to *Arath*;WEE1 over-expressors (WEE1-58 and -61) and wild type (WT) *Arabidopsis*. a, b = significantly different from GFP-WEE1-12, WT respectively (P<0.05).

The rate of lateral root initiation per mm of primary root after seven days growth did not vary from that of wild type in any of the transgenic lines (Table 3.2). This was supported by regression analysis which indicated a linear relationship between the primary root length and number of lateral roots in each line after seven days (r^2=0.94), confirming that the rate of lateral root formation was similar in each line. Similarly, a linear relationship between the primary root length and number of lateral roots in each line was confirmed after fourteen days (r^2=0.95). After fourteen days growth, the GFP-*Arath*;WEE1-12 line produced an increased number of lateral roots per mm of primary root compared to wild type (Table 3.2).

Table 3.2 Rate of lateral root formation per mm of primary root (±SE) after 7 days and 14 days growth in the GFP-*Arath*;WEE1 line compared to *Arath*;WEE1 over-expressors (WEE1-58 and -61) and wild type *Arabidopsis*. * = significantly different from wild type (P<0.05).

	Rate of lateral root formation per mm of primary root (±SE)	
***Arabidopsis* line**	**7 day old seedlings (n=9-28)**	**14 day old seedlings (n=11-29)**
GFP-*At*;WEE1-12	0.27 ±0.01	0.60 ±0.02 *
WEE1-58	0.20 ±0.02	0.58 ±0.02
WEE1-61	0.25 ±0.03	0.58 ±0.03
Wild type	0.24 ±0.01	0.54 ±0.01

Seeds from the GFP-*Arath*;WEE1-12 line were surface sterilised and sown (Section 2.3.3) and, after 5 days growth, imaged using a confocal microscope (Section 2.3.7). The GFP signal observed demonstrated that *Arath*;WEE1 is expressed at the protein level in the nucleus in *Arabidopsis* root cells (Figure 3.13). Also, the GFP signal appeared to be lower in the cortical cells and the cell lineage destined to become the stelar cells of the meristem (Figure 3.13). However, despite being under the control of the strong constitutive 35S promoter, this strong GFP expression was only observed in one of 54 homozygous seedlings screened, so new lines were sought in order to further confirm and quantify these results.

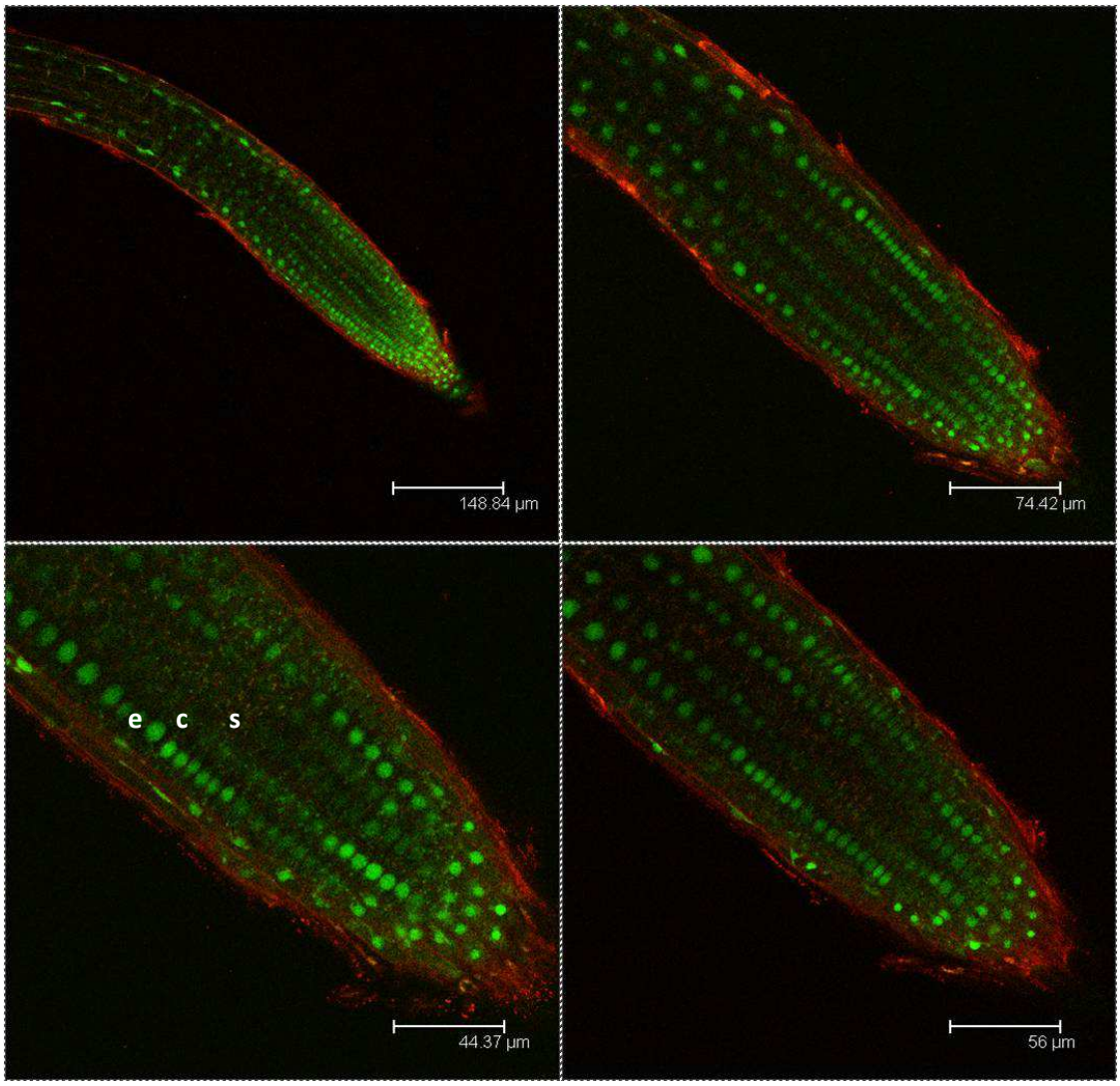

Figure 3.13 Confocal images of the root tip of one seedling of the GFP-*Arath*;WEE1-12 line. Green colouring indicates GFP-*Arath*;WEE1 expression, red colouring is propidium iodide counter-stain for the cell walls. e: epidermis, c: cortex, s: stele.

Seed from the original transformation was used for selection (Section 2.3.2; 100µg/mL kanamycin) and 70 plants were isolated. These plants were transferred to soil and allowed to self and set seed. A mature leaf was taken from each plant, DNA extracted, and used for PCR (Section 2.4; Table 2.3) to confirm the presence of the GFP-*Arath*;WEE1 construct in 68 of the 70 plants. Seed from 62 plants was collected, surface sterilised and sown (Section 2.3.3) and the resulting 5 day-old seedlings screened for GFP signal compared to wild type and the weak GFP-*Arath*;WEE1-12 line under a high power fluorescent microscope (Section 2.3.6). An *Arabidopsis* line transformed with a H2B-YFP construct, under the 35S promoter and known to localise to the nucleus, was obtained as a positive control (by kind

donation from J. A. H. Murray, Cardiff University; Boisnard-Lorig et al., 2001). While none of the new GFP-*Arath*;WEE1 lines exhibited a very strong nuclear fluorescent signal similar to the H2B-YFP control line, several lines were clearly and consistently expressing GFP-*Arath*;WEE1 at a higher level than the GFP-*Arath*;WEE1-12 line. Two lines, 10 and 67, were chosen for further analysis. Seedlings from each of these lines were transferred to soil and allowed to self and set seed. A homozygous line (exhibiting 100% survival of seedlings on kanamycin selection) was obtained from each line and used for further analysis.

Semi-quantitative RT-PCR was used to compare levels of *Arath*;*WEE1* expression in mature leaves relative to wild type and WEE1-58 plants (Section 2.5; Table 2.3). Both GFP-*Arath*;WEE1-10 and GFP-*Arath*;WEE1-67 were found to be over-expressing *Arath*;*WEE1*, a 4-fold and 2-fold increase compared to wild type, respectively (Figure 3.14). However, both were over-expressing *Arath*;*WEE1* at a lower level than WEE1-58, which was expressing *Arath*;*WEE1* at a level approximately five times higher than wild type (Figure 3.14).

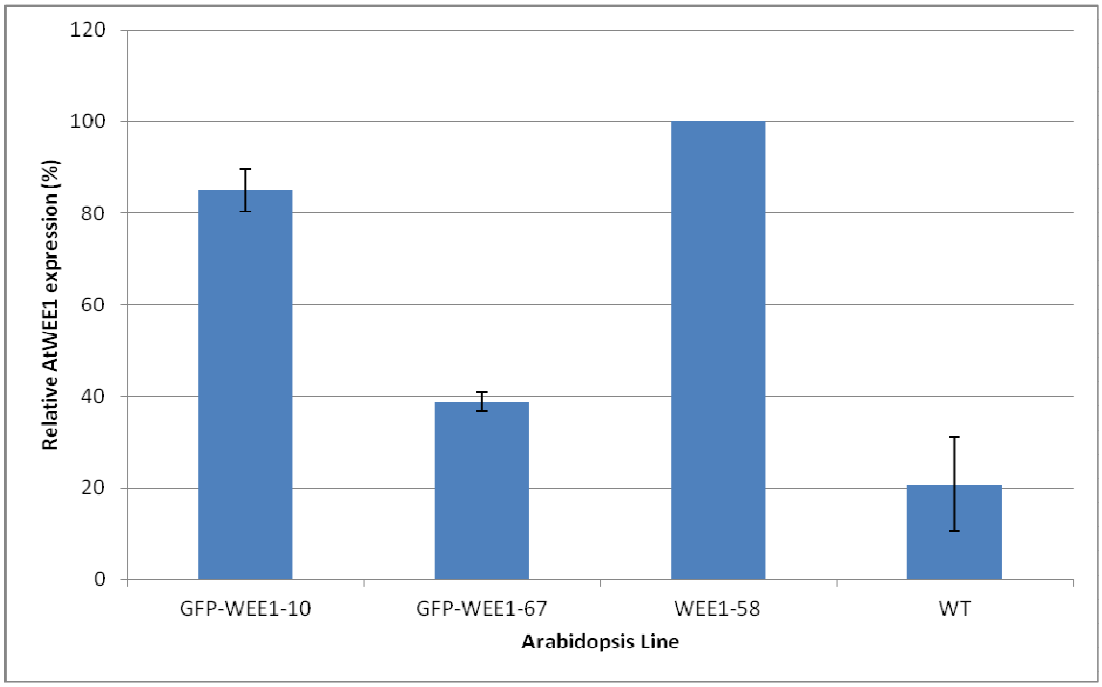

Figure 3.14 Results of semi-quantitative RT-PCR: Mean (±SE, n=3) *Arath*;WEE1 gene expression in the GFP-*Arath*;WEE1-10 and -67 transformed lines compared to wild type (WT) and the *Arath*;WEE1 over-expressor WEE1-58.

To test for the number of insertions of the GFP-*Arath*;WEE1 transgene into the *Arabidopsis* genome in each line, T_2 seeds (200) from lines GFP-*Arath*;WEE1-10 and -67 were surface sterilised and sown on MS medium containing kanamycin selection. The ratio of kanamycin-resistant to kanamycin-sensitive plants was calculated for each line and compared to the ratio of 3:1 (75% kanamycin-resistant) which is expected for a single insertion. The ratio of kanamycin-resistant to kanamycin-sensitive in the GFP-*Arath*;WEE1-10 line was approximately 3:1 (75.8%), implying that this line contained a single insertion of the GFP-*Arath*;WEE1 transgene. In the GFP-*Arath*;WEE1-67 line, 97.3% of seedlings were kanamycin-resistant, implying that the genome of the GFP-*Arath*;WEE1-67 line contained more than one copy of the GFP-*Arath*;WEE1 transgene.

The root phenotypes of the GFP-*Arath*;WEE1-10 and -67 lines were compared to wild type and the *Arath*;WEE1 over-expressors WEE1-58 and WEE1-61 (Section 2.3.5). The primary root growth data were analysed by linear regression in order to calculate rates of primary root elongation in each line (Table 3.3). Contrary to the results described for the GFP-*Arath*;WEE1-12 line, although the primary root elongation rate of 5.5 mm per day in WEE1-61 was slower than wild type (5.8 mm per day), that of WEE1-58 (6.8 mm per day) was actually found to be faster on this occasion (Figure 3.15; Table 3.3). The primary root elongation rates of GFP-*Arath*;WEE1-10 and -67 were also faster than wild type (6.9 and 7 mm per day, respectively), similar to WEE1-58 (Figure 3.15; Table 3.3).

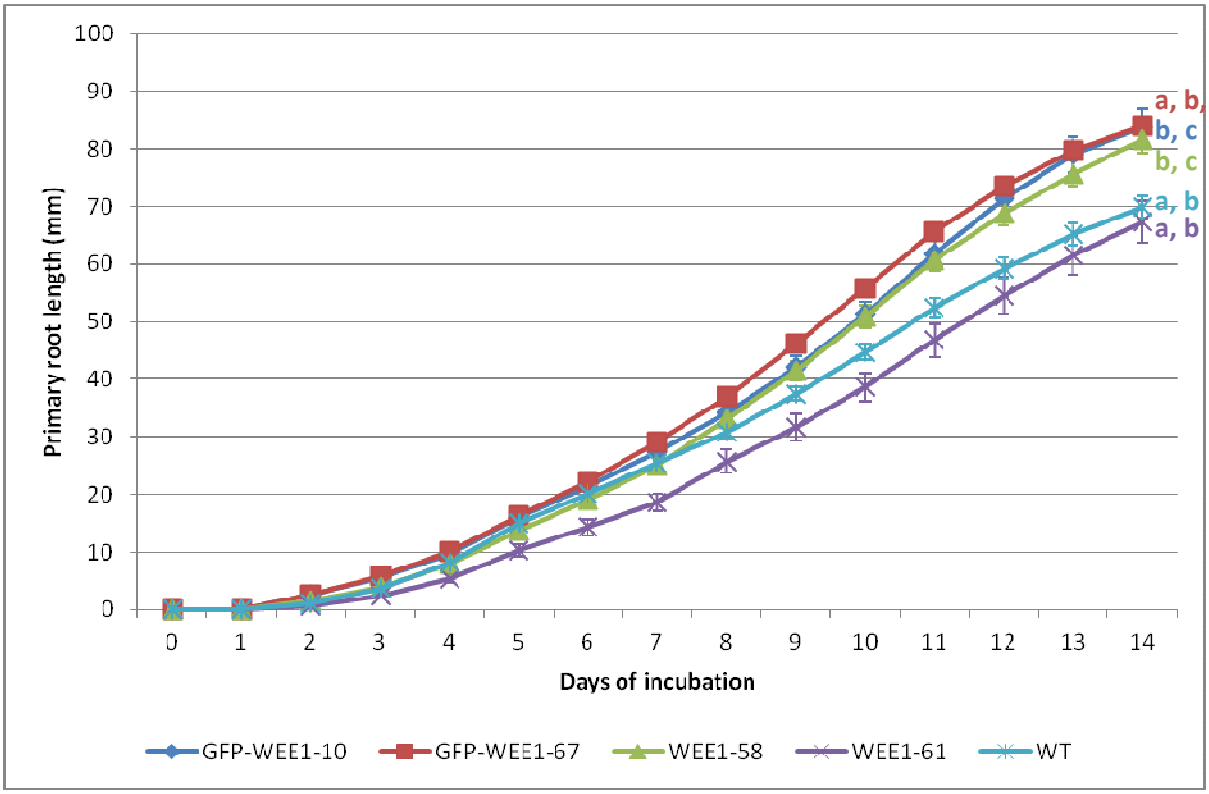

Figure 3.15 Mean primary root length (±SE, n=17-60) over time in the GFP-*Arath*;WEE1-10 and -67 lines compared to *Arath*;WEE1 over-expressors (WEE1-58 and -61) and wild type (WT) *Arabidopsis*. a, b, c = significantly different from WEE1-58, WEE1-61, WT respectively (P<0.05).

Table 3.3 Rate of primary root elongation in GFP-*Arath*;WEE1 lines 10 and 67 compared to *Arath*;WEE1 over-expressors (WEE1-58 and -61) and wild type *Arabidopsis*.

***Arabidopsis* line**	**Linear regression equation (P=0.000)**	**Rate of primary root elongation (mm per day)**
GFP-*Arath*;WEE1-10	y = 6.88x + 15.4	6.88
GFP-*Arath*;WEE1-67	y = 7.06x + 15.2	7.06
WEE1-58	y = 6.80x + 16.4	6.80
WEE1-61	y = 5.51x + 14.3	5.51
Wild type	y = 5.78x + 12.4	5.78

After 7 days, WEE1-61 had significantly shorter primary roots and fewer lateral roots than wild type, as expected (Figure 3.16). However, WEE1-58 primary root length and number of lateral roots were similar to wild type (Figure 3.16). GFP-*Arath*;WEE1-10 and -67 both had significantly more lateral roots and primordia than wild type and both *Arath*;WEE1 over-expressors, and GFP-*Arath*;WEE1-67 also had significantly longer primary roots (Figure 3.16).

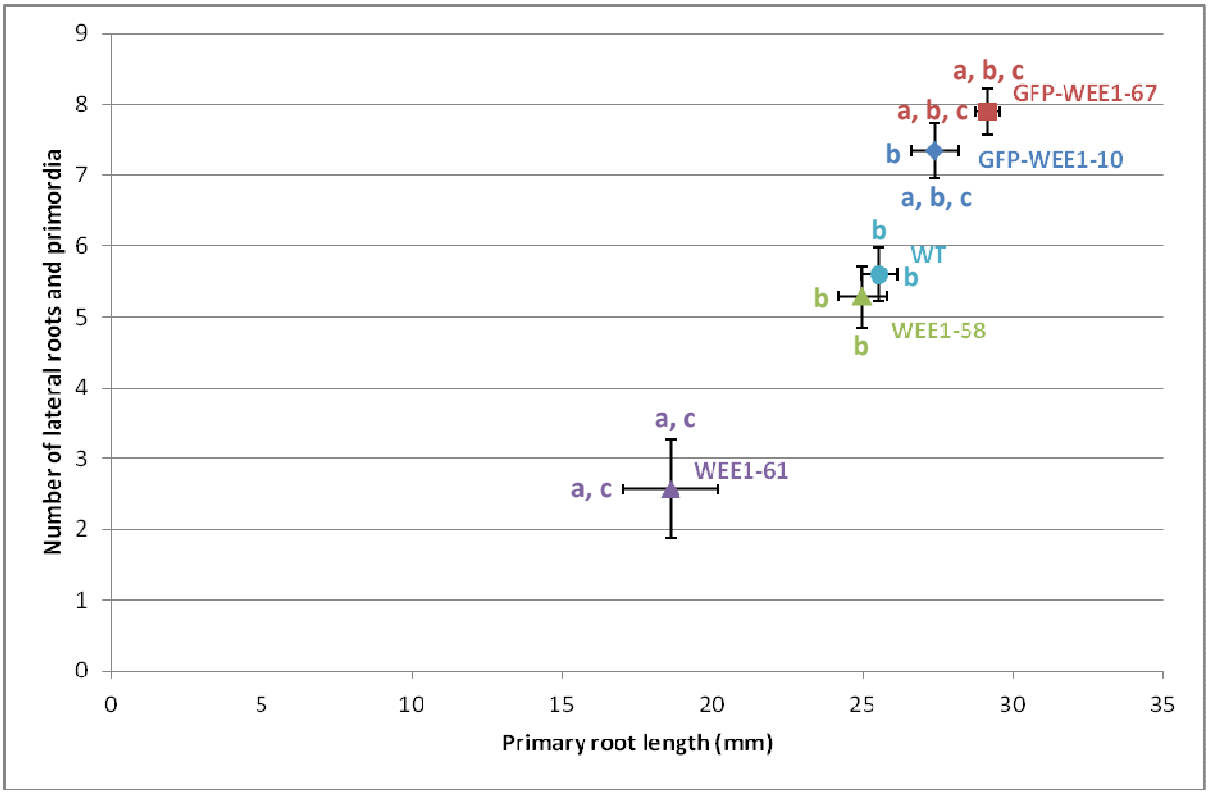

Figure 3.16 Mean primary root length and number of lateral roots and primordia (±SE, n=14-30) after 7 days growth in the GFP-*Arath*;WEE1-10 and -67 lines compared to *Arath*;WEE1 over-expressors (WEE1-58 and -61) and wild type (WT) *Arabidopsis*. a, b, c = significantly different from WEE1-58, WEE1-61, WT respectively ($P<0.05$).

After 14 days growth, the root phenotype of the WEE1-61 line was similar to wild type (Figure 3.17). WEE1-58 had significantly longer primary roots than wild type, but similar numbers of lateral roots (Figure 3.17). The GFP-*Arath*;WEE1-10 line displayed a similar pattern to WEE1-58 (Figure 3.17). The GFP-*Arath*;WEE1-67 line also had significantly longer primary roots than wild type, but also had more lateral roots than both wild type and WEE1-58 (Figure 3.17).

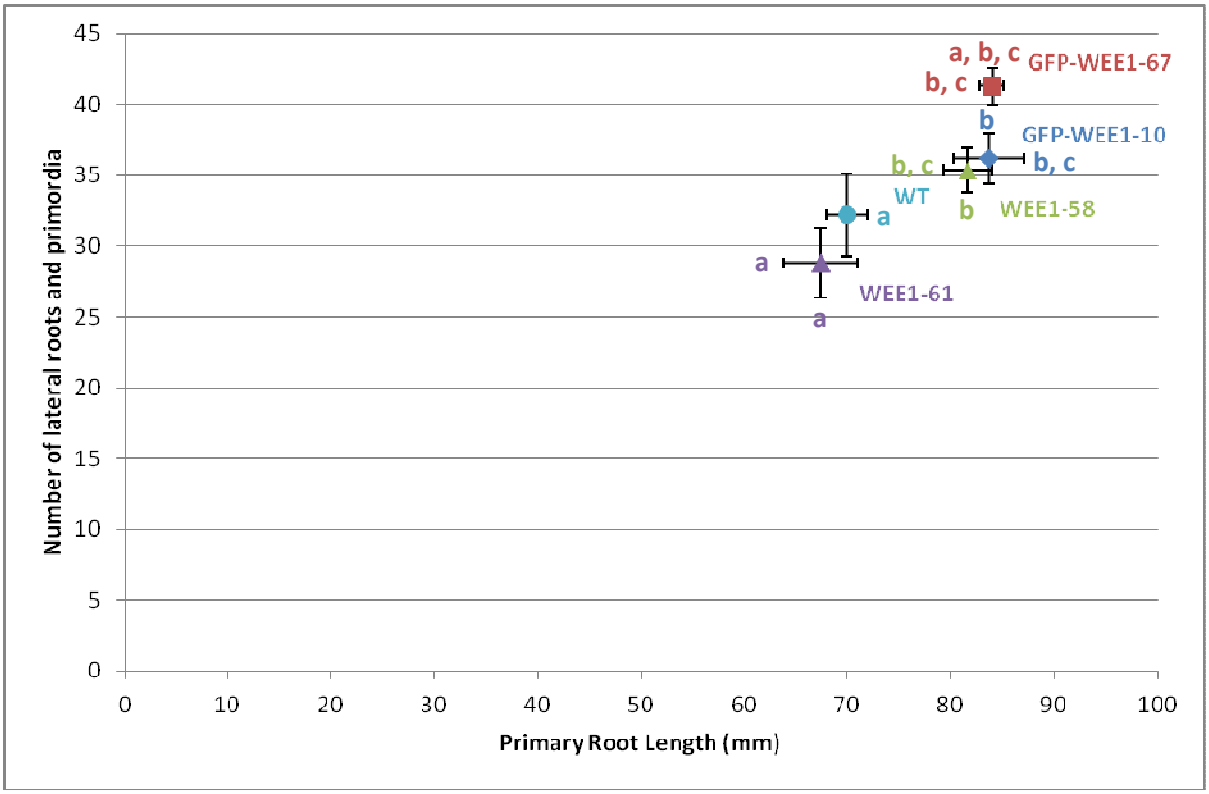

Figure 3.17 Mean primary root length and number of lateral roots and primordia (±SE, n=10-11) after 14 days growth in the GFP-*Arath*;WEE1-10 and -67 lines compared to *Arath*;WEE1 over-expressors (WEE1-58 and -61) and wild type (WT) *Arabidopsis*. a, b, c = significantly different from WEE1-58, WEE1-61, WT respectively ($P<0.05$).

The rate of lateral root initiation per mm of primary root after seven days growth was increased compared to wild type in the GFP-*Arath*;WEE1 lines (Table 3.4). In contrast, the rate of lateral root initiation per mm of primary root was decreased in WEE1-61 compared to wild type after seven days (Table 3.4). The rate of lateral root initiation was similar to wild type in the WEE1-58 line after seven days (Table 3.4). After fourteen days, however, the rate of lateral root formation was decreased compared to wild type in both the GFP-*Arath*;WEE1-10 and WEE1-58 lines, while GFP-*Arath*;WEE1-67 and WEE1-61 were similar to wild type (Table 5.2).

Table 3.4 Rate of lateral root formation per mm of primary root (±SE) after 7 days and 14 days growth in the GFP-*Arath*;WEE1 lines 10 and 67 compared to *Arath*;WEE1 over-expressors (WEE1-58 and -61) and wild type *Arabidopsis*. * = significantly different from wild type (P<0.05).

	Rate of lateral root formation per mm of primary root (±SE)	
***Arabidopsis* line**	**7 day old seedlings (n=14-30)**	**14 day old seedlings (n=10-11)**
GFP-*At*;WEE1-10	0.26 ±0.01 *	0.41 ±0.02 *
GFP-*At*;WEE1-67	0.27 ±0.01 *	0.49 ±0.01
WEE1-58	0.21 ±0.01	0.42 ±0.02 *
WEE1-61	0.11 ±0.03 *	0.48 ±0.02
Wild type	0.21 ±0.01	0.48 ±0.02

The meristematic cell sizes in these lines were also measured and compared (Section 3.2.1, see Appendix II for images). In the epidermis, WEE1-61 cells were a similar width and length to wild type cells, while WEE1-58 epidermal cells were significantly wider and longer (Figure 3.18a). The GFP-*Arath*;WEE1-67 epidermal cells were similar in length to wild type, but significantly wider, resulting in a similar width to WEE1-58 (Figure 3.18a). GFP-*Arath*;WEE1-10 epidermal cells were also similar in length to wild type, however cells were approximately twice as wide (Figure 3.18a). In the cortex, on the other hand, the cells in the *Arath*;WEE1 over-expressors and GFP-*Arath*;WEE1 lines were all similar in width to wild type cortical cells (Figure 3.18b). WEE1-58 and GFP-*Arath*;WEE1-67 cortical cells were also similar to wild type in length, while WEE1-61 and GFP-*Arath*;WEE1-10 were significantly shorter (Figure 3.18b). The length and width of stele initial cells was similar in all lines, except for GFP-*Arath*;WEE1-67 which had longer stele initial cells than wild type (Figure 3.18c).

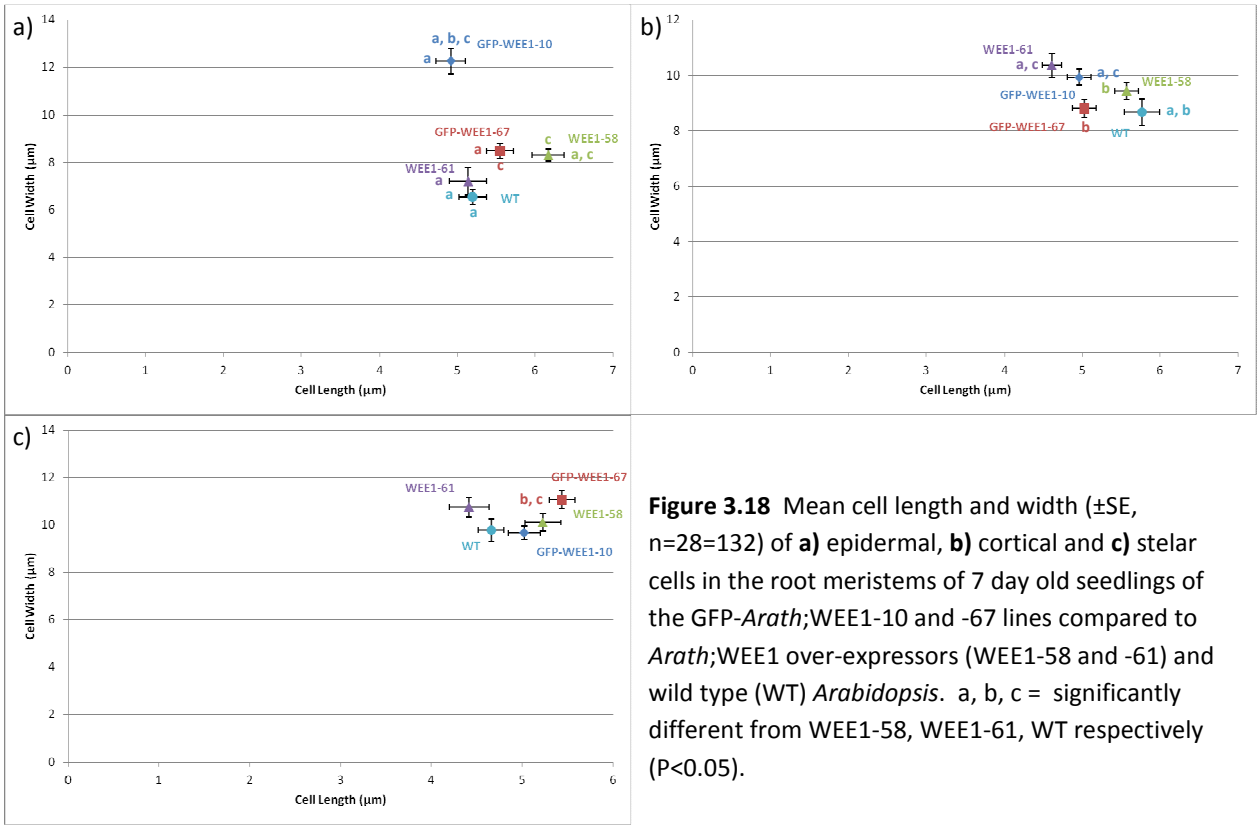

Figure 3.18 Mean cell length and width (±SE, n=28=132) of **a)** epidermal, **b)** cortical and **c)** stelar cells in the root meristems of 7 day old seedlings of the GFP-*Arath*;WEE1-10 and -67 lines compared to *Arath*;WEE1 over-expressors (WEE1-58 and -61) and wild type (WT) *Arabidopsis*. a, b, c = significantly different from WEE1-58, WEE1-61, WT respectively ($P<0.05$).

Cell number in each tissue in each line was also measured in order to determine whether or not cell number was altered to compensate for changes in cell size. Statistical analyses indicate that there were no differences in cell number between any of the lines in any tissue (Figure 3.19). Subjective analysis of the overlap in error bars suggests that cortical and stelar cell numbers were indeed similar in all lines, however there seemed to be more epidermal cells in the GFP-*Arath*;WEE1-67 line compared to wild type, and less in WEE1-61 (Figure 3.19).

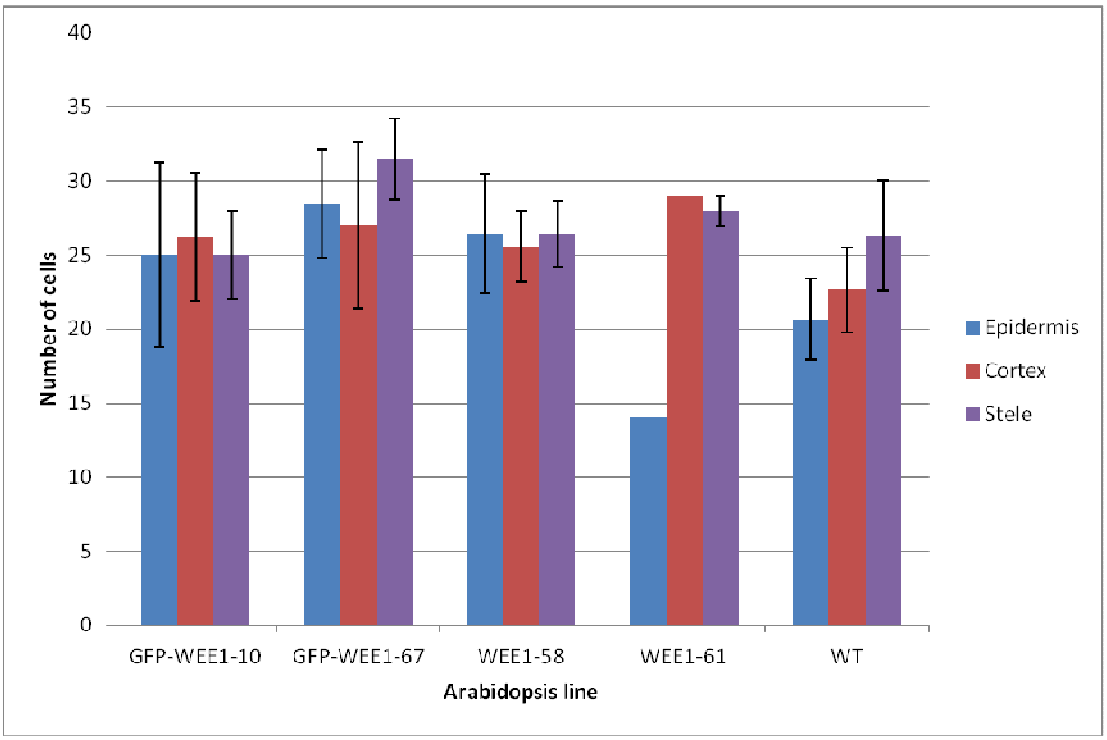

Figure 3.19 Cell number (±SE, n=2-5) in the meristems of 7 day old seedlings of the GFP-*Arath*;WEE1-10 and -67 lines compared to *Arath*;WEE1 over-expressors (WEE1-58 and -61) and wild type (WT) *Arabidopsis*.

Finally, the area of the whole meristem was measured in each line. Statistical analysis indicates that GFP-*Arath*;WEE1-10 and -67 and WEE1-58 meristems were similar in area to each other and wild type, but larger than WEE1-61 , while WEE1-61 meristems were a similar size to wild type (Figure 3.20). Subjective analysis of the overlap in error bars suggests that the meristematic areas of lines GFP-*Arath*;WEE1-10 and -67 and WEE1-58 were larger than both wild type and WEE1-61, while WEE1-61 meristems were smaller than wild type (Figure 3.20).

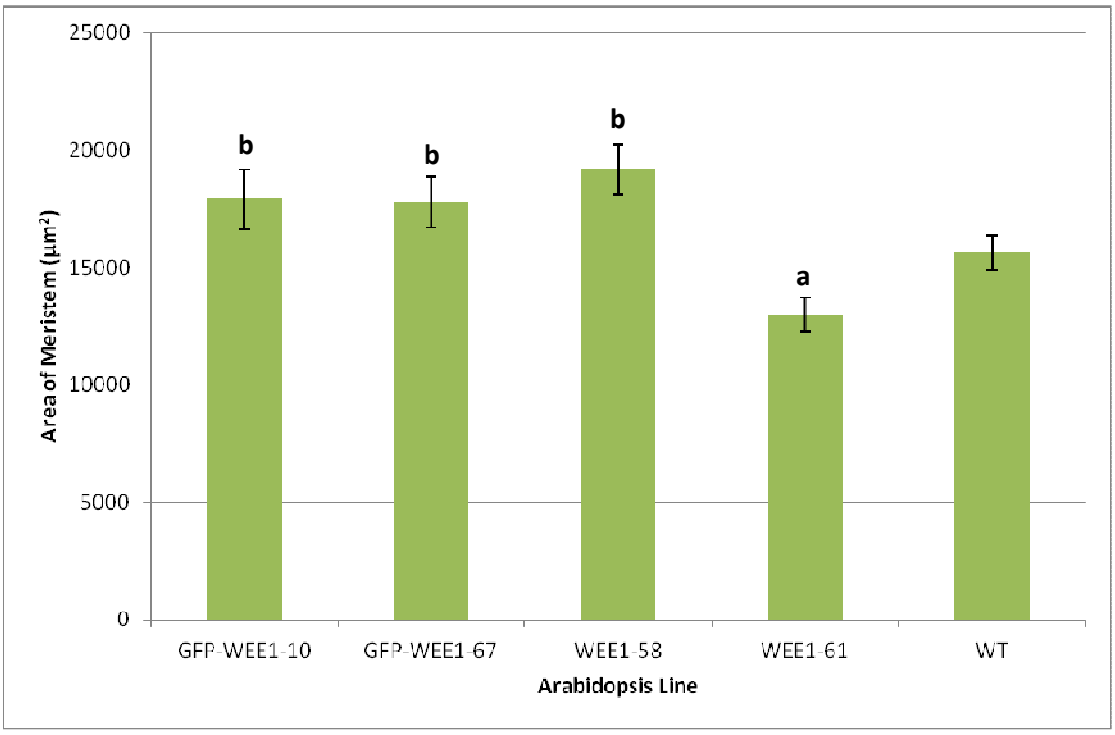

Figure 3.20 Meristem area (±SE, n=2-5) of 7 day old seedlings of the GFP-*Arath*;WEE1-10 and -67 lines compared to *Arath*;WEE1 over-expressors (WEE1-58 and -61) and wild type (WT) *Arabidopsis*. a, b, c = significantly different from WEE1-58, WEE1-61, WT respectively ($P<0.05$).

Roots from each line (7 days old) were stained using Hoechst, the root tip squashed on a microscope slide, and mitotic index scored (Section 3.2.2), to test for any effects of *Arath*;WEE1 over-expression on the cell cycle in root meristems. It was found that WEE1-58, WEE1-61 and wild type all had similar mitotic indices of approximately 2% per meristem (Figure 3.21). However, the GFP-*Arath*;WEE1-10 and -67 lines both had a higher percentage of mitotic figures than both the *Arath*;WEE1 over-expressers and wild type, at approximately 4-5% respectively (Figure 3.21).

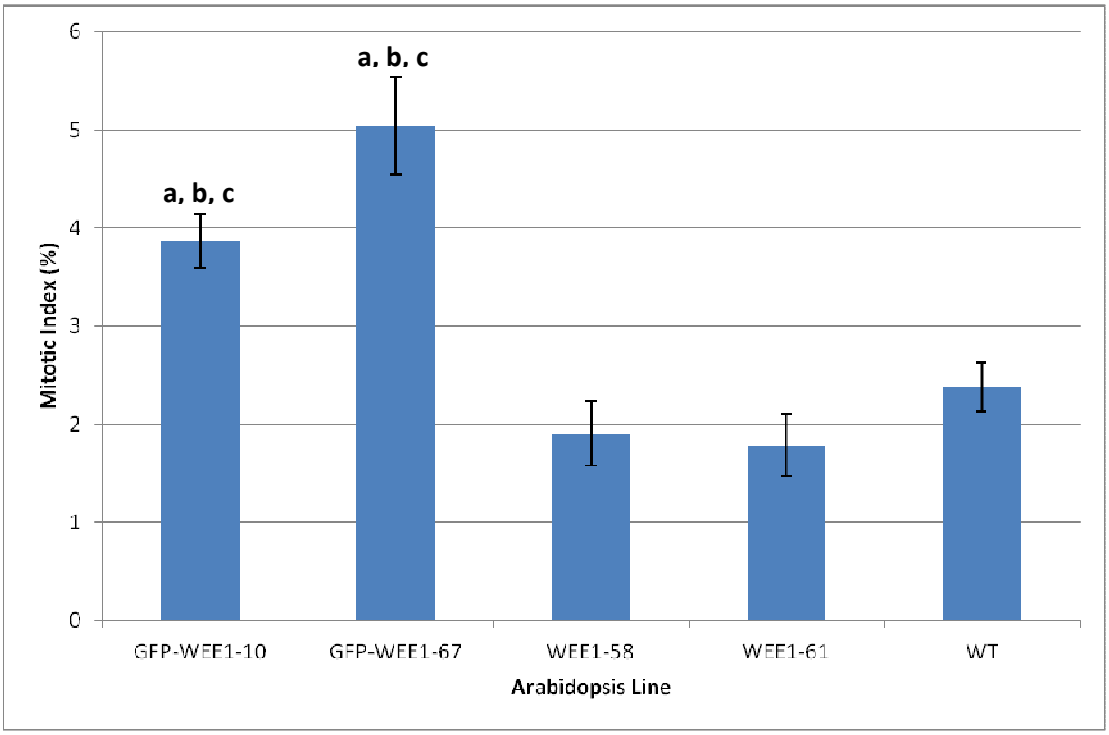

Figure 3.21 Mitotic index (±SE, n=3-6) in the root meristem of 7 day old seedlings of the GFP-*Arath*;WEE1-10 and -67 lines compared to *Arath*;WEE1 over-expressors (WEE1-58 and -61) and wild type (WT) *Arabidopsis*. a, b, c = significantly different from WEE1-58, WEE1-61, WT

3.3.4 *ARATH*;WEE1 LOCALISES TO THE NUCLEUS IN *ARABIDOPSIS* ROOT CELLS, AND ITS STABILITY IS TISSUE-DEPENDENT

In order to study the subcellular localisation of WEE1 in *Arabidopsis*, 5 day old seedlings from lines GFP-*Arath*;WEE1-10 and -67, and the control H2B-YFP, were counter-stained using propidium iodide and imaged under the confocal microscope (Section 2.3.7). As expected, a strong constitutive fluorescent signal was detected in the nuclei of H2B-YFP root cells (Figure 3.24). In the GFP-*Arath*;WEE1 lines a clear nuclear fluorescent signal was also detected (Figures 3.22 and 3.23). However, as seen in the GFP-*Arath*;WEE1-12 line, the signal appeared to be weaker in certain areas and tissues of the root (Figures 3.22, 3.23 and 3.24).

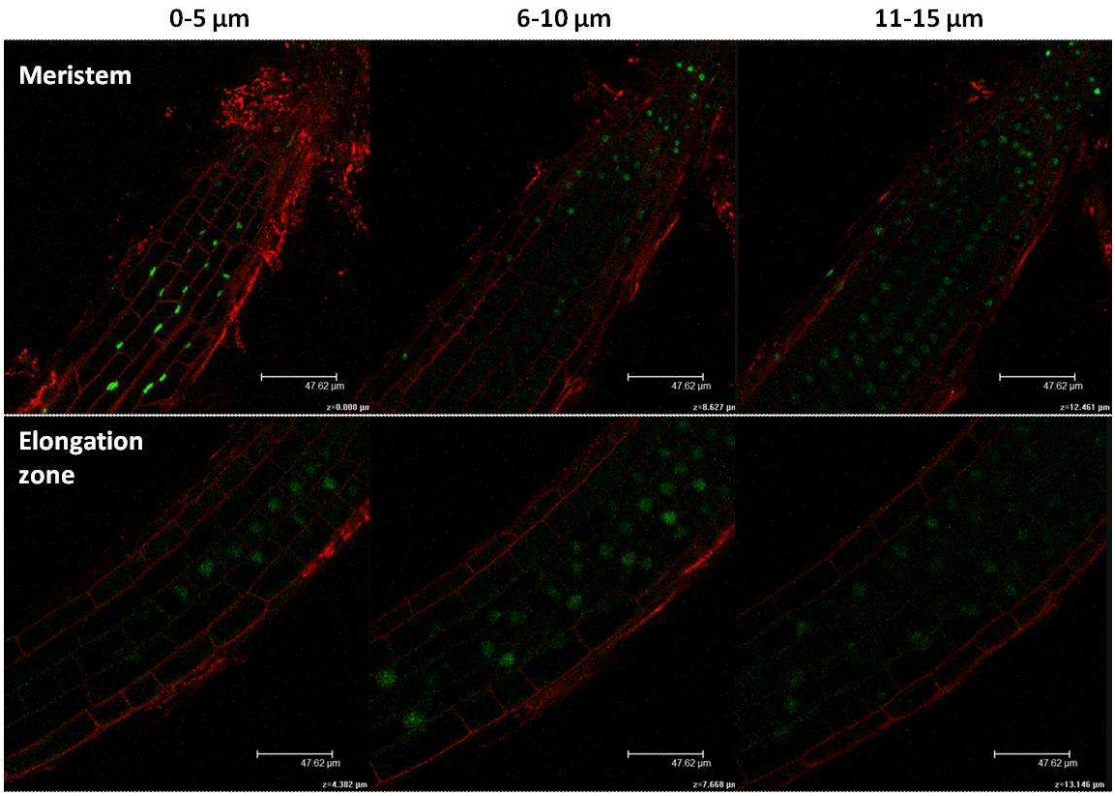

Figure 3.22 Confocal images of the GFP-*Arath*;WEE1-10 *Arabidopsis* line, showing the root tip and root elongation zone at sections 0-5, 6-10 and 11-15 µm from the surface of the root. Green colouring indicates GFP-*Arath*;WEE1 expression, red colouring is propidium iodide counter-stain for the cell walls. Representative images of at least 8 seedlings examined.

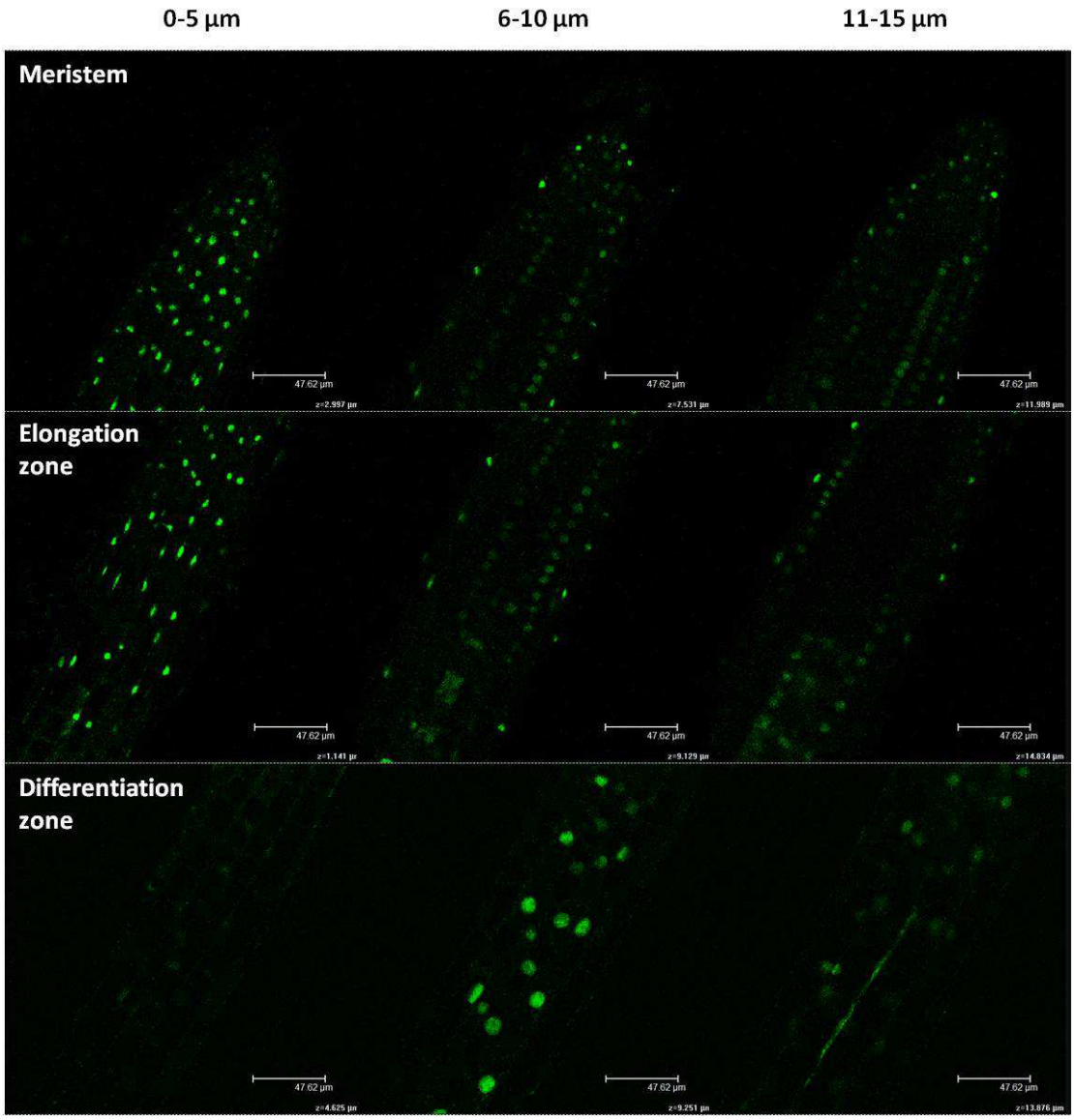

Figure 3.23 Confocal images of the GFP-*Arath*;WEE1-67 *Arabidopsis* line, showing the root tip and root elongation and differentiation zones at sections 0-5, 6-10 and 11-15 µm from the surface of the root. Green colouring indicates GFP-*Arath*;WEE1 expression. Representative images of at least 7 seedlings examined.

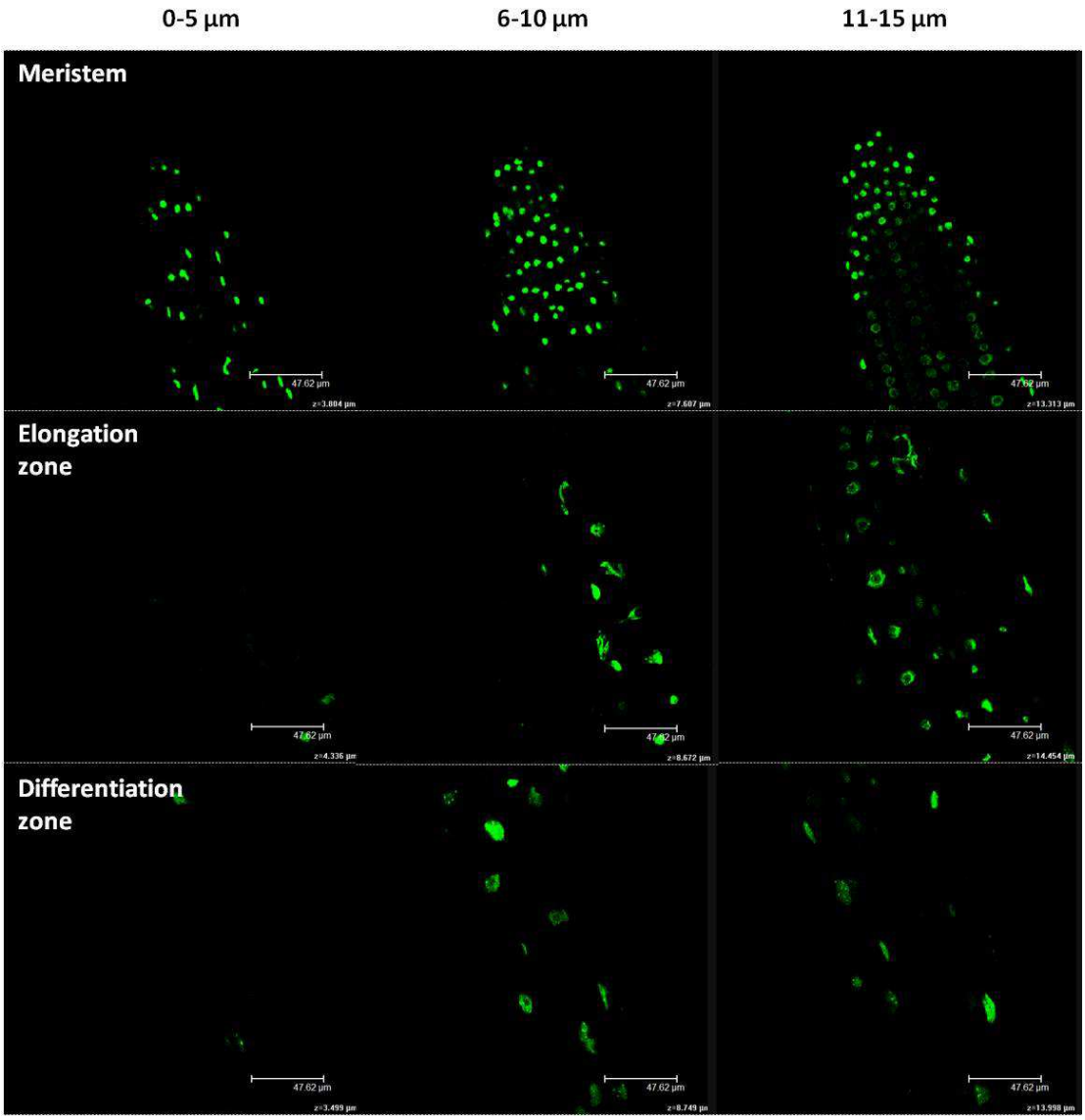

Figure 3.24 Confocal images of the H2B-YFP *Arabidopsis* line, showing the root tip and root elongation and differentiation zones at sections 0-5, 6-10 and 11-15 µm from the surface of the root. Green colouring indicates H2B-YFP expression. Representative images of at least 5 seedlings examined.

To investigate the potential differences in *Arath*;WEE1 protein levels in the different root tissues further and to try to confirm this observation, the fluorescent signal from each nucleus was quantified (expressed as average pixel intensity) in each line, and the signal in each tissue (epidermis, cortex and stele) compared to the other tissues in the same root zone (meristem, elongation zone and differentiation zone). Due to differences in confocal settings, the raw data could not be directly compared. However, the intensity of fluorescence in the nuclei of the epidermal cells was consistently higher than that of both the cortex and stele in all root zones in all three

lines. Therefore, by expressing the cortex and stele results as a ratio to epidermal signal intensity, differences in the pattern of GFP expression could be analysed.

Unlike the epidermis, in the meristem and elongation zone the fluorescent signals in the cortex and stele relative to that of the epidermis varied between the GFP-*Arath*;WEE1 lines and the H2B-YFP control line. In the meristem, the fluorescent signal in the cortex was 75% that of the epidermis in the H2B-YFP line (Figure 3.25). Similarly, signal intensity in the cortex of the GFP-*Arath*;WEE1-10 line was 68% that of the epidermis (Figure 3.25). However, in the GFP-*Arath*;WEE1-67 line the GFP signal in the cortex was significantly different from the H2B-YFP control, at 50% that of the epidermis (Figure 3.25). The fluorescence signal in the cell lineages destined to become the stele of the H2B-YFP meristem was only 42% of the epidermal signal (Figure 3.25). Both of the GFP-*Arath*;WEE1 lines had a higher GFP signal in the cell lineages destined to become the stele compared to the epidermis in the meristem compared to the H2B-YFP line, of 54% in line 10 and 57% in line 67 (Figure 3.25).

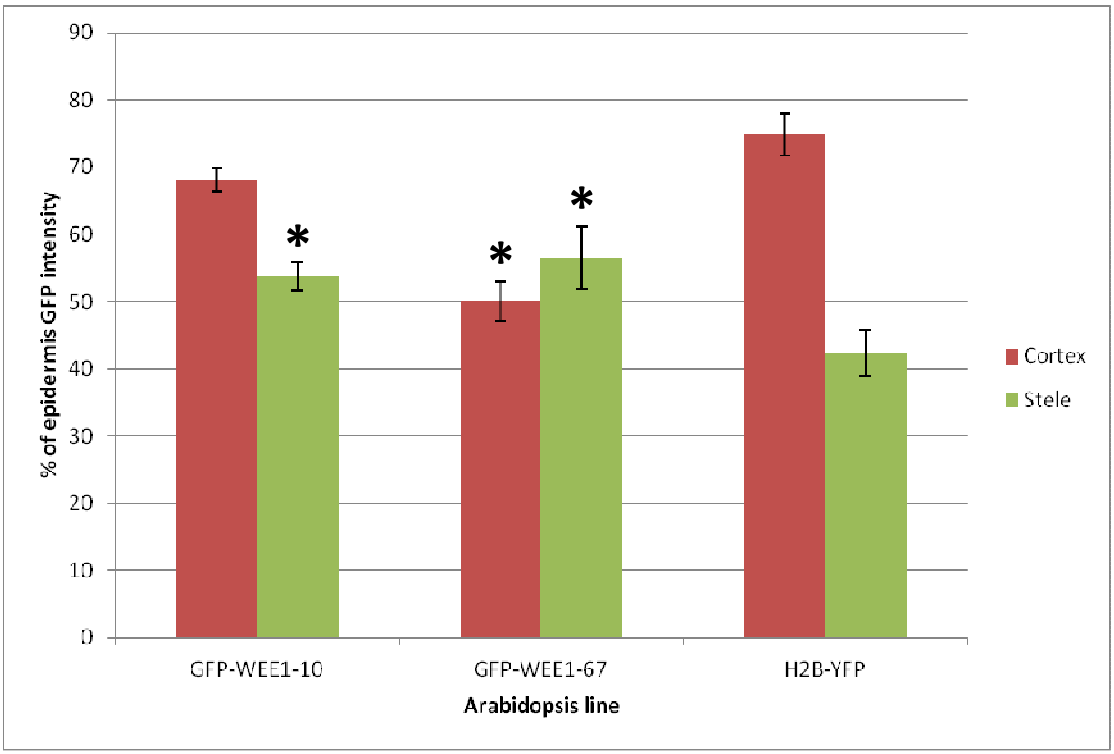

Figure 3.25 Ratio to epidermal GFP signal intensity (%, ±SE, n=75-433) in the cortex and cell lineages destined to become the stele of the root meristem of the GFP-*Arath*;WEE1-10, GFP-*Arath*;WEE1-67 and H2B-YFP *Arabidopsis* lines. * = significantly different from H2B-YFP (P<0.05).

In the root elongation zone, the fluorescent signal in the cortex of the H2B-YFP line was similar to that of the epidermis (Figure 3.26). In contrast, the signal in the cortex in both GFP-*Arath*;WEE1 lines was significantly lower than that of the epidermis than in the H2B-YFP line (Figure 3.26). The signal in the cortex of the GFP-*Arath*;WEE1-10 line was 78% that of the epidermis, while the signal of the GFP-*Arath*;WEE1-67 line was only 33% that of the epidermis (Figure 3.26). In the H2B-YFP line in the stele of the elongation zone the fluorescent signal was 74% that of the epidermis (Figure 3.26). The signal in the stele of the GFP-*Arath*;WEE1-10 line compared to the epidermis was similar to that of the H2B-YFP line, at 65% of the epidermis (Figure 3.26). However, in the GFP-*Arath*;WEE1-67 line the difference between the signal in the stele and epidermis was much larger, with the signal in the stele being only 30% that of the epidermis (Figure 3.26).

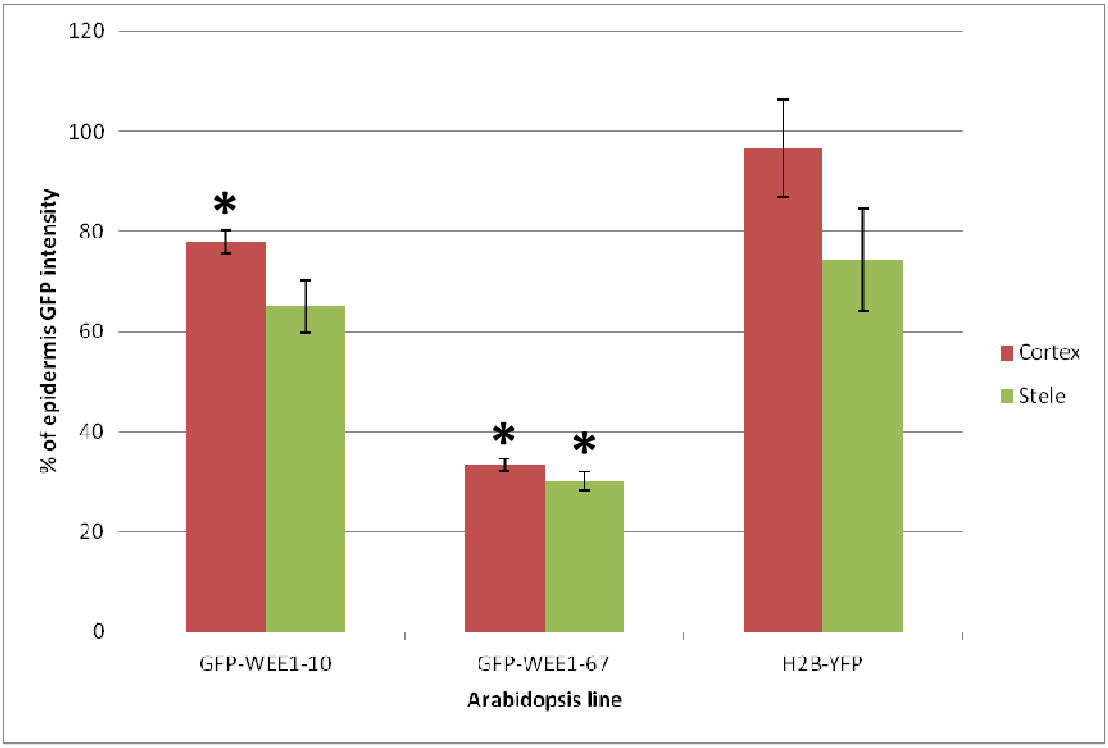

Figure 3.26 Ratio to epidermal GFP signal intensity (%, ±SE, n=18-192) in the cortex and stele of the root elongation zone of the GFP-*Arath*;WEE1-10, GFP-*Arath*;WEE1-67 and H2B-YFP *Arabidopsis* lines. * = significantly different from H2B-YFP (P<0.05).

In the root differentiation zone, the fluorescence signal compared to the epidermis in both the cortex and the stele of the GFP-*Arath*;WEE1-67 line was similar to that of the H2B-YFP line (Figure 3.27). No data were collected from the differentiation zone of the GFP-*Arath*;WEE1-10 line.

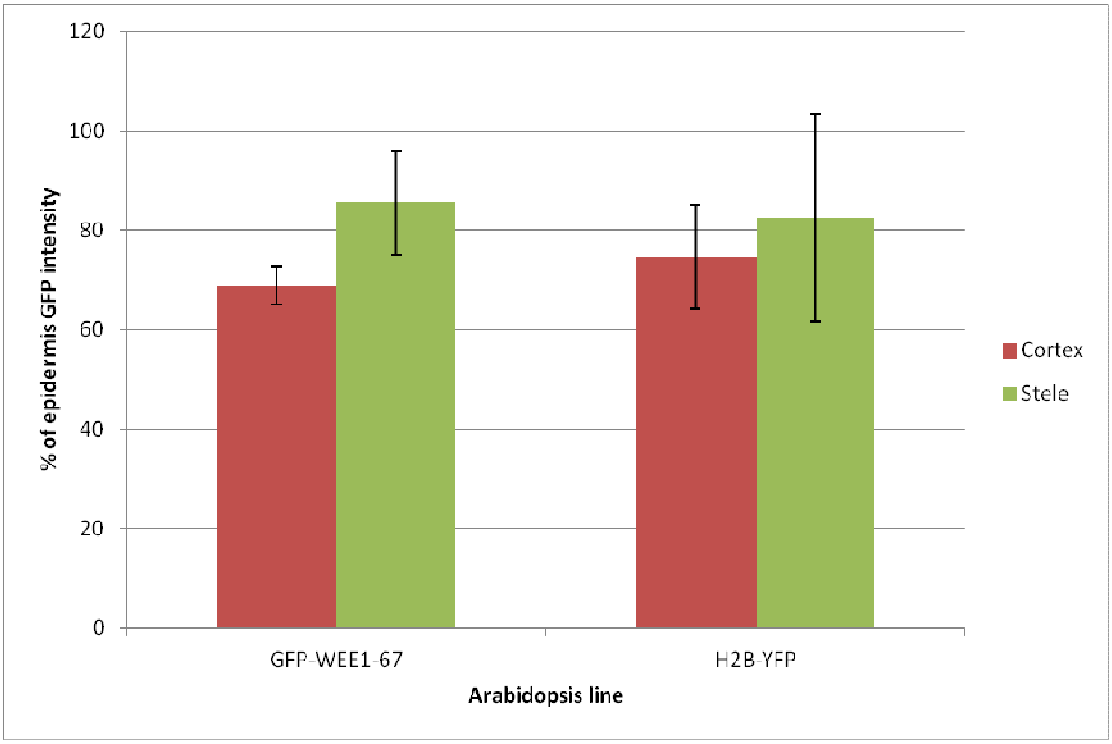

Figure 3.27 Ratio to epidermal GFP signal intensity (%, ±SE, n=5-157) in the cortex and stele of the root differentiation zone of the GFP-*Arath*;WEE1-67 and H2B-YFP *Arabidopsis* lines.

Propidium iodide is able to enter and label dead cells. In several seedlings, especially in line GFP-*Arath*;WEE1-10, dead cells, heavily stained by propidium iodide, were observed in the elongating and differentiating stelar cells (Figure 3.28). This was primarily assumed to be caused by damage to the seedlings on removal from the agar, but the phenomenon was not observed in H2B-YFP or wild type seedlings.

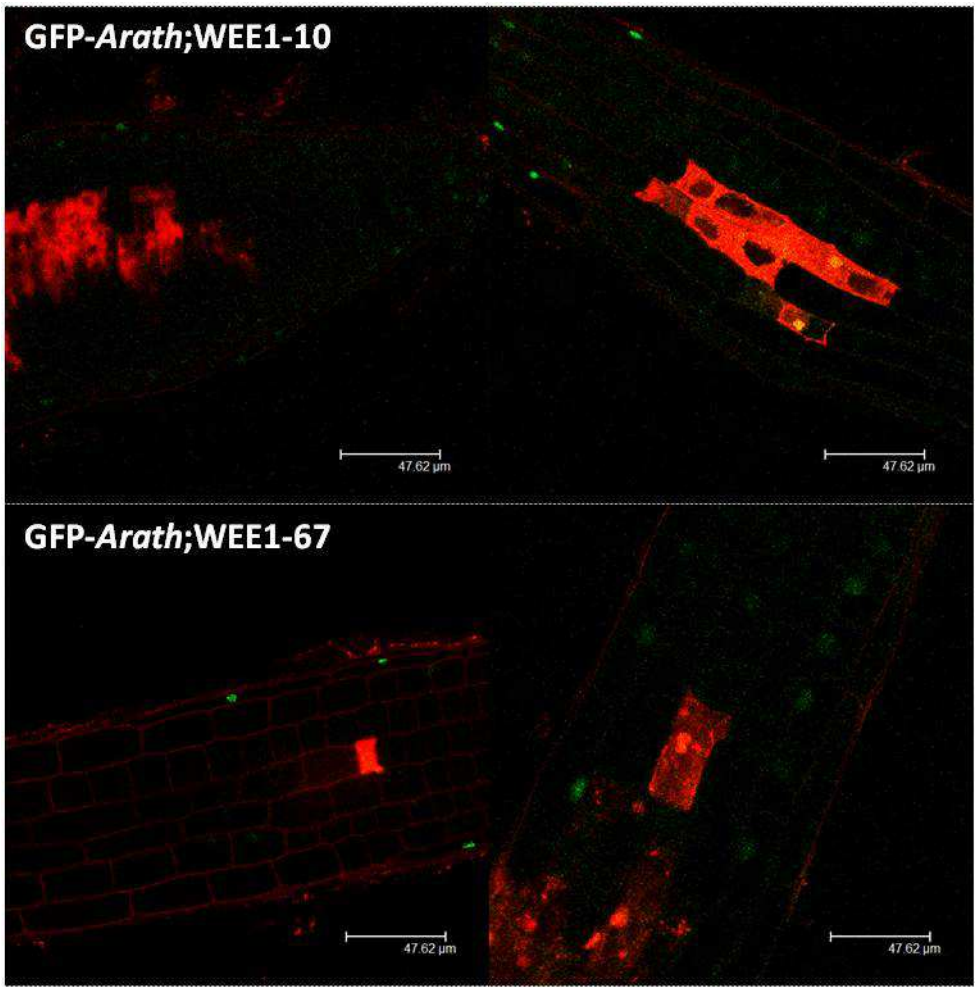

Figure 3.28 Propidium iodide staining of dead cells in the elongation and differentiation zones of GFP-*Arath*;WEE1-10 and -67 roots. Green colouring indicates GFP-*Arath*;WEE1 expression, red colouring is propidium iodide counter-stain for the cell walls. Representative images of at least 7 seedlings examined.

WEE1 localisation in lateral root primordia was also examined. Fourteen day old seedlings were counter-stained with propidium iodide and imaged using the confocal microscope (Section 2.3.7). In line GFP-*Arath*;WEE1-10 a weak GFP signal was observed in the nuclei of the basal cells of the lateral root primordia, but fluorescence was not detected in the rest of the primordium (Figure 3.29). In line GFP-*Arath*;WEE1-67 a fluorescent signal could not be detected in the cells of the lateral root primordia (Figure 3.29). In contrast, in the H2B-YFP line, strong constitutive nuclear YFP expression was observed throughout the lateral root primordia (Figure 3.29).

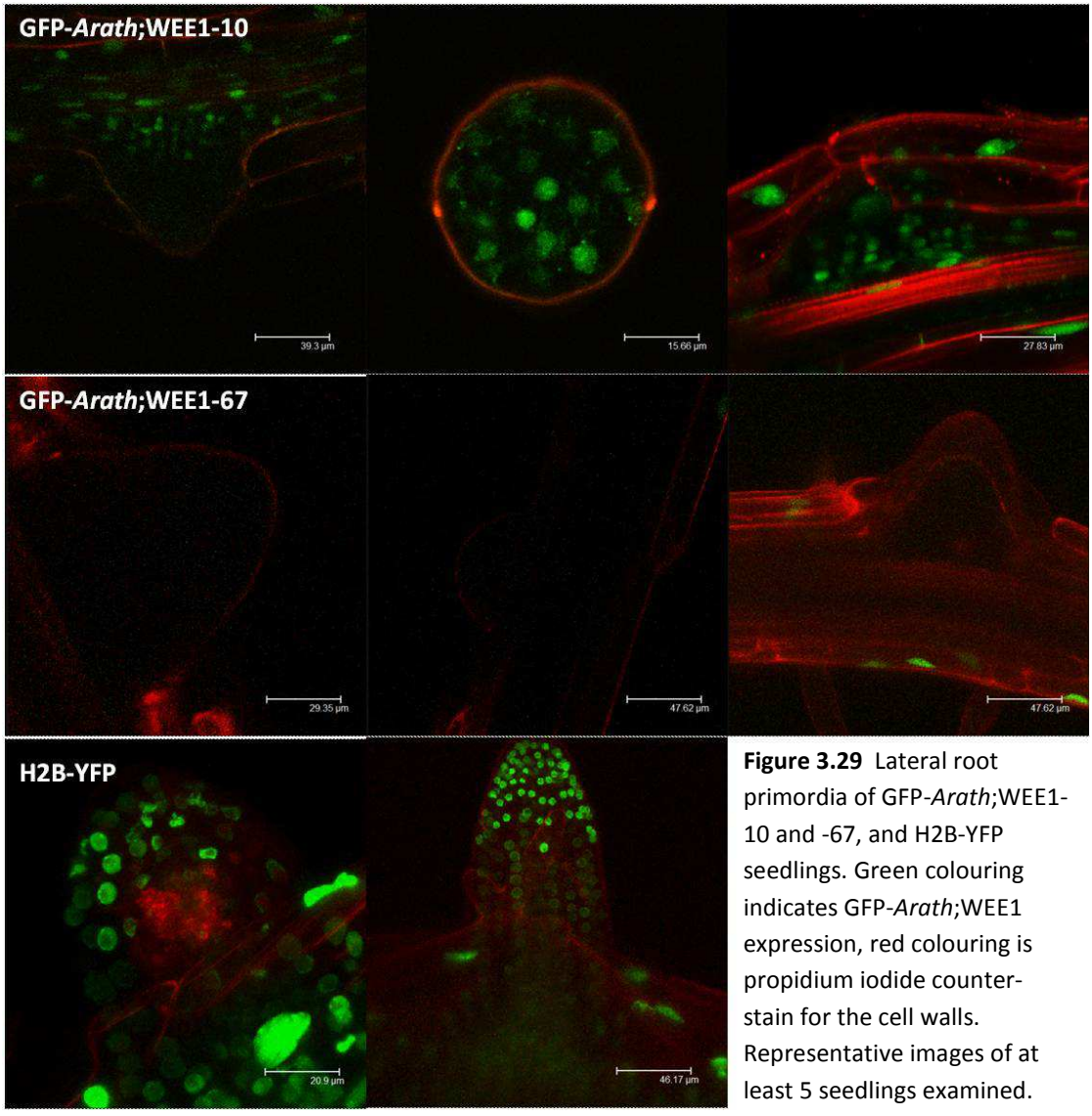

Figure 3.29 Lateral root primordia of GFP-*Arath*;WEE1-10 and -67, and H2B-YFP seedlings. Green colouring indicates GFP-*Arath*;WEE1 expression, red colouring is propidium iodide counter-stain for the cell walls. Representative images of at least 5 seedlings examined.

3.3.5 *ARATH*;WEE1 IS DEGRADED VIA THE 26S PROTEASOME DEGRADATION PATHWAY

The proteasome inhibitor MG132 was used to determine whether the differences in the level of fluorescent signal between tissues in the GFP-*Arath*;WEE1 lines were caused by differences in *Arath*;WEE1 stability. Five day old GFP-*Arath*;WEE1-67 seedlings were treated with MG132 or mock-treated with DMSO (Section 3.2.3), counter-stained with propidium iodide and imaged using the confocal microscope (Section 2.3.7). The confocal settings were not altered between the imaging of the MG132-treated and mock-treated seedlings to allow for accurate and direct comparison between the two treatments. GFP signal was clearly increased in the MG132-treated seedlings relative to the mock-treated seedlings (Figure 3.30). Quantification of the fluorescent signal showed that there was a significant, two-fold increase in GFP signal in the MG132 treated seedlings compared to the mock-treated seedlings (Figure 3.31). Additionally, western blotting was used in an attempt to confirm the increase in *Arath*;WEE1 protein level in MG132-seedlings compared to the mock-treated seedlings, however this was unsuccessful (see Appendix III).

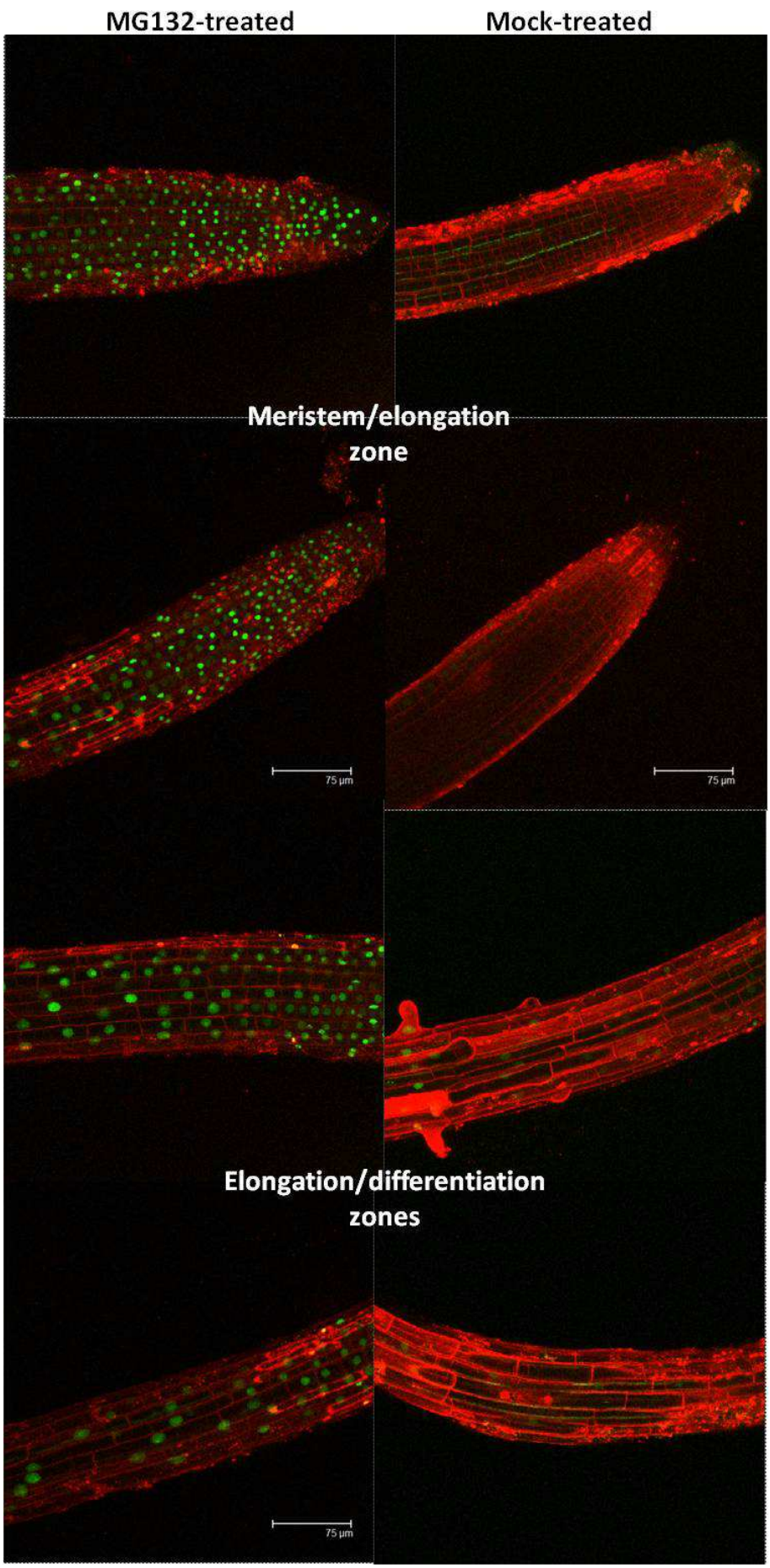

Figure 3.30 Roots of MG132- and mock-treated GFP-*Arath*;WEE1-67 seedlings. Green colouring indicates GFP-*Arath*;WEE1 expression, red colouring is propidium iodide counter-stain for the cell walls. Representative images of 3 seedlings examined for each treatment.

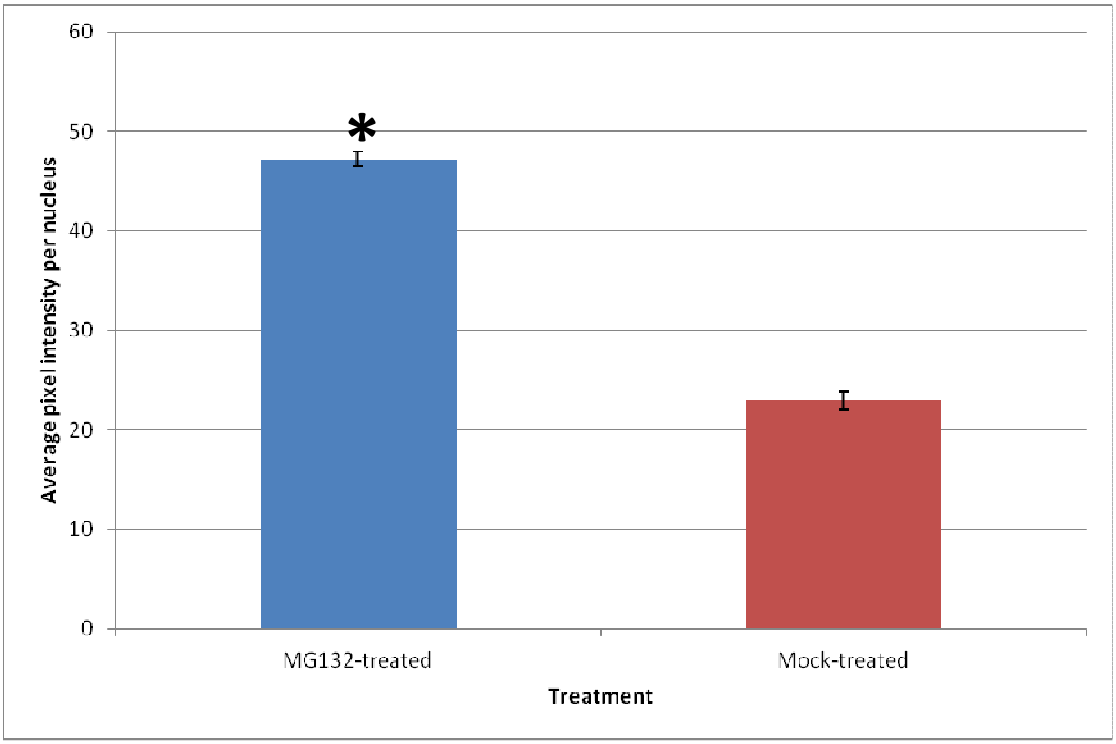

Figure 3.31 GFP signal intensity (±SE, n=466-2121) in the roots of 5 day old seedlings of the GFP-*Arath*;WEE1-67 line treated with MG132 or mock-treated. * = significantly different from mock treatment (P<0.05).

The levels of fluorescence in each tissue type (epidermis, cortex and stele) were compared between MG132- and mock-treated seedlings. In the meristem/elongation zone the fluorescent signal in the epidermis of MG132-treated roots was approximately 3-fold higher compared with mock-treated seedlings, while the fluorescent signal in the stele of MG132-treated roots was significantly higher than the zero signal recorded in the stele of mock-treated seedlings (Figure 3.32a). In contrast, the level of fluorescent signal in the cortex was similar whether MG132-treated or mock-treated (Figure 3.32a). In the elongation/differentiation zones, the fluorescent signal was significantly higher in the epidermis and cortex of the MG132-treated roots than in the epidermis and cortex of the mock-treated roots (Figure 3.32b). In the stele, however, the level of fluorescence was similar between MG132-treated and mock-treated seedlings (Figure 3.32b).

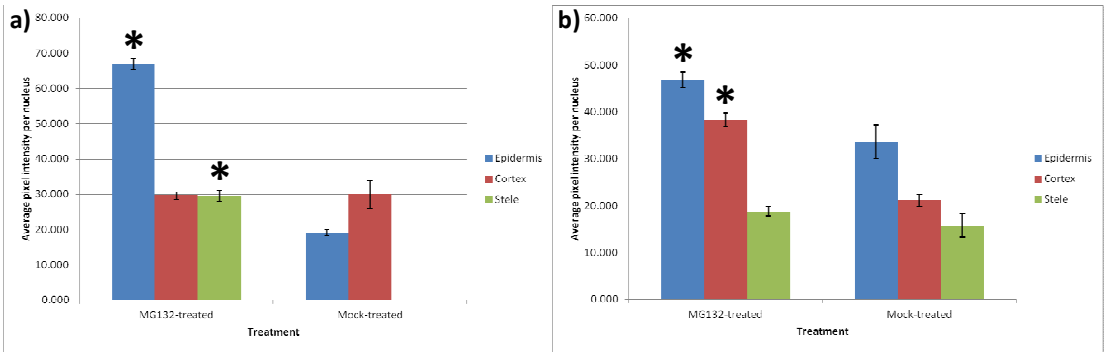

Figure 3.32 GFP signal intensity (±SE, n=23-770) in the a) meristem/elongation zone and b) elongation/differentiation zones in the roots of 5 day old seedlings of the GFP-*Arath*;WEE1-67 line treated with MG132 or mock-treated. * = significantly different from mock treatment (P<0.05).

3.4 DISCUSSION

The spatial and temporal control of cell cycle regulators is important for ensuring that cell cycle progression occurs in an accurate and timely manner. Therefore the localisation and stability of higher plant WEE1 could provide information about its role in the plant cell cycle. In the work described here, the expression of GFP-*Arath*;WEE1 under the 35S promoter in tobacco BY-2 cell cultures allowed the study of the change in localisation of the protein during the cell cycle. Synchronised GFP-*Arath*;WEE1 and control 35S-GFP BY-2 cultures both peaked in mitotic index after 9 and 22 hours, similar to wild type, but unlike previously recorded results for BY-2 cultures expressing *Arath*;WEE1, where premature mitosis was observed (Siciliano, 2006; Lentz Grønlund, 2007; Spadafora, 2008). However, in the previous studies the premature mitosis was found to be due to a reduced G2 phase (Siciliano, 2006), which was also observed in the GFP-*Arath*;WEE1 line, compensated by a lengthening of G1 (Figure 3.3, Appendix I). This resulted in a cell cycle duration of 13 hours (Figure 3.3), which was typical of both wild type and *Arath*;WEE1 expression (Orchard et al., 2005; Siciliano, 2006; Spadafora, 2008).

The mitotic cell size of the 35S-GFP BY-2 cells was double that of the approximately 3000 μm^2 previously recorded for wild type BY-2 cells (Figure 3.4; Siciliano, 2006; Spadafora, 2008). However, GFP-*Arath*;WEE1 BY-2 mitotic cells were 3-fold smaller than 35S-GFP cells (Figure 3.4), showing a similar small cell

phenotype to that previously recorded for the expression of *Arath*;WEE1 in BY-2 cells (Siciliano, 2006; Spadafora, 2008). It is important to note that the cells measured here were taken from a culture grown in 29 mL of medium as opposed to the more standard 95 mL, which could have an effect on cell size. It would be interesting, therefore, to compare this cell size data with measurements from wild type cells grown in only 29 mL of medium.

In human cells, WEE1 localisation alters early in mitosis, being removed from the nucleus. This physically removes WEE1 inhibition from the CDK-cyclin complex driving mitotic progression (Baldin and Ducommun, 1995). The GFP BY-2 lines were used to assess changes in *Arath*;WEE1 localisation during mitosis. In the 35S-GFP BY-2 line, GFP expression was observed in 100% of cells in all cell cycle phases (Figure 3.7). This is to be expected; although the levels of expression from the 35S promoter may vary with cell cycle phase (Nagata et al., 1987), the GFP protein is expected to remain stable throughout the cell cycle, since GFP degradation during the cell cycle is dependent upon signals targeting the protein to which it is fused (Corish and Tyler-Smith, 1999). This means that in the GFP-*Arath*;WEE1 BY-2 line, which was also under the control of the 35S promoter, any removal of GFP signal would be due to the targeted degradation of *Arath*;WEE1. In the GFP-*Arath*;WEE1 BY-2 line, *Arath*;WEE1 expression was only observed in 4% of prophase cells, and was never observed in metaphase cells, with expression increasing in anaphase and telophase cells (Figures 3.5 and 3.6). This indicates that *Arath*;WEE1 is removed during prophase and suggests that *Arath*;WEE1 degradation may be a requirement for mitotic progression. These results are supported by the confocal imaging of a cross between the GFP-*Arath*;WEE1 line 12 and a line containing RFP-*Arath*;SUN1, a nuclear envelope marker (Figure 3.8; Graumann et al., 2009). In this *Arabidopsis* line, a nuclear GFP signal was observed in root cells during interphase and telophase, but no GFP signal was visible during metaphase (Figure 3.8).

GFP-*Arath*;WEE1 was also expressed in *Arabidopsis* plants under the strong constitutive 35S promoter. Three homozygous lines (12, 10 and 67) were isolated and found to be over-expressing *Arath*;*WEE1* at levels 2- to 4-fold higher than *Arath*;*WEE1* expression levels in wild type plants (Figures 3.9 and 3.14). The

number of insertions of the GFP-*Arath*;WEE1 transgene was analysed in lines GFP-*Arath*;WEE1-10 and -67. Interestingly, line GFP-*Arath*;WEE1-10, which was shown by semi-quantitative RT-PCR to be expressing *Arath*;*WEE1* at a level 4-fold higher than that of wild type, was found to contain only one copy; while line GFP-*Arath*;WEE1-67, which was only expressing *Arath*;*WEE1* at a level double that of wild type, was calculated to contain more than one copy of the GFP-*Arath*;WEE1 transgene (Section 3.3.3). It is therefore possible that the introduction of more than one copy of the transgene led to partial silencing, as has been found in other systems (reviewed by Stam et al., 1997; Fagard and Vaucheret, 2000).

The root phenotypes of the three GFP-*Arath*;WEE1 lines were compared to the root phenotypes of wild type plants and the previously described *Arath*;WEE1 over-expressors, WEE1-58 and WEE1-61 (Spadafora, 2008). In both the WEE1-58 and WEE1-61 lines, *Arath*;*WEE1* was expressed at levels ten-fold higher than wild type (Spadafora, 2008). It was expected that the GFP-*Arath*;WEE1 lines would display a similar phenotype to that already described for the *Arath*;WEE1 over-expressing lines, with slower primary root growth and fewer lateral roots and primordia compared to wild type (Spadafora, 2008). This WEE1 over-expression phenotype was observed in WEE1-58 and WEE1-61, however the root phenotype of GFP-*Arath*;WEE1-12 was similar to wild type and roots developed normally (Figures 3.10, 3.11 and 3.12). This might imply that the fusion protein was not functional in the GFP-*Arath*;WEE1-12 line.

In a separate experiment, the root phenotypes of GFP-*Arath*;WEE1 lines 10 and 67 were also compared to that of wild type and the *Arath*;WEE1 over-expressors. While the root phenotype of WEE1-61 was consistent with previous results, the WEE1-58 line exhibited faster primary root growth and a similar number of lateral roots and primordia compared to wild type, despite the seed originating from the same stock as those used above (Figures 3.15, 3.16 and 3.17). This difference in results could be due to the inherent variability of *Arabidopsis*, or due to a subtle difference in the growth conditions. *Arabidopsis* seedlings are particularly sensitive to changes in the sucrose concentration of the medium, so a very small difference between experiments could have led to the opposing phenotypes (Rognoni et al., 2007; Gibson, 2005). The root phenotypes of lines GFP-*Arath*;WEE1-10 and -67 were

consistent with WEE1-58 in having faster primary root elongation (Figures 3.15). However, roots of both GFP-*Arath*;WEE1 lines also had a higher rate of lateral root production than wild type after seven days, and roots of GFP-*Arath*;WEE1-67 also had more lateral roots after fourteen days (Table 3.4). The increase in lateral roots is more similar to an *Arath*;WEE1 knockout phenotype (Lentz Grønlund, 2007), therefore may indicate a loss of WEE1 function in the GFP-*Arath*;WEE1 lines. This could be caused by the mis-folding of the protein due to the attached GFP fragment leading to the removal of both WT and transgenic WEE1. A similar mechanism has been postulated in the Cardiff lab to explain anomalous results obtained when *Arath;WEE1* is expressed in tobacco cells (Cardiff lab, unpublished data).

An increase in WEE1 expression levels is known to result in increased cell length in other systems, such as fission yeast, by the inhibition of cell division (Russell and Nurse, 1987). *Arabidopsis* WEE1 has been previously demonstrated to induce long cells when expressed in fission yeast (Sorrell et al., 2002). It was expected that the over-expression of *Arath*;WEE1 in the GFP-*Arath*;WEE1 lines would lead to an increase in cell size in the root meristem compared to wild type. Cell length and width varied between lines in all cell layers. In the epidermis, the cell width in WEE1-58 was greater compared to wild type, as were the widths of epidermal cells in the GFP-*Arath*;WEE1-10 and -67 lines (Figure 3.18). However cell width was similar in all lines in the cortex and cell lineages destined to become the stele (Figure 3.18). Cell length was more variable. While WEE1-58 epidermal cell length was greater compared to wild type, the epidermal cell lengths of the GFP-*Arath*;WEE1 lines were similar to wild type (Figure 3.18). In the cortex, GFP-*Arath*;WEE1-67 and WEE1-58 cells were similar in length to wild type, whereas GFP-*Arath*;WEE1-10 and WEE1-61 cells were shorter than wild type. In the cell lineages destined to become the stele, only GFP-*Arath*;WEE1-67 cells were longer than wild type (Figure 3.18). The overall area of the root meristem was found to be similar to wild type in all lines, however the meristems of GFP-*Arath*;WEE1-10 and -67 and WEE1-58 were larger than WEE1-61 meristems (Figure 3.20), which could be explained by the differences observed in cell size. The most pronounced changes in cell length and width in the GFP-*Arath*;WEE1 lines compared to wild type were seen in the epidermis, which may imply a role for *Arath*;WEE1 in this tissue. In the

Arath;WEE1 insertion mutant line, *wee1-1*, shorter epidermal cells were observed, as expected for a line deficient in WEE1 expression (G. Rafiei, Cardiff lab, unpublished data). Overall the cell size results are as expected for WEE1 over-expression, with generally longer cells observed, contradicting the root phenotyping results described above which implied an impairment of *Arath*;WEE1 function in the GFP-*Arath*;WEE1 lines. This could indicate that the gene was actually functional in these lines, with the phenotypic variation being caused by variation in the media, as postulated for the differences in phenotype recorded for WEE1-58.

If *Arath*;WEE1 has a role in the inhibition of mitosis during an unperturbed cell cycle, as recorded in other organisms (Den Haese et al., 1995; Booher et al., 1993; Russell and Nurse, 1987; Featherstone and Russell, 1991) it would be expected that an increase in *Arath*;WEE1 expression would lead to a reduction in the incidence of mitosis in the root meristem. However, in the GFP-*Arath*;WEE1 lines the mitotic index in the *Arabidopsis* root meristem was found to be significantly greater in comparison to wild type and the *Arath*;WEE1 over-expressors (Figure 3.21). Strangely this is not reflected by an increase in cell number in the root meristems of the GFP-*Arath*;WEE1 lines (Figure 3.19). The increased mitotic index could explain the increase in number of lateral roots in the GFP-*Arath*;WEE1 lines compared to wild type (Figures 3.16 and 3.17). Overall it is unclear from the comparison of root phenotypes whether or not the *Arath*;WEE1 protein expressed as part of the GFP fusion was functional, however this does not necessarily mean that the localisation of *Arath*;WEE1 observed in these lines is not accurate. In fact, the functionality of the fusion protein is rarely published alongside localisation data (Boruc et al., 2010; Sozzani et al., 2010; Srilunchang et al., 2010).

Roots of the GFP-*Arath*;WEE1-12 line were screened using confocal microscopy, however only one seedling exhibited a fluorescent signal strong enough to be imaged (Figure 3.13). An explanation for this could be the lack of functionality of the fusion protein demonstrated above by the lack of abnormal root phenotype (Figures 3.10, 3.11 and 3.12), for example, if the protein was mis-folded, it could be targeted for degradation. The GFP-*Arath*;WEE1-10 and -67 lines were isolated as lines exhibiting a stronger GFP signal, and imaged alongside 35S-H2B-YFP as a control. The H2B-YFP fusion protein is known to localise to the nucleus in Arabidopsis root

cells (Boisnard-Lorig et al., 2001; Figure 3.24). *Arath*;WEE1 was confirmed to localise to the nucleus in both GFP-*Arath*;WEE1 lines, as previously described (Figures 3.22 and 3.23; Boruc et al., 2010; Cools et al., 2011).

The strength of the GFP signal in both GFP-*Arath*;WEE1 lines appeared to vary according to tissues and sections of the root, so the strength of the fluorescent signal was quantified to allow for more objective comparisons. In all root sections, the GFP signal was consistently higher in the epidermis than in the other tissues, in the H2B-YFP line as well as in the GFP-*Arath*;WEE1 lines, indicating that this is not a WEE1 effect. In the cortex of the meristem, the lower signal compared to the epidermis observed in the GFP-*Arath*;WEE1-67 line compared to that of the H2B-YFP line was not reflected in the GFP-*Arath*;WEE1-10 line, so this may be a positional effect (Figure 3.25). In contrast, the GFP signal in the cell lineages destined to become the stele was higher compared to the epidermis in both GFP-*Arath*;WEE1 lines compared to the H2B-YFP line (Figure 3.25). This suggests that WEE1 degradation is reduced in the cell lineages destined to become the stele compared to the other tissues, so WEE1 may be important for inhibiting mitosis in the cell lineages destined to become the stelar tissue of the meristem. This is in contrast to data from *in situ* hybridisation in the root apical meristem of *Arabidopsis*, where weak *Arath*;*WEE1* expression was observed in the cortex and stele, with a slightly stronger signal in the epidermis (Engler et al., 2009).

In the elongation zone this pattern was reversed. In the stele, the lower signal in the GFP-*Arath*;WEE1-67 line compared to the H2B-YFP line was not reflected in the GFP-*Arath*;WEE1-10 line, so again this is likely to be a positional effect (Figure 3.26). In contrast, the GFP signal in the cortex was lower compared to the epidermis in both GFP-*Arath*;WEE1 lines compared to the H2B-YFP line (Figure 3.26). This suggests that more WEE1 is removed in the cortical tissue, indicating that perhaps WEE1 is no longer required. This could either be because these cells are no longer going through the cell cycle, or because WEE1 must be removed for mitosis to proceed. However, this pattern is again in contrast to data from *in situ* hybridisation, where *WEE1* expression was not detected in the epidermis or stele of the *Arabidopsis* root elongation zone, but a weak signal was observed in the cortex (Engler et al., 2009).

In the differentiation zone, the fluorescence signal compared to the epidermis in both the cortex and stele of the GFP-*Arath*;WEE1-67 line was similar to that of the H2B-YFP line (Figure 3.27). This implies that WEE1 is stable in this section of the root and may reflect the fact that differentiated cells are no longer going through the cell cycle, so may not possess the mechanism for WEE1 removal. Data from *in situ* hybridisation indicated that while *WEE1* was sometimes expressed in the epidermis and cortex of young *Arabidopsis* roots, it was strongly expressed in the vascular tissue, and patchy expression in the xylem indicated tight regulation (Engler et al., 2009).

It is important to remember that, due to the use of the 35S promoter, *WEE1* was expressed ectopically in these transgenic lines, hence the differential removal of WEE1 protein in these tissues may not reflect the *in vivo* situation. The results would need to be further verified through the expression of the GFP-*Arath*;*WEE1* fusion under the native *Arath*;*WEE1* promoter.

Timely degradation of cell cycle proteins is frequently achieved via the 26S proteasome degradation pathway, including cyclins in plants (Genschik et al., 1998). WEE1 degradation is also achieved via the 26S proteasome degradation pathway, as demonstrated in budding yeast (Simpson-Lavy and Brandeis, 2010), *Xenopus* (Michael and Newport, 1998) and humans (Watanabe et al., 2004). However, the mechanism for the degradation of WEE1 protein in plants is yet to be described. A 26S proteasome inhibitor, MG132 (Rock et al., 1994), was used to treat seedlings from line GFP-*Arath*;WEE1-67, halving degradation of *Arath*;WEE1 protein (Figures 3.30 and 3.31). This clearly indicates that *Arath*;WEE1 protein is degraded via the 26S proteasome degradation pathway and that the low level of GFP-*Arath*;WEE1 signal observed in root cells was likely to be due to high levels of *Arath*;WEE1 proteolysis.

The results described in this chapter were all obtained using the GFP-*Arath*;WEE1 construct under the control of the 35S promoter. It provided a useful tool for looking at the stability of *Arath*;WEE1 protein, but may not accurately reflect the tissues in which endogenous *Arath;*WEE1 is expressed. The expression pattern of *Arath*;WEE1-GFP under the endogenous *Arath*;*WEE1* promoter was recently

described by Cools et al. (2011). A GFP signal was only observed in roots subjected to replication stress (imposed by hydroxyurea treatment), leading to the conclusion that *Arath*;WEE1 is not expressed in unperturbed roots. However, it could be argued that turnover of *Arath*;WEE1 in the roots was so high that levels of GFP-*Arath*;WEE1 were too low to allow detection. Hence, it would be interesting to study the effects of MG132-treatment on P_{WEE1}:*Arath*;WEE1-GFP plants.

The effect of MG132 treatment on the pattern of *Arath*;WEE1 degradation in the different root tissues of the GFP-*Arath*;WEE1 lines 10 and 67 was also examined. In the meristem/elongation zone, *Arath*;WEE1 protein was highly stabilised in the epidermis and stele by MG132-treatment (Figure 3.32), implying that *Arath*;WEE1 degradation is usually higher in these tissues. In contrast, *Arath*;WEE1 protein levels were similar in the cortex of the meristem/elongation zone of MG132- and mock-treated seedlings (Figure 3.32), indicating that degradation of *Arath*;WEE1 is usually low in cortical cells. This is supported by data on *Arath*;*WEE1* transgene levels from *in situ* hybridisation, which indicated that *WEE1* is not usually expressed in the epidermis and stele of the elongation zone, with weak expression in the cortex (Engler et al., 2009). Similarly, *Arath*;WEE1 degradation was decreased in the epidermis and cortex in the elongation/differentiation zones of MG132-treated roots, while there was no change in the degradation of *Arath*;WEE1 in stele cells (Figure 3.32), suggesting that there is usually a relatively higher degradation of *Arath*;WEE1 in the epidermis and cortex. Again, this is supported by data from *in situ* hybridisation, which indicated that *Arath*;*WEE1* expression is high in the vascular tissue of young roots, and sometimes expressed in the epidermis and cortex (Engler et al., 2009). The MG132 data also fit with the conclusions drawn from the GFP signals in the root tissues of untreated GFP-*Arath*;WEE1 seedlings, which indicated that WEE1 may be important in the cell lineages destined to become the stele of meristematic cells and in the cortex of cells of the root elongation zone (Section 3.3.4). However, the relatively higher levels of degradation in the epidermis contrast with the observation that the GFP signal was consistently higher in the epidermis of untreated seedlings (Section 3.3.4). This may be a compensation for the ectopic expression of *Arath*;*WEE1* in these lines via the 35S promoter, as *Arath*;*WEE1* is

usually expressed at low levels in the epidermis of both the elongation zone and young roots (Engler et al., 2009).

The root phenotype results implied a role for *Arath*;WEE1 in lateral root initiation, so GFP-*Arath*;WEE1 expression was examined in lateral root primordia. *Arath*;WEE1 expression was reduced in both GFP-*Arath*;WEE1 lines, to the point of being undetectable in line GFP-*Arath*;WEE1-67, whereas H2B-YFP was strongly and constitutively expressed in the lateral root primordia (Figure 3.29). This implies a high turnover of *Arath*;WEE1 in lateral root primordia, supporting a role for *Arath*;WEE1 degradation in the initiation of lateral root growth. This is further supported by the down-regulation of *Arath*;*WEE1*, compared to its usual expression in the pericycle, observed in roots stimulated to produce laterals by NAA-treatment (Engler et al., 2009). It would be interesting to study whether or not the GFP signal is re-established in more mature lateral roots to match the pattern of *Arath*;WEE1 protein turnover observed in primary roots. Another interesting application of MG132 would be to confirm that the low level of GFP-*Arath*;WEE1 signal observed in lateral roots was due to high *Arath*;WEE1 protein turnover.

It would also be interesting to study the effects of MG132-treatment on GFP-*Arath*;WEE1 degradation in BY-2 cells. It might be expected that MG132 would stabilise *Arath*;WEE1 protein, allowing it to be visible at metaphase. MG132-treatment has been shown to block cell cycle progression in BY-2 cells, due to the prevention of the degradation of cyclins, but cells were arrested in metaphase (Genschik et al., 1998), which should be sufficient to see the effect on *Arath*;WEE1 degradation. MG132 could also be applied to seedlings of the GFP-*Arath*;WEE1/RFP-*Arath*;SUN1 cross.

Recently, *Arath*;WEE1 was shown to have a role in protecting against premature vascular differentiation in *Arabidopsis* roots under replication stress (Cools et al., 2011). Differentiated vascular tissue is characterised by dead cells, which propidium iodide is able to penetrate and stain fully. During the confocal imaging of both the GFP-*Arath*;WEE1 lines 10 and 67, dead cells were frequently observed in the stele of the elongation and differentiation zones (Figure 3.28). These were never observed in the wild type and H2B-YFP lines, implying a WEE1 effect. However, in the

previously described study, these prematurely differentiating cells were only observed in a *wee1* knockout background when the plants were under replication stress (imposed by hydroxyurea treatment; Cools et al., 2011). Here the GFP-*Arath*;WEE1 seedlings were not grown under conditions of replication stress, so the putative premature differentiation seen in these lines could support a role for *Arath*;WEE1 in an unperturbed cell cycle, protecting against premature vascular differentiation under normal conditions as well as when under replication stress. Alternatively, the observation of these dead cells in the GFP-*Arath*;WEE1 lines could be an indication that the *Arath*;WEE1 fusion protein was not functioning normally in these lines and instead causing them to behave as replication-stressed *wee1* knockout lines. Or the effect could be due to the ectopic expression of the *WEE1* transgene by the 35S promoter, as discussed above. Again, transgenic lines expressing GFP-*Arath*;*WEE1* under the endogenous *Arath*;*WEE1* promoter may help to resolve this issue.

The expression of a GFP-*Arath*;WEE1 construct under the 35S promoter in both the tobacco BY-2 cell line and *Arabidopsis* roots has provided several new insights into the stability of the *Arath*;WEE1 protein. The subcellular localisation of *Arath*;WEE1 was confirmed to be nuclear during interphase in both tobacco BY-2 cells and *Arabidopsis* roots. It was observed that *Arath*;WEE1 protein appears to be removed during prophase, and absent during metaphase, which suggests that the removal of WEE1 may be required for mitotic progression in plants. The application of the proteasome inhibitor MG132 allowed the demonstration that *Arath*;WEE1 is degraded via the 26S proteasome in *Arabidopsis*. Also, interestingly, levels of *Arath*;WEE1 proteolysis appeared to vary in different tissues of the *Arabidopsis* root, being relatively higher in the epidermis and stele of the root elongation zone, and in the epidermis and cortex of differentiating root tissue. *Arath*;WEE1 degradation was also high in lateral root primordia, suggesting that the removal of WEE1 may be important for the initiation of lateral roots. Finally, the detection of dead cells in the stele of the differentiation and elongation zones in the GFP-*Arath*;WEE1 lines may indicate that *Arath*;WEE1 is involved in the protection against premature differentiation under normal conditions, as well as under conditions of replication stress as previously described.

4. THE INTERACTIONS OF *ARATH;*WEE1 KINASE WITH OTHER PROTEINS

4.1 INTRODUCTION

Discovering the proteins with which core cell cycle components interact is useful for building networks in order to discover specific pathways and also may point towards unknown functions of individual proteins. Several techniques are now available to researchers to build knowledge of protein-protein interaction networks (interactomes; reviewed by Zhang et al., 2010). Recently an interactome network of *Arabidopsis* core cell cycle proteins was constructed using the yeast two-hybrid assay and bimolecular fluorescence complementation analysis, correlated with already available cell cycle phase-dependent gene expression data and subcellular localisation information (Boruc et al., 2010b; Van Leene et al., 2011). It was found that *Arath;*WEE1 only interacted with one core cell cycle gene, CDKA;1, which occurred in the nucleus (Boruc et al., 2010b).

A yeast two-hybrid assay was used by the Cardiff team to discover which proteins interact with *Arath;*WEE1, in order to obtain more information about the protein's function in *Arabidopsis* (Lentz Grønlund, 2007). The yeast two-hybrid assay is a technique which uses a protein of known function as bait to determine whether it interacts with candidate proteins, or to identify new interactors in a screen (Thorner et al., 2000). This method was devised by Fields and Song (1989) and utilises budding yeast (*Saccharomyces cerevisiae*) cells, making use of the GAL4 protein. GAL4 is a transcriptional activator protein responsible for the expression of genes encoding enzymes involved in galactose metabolism, and contains two domains: a DNA-binding domain (DBD) and a transcriptional activator domain (AD). In the assay these two domains are separated and fused to the proteins under scrutiny, one domain to each protein (eg. DBD to the protein of interest and AD to the bait protein; Figure 4.1; Thorner et al., 2000). If the two proteins interact with each other in the yeast cell the two domains come together and GAL4 is expressed (Figure 4.1). This leads to the expression of marker enzymes such as β-galactosidase, detectable by the indicator X-gal, meaning that any colonies exhibiting the interacting proteins

will be dark blue, as opposed to white colonies where no interaction occurs (Fields and Song, 1989). In the system used in the Cardiff lab, an additional transcriptional activator was utilised, which promotes the transcription of *HIS3*, conferring the ability to grow on media lacking histidine when two proteins interact. Over 90 cellular proteins were able to interact with *Arath;*WEE1 in yeast cells (Lentz Grønlund, 2007). The functions of these proteins included transcription, RNA and DNA binding, histone modification, plant growth regulation, signal transduction, stress response, detoxification, pathogen response, cell division, cell growth, protein biosynthesis and ubiquitin-mediated degradation (Lentz Grønlund, 2007).

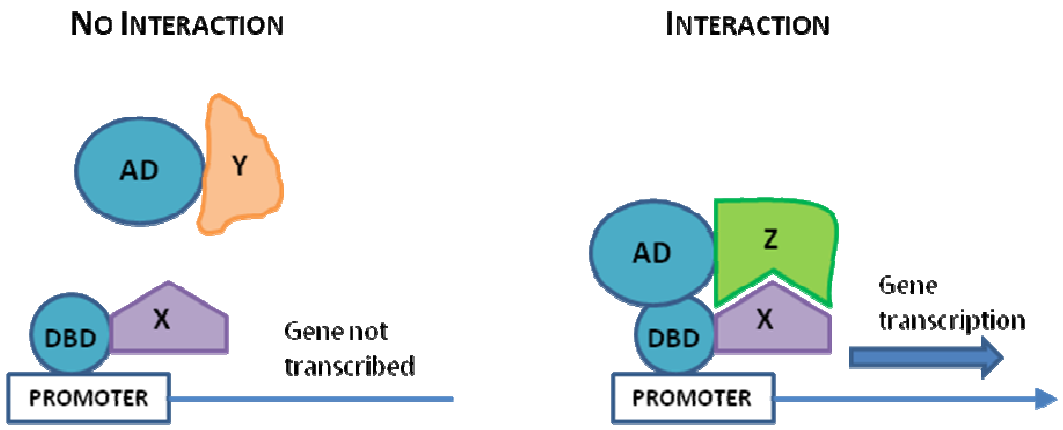

Figure 4.1 The yeast two-hybrid system. The DNA-binding domain (DBD) of a transcriptional activator protein is fused to a bait protein (X). The transcriptional activator domain (AD) of the transcriptional activator protein is fused to proteins of interest (eg. Y and Z). If no interaction occurs between the proteins (eg. X and Y), the AD and DBD of the transcriptional activator remain separated and transcription of the marker gene does not occur. If the two proteins interact (X and Z), the AD and DBD of the transcriptional activator protein are able to come together to activate the transcription of the marker gene.

Among these proteins, an F-box protein, *Arath*;SKIP1, was identified, which probably has a role in the ubiquitin/26S proteasome pathway, and may target *Arath*;WEE1 protein for degradation. Additionally, four proteins were identified which may have a function in the cell cycle: *Arath;*GCN5, a histone-acetylating protein; *Arath;*TFCB, an α-tubulin folding cofactor; *Arath*;14-3-3ω, which may prevent dephosphorylation of *Arath*;WEE1; and *Arath;*GSTF9, a glutathione S-transferase involved in the cell's response to stress. This enzyme is involved in a redox pathway which may be linked to cell cycle control. The interactions of these four proteins were confirmed *in vivo* via bimolecular fluorescence complementation (BiFC; Cook, unpublished data, see Appendix IV; Lentz Grønlund et al., 2009).

The BiFC procedure uses the linkage of two interacting proteins to bring together two fragments of yellow fluorescence protein (YFP) fused to these proteins by the use of complementary expression vectors (Hu et al., 2002) both expressed in the same plant cell. When the proteins interact and the portions of YFP are brought together, the resulting fluorescence can be viewed under a light microscope using ultraviolet (UV) light. Two advantages of this technique for viewing protein-protein interactions in plant cells include the visualisation of these interactions *in vivo*, and the discovery of the subcellular compartments in which they take place. A disadvantage of the BiFC procedure is that the YFP fragments may associate non-specifically at high expression levels, which generates background fluorescence (Stephens and Banting, 2000).

The BiFC vectors developed for use in plant cells (Walter et al., 2004) are known as pSPYCE and pSPYNE (split YFP C-terminal/N-terminal fragment expression; Figure 4.2), enabling proteins of interest to be expressed and fused to either the 86 amino acids at the C-terminal or the 155 amino acids at the N-terminal of YFP, respectively. Each plasmid contains an affinity tag – HA in pSPYCE and C-MYC in pSPYNE – which allows the fusion protein to be detected, for example by PCR or through the use of commercially available antibodies (Figure 4.2). Transcription is driven by the 35S promoter of the cauliflower mosaic virus which ensures high levels of expression of the fusion proteins within plant cells (Figure 4.2). The pSPYNE and pSPYCE vectors originally adopted in the Cardiff lab carried a gene conferring resistance to the antibiotic hygromycin, and to the herbicide glufosinate (BASTA) respectively (Walter et al., 2004).

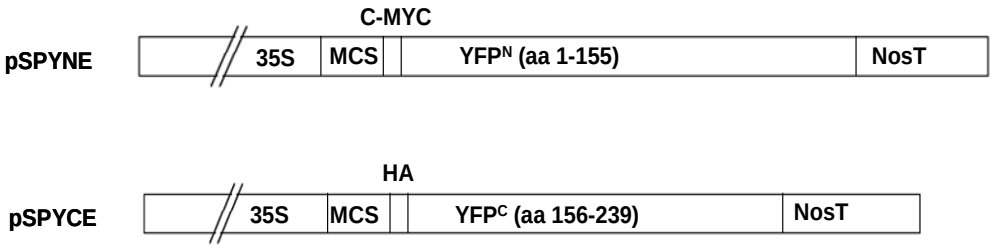

Figure 4.2 Plasmid vectors designed for the use of BiFC in plant cells. Both vectors contain the cauliflower mosaic virus 35S promoter sequence, a multi-cloning site (MCS) containing target sites for the restriction enzymes Asc1 and Xma1 (among others) and the terminator for the Nos gene (NosT). The pSPYNE vector codes for the 155 amino acids from the N-terminal of the split-YFP, and contains a C-MYC affinity tag. The pSPYCE vector codes for the 83 amino acids from the C-terminal of the split YFP, and contains a hemagglutinin affinity tag. (Diagram adapted from Walter et al., 2004).

Recently, new sets of vectors have been developed for multi-colour BiFC (mc-BiFC), allowing the visualisation of more than one protein-protein interaction simultaneously (Waadt et al., 2008). BiFC and mc-BiFC have both been used successfully to show the interactions of proteins in BY-2 cells (Liu et al., 2008; Lee et al., 2008; Lentz Grønlund et al., 2009; Yano et al., 2006). BiFC can in theory be used in all cell types of all organisms, and has been used to confirm protein-protein interactions in many plant processes, including the cell cycle (Boruc et al., 2010c, Van Damme et al., 2011), processes associated with protein degradation (Dowil et al., 2011; Li et al., 2011) and DNA damage (Halimi et al., 2011). Previous work in the Cardiff lab used transient transformation of tobacco BY-2 cells. This was either achieved by co-transformation of the two vectors simultaneously or by generating a stable BY-2 culture carrying the pSPYNE vector and transforming the cells transiently with the pSPYCE vector. This enabled visualisation and localisation of the interactions but due to the low efficiency of this method it was not possible to chart the interaction between WEE1 and interacting proteins through the stages of the cell cycle. To do this, stable cultures carrying both vectors would be required. It is expected that these stable cultures would allow the study of the dynamics of *Arath*;WEE1's interactions with other proteins at different stages of the cell cycle, which is not possible using the transient BiFC system. It should also allow the visualisation of a higher percentage of cells positive for fluorescence caused by BiFC.

4.1.1 EXPERIMENTAL AIMS

The interactions of *Arath*;WEE1 with *Arath*;SKIP1 and *Arath*;GSTF9 were studied further to:

1. Verify *in vivo* the interaction between *Arath*;WEE1 and *Arath*;SKIP1 by transient BiFC.
2. Develop stable, double-transformed tobacco BY-2 cultures carrying both pSPYCE-*Arath*;WEE1 and pSPYNE constructs containing the WEE1-interacting proteins of interest.
3. Use these cultures to study any changes in the subcellular localisation of the *Arath*;WEE1 complexes with proteins of interest during the cell cycle.

4.2 MATERIALS AND METHODS

All standard chemicals were sourced from Sigma-Aldrich, Poole, UK unless otherwise specified.

4.2.1 CLONING

For a flow diagram of methods used see Figure 4.3.

Table 4.1 Summary of cloning completed:

TARGET	FROM PLASMID	TO PLASMID	RESTRICTION ENZYMES	DIGESTION BUFFER
Arath;WEE1	pSPYCE	pkanII-SPYCE(M)	AscI/XmaI	NEB buffer 4
Arath;WEE1 (S485A)	pSPYCE	pkanII-SPYCE(M)	AscI/XmaI	NEB buffer 4

4.2.1.1 PLASMID DNA EXTRACTION

Plasmid DNA was extracted from *Escherichia coli* using a Qiagen® miniprep kit, which uses several different buffers to elute DNA. The bacteria are lysed under alkaline conditions and the DNA bound to a silica gel membrane under high salt

conditions, before being eluted into Tris buffer (QIAprep® miniprep handbook, December 2006). The bacteria were inoculated into LB (5 mL) containing appropriate selection in growth tubes, from a glycerol stock of the appropriate *E. coli* culture. The cultures were grown overnight shaking at 200 rpm at 37°C in a Gallenkamp Cooled Orbital Shaker.

Each culture was used in a Qiagen® miniprep by pipetting aliquots into each of four Eppendorf tubes and centrifuging at 8000 rpm in an Eppendorf MiniSpin® microcentrifuge for 3 minutes. All supernatant was then removed and the bacterial pellets resuspended in buffer P1 (250 μL) in a single Eppendorf. Buffer P2 (250 μL) was added and the tube gently inverted 4-6 times to mix. Buffer N3 (350 μL) was added and the tube gently inverted 4-6 times to mix, before being centrifuged at 13000 rpm in an Eppendorf MiniSpin® microcentrifuge for 10 minutes to give a white pellet. The supernatants were then applied to QIAprep® spin columns and the white pellet discarded. These supernatants were centrifuged at 13000 rpm in an Eppendorf MiniSpin® microcentrifuge for 60 seconds, and the flow-through discarded from the collection tube. The spin column was washed by adding buffer PE (750 μL), left to stand for 2-3 minutes and then centrifuged for 60 seconds. This step was then repeated once. The flow-through was discarded and the column centrifuged dry for 60 seconds in order to remove residual wash buffer. The spin column was then placed into a clean Eppendorf tube and warm buffer EB (elution buffer; 50 μL) added to the centre of the column, left to stand for 3 minutes and centrifuged for 60 seconds to elute DNA (QIAprep® miniprep handbook, December 2006). The concentration of the DNA miniprep was measured and calculated using a ThermoScientific NanoDrop 1000 UV-Vis Spectrophotometer.

4.2.1.2 VECTOR PREPARATION FOR CLONING

Vector DNA was extracted from *E. coli* using a Qiagen® miniprep as described above (Section 4.2.1.1). The vector was digested with restriction enzymes in order to allow insertion of the desired DNA. Parallel reactions were set up, one for each restriction enzyme, containing: appropriate restriction enzyme buffer (4 μL), bovine serum albumin (1 μg/mL; BSA; New England Biolabs, Hertfordshire, UK), vector DNA (2 μg), 10 units of either restriction enzyme (RE), and sterile distilled water added to 40 μL. Reactions were incubated at 37°C for 3 hours and the results

viewed by checking 100 ng of the digested DNA on a 0.8% agarose gel (as described in Section 2.4.3) and comparing to undigested DNA. If digestion was complete, RE2 (10 units) was added to the RE1 digest and RE1 (10 units) to the RE2 digest, then digested at 37°C for 3 hours. Otherwise the first digestion was repeated.

Phosphatase treatment was used to prevent rejoining of digested ends. To the digest, 1% Calf Intestine Alkaline Phosphatase (CIAP; 0.5 units; Fermentas, York, UK), 10x CIAP buffer (5 μL; Fermentas, York, UK) and sterile distilled water (4.5 μL) were added, mixed and the sample incubated at 37°C for 30 minutes. Another 0.5 units of 1% CIAP were added and the sample incubated at 37°C for a further 30 minutes before the digests were pooled and purified using a QiaQuick PCR purification kit (as described in Section 4.2.1.3).

4.2.1.3 PURIFICATION OF DNA FRAGMENTS USING A QIAQUICK PCR PURIFICATION KIT

A QIAquick® PCR purification kit (Qiagen, Crawley, UK) was used to remove contaminants from DNA samples using a similar method to the Qiagen® miniprep (described in Section 4.2.1.1). PB buffer was added to the sample (5:1), applied to a spin column and centrifuged at 13000 rpm in an Eppendorf MiniSpin® microcentrifuge for 60 seconds to bind the DNA. The flow-through was discarded from the collection tube and the spin column washed by adding PE buffer (750 μL) and centrifuging at 13000rpm in an Eppendorf MiniSpin® microcentrifuge for 60 seconds. The flow-through was discarded from the collection tube and centrifuged dry for another 60 seconds. The spin column was then placed into a clean Eppendorf tube and elution buffer (buffer EB; 30 μL) was added to the centre of the membrane, left to stand for 60 seconds and centrifuged at 13000rpm in an Eppendorf MiniSpin® microcentrifuge for 60 seconds in order to elute the DNA (QIAquick® Spin Handbook, November 2006).

4.2.1.4 PREPARATION OF INSERT FRAGMENTS FOR CLONING BY DIGESTION FROM PLASMID DNA

Plasmid DNA was extracted from *E. coli* using a Qiagen® miniprep (described in Section 4.2.1.1). Products were digested as described above in Section 4.2.1.2, except that both enzymes were added at the same time. The products of this

digestion were separated on a 0.8% agarose gel (see Section 2.4.3) and extracted using the QIAquick® Gel Extraction kit (Qiagen), using a method similar to the PCR purification (described in Section 4.2.1.3). Firstly the DNA fragment was excised from the agarose gel using a clean sharp razor blade and QG buffer added to the gel (3:1). This was then incubated at 50°C for 10 minutes, and mixed by vortexing every 2-3 minutes during this incubation to help dissolve the gel. Having dissolved the gel completely, isopropanol (1:1) was added to the tube and mixed (this was only required for fragments sized <500 bp and >4 kb). This sample was then applied to a spin column and microcentrifuged at 13000 rpm in an Eppendorf MiniSpin® microcentrifuge for 1 minute to bind DNA. The flow-through was discarded from the collection tube and PE buffer (750 μL) added and microcentrifuged at 13000rpm in an Eppendorf MiniSpin® microcentrifuge for 60 seconds to wash. The flow-through was discarded and the column centrifuged again at 13000rpm in an Eppendorf MiniSpin® microcentrifuge for 60 seconds. The spin column was then placed into a clean Eppendorf tube and elution buffer (buffer EB; 30 μL) added to the centre of the membrane, left to stand for 60 seconds, and then centrifuged at 13000rpm in an Eppendorf MiniSpin® microcentrifuge for 60 seconds, eluting the DNA (QIAquick® Spin Handbook, November 2006). A 0.8% agarose gel was used to test the quantity and quality of the recovered DNA (see Section 2.4.3).

4.2.1.5 LIGATIONS

Three parallel reactions were set up. Reactions one and two were controls, containing no insert DNA, and no insert DNA and no ligase respectively (Table 4.2). Ligations were incubated at 4°C overnight and stored at -20°C if required.

Table 4.2 Ligation reactions

Reaction one	**Reaction two**	**Reaction three**
2μL empty vector (50-100ng)	2μL empty vector (50-100ng)	2μL empty vector (50-100ng)
1μL ligase buffer	1μL ligase buffer	1μL ligase buffer
1μL ligase		1μL ligase
6μL sterile distilled water	7μL sterile distilled water	6μL insert DNA

4.2.1.6 TRANSFORMATION INTO E.COLI

Competent cells (strain DH5α) were prepared in house (Section 4.2.2), snap frozen in liquid nitrogen and stored at -80 ^{o}C. The cells were thawed on ice and divided into four aliquots (100 μL) in 1.5 mL Eppendorf tubes. Ligated DNA (2 μL) was added to separate aliquots of the cells. Undigested vector (10-20 ng) was added to the final aliquot of cells as a control. Transformations were mixed thoroughly, then left on ice for 20 minutes. The cells were then heat shocked at 42°C for exactly 45 seconds, before being transferred back to ice for 2 minutes. LB medium (900 μL) was then added to the cells, before being incubated at 37°C shaking horizontally at 100 rpm in a Gallenkamp Cooled Orbital Shaker for approximately 1 hour. Each transformation (200 μL) was plated onto an LB agar plate (Table 2.1) in the presence of appropriate antibiotic selection (see Table 2.2) and incubated at 37°C overnight (approximately 17 hours). The next morning the resultant colonies were counted.

4.2.1.7 COLONY PCR

PCR was used to identify positive clones. Colonies were inoculated into aliquots (200 μL) of LB (Table 2.1) in the presence of appropriate antibiotic selection (see Table 2.2) in Eppendorf tubes and incubated at 37°C shaking horizontally at 100 rpm in a Gallenkamp Cooled Orbital Shaker for approximately 5 hours. PCR mix was prepared for each culture, as described in Section 2.4.2, using 1 μL of culture for each sample and appropriate primers. Undigested empty vector (1 μL containing approx 1 ng of DNA) was used as a positive control and sterile distilled water (1 μL) as a negative control.

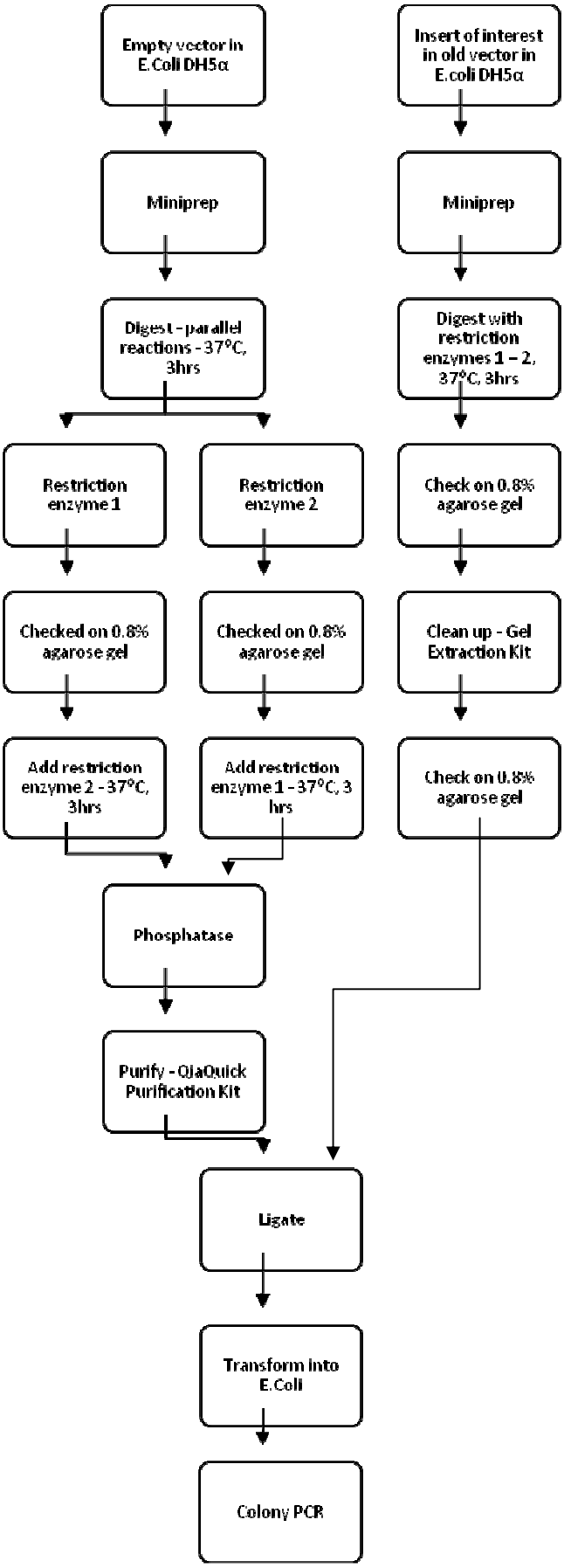

Figure 4.3 Sequence of methods used for cloning – vector and insert are digested, checked and cleaned before being ligated and transformed into *E. coli*.

4.2.2 *E. COLI* DH5α COMPETENT CELLS

E. coli DH5α cells were streaked out on a LB-agar plate and incubated at 37^0C overnight. A single colony from this plate was inoculated into 3 mL LB medium and incubated at 37^oC overnight, 200 rpm in a Gallenkamp Cooled Orbital Shaker. 100 μL of this starter culture was inoculated into 100 mL of Psi broth (0.5% bacto yeast extract, 2% bacto tryptone, 0.5% magnesium hydroxide, pH 7.6) and incubated at 37^0C, 200 rpm in a Gallenkamp Cooled Orbital Shaker until the culture reached an optical density of 0.6-0.7 at 600 nm (2-3 hours). The culture was then put on ice for 15 minutes. The cells were pelleted at 3000g for 5 minutes at 4^0C and the supernatant discarded. The pellet was resuspended in 0.4 volume (20 mL) of TfbI (30 mM potassium acetate, 100 mM rubidium chloride, 10 mM calcium chloride, 50 mM manganese chloride, 15% glycerol, pH5.8) and put on ice for 15 minutes. The cells were again pelleted at 3000g for 5 minutes at 4^0C and the supernatant discarded. The pellet was resuspended in 0.04 volume (2 mL) of TfbII (10 mM MOPS, 75 mM calcium chloride, 10 mM rubidium chloride, 15% glycerol, pH6.5) and put on ice for 15 minutes. The cells were aliquoted into 100 μL or 400 μL aliquots, frozen rapidly in liquid nitrogen and stored at -80^0C. The competency of the cells was checked by transformation (see Section 4.2.1.6) with 2 ng of a plasmid with a known concentration and colonies counted. The cells were deemed competent if they produced 10^5-10^7 colonies/μg of DNA.

4.2.3 TRANSIENT BIMOLECULAR FLUORESCENCE COMPLEMENTATION (BiFC)

Agrobacterium transformed with the appropriate constructs (Section 2.2) were plated from glycerol stocks onto LB agar plates (Table 2.1) in the presence of rifampicin (100 μg/mL) and kanamycin (50 μg/mL) and grown at 30°C for 3 days. They were then subcultured onto a fresh LB-rifampicin-kanamycin agar plate and grown at 30°C for 2 days (these cell lines were maintained by subculturing onto fresh agar plates every 7 days). Overnight cultures of the appropriate *Agrobacterium* cultures were established, inoculating from the 2 day old colonies into LB medium (2 mL; Table 2.1) in 15 mL growth tubes.

To transiently transform BY-2 cells with plasmids, 7 mL of four day-old cells was pipetted onto a BY-2 agar plate (Table 2.1) and swirled to fill the plate to the edges. 19.6 g/L acetosyringone (12 µL; prepared in 100% ethanol) was added and swirled to mix. 100 µL of each appropriate *Agrobacterium* culture was added to the plate and swirled to mix. Each plate was then sealed in Nesco film, wrapped in aluminium foil and incubated at 27°C in the dark for 72 hours. Cells were monitored for fluorescence as described in Section 2.1.5.

Stable transformation of BY-2 cells with BiFC vectors was achieved as described in Section 2.1.2. For antibiotic selection see Table 4.3.

Table 4.3 Antibiotic selection of stable tobacco BY-2 cell lines for bimolecular fluorescence complementation (BiFC)

CONSTRUCT	BY-2 FORM	ANTIBIOTIC
kanSPYCE-*Arath*;WEE1/ pSPYNE-*Arath*; (gene) constructs	Callus	Kanamycin 10 µg/mL Hygromycin 80 µg/mL Timentin 250 µg/mL
	Liquid	Kanamycin 25 µg/mL Hygromycin 80 µg/mL Timentin 250 µg/mL

4.3 RESULTS

Transient BiFC was used to confirm the *Arath*;WEE1/*Arath*;SKIP1 interaction revealed by the yeast two-hybrid assay and in parallel stable BY-2 cultures carrying both SPYNE and SPYCE constructs were created. These cultures were used to identify the localisation of the interaction of *Arath*;WEE1 with other proteins of interest in different cell cycle stages.

4.3.1 VERIFICATION OF THE *ARATH*;WEE1- *ARATH*;SKIP1 INTERACTION BY TRANSIENT BiFC

Arath;SKIP1 in the pSPYNE vector was transformed transiently into BY-2 cells via *Agrobacterium* EHA105 along with pSPYCE- *Arath*;WEE1 to facilitate the investigation of the subcellular localisation of the interaction between these two proteins (as described in Section 4.2.3). Transformation efficiency was relatively high with approximately 230 cells per 20 μL exhibiting fluorescence in the positive control (BZIP63 heterodimer) and approximately 40 clusters of cells per 20 μL exhibiting fluorescence in the experimental transformation (*Arath*;WEE1/*Arath*;SKIP1). The proteins, when interacting, were mostly localised in the nucleus, however the interaction was also detected at the cell wall, especially where two cells joined (Figure 4.4; Appendix V). Images were not acquired from the negative control transformations (*Arath*;WEE1/*Arath*;BZIP63 and *Arath*;BZIP63/*Arath*;SKIP1) on this occasion (for representative images of negative controls see Appendix IV).

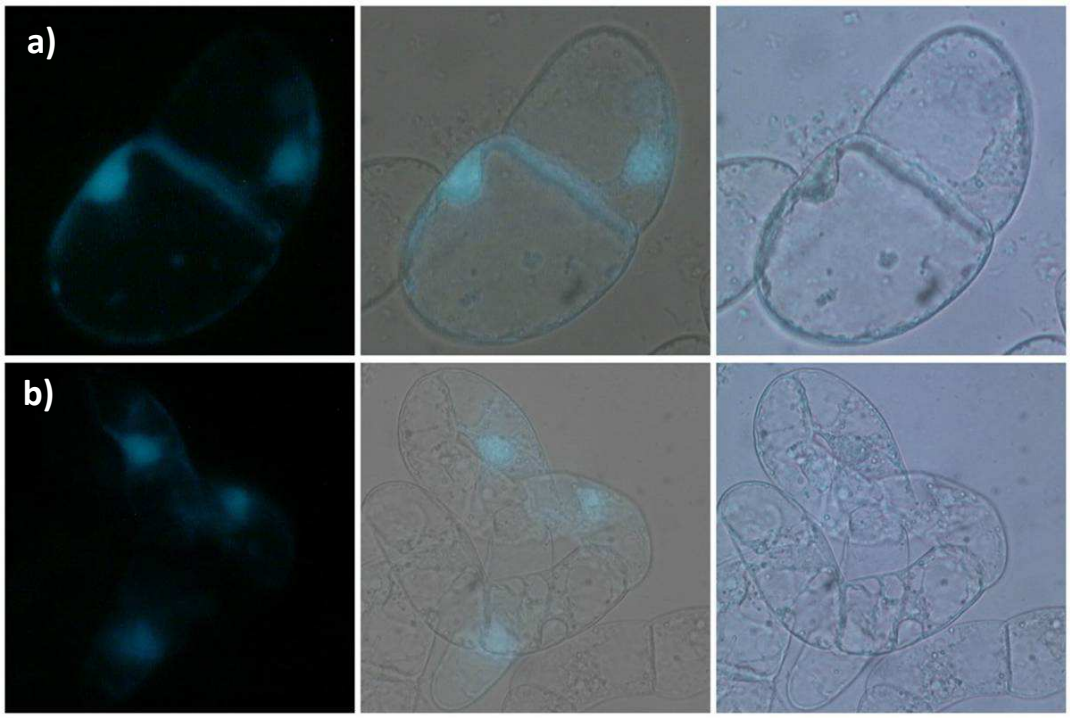

Figure 4.4 Tobacco BY-2 cells co-transformed with a) *Arath*;WEE1 fused to the split-YFP vector pSPYCE and *Arath*;SKIP1 fused to pSPYNE, and b) *Arath*;BZIP63 fused to both pSPYCE and pSPYNE (positive control); under UV light (left), white light (right) and the two merged (centre). Blue colouring indicates a positive interaction between the two proteins (representative images).

4.3.2 DEVELOPMENT OF STABLE BiFC BY-2 TRANSGENIC LINES

Initial efforts aimed at creating stable double transformants using the original pSPYCE vector used in the Cardiff lab were hampered by the use of BASTA selection. pSPYCE- *Arath*;WEE1 was transformed into tobacco BY-2 cells via *Agrobacterium* EHA105 (see Section 2.1.2), however due to problems with BASTA selection calli were not isolated at any concentration of BASTA (2.5, 5, 7, 10 and 15 mg/mL) attempted. Consequently the decision was made to clone the *Arath*;WEE1 fragment into the pkanII-SPYCE(M) vector conferring kanamycin resistance *in planta* (as described in Section 4.2.1). The resulting construct was transformed into *Agrobacterium* LBA4404 competent cells (see Section 2.2.2) resulting in many colonies, one of which was grown up and used to transform BY-2 cells. Many individual calli were selected. One of these calli was inoculated into liquid BY-2 medium (Table 2.1) and a stable culture obtained (see Section 2.1.2). DNA was extracted from this liquid culture and checked for the transgene by PCR using primers P81F and HATAGR (as described in section 2.4, for primers see Table 2.3). This line was shown to be positive for the SPYCE-*Arath*;WEE1 construct (Figure 4.5).

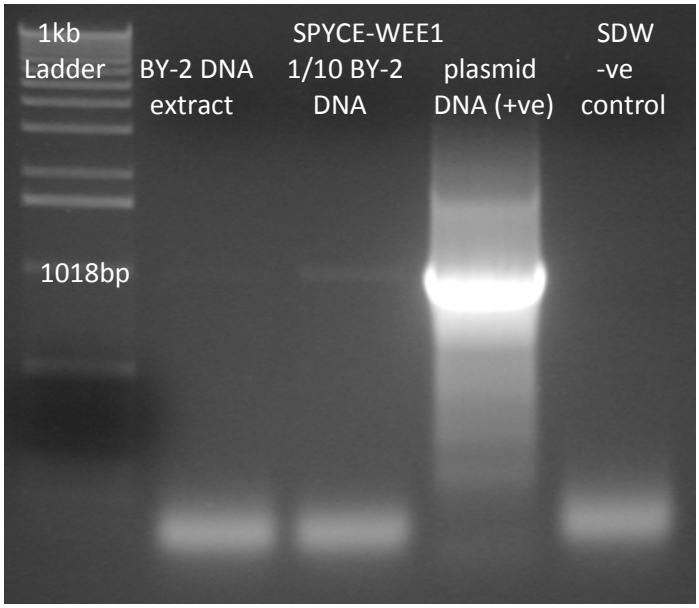

Figure 4.5 Results of PCR for the pSPYCE-*Arath*;WEE1 construct in transformed tobacco BY-2 cells, using primers P81F and HATAGR. The first two lanes show the fragment amplified from a DNA extract from the transformed BY-2 culture, and a 10% dilution of the same extract. Both show a faint band of the expected size (~1000bp). A very strong band was amplified from the positive control, purified pSPYCE-*Arath*;WEE1 plasmid DNA.

Expression of the SPYCE-*Arath*;WEE1 transgene was tested by transiently transforming the liquid BY-2 culture with the SPYNE-*Arath*;SKIP1 construct (as described in Section 4.2.3). Positive and negative controls were also set up (see Table 4.4). Fluorescence was detected in the nuclei of SPYCE-*Arath*;WEE1 cells transiently transformed with both the BZIP63 constructs, and those transformed with the SPYNE-*Arath*;SKIP1 construct (Figure 4.6 and Appendix VI) the latter indicating that the transgenic BY-2 cells were expressing SPYCE-*Arath*;WEE1. Fluorescence above background was not detected in negative control cells (Figure 4.6 and Appendix VI).

Table 4.4 Controls for transient BiFC in stable pKanSPYCE-*Arath*;WEE1 BY-2 line

Control/Experiment	BY-2 Cell Line	SPYCE	SPYNE	OUTCOME
1. Experiment	pSPYCE-*Arath*;WEE1	-	*Arath*;SKIP1	Positive
2. Positive control	WT	*Arath*;WEE1	*Arath*;SKIP1	Negative
3. Positive control	pSPYCE-*Arath*;WEE1	BZIP63	BZIP63	Positive
4. Positive control	WT	BZIP63	BZIP63	Positive
5. Negative control	pSPYCE-*Arath*;WEE1	-	BZIP63	Negative
6. Negative control	WT	*Arath*;WEE1	BZIP63	Negative
7. Negative control	WT	BZIP63	*Arath*;SKIP1	Negative

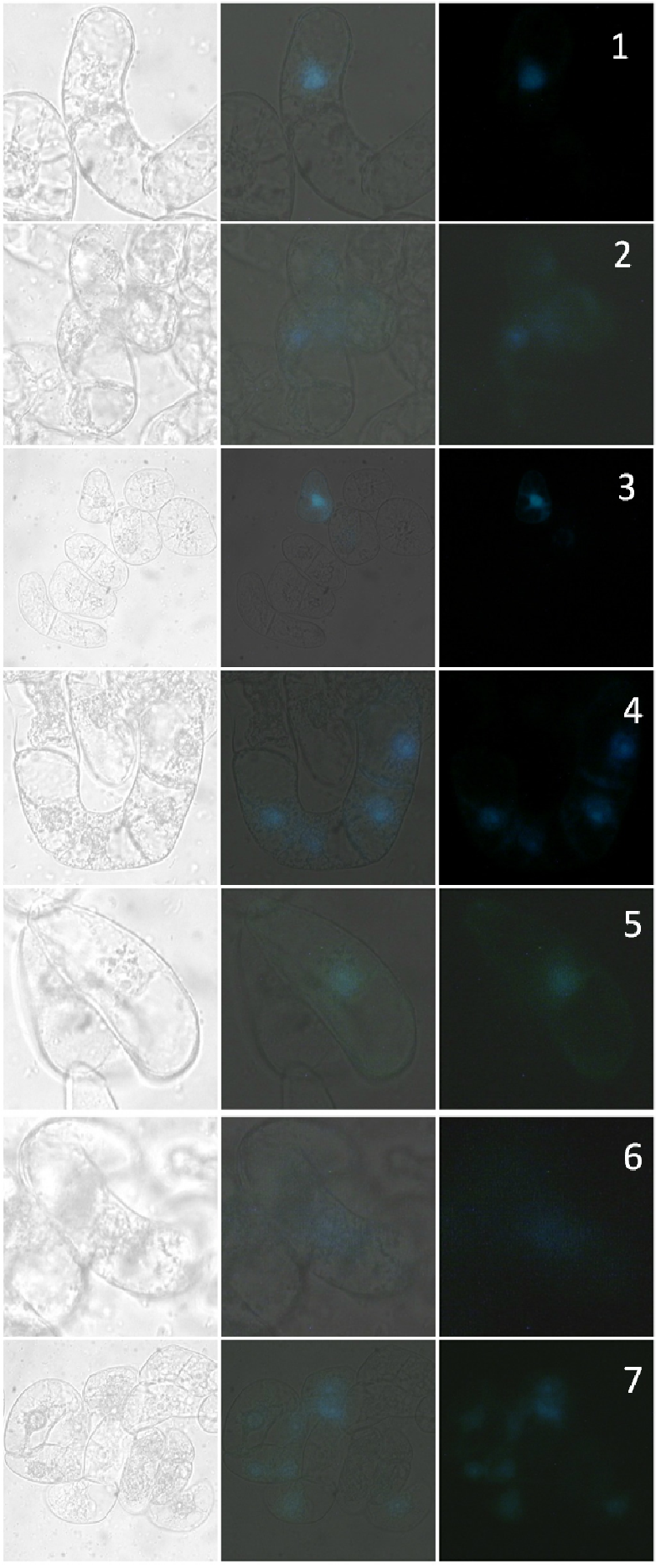

Figure 4.6 Results of experiment to test for expression of pkanSPYCE-*Arath*;WEE1 in stably transformed tobacco BY-2 cells by semi-transient BiFC, under white light (left), UV light (right) and the two merged (centre). Clear blue colouring indicates a positive interaction, whereas grainy unclear blue colouring indicates background, or false positive, fluorescence. See Table 4.4 for key to numbering.

Having verified expression of the transgene, the SPYCE-*Arath*;WEE1 BY-2 culture was co-transformed with several co-interactors, including *Arath*;SKIP1, *Arath*;GSTF9, *Arath*;GCN5 and *Arath*;TFCB, in the SPYNE vector (as described in Section 2.1.2). Co-transformed cells were selected using hygromycin for the SPYNE vectors and low level kanamycin to ensure the presence of the SPYCE vector (Table 4.3). Many calli were obtained from transformation with all constructs, several of which were maintained on solid medium for each line (Section 2.1.2). A liquid culture was obtained from at least one line each of SPYCE-*Arath*;WEE1/SPYNE-*Arath*;SKIP1, -*Arath;*GSTF9 and – *Arath;*BZIP63 (as described in Section 2.1.2). DNA was extracted from these liquid cultures and checked for both the SPYCE and SPYNE transgenes by PCR (as described in Section 2.4, for primers see Table 2.3)**.**

All the lines were positive for the SPYCE-*Arath*;WEE1 fusion, with a band amplified of approximately 500bp, as expected for these primers (Figure 4.7). However, the band amplified from the positive control, SPYCE-*Arath*;WEE1 plasmid, appears to be 500bp larger (Figure 4.7). The SPYCE-*Arath*;WEE1/SPYNE-*Arath*;SKIP1 culture was positive for SPYNE-*Arath*;SKIP1 (Figure 4.7). The SPYCE-*Arath*;WEE1/SPYNE-BZIP63 culture was positive for SPYNE-BZIP63 (Figure 4.7). And finally the SPYCE-*Arath*;WEE1/SPYNE-*Arath*;GSTF9 culture was positive for SPYNE-*Arath*;GSTF9 (Figure 4.7).

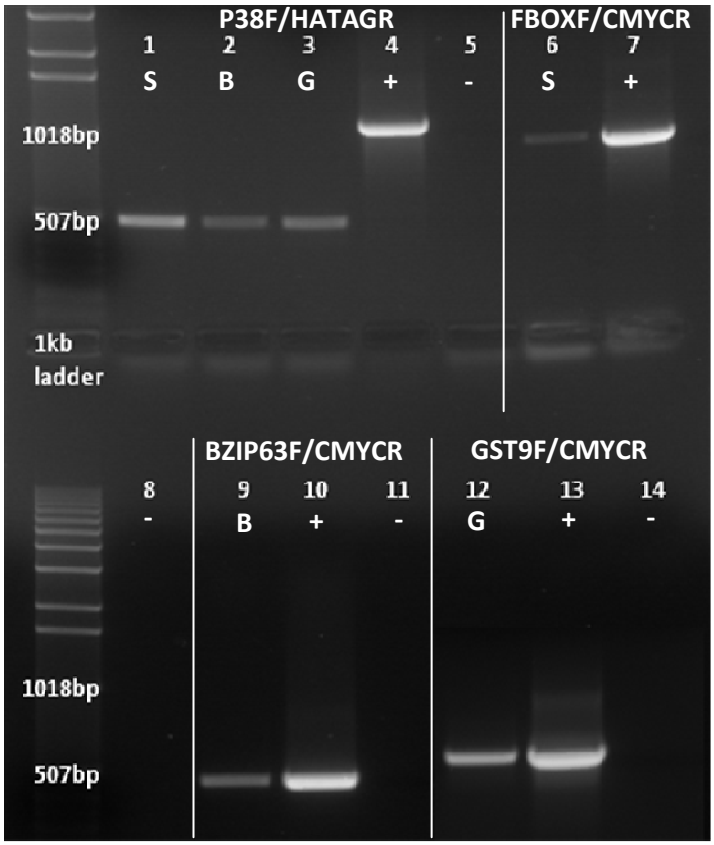

Figure 4.7 Results of PCR to confirm presence of BiFC constructs in stable co-transformed BY-2 cultures.
P38F/HATAGR = primers for pSPYCE-*Arath*;WEE1;
FBOXF/CMYCR = primers for pSPYNE-*Arath*;SKIP1;
BZIP63F/CMYCR = primers for pSPYNE-BZIP63;
GST9F/CMYCR = primers for pSPYNE-*Arath*;GSTF9
S = pSPYNE-*Arath*;SKIP1 culture;
B = pSPYNE-BZIP63 culture;
G = pSPYNE-*Arath*;GSTF9;
+ = positive control, appropriate plasmid; **-** = negative control, SDW

The SPYCE-*Arath*;WEE1/SPYNE-*Arath*;SKIP1 and SPYCE-*Arath*;WEE1/SPYNE-BZIP63 cultures were transferred to 95mL culture (as described in Section 2.1.1). Growth was monitored and the mitotic index was measured every day over the course of 7 days (as described in Section 2.1.4), in order to compare the growth profiles of the transgenic lines with those of wild type. The cultures both reached stationary phase after 7 days, similarly to wild type culture (Figure 4.8a). The mitotic index of the SKIP1 culture peaked at approximately 18% on day 4, while the BZIP63 culture also peaked at approximately 18% but on day 3, compared to the peak in mitosis in wild type at 15% on day 4 (Figure 4.8b).

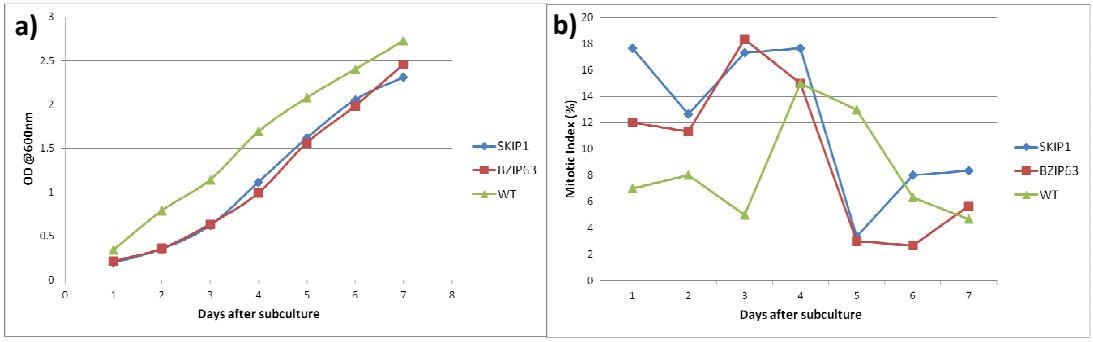

Figure 4.8 Growth characteristics of the pSPYCE-*Arath*;WEE1/pSPYNE-*Arath*;SKIP1 and pSPYCE-*Arath*;WEE1/pSPYNE-BZIP63 BY-2 cell cultures compared to wild type (WT). a) Growth measured as increase in absorbance at 600nm (turbidity) of culture sampled daily for 7 days. b) Mitotic index (% frequency of cells in mitosis) sampled daily for 7 days.

The next step was to use these cultures to study the changes in the subcellular localisations of WEE1's interactions during the cell cycle. However the cultures were extremely heterogeneous, with only a very small proportion of the cells actually expressing YFP. A recently described protocol (Nocarova and Fischer, 2009; see Section 2.1.6) was used in an attempt to clone the cells which are expressing YFP and increase homogeneity. However, this experiment proved to be unsuccessful, with none of the isolated calli exhibiting an improved level of YFP expression, so following several attempts the decision was made to continue the study using the existing cultures.

4.3.3 THE INTERACTION OF *ARATH*;WEE1 WITH *ARATH*;SKIP1 ALTERS DEPENDING ON CELL CYCLE PHASE

Wild type, SPYCE-*Arath*;WEE1, SPYCE-*Arath*;WEE1/SPYNE-*Arath*;SKIP1 and SPYCE-*Arath*;WEE1/SPYNE-*Arath*;GSTF9 BY-2 lines were cultured in 29mL of medium and cell division synchronised (as described in Section 2.1.3). After release from G1 by the removal of aphidicolin, samples were taken from each BY-2 line every hour for at least 27 hours, stained with Hoechst and scored for percentage mitosis. The duration of each cell cycle phase was also calculated in each line (see Appendix I). In the wild type BY-2 line mitotic cells could be seen after four hours, with the first peak in mitotic index occurring nine hours after the removal of aphidicolin (Figure 4.9a). A second peak occurred 22 hours after the removal of aphidicolin allowing an estimation of cell cycle duration as 13 hours (Figure 4.9a).

In the SPYCE-*Arath*;WEE1 line, mitotic cells could be seen only two hours after the removal of aphidicolin, with the first peak in mitosis occurring seven hours after the removal of aphidicolin, both two hours earlier than in the wild type line (Figure 4.9b). However, similarly to wild type, the second peak in mitosis in the SPYCE-*Arath*;WEE1 line occurred 22 hours after removal of aphidicolin (Figure 4.9b). This results in a longer cell cycle duration of 15 hours for the SPYCE-*Arath*;WEE1 line, two hours longer than in wild type. This is accounted for by an increase in duration of both S-phase and mitosis by one hour each (Figure 4.9b)

Two independent SPYCE-*Arath*;WEE1/SPYNE-*Arath*;SKIP1 lines, 6 and 2, were synchronised and scored for mitotic index. In both *Arath*;SKIP1 lines mitotic cells were seen three hours after the removal of aphidicolin, one hour later than in the SPYCE-*Arath*;WEE1 line, but one hour earlier than in wild type (Figure 4.9c and d). However, peaks in mitotic index did not occur until nine hours after removal of aphidicolin in line 6, 2 hours later than in the SPYCE-*Arath*;WEE1 line, but similar to wild type; or 11 hours after removal of aphidicolin in line 2, four hours later than in the SPYCE-*Arath*;WEE1 line and two hours later than in wild type (Figure 4.9c and d). This is accounted for by an increase in the duration of G2, lasting six and seven hours in line 6 and line 2, respectively (Figure 4.9c and d). A second peak in mitosis occurred 22 hours after removal of aphidicolin in line 6, giving a cell cycle duration of 13 hours, similar to wild type (Figure 4.9c). No clear second peak

occurred in line 2, although the mitotic index rose to a small peak 26 hours after the removal of aphidicolin, giving a cell cycle duration of 15 hours, similar to the SPYCE-*Arath*;WEE1 line (Figure 4.9d). The lengthened G2 phase in these lines was compensated for by a short G1 of 1.3 and 1.9 hours in line 6 and line 2, respectively, accounting for the similarity in cell cycle duration to wild type (Figure 4.9c and d).

An interesting attribute of the *Arath*;SKIP1 lines was the size of the mitotic peaks. The scaled-down method used here resulted in a peak wild type mitotic index of approximately 23% (Figure 4.9a). The peak mitotic index in the SPYCE-*Arath*;WEE1 line was similar, approximately 24% (Figure 4.9b). The peaks in mitotic index seen in the *Arath*;SKIP1 lines, however, were considerably higher: approximately 32% in line 6 and 38% in line 2, an increase of 9-14% compared to wild type and SPYCE-*Arath*;WEE1 (Figure 4.9c and d).

To test whether the results from the SPYCE-*Arath*;WEE1/SPYNE-*Arath*;SKIP1 lines were the effects of the double transformation, or of the WEE1 protein-protein interaction generally rather than a specific effect of the interaction with *Arath*;SKIP1, the SPYCE-*Arath*;WEE1 line was stably transformed with a different second construct, SPYNE-*Arath*;GSTF9. One independent line, line 3, was selected and used in a partial synchrony (ie. measurements were taken every hour up to only 11 hours, rather than the full 27 hours) in order to gather preliminary mitotic index data for this line. Mitotic cells were first seen 2 hours after removal of aphidicolin, although the mean percentage did not rise significantly above 0% until 8 hours after removal of aphidicolin, 5 hours after the same occurrence in the SPYCE-*Arath*;WEE1 line, and 4 hours after wild type (Figure 4.9e). Due to the limited number of measurements it was not possible to ascertain the time of peak mitosis in the *Arath*;GSTF9 line, although it was at least 11 hours after the removal of aphidicolin, so at least 4 hours later than in the SPYCE-*Arath*;WEE1 line and at least 2 hours later than in wild type, giving a delay similar to that in the *Arath*;SKIP1 lines (Figure 4.9e). Again due to the limited measurements, a second peak was not recorded therefore it was not possible to estimate cell cycle duration for the *Arath*;GSTF9 line. However, the length of G2 phase was estimated as eight hours, twice the length of G2 in wild type, and similar to the SPYCE-*Arath*;WEE1/SPYNE-*Arath*;SKIP1 lines (Figure 4.9e). The size of the mitotic peak in the *Arath*;GSTF9 line also cannot be meaningfully estimated.

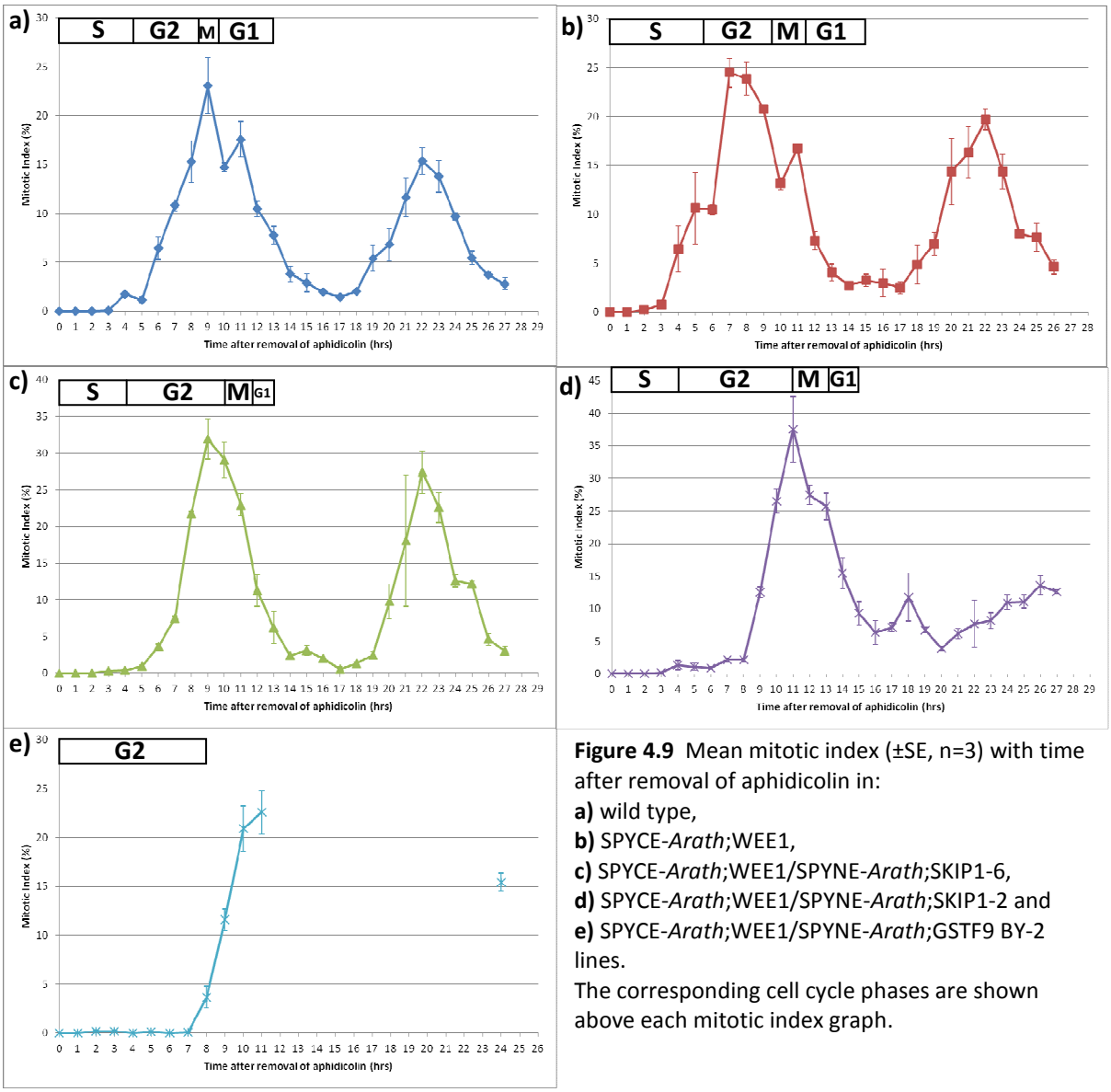

Figure 4.9 Mean mitotic index (±SE, n=3) with time after removal of aphidicolin in:
a) wild type,
b) SPYCE-*Arath*;WEE1,
c) SPYCE-*Arath*;WEE1/SPYNE-*Arath*;SKIP1-6,
d) SPYCE-*Arath*;WEE1/SPYNE-*Arath*;SKIP1-2 and
e) SPYCE-*Arath*;WEE1/SPYNE-*Arath*;GSTF9 BY-2 lines.
The corresponding cell cycle phases are shown above each mitotic index graph.

During each synchrony, images of mitotic cells from each of the transgenic lines were captured and used for measurements of mitotic cell size (as described in Section 2.1.4). Mitotic cells from the SPYCE-*Arath*;WEE1 line were, on average, 4400 μm^2 (Figure 4.10). The addition of the SPYNE-*Arath*;SKIP1 construct had no significant effect on the cell size in line 6, however in line 2 mitotic cells were significantly smaller than in the SPYCE-*Arath*;WEE1 line, by approximately 43%, and also smaller than the 3000 μm^2 usually recorded for wild type, with a mean mitotic cell area of 2500 μm^2 (Figure 4.10). Cells from the SPYCE-*Arath*;WEE1/SPYNE-*Arath*;GSTF9 BY-2 line were also significantly smaller than SPYCE-WEE1 alone, by approximately 23%, with a mean area of 3400μm^2 (Figure 4.10), similar to the size of wild type cells.

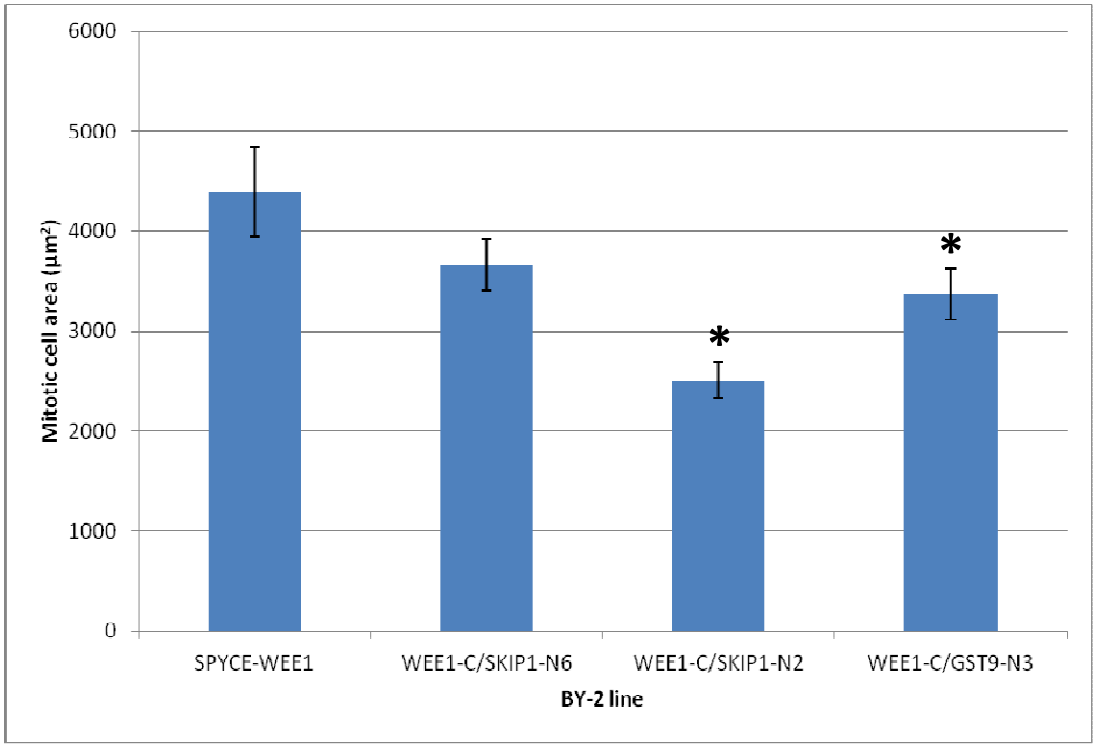

Figure 4.10 Differences in the mean area (±SE, n=27-41) of mitotic cells in the following transgenic BY-2 lines: SPYCE-*Arath*;WEE1 (SPYCE-WEE1), SPYCE-*Arath*;WEE1/SPYNE-*Arath*;SKIP1, lines 6 and 2 (WEE1-C/SKIP1-N6 and WEE1-C/SKIP1-N2) and SPYCE-*Arath*;WEE1/SPYNE-*Arath*;GSTF9, line 3 (WEE1-C/GST9-N3). * = significantly different from SPYCE-WEE1 ($P<0.05$).

The aim of the BiFC experiment was to study the dynamics of *Arath*;WEE1's interactions with the known interactors (described in Section 4.1) at different stages of the cell cycle. The double transformants, SPYCE-*Arath*;WEE1/SPYNE-*Arath*;SKIP1 (line 6) and SPYCE-*Arath*;WEE1/SPYNE-*Arath*;GSTF9 (line 3) were synchronised using aphidicolin and once a high mitotic index was reached (8 and 11

hours after the removal of aphidicolin respectively) a sample was taken and scored for the percentage of cells exhibiting a YFP signal in each cell cycle phase (as described in Section 2.1.5). The pattern of fluorescence is compared to that of GFP-*Arath*;WEE1 (as described in Section 3.3.1). In all 3 lines, a contingency chi-squared test confirmed that the proportion of fluorescence changed with respect to cell cycle phase (see legend of Figure 4.11).

As described in Section 3.3.1, the percentage of cells exhibiting GFP fluorescence, or, in other words, expressing *Arath*;WEE1, dropped sharply as cells entered mitosis, from 100% in interphase to only 4% and 0% in prophase and metaphase respectively, but rose again to 61% and 88% in anaphase and telophase (Figure 4.11). Both of the BiFC lines displayed a similar pattern to the GFP line with *Arath*;WEE1 alone (Figures 4.12 and 4.13), although the proportion of cells fluorescing in each line was somewhat different (Figure 4.11). Due to the inherent heterogeneity of fluorescence in the BiFC lines, which it was not possible to decrease (as described in Section 4.3.2), 100% fluorescence was neither expected nor observed in either BiFC line. Instead, in the *Arath*;SKIP1 line 64% of cells exhibited fluorescence during interphase, while only 48% of cells exhibited fluorescence during interphase in the *Arath*;GSTF9 line (Figure 4.11). In the *Arath*;SKIP1 line a 95% drop in fluorescence was seen between interphase and prophase, with only 3% of prophase cells fluorescing (Figure 4.11). This is similar to the 96% drop in fluorescence seen in the GFP- *Arath*;WEE1 line (Figure 4.11). However in the *Arath*;GSTF9 line there was only a 54% drop in fluorescence between interphase and prophase (Figure 4.11). In metaphase, no fluorescence was observed in any of the BY-2 lines (Figures 4.11, 4.12 and 4.13). While in anaphase the signal from GFP-*Arath*;WEE1 rose to 61%, the *Arath*;SKIP1 and *Arath*;GSTF9 lines exhibited fluorescence in only 31% and 20% of cells respectively, although both were highly variable (Figure 4.11). Between anaphase and telophase the proportion of cells exhibiting a GFP signal in the GFP- *Arath*;WEE1 line increased by 44%, however there was no change in the proportion of fluorescing cells in the *Arath*;SKIP1 line between anaphase and telophase, due to the high variability at anaphase (Figure 4.11). In the *Arath*;GSTF9 line there was a three-fold increase in the percentage of fluorescing cells between anaphase and telophase, bringing the percentage fluorescence in telophase to 66% (Figure 4.11). Interestingly this is 37.5% higher

than the percentage of cells fluorescing during interphase in this line, contrasting with the situation seen in the GFP- *Arath*;WEE1 line where fluorescence in telophase was 12% lower than in interphase (Figure 4.11). There was an even larger difference in the *Arath*;SKIP1 line, where fluorescence in telophase was 31% lower than in interphase (Figure 4.11).

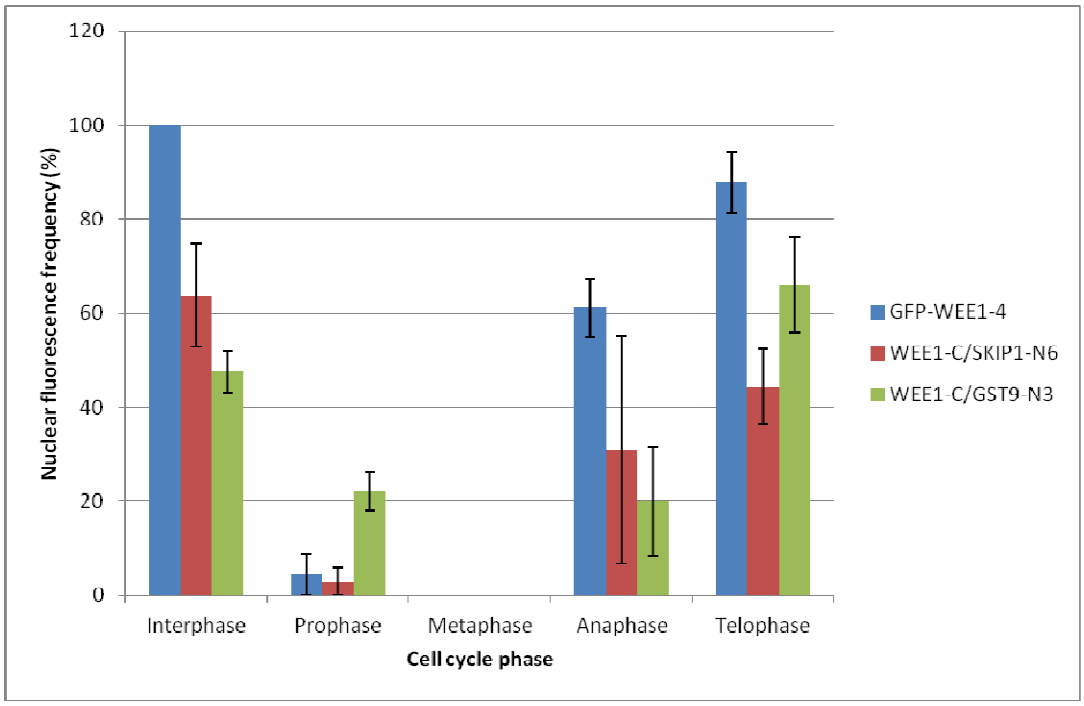

Figure 4.11 Mean nuclear fluorescence frequency (%; ±SE, n=3) in each cell cycle phase in cells from the following transgenic BY-2 lines: GFP-*Arath*;WEE1, line 4 (GFP-WEE1-4), SPYCE-*Arath*;WEE1/SPYNE-*Arath*;SKIP1, line 6 (WEE1-C/SKIP1-N6) and SPYCE-*Arath*;WEE1/SPYNE-*Arath*;GSTF9, line 3 (WEE1-C/GST9-N3). GFP-WEE1-4: Contingency $\chi 2 = 30.031$, df = 6, P =0.000. WEE1-C/SKIP1-N6: Contingency $\chi 2 = 98.585$, df = 6, P =0.000. WEE1-C/GST9-N3: Contingency $\chi 2 = 50.526$, df = 6, P =0.000.

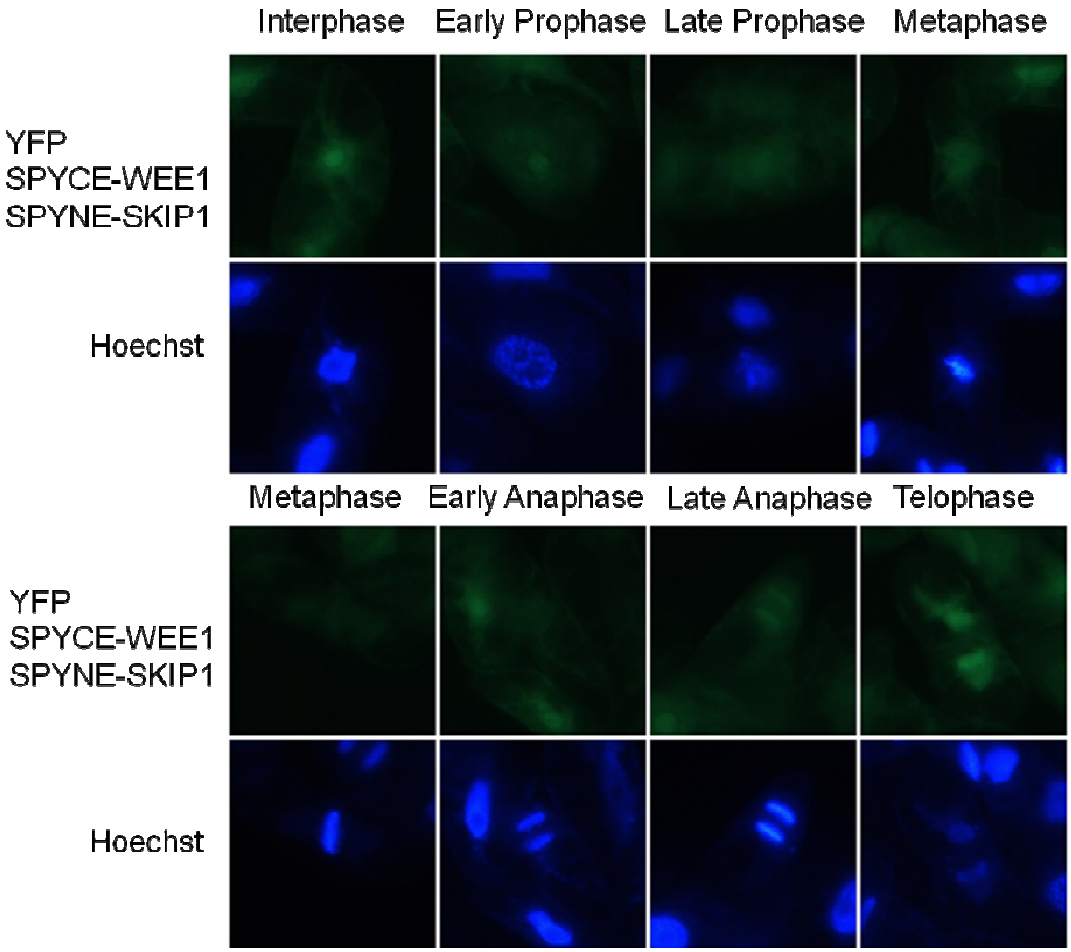

Figure 4.12 YFP expression in BY-2 line stably transformed with SPYCE-*Arath*;WEE1 and SPYNE-*Arath*;SKIP1 constructs. Hoechst was used as a counterstain to indicate mitotic phase. (Representative figures).

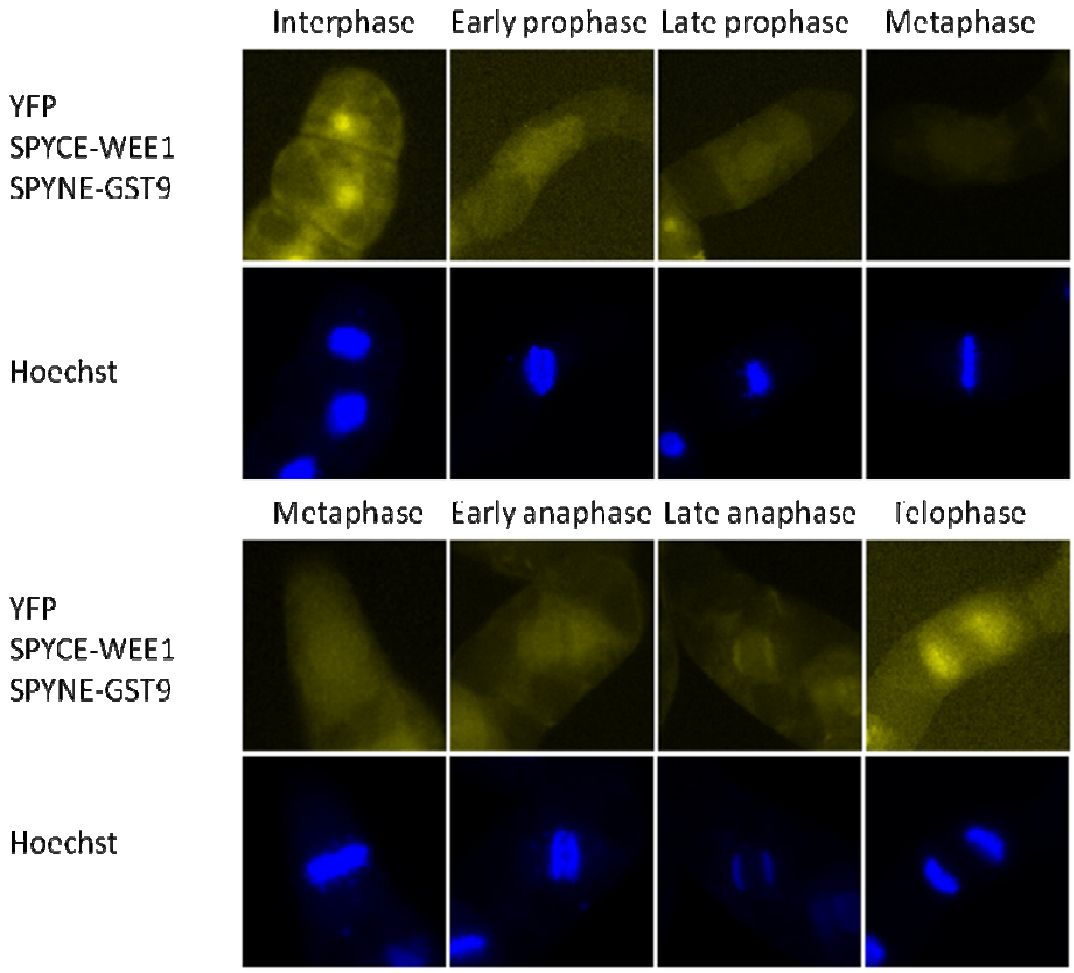

Figure 4.13 YFP expression in BY-2 line stably transformed with SPYCE-*Arath*;WEE1 and SPYNE-*Arath*;GSTF9 constructs. Hoechst was used as a counterstain to indicate mitotic phase. (Representative figures).

4.4 DISCUSSION

Previous work in the Cardiff lab has shown by yeast two-hybrid screening that *Arath*;WEE1 interacts with over 90 different proteins (Lentz Grønlund, 2007), several of which have been confirmed *in vivo* by bimolecular fluorescence complementation (Appendix IV, Lentz Grønlund et al., 2009). In the course of this work a further interaction was confirmed by BiFC, between *Arath*;WEE1 and *Arath*;SKIP1, an F-box protein (see Section 4.3.1). This interaction suggests that *Arath*;WEE1 is targeted for protein degradation via the 26S proteasome by *Arath*;SKIP1 (see Chapter 5).

WEE1 has been well characterised in many organisms as a cell cycle regulator (Den Haese et al., 1995; Booher et al., 1993; Russell and Nurse, 1987; Featherstone and Russell, 1991) and recent results seem to indicate that *Arath*;WEE1 may also have a role to play in the cell cycle in plants (see Chapter 3). In determining the functionality of *Arath*;WEE1's interactions with other proteins it is therefore of interest to study the dynamics of these interactions in different cell cycle phases. To this end, the highly synchronous tobacco BY-2 line was stably transformed with the split-YFP vectors for BiFC, first with the pSPYCE-*Arath*;WEE1 construct. The expression of this transgene was confirmed via semi-transient BiFC with *Arath*;SKIP1 (see Section 4.3.2), as used for BiFC experiments in previous work (Lentz Grønlund et al., 2009). Having confirmed SPYCE-*Arath*;WEE1 expression, the line was then stably co-transformed with interacting proteins in the pSPYNE vector: *Arath*;SKIP1, *Arath*;BZIP63 and *Arath*;GSTF9 (see section 4.3.2).

The co-transformed cultures were studied for growth characteristics in comparison to wild type BY-2 culture, before their use in the study of protein-protein interactions. Both SPYCE-*Arath*;WEE1/SPYNE-*Arath*;SKIP1 and the negative control, SPYCE-*Arath*;WEE1/SPYNE-*Arath*;BZIP63, grew in a similar manner to wild type over the course of seven days, in 95 mL culture (see section 4.3.2). The growth of the cultures in 8 mL and 29 mL of medium was not studied, however this would be interesting, especially as the cultures can take 14 days, ie. twice as long, to reach stationary phase in 8 mL of medium. However, the small amount of culture is limiting for these measurements, as at least 1 mL is required each day.

Cell division in the co-transformed cultures was synchronised and assessed for changes in mitotic index and mitotic cell size in comparison to wild type and SPYCE-*Arath*;WEE1 lines. It was expected that the SPYCE-*Arath*;WEE1 line would behave as the previously described *Arath*;WEE1 line, which leads to premature mitosis due to a reduced G2 phase (Siciliano, 2006; Lentz Grønlund, 2007; Spadafora, 2008). Indeed, the premature mitosis in this line compared to wild type (two hours, see Section 4.3.3) fits with predictions and supports the previously recorded phenotype associated with expression of *Arath*;WEE1 in tobacco BY-2 cells. However, the SPYCE-*Arath*;WEE1 line had a cell cycle duration of 15 hours, two hours longer than the typical 13-hour cell cycle duration of both the wild type and *Arath*;WEE1 lines (Orchard et al., 2005; Siciliano, 2006; Spadafora, 2008). In

the *Arath*;WEE1 line the short G2 leading to an early mitotic peak was compensated for by a long G1 (Siciliano, 2006; Spadafora, 2008). However, in the SPYCE-*Arath*;WEE1 line the durations of both G2 and G1 were similar to wild type, and the increased cell cycle duration could be attributed to the lengthening of both S-phase and mitosis (Figure 4.9). The differences in the BiFC lines compared to the previously described *Arath*;WEE1 line (Siciliano, 2006) may be related to the different vector systems used, with the SPYCE-*Arath*;WEE1 fusion protein containing a fragment of YFP. It would be useful to use semi-quantitative or real time RT-PCR to test the relative expression levels of *Arath*;WEE1 in the different lines.

Two SPYCE-*Arath*;WEE1/SPYNE-*Arath*;SKIP1 co-transformed lines were synchronised and mitotic index measured. The mitotic peak of line 6 was similar to wild type and had a normal cell cycle duration, while the mitotic peak of line 2 was later than both wild type and the SPYCE-*Arath*;WEE1 line, with a long cell cycle. Both SPYCE-*Arath*;WEE1/SPYNE-*Arath*;SKIP1 lines had a long G2, compensated for by a short G1 (Figure 4.9c and d). This suggests that the SPYNE-*Arath*;SKIP1 construct may be able to rescue the abnormal effects of *Arath*;WEE1 expression on the cell cycle of BY-2 cells. This could either be due to the stabilisation of *Arath*;WEE1 protein via the BiFC complex, or due to the over-expression of *Arath*;SKIP1 which may accelerate degradation of the *Arath*;WEE1 protein via the 26S proteasome. It would also be useful to use semi-quantitative or real time RT-PCR to quantify the levels of *Arath*;SKIP1 expression in these lines.

Typically, in a standard synchronisation experiment using the wild type line, peaks in mitotic index of 40-50% can be expected (e.g. Herbert et al., 2001), but this can drop to 20-30% for some transgenic BY-2 lines (e.g. Orchard et al., 2005). An interesting feature of the SPYCE-*Arath*;WEE1/SPYNE-*Arath*;SKIP1 co-transformed lines was the high mitotic peaks compared to wild type and SPYCE-*Arath*;WEE1. This could be indicative of a decrease in the inhibition of cell cycle progression by *Arath*;WEE1 due to it being targeted for removal by an increase in *Arath*;SKIP1. It would be interesting to know if there was less *Arath*;WEE1 protein, or even less total WEE1 protein (endogenous *Nicta*;WEE1 and *Arath*;WEE1) in the SPYCE-*Arath*;WEE1/SPYNE-*Arath*;SKIP1 co-transformed lines compared to SPYCE-*Arath*;WEE1 and wild type lines.

The SPYCE-*Arath*;WEE1/SPYNE-*Arath*;GSTF9 co-transformed line was used as a control to test whether the effects recorded for the SPYCE-*Arath*;WEE1/SPYNE-*Arath*;SKIP1 line were due to the BiFC interaction or due to *Arath*;SKIP1 over-expression. The peak in mitosis in the SPYCE-*Arath*;WEE1/SPYNE-*Arath*;GSTF9 co-transformed line was also later than that of both SPYCE-*Arath*;WEE1 and wild type lines, similar to the SPYCE-*Arath*;WEE1/SPYNE-*Arath*;SKIP1 lines. Additionally, the duration of G2 in the SPYCE-*Arath*;WEE1/SPYNE-*Arath*;GSTF9 line was also long, again similar to the SPYCE-*Arath*;WEE1/SPYNE-*Arath*;SKIP1 lines. This implies that the rescue of the abnormal effects caused by *Arath*;WEE1 over-expression, specifically the reversal of the premature mitosis due to a shortened G2 phase, is most likely due to the BiFC interaction rather than *Arath*;SKIP1 over-expression. Due to the limited number of measurements from the SPYCE-*Arath*;WEE1/SPYNE-*Arath*;GSTF9 line, it is not possible to draw any meaningful conclusions about the size of the mitotic peak in this line. However, the difference in mitotic index between 10 and 11 hours after the removal of aphidicolin is much smaller than the difference between 9 and 10 hours, which could lead to the conclusion that the peak in mitotic index was imminent and would be approximately 23-25% mitosis (Figure 4.9e). This is similar to wild type and SPYCE-*Arath*;WEE1, and much lower than the *Arath*;SKIP1 lines, which would confirm the high mitotic index to be an *Arath*;SKIP1 effect, rather than the effect of the double transformation. Of course it is also possible that the mitotic index of the *Arath*;GSTF9 line would have continued to increase after 11 hours, to reach the same levels as the *Arath*;SKIP1 lines or higher. The mitotic index measurements of this line would need to be repeated in full, to a total of at least 27 hours, to allow meaningful conclusions to be drawn. It would also be interesting to see the results of a synchrony using the SPYCE-*Arath*;WEE1/SPYNE-*Arath*;BZIP63 co-transformed line. There should be no BiFC interaction in this line, giving a negative control to further confirm that the delay in mitosis in the co-transformed lines was caused by the stabilisation of *Arath*;WEE1 protein via the BiFC interactions in the *Arath*;SKIP1 and *Arath*;GSTF9 lines.

Previous studies on the effects of WEE1 over-expression have shown a cell size effect. In fission yeast, when WEE1 is over-expressed, cell division is inhibited, leading to a long cell size phenotype (Russell and Nurse, 1987). Long cells are also

induced when *Arabidopsis* WEE1 is expressed in fission yeast (Sorrell et al., 2002), and this has also been demonstrated with human and maize WEE1 (Igarashi et al., 1991; Sun et al., 1999). This long cell phenotype would also be expected when expressing *Arath*;WEE1 in tobacco BY-2 cells, however it has been routinely found that this actually causes a small size (Siciliano, 2006; Spadafora, 2008). The expression of *Arath*;WEE1 in tobacco plants also leads to a small cell size (G. Rafiei, Cardiff University, unpublished data). Measurements of mitotic cell size were taken from synchronised SPYCE-*Arath*;WEE1 and co-transformed BY-2 lines. Cells from the SPYCE-*Arath*;WEE1 line were, on average, larger than the 3000 μm^2 usually recorded for synchronised wild type cells (Orchard et al., 2005; Siciliano, 2006; Spadafora, 2008). This is the opposite effect of that seen in *Arath*;WEE1 over-expressing BY-2 cells (Siciliano, 2006; Spadafora, 2008). However the large cell size phenotype is as would generally be expected for an over-expression of WEE1. It is possible that the differences are caused by the different vectors used in the different *Arath*;WEE1 lines, with the SPYCE-*Arath*;WEE1 construct containing a fragment of YFP. The effect may alternatively be due to the different size of these cultures, grown in 29 mL of medium as opposed to the previously used 95 mL. The study of change in mitotic cell size in wild type cultures of varying sizes could be an interesting area of future research.

The addition of both SPYNE-*Arath*;SKIP1 (line 2 only) and SPYNE-*Arath*;GSTF9 led to mitotic cell sizes which were, on average, significantly smaller than in the SPYCE-*Arath*;WEE1 line alone. This gives them a similar cell size to the wild type line (Siciliano, 2006; Spadafora, 2008), which, taken with the mitotic index results above, probably confirms that the BiFC interactions were stabilising *Arath*;WEE1, preventing the effects of its over-expression. It is also possible that the BiFC interaction was preventing the catalytic function of the WEE1 enzyme.

The overall aim of the BiFC experiment was to study the dynamics of *Arath*;WEE1's interactions with *Arath*;SKIP1 and *Arath*;GSTF9 at different stages of the cell cycle. The percentage of cells demonstrating fluorescence associated with the chromosomes in each cell cycle phase was calculated for each line. A fluorescent signal was indicative of an interaction between *Arath*;WEE1 and either *Arath*;SKIP1 or *Arath*;GSTF9. The results were compared to those of the GFP-*Arath*;WEE1 line, described in Section 3.3.1. The results from the BiFC lines were more variable than

the GFP-*Arath*;WEE1 results, as expected due to the low efficiency of the technique (see Section 4.3.3). However, the overall pattern of fluorescence from both BiFC lines was similar to the pattern seen in the GFP-*Arath*;WEE1 line, being relatively high in interphase, low and completely absent in prophase and metaphase respectively, and rising again into anaphase and telophase (see Section 4.3.3). It is difficult to tell whether or not this is genuinely the pattern of interaction between *Arath*;WEE1 and *Arath*;SKIP1 or *Arath*;GSTF9, or merely an effect of the removal of *Arath*;WEE1 at mitosis. This is discussed in detail below.

Between interphase and prophase the proportion of cells indicating an interaction between *Arath*;WEE1 and *Arath*;SKIP1 dropped by a similar amount to the proportion of cells expressing GFP-*Arath*;WEE1 between the same two phases. On the other hand, the proportion of cells indicating an interaction between *Arath*;WEE1 and *Arath*;GSTF9 only dropped by almost half as much as the other two lines between interphase and prophase. One explanation for this could be that while both the *Arath*;SKIP1 and *Arath*;GSTF9 interactions stabilised *Arath*;WEE1 via BiFC, as implied by the mitotic index and mitotic cell size results described above, the over-expression of *Arath*;SKIP1 leads to an increase in *Arath*;WEE1 degradation. This could compensate for the effects of stabilisation by decreasing the amount of *Arath*;WEE1 protein to the levels seen in the GFP-*Arath*;WEE1 line alone, leading to the similar decrease in fluorescence at prophase. This theory is also supported by the high percentage of mitotic cells seen in the SPYCE-*Arath*;WEE1/SPYNE-*Arath*;SKIP1 lines compared to the SPYCE-*Arath*;WEE1 and SPYCE-*Arath*;WEE1/SPYNE-*Arath*;GSTF9 lines, which could imply a removal of mitotic inhibition by *Arath*;WEE1 by its degradation via excess *Arath*;SKIP1.

In the GFP-*Arath*;WEE1 line it was discovered that *Arath*;WEE1 is never observed during metaphase (see Section 3.3.1). In both BiFC lines an interaction was also never seen during metaphase (Section 4.3.3), confirming that the stabilisation of the protein via the BiFC interaction was not sufficient to prevent its degradation. This also implies a strong mechanism for the complete removal of all WEE1 protein before mitosis is able to proceed beyond prophase.

The high variability in the proportion of fluorescence seen in the BiFC lines at anaphase and telophase make it difficult to draw any meaningful conclusions about

the dynamics of the interactions between *Arath*;WEE1 and the interacting proteins of interest during these mitotic phases. It is known from previous work that WEE1 protein levels peak in S-phase (Lentz Grønlund, 2007) and the results from the GFP-*Arath*;WEE1 line show that WEE1 is removed prior to metaphase (see Section 3.3.1). So, it is interesting in itself that there is evidence of interactions occurring during anaphase. This means that interactions between *Arath*;WEE1 and its interactors take place soon after *Arath*;WEE1 is expressed again, which is not necessarily to be expected, especially in the *Arath*;SKIP1 line with its expected role in targeting WEE1 for degradation. In human cells WEE1 protein localises to the microtubules at telophase and cytokinesis (Baldin and Ducommun, 1995). It has been proposed that this could function to inhibit CDK1 activity on exit from mitosis (Baldin and Ducommun, 1995). The return of the interactions observed in the BiFC lines during anaphase and telophase may also indicate a role for *Arath*;WEE1 at this stage of the cell cycle. Another possibility is that the *Arath*;WEE1 is being targeted as a non-endogenous protein, but then the interactor in question is *Arath*;SKIP1, itself not an endogenous protein. It would be interesting to see if the pattern of interactions were different if *Nicta*;WEE1 and *Nicta*;SKIP1, expressed under their native promoters, were used instead. It is more difficult to interpret the pattern of localisation during mitosis in the SPYCE-*Arath*;WEE1/SPYNE-*Arath*;GSTF9 line as *Arath*;GSTF9 localisation has not been characterised. Therefore it is not clear what pattern is expected between *Arath*;WEE1 and *Arath*;GSTF9.

There are of course several limitations to the use of the BiFC technique. Firstly, the efficiency is low, with only a small proportion of cells exhibiting an interaction between the two proteins. However, stably co-transforming the BY-2 cells with both constructs rather than using transient transformation did improve the efficiency considerably. It is known that false positives can occur using the BiFC technique, as the YFP fragments may associate non-specifically at high expression levels, which generates background fluorescence (Stephens and Banting, 2000). However the difference between these and real positive interactions is easy to distinguish with some experience. This does, of course, add an element of subjectivity to the procedure. A considerable disadvantage of the technique is the lack of potential to follow the change in an interaction in real time. This is because once the interaction occurs, the YFP is stable and the two fragments do not part (Kerppola, 2009).

This also restricts the interpretation of the cell cycle phase results, although does not entirely explain the reason why the BiFC lines follow the same pattern as the GFP-*Arath*;WEE1 line. It should not mean that whenever *Arath*;WEE1 is expressed, the interaction occurs. Although under the control of the 35S promoter and therefore constitutively expressed, a positive signal is only observed when the two proteins interact. The possibility remains that the two proteins could be sequestered in distinct subcellular compartments, preventing the interaction. *Arath*;WEE1 is not expressed during metaphase, and a recurrence of the interaction between *Arath*;WEE1 and *Arath*;SKIP1 is not expected until interphase. However, if the BiFC interaction was stabilising the *Arath*;WEE1 so that it was not degraded during mitosis we would expect to see the signal in metaphase as well as anaphase and telophase. So both the loss of the signal at metaphase and the observation of the signal in anaphase imply a real recurrence of the interactions at this stage. It may, however, explain the relatively higher proportions of fluorescence between anaphase and telophase and between telophase and interphase in the SPYCE-*Arath*;WEE1/SPYNE-*Arath*;GSTF9 line, as the complexes are able to accumulate over time. A final restriction of the method used is that *Arabidopsis* proteins were studied in a tobacco system, and were also (probably) expressed at high levels, meaning that the results may not accurately reflect the *in vivo* situation.

Although BiFC has been used in BY-2 cells previously, this is usually done by transient transformation so, to our knowledge, this work represents the first demonstration of the BiFC technique used in stably transformed tobacco BY-2 cultures, although BiFC has been demonstrated in stably transformed *Arabidopsis* plants (Boruc et al., 2010c). Most frequently BiFC is used by transient transformation via infiltration into *Nicotiana benthamiana* leaves (Boruc et al., 2010c; Dowil et al., 2011; Halimi et al., 2011; Van Damme et al., 2011) although the method can also be used in rice protoplasts (Li et al., 2011), and has of course been demonstrated previously in tobacco BY-2 cells (Liu et al., 2009; Lee et al., 2008; Lentz Grønlund et al., 2009; Yano et al., 2006).

It would be interesting to use other methods to further confirm the dynamics of the *Arath*;WEE1 interactions at different stages of the cell cycle. A frequently used method is to introduce mutations to the putative binding sites of the proteins followed by BiFC to test for the abolition of the interactions (Lentz Grønlund et al.,

2009; Li et al., 2011). Co-localisation of the proteins separately can be tested using full-length fluorescent protein fusions (Boruc et al., 2010c; Van Damme et al., 2011). Co-immunoprecipitation could be used (Dowil et al., 2011; Halimi et al., 2011; Van Damme et al., 2011), although there are limitations, for example the cells would need to be sorted into cell cycle phases prior to analysis. One study couples BiFC with flow cytometry to produce a high throughput method of screening the strength of protein-protein interactions (Morell et al., 2008). BiFC can also be used alongside methods such as fluorescence resonance energy transfer (FRET; Kerppola, 2009). It would be interesting to repeat the BiFC experiment using tobacco proteins, especially if introduced into a mutant background to ensure there was no net over-expression. Of course the further study of the function of these interactions is probably the most interesting aspect, and should prove very useful towards our understanding of the role of WEE1 in plants. The following chapter (Chapter 5) outlines the results of experiments completed to verify the role of *Arath*;SKIP1 in targeting *Arath*;WEE1 for degradation via the 26S proteasome.

5. PERTURBATION OF THE *ARATH*;WEE1 INTERACTOR, *ARATH*;SKIP1, AFFECTS ROOT PHENOTYPE IN *ARABIDOPSIS* SEEDLINGS

5.1 INTRODUCTION

One of the proteins found to interact with *Arath*;WEE1 via yeast-two hybrid was SKIP1 (SKP1 interacting protein, At5g57900), an F-box protein (Lentz Grønlund, 2007). F-box proteins are involved in protein degradation via the ubiquitin/26S proteasome-mediated pathway (see Section 1.6.2.1; reviewed by Wang et al., 2004 and Sullivan et al., 2003). *Arath*;SKIP1 is a 35 kDa protein which has an F-box domain at its N-terminus and is able to interact with the *Arabidopsis* SKP1 homologue, *Arath*;ASK1 (Farras et al., 2001). Although the F-box proteins form a superfamily, *Arath*;SKIP1 is not closely related to any other proteins in *Arabidopsis*. The closest homologue is a member of the RNI-superfamily, the *Arabidopsis* putative F-box/leucine-rich repeat protein 19 (At4g30640), which shares 40% gene sequence identity with *Arath*;*SKIP1*. *Arath*;SKIP1 is also related to several cyclin-like F-box proteins from *Medicago truncatula*. There is evidence to suggest that SKIP1 is involved in the response to abiotic stress in *Arabidopsis*. *Arath*;*SKIP1* expression increases when the plant is subjected to a combination of drought and heat stress (Rizhsky et al., 2004), and is also up-regulated in response to cold de-acclimation (recovery from cold stress; Oono et al., 2004). Additionally, SKIP1 may be involved in ethylene and cytokinin signalling (Hass et al., 2004), and in the response to viral infection (Ascencio-Ibanez et al., 2008).

In both yeasts and mammals there is evidence that WEE1 is degraded via the 26S proteasome pathway. The budding yeast and human homologues to the SCF component, SKP1, were both required for the transition from G2-phase into mitosis (Bai et al., 1996), demonstrating a link between the cell cycle and the SCF complex. In the African frog, *Xenopus laevis*, the degradation of WEE1 requires CDC34, an E2, or ubiquitin-conjugating, enzyme (Michael and Newport, 1998). This degradation of WEE1 was required for the correct timing of mitosis, and was blocked by inhibition of DNA replication, clearly indicating a link between the

completion of S-phase and the progression of mitosis (Michael and Newport, 1998). The *S. cerevisiae* WEE1 homologue, SWE1, is degraded in a cell cycle dependent manner, requiring CDC28 activity for degradation (Sia et al., 1998). Recently it was discovered that SWE1 is targeted for degradation by a SUMO (Small-Ubiquitin Modifier proteins, similar to ubiquitin) protein, SMT3, via the E3 ligase SIZ1 (Simpson-Lavy and Brandeis, 2010). F-box proteins have also been previously implicated in WEE1 degradation, including MET30 in *S. cerevisiae* (Kaiser et al., 1998) and TOME-1 in *Xenopus* (Ayad et al., 2003).

The 26S proteasome is also important for cell cycle regulation in plants. Another type of ubiquitin E3 ligase, the APC, is conserved in plants and is important for mitotic progression and exit (Capron et al., 2003). The CDK inhibitor KRP1 is targeted for degradation by two ubiquitin E3 ligases, including SCF^{SKP2b} (Ren et al., 2008). Protein degradation is also important for plant development, for example APC is active in post-mitotic cells and is important for the development and organisation of vascular tissue in *Arabidopsis* (Marrocco et al., 2009). An *Arabidopsis* F-box protein, FBL17, is important for male gametogenesis, highlighting the diverse functions of the F-box proteins in plants (Gusti et al., 2009).

In tobacco BY-2 cells *Nicta*;WEE1 protein levels decrease as the percentage of cells in mitosis increase, which may imply that a certain level of WEE1 degradation is required for mitotic progression (Lentz Grønlund, 2007). WEE1 activity can also be negatively controlled by phosphoregulation (reviewed by Dunphy, 1994), which may explain why some *Nicta*;WEE1 protein is still present at mitosis (Lentz Grønlund, 2007), as it could be present in an inactive form.

Expression data from microarrays show that *Arath*;*WEE1* and *Arath*;*SKIP1* are sometimes co-expressed, both spatially and temporally (Schmid et al., 2005). Both are moderately expressed in the roots, stems and cotyledons, as well as flower buds, early embryos and young siliques (Schmid et al., 2005). Both *Arath*;*WEE1* and *Arath*;*SKIP1* are also moderately expressed in the shoot apical meristem (Yadav et al., 2009). However, neither gene is ever highly expressed at the same time. *Arath*;*WEE1* is highly expressed in both the shoot apex and mature pollen, while *Arath*;*SKIP1* is low (Schmid et al., 2005). Conversely, *Arath*;*WEE1* is expressed at a

low level in mature flowers and dry seed, where *Arath*;*SKIP1* is highly expressed (Schmid et al., 2005). In the leaves, *Arath*;*WEE1* is highly expressed in stage 10 leaves while *Arath*;*SKIP1* is highly expressed in cauline and senescent leaves (Schmid et al., 2005). Finally, in the embryo *Arath*;*SKIP1* is highly expressed in the seed coat, while *Arath*;*WEE1* is highly expressed in the embryo and endosperm, especially at the linear cotyledon stage (Schmid et al., 2005). The co-expression of the genes in certain organs supports a role for *Arath*;SKIP1 in the degradation of *Arath*;WEE1. The lack of *Arath*;*SKIP1* expression in organs where *Arath*;*WEE1* is highly expressed could be due to an underlying mechanism ensuring that *Arath*;WEE1 is not degraded when its activity is needed.

Arabidopsis provides the tools to manipulate levels of gene expression and thus test whether altering the levels of WEE1-interacting proteins impacts on WEE1 function. One hypothesis is that increased expression of *Arath*;*SKIP1* would lead to increased levels of SCF ubiquitin E3 ligase, which would increase the ubiquitination of *Arath*;WEE1 and decrease WEE1 abundance, leading to premature mitosis. Conversely, a knockout of SKIP1 should decrease the levels of suitable SCF complex, decreasing ubiquitination of WEE1 and increasing WEE1 abundance, delaying mitosis and inducing G2 arrest. Additionally, an alteration in cell size would be expected in these lines, with small cells evident where SKIP1 is over-expressed and large cells where SKIP1 expression is decreased, due to the difference in WEE1 protein abundance.

5.1.1 EXPERIMENTAL AIMS

Further characterisation of the *Arath*;SKIP1 F-box protein is required in order to assess its impact on *Arath*;WEE1 protein levels and function. This was investigated by generating transgenic lines carrying an extra copy of *Arath*;SKIP1 and thorough analysis of an *Arath*;SKIP1 T-DNA insertion line, asking:

1. What is the effect of perturbing *Arath*;*SKIP1* gene expression on *Arabidopsis* root phenotype compared with *Arath*;*WEE1* over-expression?
2. What is the effect of knocking-down *Arath*;*SKIP1* gene expression on *Arath*;WEE1 protein levels?

5.2 MATERIALS AND METHODS

For full details of methods used in this chapter please refer to Chapter 2: General Materials and Methods.

5.3 RESULTS

The *Arath*;WEE1 interactor *Arath*;*SKIP1* was transformed into *Arabidopsis* in an attempt to over-express this F-box gene. However, unexpectedly, this transformation resulted in decreased expression of endogenous *Arath*;*SKIP1*. These lines were analysed and the phenotype compared to wild type and plants over-expressing *Arath*;*WEE1*. Attempts were made to further analyse these lines both by western blotting for the abundance of *Arath*;WEE1 protein, and crossing with a GFP-*Arath*;WEE1 line, however these proved unsuccessful.

5.3.1 ISOLATION OF SENSE KNOCK-DOWN LINES OF *ARATH*;*SKIP1* IN *ARABIDOPSIS* PLANTS

The split-YFP construct pSPYNE- *Arath*;*SKIP1* was transformed into *Arabidopsis* via *Agrobacterium* EHA105 and the floral dip method in an attempt to over-express this gene (see Section 2.3.1). Seed harvested from the dipped plants was selected on hygromycin and growing seedlings were transferred from the selection plates onto soil (see Section 2.3.2). After several weeks of growth of first generation seedlings in soil, DNA was extracted from the leaves of eight plants and tested for the presence of the pSPYNE-*Arath*;*SKIP1* construct by PCR (see Section 2.4). A primer specific for *Arath*;*SKIP1* was used to verify the presence of *Arath*;*SKIP1* and a primer directed against the CMYC affinity tag was used to verify the presence of the vector (see Table 2.3). A fragment of the expected size of 900bp was amplified from the DNA extracts of all eight plants, confirming the presence of the construct in the transgenic plants (Figure 5.1). After material was taken for RNA extraction, plants were allowed to self and set seed, and seeds collected for further work.

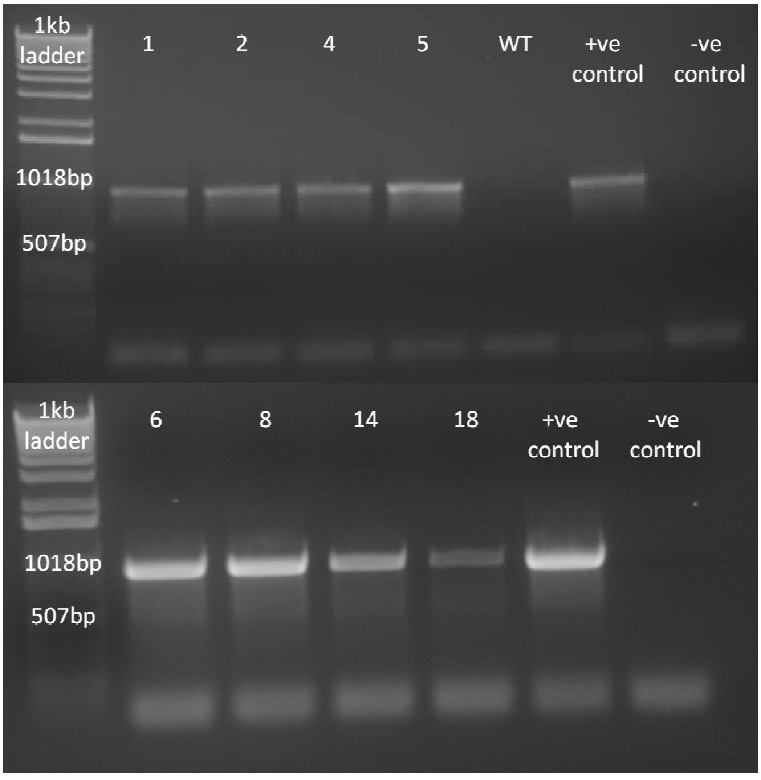

Figure 5.1 Results of PCR for the pSPYNE-*Arath*;SKIP1 construct in transformed *Arabidopsis* plants using FBOXF and CMYCR primers. Numbers **1-18** refer to each individual plant sampled.
WT = wild type.
+ve control = positive control, SPYNE-*Arath*;SKIP1 plasmid.
–ve control = negative control, SDW.

RNA was extracted from the leaves of all eight plants and, following DNase treatment, tested by PCR to ensure the absence of genomic DNA (see Section 2.5). cDNA was synthesised for use in semi-quantitative RT-PCR to confirm levels of transgene expression (as described in Section 2.5). The pSPYNE-*Arath*;*SKIP1* transgene could consistently only be detected in cDNA of lines 4 and 6 (Figure 5.2), leading to the question of whether the transgene was in fact inhibiting the expression of the endogenous *Arath*;*SKIP1* gene.

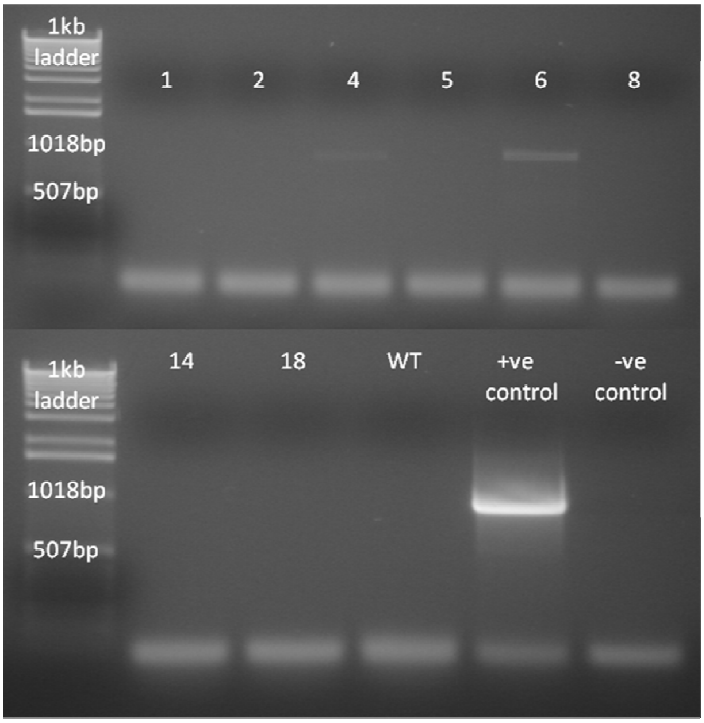

Figure 5.2 Results of PCR for the pSPYNE-*Arath*;SKIP1 transgene in transformed *Arabidopsis* plants using FBOX and CMYCR primers. Numbers **1-18** refer to each individual plant sampled.
WT = wild type.
+ve control = positive control, SPYNE-*Arath*;SKIP1 plasmid.
–ve control = negative control, SDW.

To test this, the cDNA was used for semi-quantitative RT-PCR in comparison with wild type cDNA for expression of the endogenous *Arath*;*SKIP1* gene using *Arath*;*SKIP1* specific primers (Table 2.3). The results show that all eight plants were expressing *Arath*;*SKIP1* to varying degrees, but all less than wild type (Figure 5.3). The expression of endogenous *Arath*;*SKIP1* was reduced by at least 50% compared to wild type in each line, with the highest expression seen in line 6 at 48% of wild type expression (Figure 5.3). Seed from all eight *Arath*;SKIP1 sense knockdown lines were sown on selective medium and two homozygous lines, 1b and 5b, selected for phenotypic analysis. Lines were considered homozygous if 100% of germinated seedlings survived on MS medium supplemented with hygromycin.

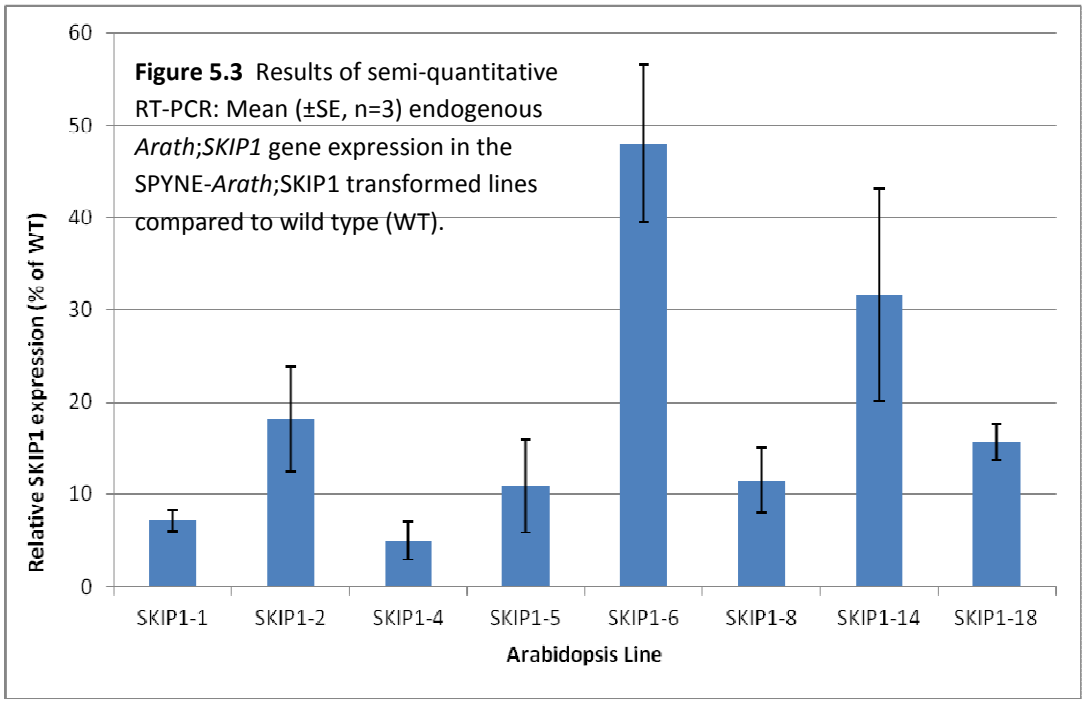

Figure 5.3 Results of semi-quantitative RT-PCR: Mean (±SE, n=3) endogenous *Arath*;*SKIP1* gene expression in the SPYNE-*Arath*;SKIP1 transformed lines compared to wild type (WT).

5.3.2 ANALYSIS OF A T-DNA INSERTION LINE OF *ARATH*;*SKIP1* IN *ARABIDOPSIS* PLANTS

A T-DNA insertion mutant of *Arath*;*SKIP1* was acquired (GK-571F12-0231F2; NASC, Nottingham, UK), with a T-DNA insertion in the first exon, 49 bp downstream of the ATG. Seeds were sown on MS medium (see Section 2.3.3), and DNA was extracted from mature leaves and genotyped by PCR for the presence of the T-DNA (see Section 2.4). Primers specific for the wild type *Arath*;*SKIP1* allele and the insertion allele were designed and used to test the homozygosity of the plants (Table 2.3; P1, P2 and P3; Figures 5.4 and 5.5). Plants homozygous for the insertion allele were transferred to soil, mature leaves taken for RNA extraction (see Section 2.5), and the plants allowed to grow and set seed. Seed from one of these homozygous lines was selected for phenotypic analysis.

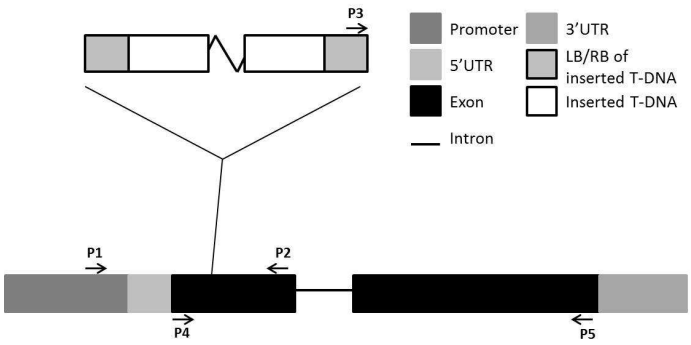

Figure 5.4 Schematic diagram of the *Arath*;*SKIP1* gene indicating position of T-DNA insertion.
P1 = AtSKIP1promF primer,
P2 = AtSKIP1exon1R primer,
P3 = GABI LB primer,
P4 = FBOXF primer,
P5 = FBOXR primer.

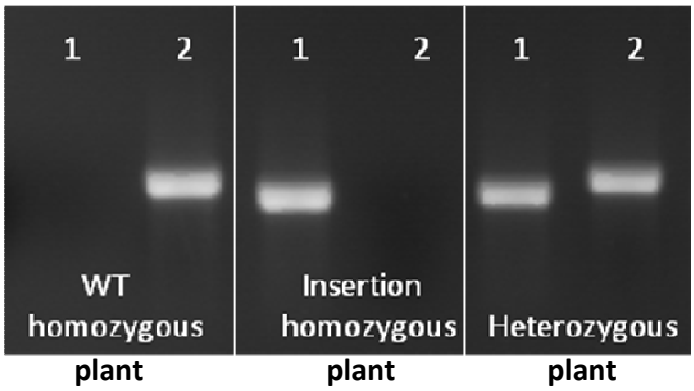

Figure 5.5 Representative image of results of genotyping for the presence of *Arath*;*SKIP1* T-DNA in three plants. Primers specific for the insertion allele (1; GABI LB and AtSKIP1exon1R; 277bp) and the wild type *Arath*;*SKIP1* allele (2; AtSKIP1promF and AtSKIP1exon1R; 377bp) were used (see Table 2.3). If a fragment was amplified using primer set 2, but not 1, the plant was wild type (WT). If a fragment was amplified using primer set 1, but not 2, the plant was homozygous for the insertion allele. If a fragment was amplified using both primer sets, the plant was heterozygous.

Semi-quantitative RT-PCR was used to compare the expression levels of endogenous *Arath*;*SKIP1* in mature leaves of the two homozygous *Arath*;SKIP1 sense knock-down lines and the homozygous T-DNA insertion line with wild type *Arabidopsis* (see Section 2.5). A line over-expressing *Arath*;*WEE1*, WEE1-58 (Spadafora, 2008), was used as a control. Primers designed to amplify the *Arath*;*SKIP1* ORF were used (P4 and P5; Figure 5.4; Table 2.3). The homozygous sense knock-down lines (SKIP1-1b and SKIP1-5b) still expressed *Arath*;*SKIP1* at a significantly lower level than wild type (Figure 5.6). The *Arath*;*SKIP1* expression levels of lines 1b and 5b were 33% and 83% of wild type expression, respectively (Figure 5.6). It was expected that the T-DNA insertion in the first exon of *Arath*;*SKIP1* would lead to reduced expression of the endogenous gene. Unexpectedly, the *Arath*;SKIP1 T-DNA insertion line was found to be expressing *Arath*;*SKIP1* at a significantly higher level than wild type (by 15%; Figure 5.6), indicating that it was, in fact, not a knock-out mutant line, despite being homozygous for the T-DNA insertion. Interestingly, the *Arath*;WEE1 over-expressing control line was also significantly over-expressing *Arath*;*SKIP1*, at a level 19% higher than wild type (Figure 5.6).

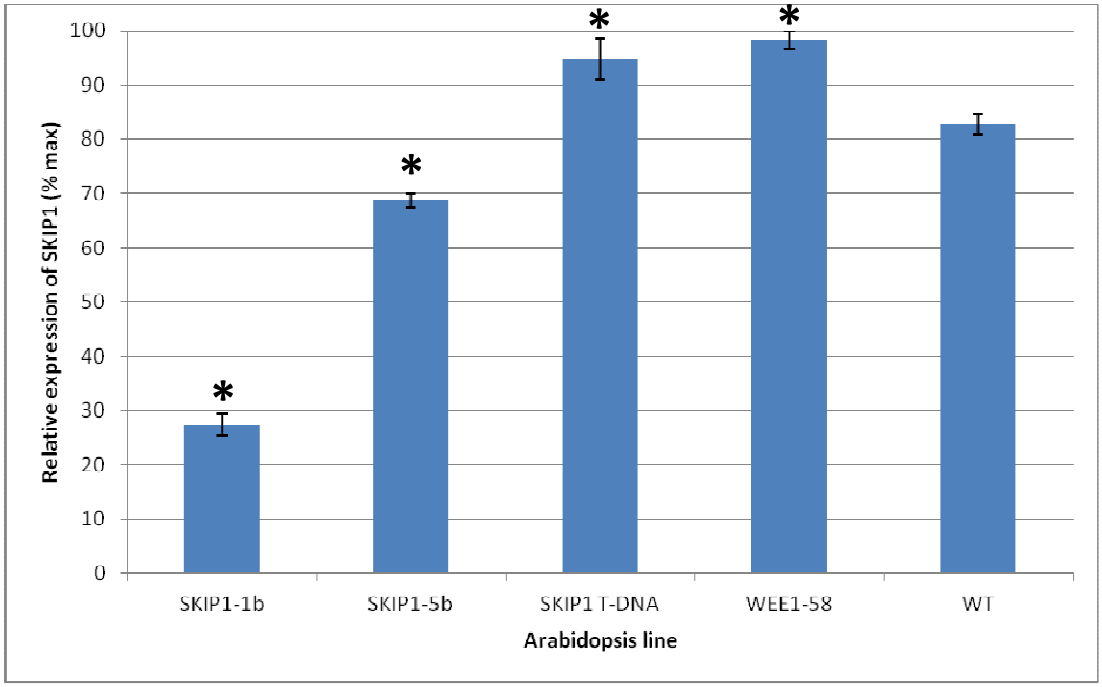

Figure 5.6 Results of semi-quantitative RT-PCR: Mean (±SE, n=3) endogenous *Arath*;*SKIP1* gene expression in the SPYNE-*Arath*;SKIP1 transformed lines (SKIP1-1b and -5b) and the *Arath*;SKIP1 T-DNA insertion line compared to wild type (WT). * = significantly different from WT (P<0.05).

To further study the expression of *Arath*;*SKIP1* in the T-DNA insertion line, the cDNA was tested by PCR (Section 2.4.2) using the primers specific for the wild type *Arath*;*SKIP1* allele and the insertion allele (P1, P2 and P3; Figure 5.4; Table 2.3). As expected, the wild type genomic DNA and cDNA were positive for the wild type allele and not the T-DNA insertion (Figure 5.7). Also as expected, and as seen in Figure 5.5, the gDNA from the *Arath*;*SKIP1* insertion line was positive for the T-DNA insertion, but not the wild type allele (Figure 5.7). The cDNA from the *Arath*;*SKIP1* insertion line was also positive for the T-DNA insertion, however a faint band was also amplified using the primers for the wild type allele (Figure 5.7).

Figure 5.7 Results of PCR to test *Arath*;*SKIP1* T-DNA insertion line (T-DNA) compared to wild type (WT). Primers for the *Arath*;*SKIP1* wild type allele (P1+2) and T-DNA insertion (P2+3) were used (Figure 5.4; Table 2.3) on genomic (g) DNA and cDNA from each line. –ve control = negative control, SDW.

The possibility that the T-DNA insertion was not inserted into the *Arath*;*SKIP1* gene was tested for by PCR (Section 2.4.2) using primers for the *Arath*;*SKIP1* ORF (P4 and P5; Figure 5.4; Table 2.3) on genomic DNA and cDNA from the *Arath*;SKIP1 T-DNA insertion line compared to wild type gDNA and cDNA. These primers used on a wild type template should amplify a fragment of 900 bp (exons only) from the cDNA and 1000 bp from wild type gDNA. No fragments should be amplified from the *Arath*;SKIP1 T-DNA insertion line gDNA or cDNA because the T-DNA insertion would make the fragment too large to be amplified. As seen in Figure 5.8, the fragments amplified from the wild type gDNA and cDNA were of the expected sizes. However the same size fragments were also amplified from the *Arath*;SKIP1 T-DNA insertion line gDNA and cDNA (Figure 5.8).

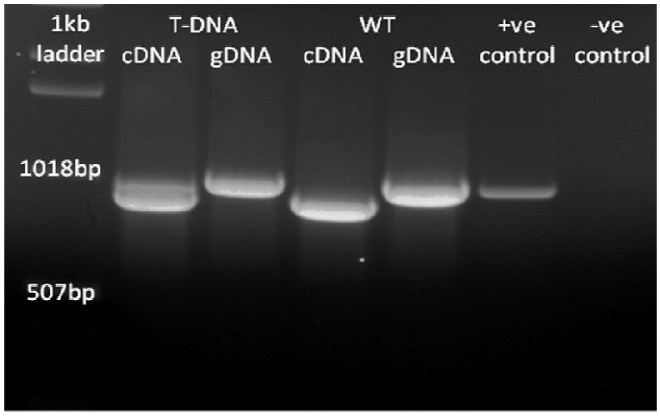

Figure 5.8 Results of PCR to test for splicing of T-DNA insertion from *Arath*;*SKIP1* T-DNA insertion line (T-DNA) compared to wild type (WT). Primers for the *Arath*;*SKIP1* ORF were used (Table 2.3) on genomic (g) DNA and cDNA from each line.
+ve control = positive control, SPYNE-*Arath*;SKIP1 plasmid.
–ve control = negative control, SDW.

5.3.3 PHENOTYPING OF SENSE KNOCK-DOWN AND T-DNA INSERTION LINES OF *ARATH*;SKIP1 IN *ARABIDOPSIS* PLANTS

The phenotypes of the two *Arath*;SKIP1 sense knock-down lines, 1b and 5b, and that of the *Arath*;SKIP1 T-DNA insertion line, were compared to wild type and two lines over-expressing *Arath*;*WEE1* (WEE1-58 and WEE1-61; Spadafora, 2008). The *Arath*;*WEE1* over-expressors were used as a control because it was expected that if *Arath*;WEE1 is targeted for degradation by *Arath*;SKIP1, a decrease in *Arath*;SKIP1 should lead to an increase in *Arath*;WEE1 protein. Half of the seedlings were fixed after seven days growth and the other half after fourteen days growth (see Section 2.3.5). Primary root length was measured daily in all seedlings until fixed (Figure 5.9). The primary root growth data were analysed by linear regression in order to calculate rates of primary root elongation in each line. Over the course of 14 days, the primary root elongation rates of the *Arath*;SKIP1 sense knock-down lines were intermediate between the *Arath*;WEE1 over-expressing lines and wild type (Figure 5.9). The *Arath*;SKIP1 sense knock-down lines elongated at a rate of 5.3 mm per day, while the roots of the *Arath*;WEE1 over-expressors elongated by 4 mm per day, and wild type 5.7 mm per day (Table 5.1). In contrast, the primary root elongation rate of the *Arath*;SKIP1 T-DNA insertion line was similar to wild type, at 5.8 mm per day (Figure 5.9; Table 5.1).

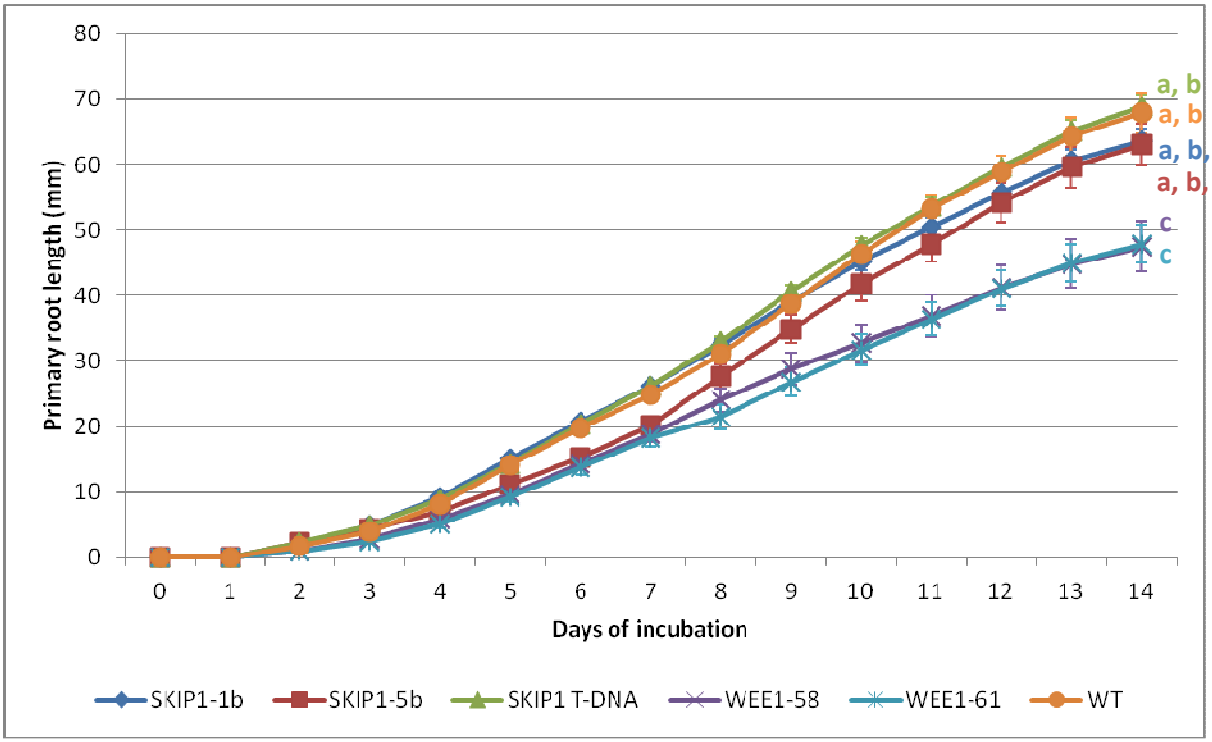

Figure 5.9 Primary root length (±SE, n=15-60) over time in *Arath*;SKIP1 sense knock-down (SKIP1-1b and -5b) and T-DNA insertion lines compared to *Arath*;WEE1 over-expressors (WEE1-58 and -61) and wild type (WT) *Arabidopsis*. a, b, c = significantly different from WEE1-58, WEE1-61, WT respectively (P<0.05).

Table 5.1 Rate of primary root elongation in *Arath*;SKIP1 sense knock-down (SKIP1-1b and -5b) and T-DNA insertion lines compared to *Arath*;WEE1 over-expressors (WEE1-58 and -61) and wild type *Arabidopsis*.

***Arabidopsis* line**	**Linear regression equation (P=0.000)**	**Rate of primary root elongation (mm per day)**
SKIP1-1b	y = 5.34x + 9.62	5.34
SKIP1-5b	y = 5.29x + 11.80	5.29
SKIP1 T-DNA	y = 5.78x + 11.5	5.78
WEE1-58	y = 4.02x + 8.06	4.02
WEE1-61	y = 4.02x + 8.69	4.02
Wild type	y = 5.73x + 12.00	5.73

Previous results have demonstrated that 10 days after sowing (equivalent to the 7 days of growth analysed here) the primary roots of WEE1-58 and WEE1-61 lines over-expressing *Arath*;*WEE1* were significantly shorter than wild type, and they produced significantly less lateral roots and primordia (Spadafora, 2008). This difference in root length was confirmed by the current phenotyping in both of the *Arath*;*WEE1* over-expressing lines, however the number of lateral roots was only reduced in WEE1-58 (Figure 5.10). The primary root was also significantly shorter than wild type in one of the *Arath*;SKIP1 knock-down lines (5b), and the number of lateral roots and primordia were reduced, similar to WEE1-58 (Figure 5.10). Both the primary root length and number of lateral roots in the other *Arath*;SKIP1 knock-down line (1b), however, were similar to wild type, as were those of the *Arath*;SKIP1 T-DNA insertion line (Figure 5.10).

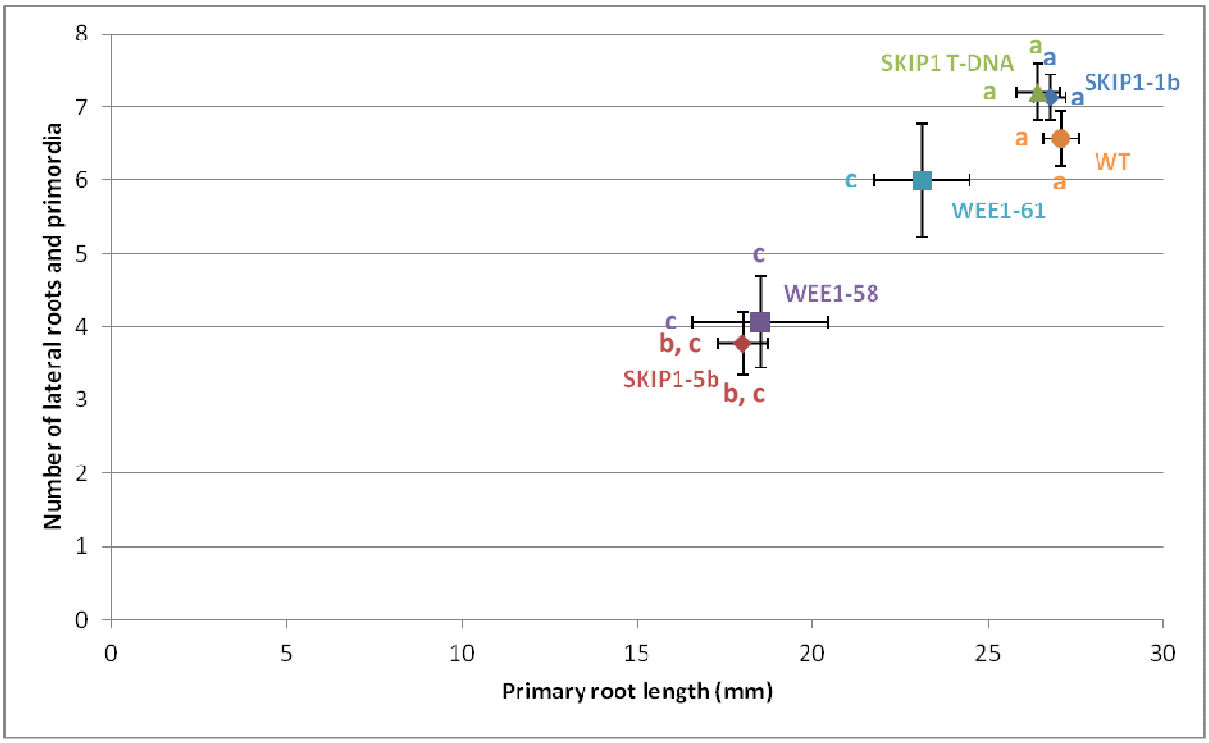

Figure 5.10 Primary root length and number of lateral roots and primordia (±SE, n=9-29) after 7 days growth in *Arath*;SKIP1 sense knock-down (SKIP1-1b and -5b) and T-DNA insertion lines compared to *Arath*;WEE1 over-expressors (WEE1-58 and -61) and wild type (WT) *Arabidopsis*. a, b, c = significantly different from WEE1-58, WEE1-61, WT respectively ($P<0.05$).

After 14 days of growth, for which there was no previous data for the lines over-expressing *Arath*;*WEE1*, both WEE1-58 and WEE1-61 had shorter primary roots and less lateral roots and primordia than wild type plants (Figure 5.11). On the other hand, both *Arath*;SKIP1 sense knock-down lines had primary root lengths and numbers of lateral roots similar to those of wild type (Figure 5.11). The root phenotype of the *Arath*;SKIP1 T-DNA insertion line was also similar to wild type after 14 days of growth (Figure 5.11).

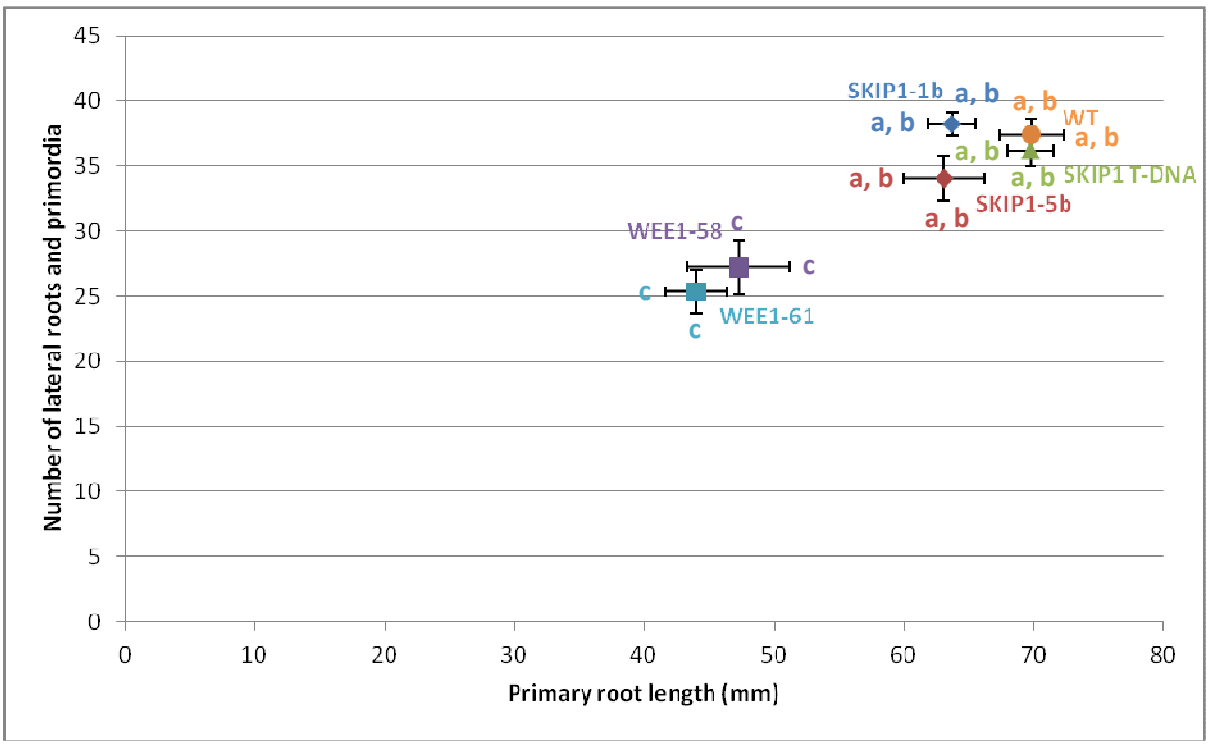

Figure 5.11 Primary root length and number of lateral roots and primordia (±SE, n=11-29) after 14 days growth in *Arath*;SKIP1 sense knock-down (SKIP1-1b and -5b) and T-DNA insertion lines compared to *Arath*;WEE1 over-expressors (WEE1-58 and -61) and wild type (WT) *Arabidopsis*. a, b, c = significantly different from WEE1-58, WEE1-61, WT respectively (P<0.05).

The rate of lateral root initiation per mm of primary root after seven days growth did not vary from that of wild type in any of the transgenic lines (Table 5.2). This was supported by regression analysis which indicated a linear relationship between the primary root length and number of lateral roots in each line after seven days (r^2=0.96), confirming that the rate of lateral root formation was similar in each line. Similarly, a linear relationship between the primary root length and number of lateral roots in each line was confirmed after fourteen days (r^2=0.87). Interestingly, SKIP1-1b was the only line in which the rate of lateral root initiation differed from that of

wild type after fourteen days growth, producing an increased number of lateral roots per mm of primary root (Table 5.2).

Table 5.2 Rate of lateral root formation per mm of primary root (±SE) after 7 days and 14 days growth in *Arath*;SKIP1 sense knock-down (SKIP1-1b and -5b) and T-DNA insertion lines compared to *Arath*;WEE1 over-expressors (WEE1-58 and -61) and wild type *Arabidopsis*. * = significantly different from wild type (P<0.05).

	Rate of lateral root formation per mm of primary root (±SE)	
***Arabidopsis* line**	**7 day old seedlings (n=9-29)**	**14 day old seedlings (n=11-29)**
SKIP1-1b	0.27 ±0.01	0.61 ±0.01 *
SKIP1-5b	0.21 ±0.02	0.54 ±0.02
SKIP1 T-DNA	0.27 ±0.01	0.52 ±0.01
WEE1-58	0.20 ±0.02	0.58 ±0.02
WEE1-61	0.25 ±0.03	0.58 ±0.03
Wild type	0.24 ±0.01	0.54 ±0.01

5.3.4 CROSS BETWEEN *ARATH*;SKIP1 SENSE KNOCK-DOWN AND GFP-*ARATH*;WEE1 LINES

The homozygous SPYNE-*Arath*;SKIP1-1b sense knock-down line was crossed with the homozygous GFP-*Arath*;WEE1-12 line (see Section 3.3.3) to study the effects of the decrease in *Arath*;SKIP1 expression on *Arath*;WEE1 protein (see Section 2.3.4). It was expected that an enhanced GFP signal would be detected in the plants carrying both transgenes compared to the original GFP-*Arath*;WEE1 line. Thirty two F1 plants were positive for the presence of both constructs by PCR (see Section 2.4.2; Table 2.3; Figure 5.12).

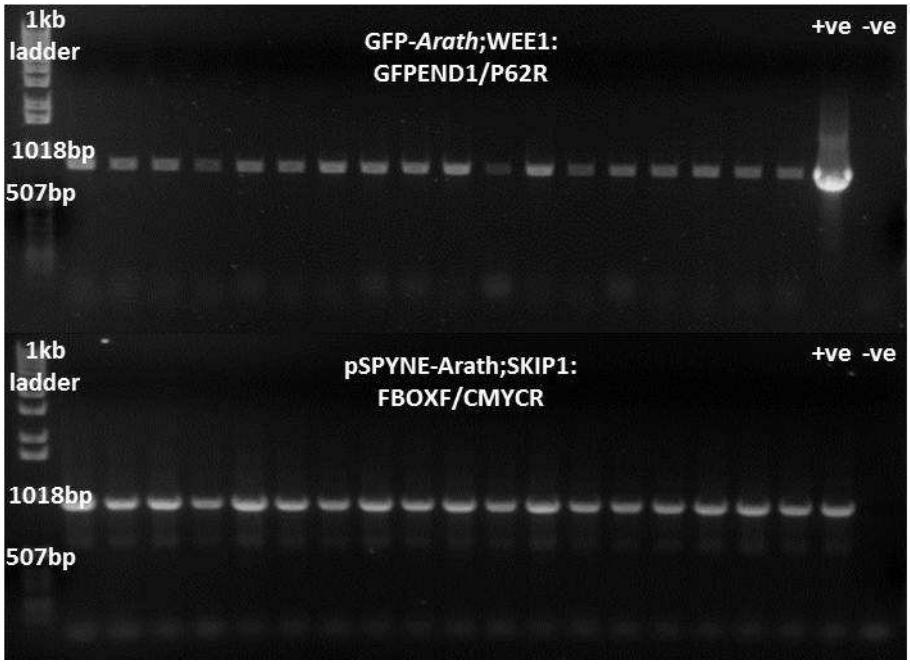

Figure 5.12 Results of PCR to test for presence of GFP-*Arath*;WEE1 (GFPEND1 and P62R primers; +ve = positive control, GFP-*Arath*;WEE1 plasmid) and pSPYNE-*Arath*;SKIP1 (FBOXF and CMYCR primers; +ve = positive control, pSPYNE-*Arath*;SKIP1 plasmid) constructs in 18 representative F1 plants. –ve = negative control, sterile distilled water.

F1 plants were allowed to self-fertilise and seeds from each line were grown on MS medium (see Section 2.3.3), with the original GFP-*Arath*;WEE1-12 and wild type lines as controls, and screened for GFP fluorescence (see Section 2.3.6). Using a high power microscope, the original line, GFP-*Arath*;WEE1-12, exhibited a weak fluorescence signal. A weak GFP signal was seen in the majority of the GFP-*Arath*;WEE1 x SPYNE-*Arath*;SKIP1 F2 lines, similar to that of the original GFP-

Arath;WEE1 line. Only two lines, 11 and 28, seemed to exhibit a stronger nuclear GFP signal. No fluorescent signal was detected in the wild type seedlings.

Seedlings from the GFP-*Arath*;WEE1 x SPYNE-*Arath*;SKIP1 F2 lines 11 and 28 were subsequently used for confocal analysis (see Section 2.3.7). Unfortunately, using the confocal microscope, no GFP signal could be detected from either of the F2 lines, or from the control, the original GFP-*Arath*;WEE1-12 line. Western blotting was used as an alternative method of testing for any increase in *Arath*;WEE1 protein levels in the *Arath*;SKIP1 sense knock-down lines and the GFP-*Arath*;WEE1 x SPYNE-*Arath*;SKIP1 F2 lines compared to wild type and the GFP-*Arath*;WEE1-12 line. However, it was not possible to isolate clear, measurable bands of *Arath*;WEE1 protein (see Appendix III).

5.3 DISCUSSION

If WEE1 is a cell cycle regulator in plants then the precise control of its activity is likely to be very important. In other organisms this control is exerted via both phosphorylation (reviewed by Dunphy, 1994) and protein degradation. *Arath*;WEE1 is degraded via the 26S proteasome pathway (see Section 3.3.5). WEE1 protein is also degraded via the 26S proteasome in other organisms, such as fission yeast, budding yeast, humans and *Xenopus* (Bai et al., 1996; Kaiser et al., 1998; Michael and Newport, 1998). In *Xenopus* this is via an SCF complex, which uses the F-box protein TOME-1 to target WEE1 for degradation (Ayad et al., 2003). *Arath*;WEE1 is able to interact with the F-box protein *Arath*;SKIP1 *in vivo* (see Section 4.3.1.1).

Arabidopsis plants were transformed with the SPYNE-*Arath*;SKIP1 construct in an attempt to over-express this gene. This in fact led to a decrease in *Arath*;*SKIP1* expression levels (Figure 5.3). This phenomenon, of a sense sequence decreasing the expression of the target gene, has been recorded previously (reviewed by Dougherty and Parks, 1995). It is thought that 75% homology is needed to decrease expression in this manner (English et al., 1996; Waterhouse et al., 1999), so it is unlikely that any other F-box proteins were knocked-down by this construct, as the closest

homologue to *Arath*;*SKIP1*, the putative *Arabidopsis* F-box/leucine-rich repeat protein 19, only shares 40% sequence identity.

The insertion of a large T-DNA into a gene, especially into the exon where it should not be spliced out, usually has the effect of reducing the expression of that gene (Azpiroz-Leehan and Feldmann, 1997; Wang, 2008). An *Arath*;SKIP1 T-DNA insertion line was acquired in the hope that it would provide a loss-of-function mutant for comparison with the sense partial knock-down lines. However, semi-quantitative RT-PCR showed these plants to express *Arath*;*SKIP1* at wild type levels or above (Figure 5.6), and their phenotype was similar to wild type (Figures 5.9, 5.10 and 5.11). The increase of gene expression levels in T-DNA insertion lines has been demonstrated previously, and this was attributed to the 35S promoter which formed part of the T-DNA. The endogenous promoter drove expression of the gene up to the insert, with the 35S promoter causing the expression of the gene downstream of the insert (Wang, 2008). It is possible that this was also the cause of *Arath*;*SKIP1* expression in the T-DNA insertion line, as the insert was present in the cDNA (Figure 5.7). However, the detection of wild type *Arath*;*SKIP1* using primers for the ORF (Figure 5.8), but the lack of detection of the wild type allele using primers for the *Arath*;*SKIP1* promoter and first exon (Figure 5.7) in the genomic DNA is yet to be explained. It is possible that the study of further generations would resolve the issue. Alternatively, a different insertion line could be acquired.

Over-expression of *Arath*;*SKIP1* was also seen in the *Arath*;*WEE1* over-expressor line, WEE1-58 (Figure 5.6). One possibility is that this is a compensation for the increased *Arath*;*WEE1* expression, leading to a requirement for increased removal of *Arath*;WEE1 protein. However, levels of *Arath*;WEE1 protein in the WEE1-58 line have not been measured, so this would need to be studied before any meaningful conclusions were drawn. Also, the level of *Arath*;*SKIP1* gene expression in the WEE1-58 line was only increased by 19% compared to wild type, so it is possible that this is due to natural variation.

The root phenotypes of the *Arath*;SKIP1 sense knock-down lines were studied in comparison with the *Arath*;WEE1 over-expressing lines, WEE1-58 and WEE1-61, and wild type *Arabidopsis*. The elongation rate of the primary root in the

Arath;WEE1 over-expressing lines was reduced (Figure 5.9), as expected and as previously described (Spadafora, 2008). In the *Arath*;SKIP1 sense knock-down lines the primary root elongation rate was also significantly slower than wild type, but was closer to the wild type primary root growth rate than to that of the *Arath*;WEE1 over-expressors (Figure 5.9). This could indicate a semi-redundant mechanism for the control of WEE1, with its activity also being controlled by phosphorylation, as seen in other organisms (Dunphy, 1994). It is of course also possible that the level of *Arath*;SKIP1 expression in these lines is not sufficiently reduced to cause an increase in *Arath*;WEE1 protein to levels similar to those of the *Arath*;WEE1 over-expressing lines.

After seven days, the primary root length and number of lateral roots and primordia of the *Arath*;SKIP1 sense knock-down line 5b were similar to those of the WEE1-58 line, however the phenotypes of line 1b, and both lines after 14 days, were similar to wild type. This may indicate that *Arath*;SKIP1 has a greater influence on *Arath*;WEE1 degradation early in development. This is supported by the high expression of *Arath*;*SKIP1* in dry seeds and in the seed coat of the embryo (Schmid et al., 2005). However the phenotypic affect would need to be confirmed in at least one additional *Arath*;SKIP1 sense knock-down line. Ideally a loss-of-function mutant would also be studied. It would also still be interesting to obtain lines over-expressing the *Arath*;*SKIP1* gene.

The rate of lateral root initiation was also calculated (Table 5.1). After seven days, the rate of lateral root initiation was similar in all six lines. This implies that although the WEE1-61 and, especially, the WEE1-58 and SKIP1-5b lines grew more slowly than wild type and the SKIP1-1b and SKIP1 T-DNA insertion lines overall, the rate of lateral root initiation remained constant. The rate of lateral root initiation was similar between most of the lines after fourteen days, with the exception of SKIP1-1b. The SKIP1-1b line produced more lateral roots per mm of primary root than wild type after fourteen days, suggesting that the *Arath*;*SKIP1* gene had a positive effect on lateral root development. This is in contrast to the expected phenotype of decreased lateral root production in lines over-expressing *Arath*;*WEE1* (Spadafora 2008) and further supports the need to confirm the SKIP1-5b phenotype in at least one additional *Arath*;SKIP1 knock-down line.

The *Arath*;SKIP1 sense knock-down line 1b was crossed with the GFP-*Arath*;WEE1 line 12 (described in Section 3.3.3). An enhanced GFP signal was expected in the F2 seedlings carrying both transgenes, as it was hypothesised that the decrease in *Arath*;*SKIP1* expression would lead to an increase in *Arath*;WEE1 protein. A GFP signal was detected in the F2 lines on a high-power fluorescent microscope, however no signal could be detected on the confocal microscope. The GFP-*Arath*;WEE1 line 12 was known to be expressing a weak GFP signal, but it was thought this would be helpful in seeing any increased signal in the crossed lines. One possibility is to image these lines on a more sensitive instrument. Another option would be to repeat the cross using a GFP-*Arath*;WEE1 line which has been identified as expressing GFP at a higher level, such as line 10 or 67 (see Section 3.3.3). The phenotype of the F2 lines might also be interesting, as the additive effects of *Arath*;*WEE1* over-expression from the GFP-*Arath*;WEE1 construct, and possible reduced *Arath*;WEE1 degradation due to reduced *Arath*;*SKIP1* expression, may lead to a clear WEE1 over-expression phenotype.

In the *Arath*;SKIP1 sense knock-down lines and the F2 lines from the cross it was hypothesised that *Arath*;WEE1 protein levels would be increased compared to wild type and GFP-*Arath*;WEE1 line 12 respectively, due to decreased degradation. Attempts were made to investigate this using western blotting, however several problems arose, including the co-migration of WEE1 with the similarly-sized large subunit of RUBISCO (57 and 55 kDa respectively; see Appendix III; Lentz Grønlund et al., 2009; Lentz Grønlund, 2007; Spreitzer and Silvucci, 2002). The high abundance of RUBISCO (Ellis, 1979) led to it being labelled non-specifically by the secondary antibody (see Appendix III). An attempt was made to remove RUBISCO from the protein extracts using calcium chloride and phytate, however this proved unsuccessful (see Appendix III). Possible solutions to this problem include improving the protocol for RUBISCO removal. A pH of 7.5 was used, this being the pH of the lysis buffer into which the proteins were extracted. In the original protocol, however, pH6.8 was used (Krishnan and Natarajan, 2009), which would require fresh protein extractions into a buffer of the suitable pH. The pH of the original extracts could be adjusted, but this may prove problematic due to the small sample size. Another option would be to obtain a more specific secondary

antibody. A GFP antibody could be used for the analysis of the crossed lines. However a second problem still remains in the inconsistency of the WEE1 protein bands, which cannot be quantified. The WEE1 signal could not be resolved using any of the methods tried, which included gel electrophoresis at a lower voltage, decreasing the percentage of acrylamide in the gel, and unfolding the protein prior to loading by treatment at 50°C for 10 minutes instead of the usual 100°C for five minutes. Another possibility is that the samples were not sufficiently homogenised, which would also require fresh protein extractions. It might also be the case that if the RUBISCO was removed, the WEE1 protein would be able to migrate normally.

There are several other methods of analysis which could be interesting for the *Arath*;SKIP1 knock-down lines. The affect of the proteasome inhibitor MG132 could be investigated. In a microarray, *Arath*;*SKIP1* expression was decreased after three hours treatment with MG132 (Winter et al., 2007; e-FP browser). In *Arabidopsis*, GFP-*Arath*;WEE1 signal was increased after six hours of treatment with MG132, demonstrating that it is targeted for degradation via the 26S proteasome pathway (see Section 3.3.5). In the *Arath*;SKIP1 knock-down lines the MG132 treatment could further decrease *Arath*;WEE1 degradation, leading to an even larger increase in *Arath*;WEE1 protein.

The effects of hydroxyurea treatment may also be interesting, as hydroxyurea inhibits the DNA replication checkpoint, of which *Arath*;WEE1 has been shown to be a key regulator (De Schutter et al., 2007). *Arath*;WEE1 mutants are hypersensitive to hydroxyurea (De Schutter et al., 2007; Lentz Grønlund, 2007), while it has little effect on the *Arath*;WEE1 over-expressors (Unpublished data, Cardiff lab). The effect of hydroxyurea treatment might, therefore, be more interesting to test on an *Arath*;SKIP1 over-expressing line, if one could be obtained, in which *Arath*;WEE1 protein levels should be decreased. These lines would be expected to be hypersensitive to hydroxyurea, like the *Arath*;WEE1 mutants.

It would also be useful to discover whether or not *Arath*;SKIP1 is cell cycle regulated. Microarray data show a large peak in *Arath*;*WEE1* gene expression at S-phase, decreasing into mitosis (Menges et al., 2003), with the same pattern seen in tobacco WEE1 protein levels in BY-2 cells (Lentz Grønlund, 2007). It would be

expected that *Arath*;*SKIP1* expression levels would follow a similar pattern to *Arath*;WEE1, peaking at S-phase and decreasing into mitosis when all WEE1 protein had been removed. However, microarray data from *Arabidopsis* cell cultures did not detect *Arath*;*SKIP1* expression during the cell cycle, with values of expression level so low that they would be considered as noise rather than true gene expression (Menges et al., 2003). Thus to determine whether *Arath*;SKIP1 is cell cycle regulated its expression in other systems may need to be studied. Alternatively, *Arath*;SKIP1 may still be important for *Arath*;WEE1 degradation, but not during a normal cell cycle. *Arath*;WEE1 has a well documented role in the DNA replication checkpoint (De Schutter et al., 2007; Cools et al., 2011), and so its degradation via *Arath*;SKIP1 may be related to recovery from this checkpoint.

6. GENERAL DISCUSSION

The activity of the WEE1 kinase protein is fundamental to the cell cycle in many organisms, including budding yeast, fission yeast and vertebrates. WEE1 prevents the premature onset of mitosis via the inhibitory phosphorylation of Cdc2 (or its homologue), the cyclin-dependent kinase responsible for the progression from G2-phase into mitosis (Den Haese et al., 1995; Booher et al., 1993; Sia et al., 1996; Featherstone and Russell, 1991; Lundgren et al., 1991; Parker and Piwnica-Worms, 1992). In higher plants, however, a role for WEE1 in the G2/M transition during an unperturbed cell cycle is yet to be identified. The results described in this thesis begin to elucidate how the localisation and stability of WEE1 protein may be regulated in higher plants.

A GFP-*Arath*;WEE1 construct under the 35S promoter was used to investigate the subcellular localisation of *Arath*;WEE1, and proved particularly useful in the study of the stability of the protein. The expression of the construct in tobacco BY-2 cells allowed the observation of *Arath*;WEE1 localisation in different cell cycle phases. While *Arath*;WEE1 was nuclear in all interphase cells, the proportion of prophase cells exhibiting fluorescence was only 4%, and no metaphase cells contained an *Arath*;WEE1 signal (Section 3.3.1). The fluorescent signal returned in anaphase and telophase (Section 3.3.1). This was confirmed in root meristem cells of a GFP-*Arath*;WEE1 *Arabidopsis* line crossed with the nuclear envelope marker RFP-*Arath*;SUN1 (Section 3.3.2). An interesting observation in the *Arabidopsis* GFP-*Arath*;WEE1 lines was that the levels of *Arath*;WEE1 degradation varied in the different root tissues (Section 3.3.4). This included the lateral root primordia, where *Arath*;WEE1 could not be detected (Section 3.3.4). The proteasome inhibitor MG132 was used to show that *Arath*;WEE1 is degraded via the 26S proteasome pathway in *Arabidopsis* roots (Section 3.3.5).

Bimolecular fluorescence complementation was used to confirm the interaction of *Arath*;WEE1 with *Arath*;SKIP1 *in vivo* (Section 4.3.1). Stable tobacco BY-2 cell cultures containing the SPYCE-*Arath*;WEE1 construct were co-transformed with the SPYNE-*Arath*;SKIP1 and SPYNE-*Arath*;GSTF9 constructs to facilitate the study of the dynamics of these interactions (Section 4.3.2). The expression of SPYCE-*Arath*;WEE1 led to premature mitosis and small mitotic cell size (Section 4.3.3). It

was discovered that the BiFC interactions rescued the abnormal effects caused by the expression of SPYCE-*Arath*;WEE1 alone (Section 4.3.3). The BY-2 culture co-transformed with SPYCE-*Arath*;WEE1 and SPYNE-*Arath*;SKIP1 differed from the other cultures in producing a high mitotic index when synchronised (Section 4.3.3). The line containing *Arath*;SKIP1 also differed by exhibiting an increased drop in fluorescence (ie. a larger decrease in the proportion of cells in which an interaction between *Arath*;WEE1 and *Arath*;SKIP1 was detected) between interphase and prophase relative to the other transgenic BY-2 lines (Section 4.3.3). No interaction with *Arath*;WEE1 was detected during metaphase in either the SPYCE-*Arath*;WEE1/SPYNE-*Arath*;SKIP1 line or the SPYCE-*Arath*;WEE1/SPYNE;*Arath*;GSTF9 line (Section 4.3.3). However, a return of the interactions could be observed in anaphase and telophase (Section 4.3.3).

An attempt was made to over-express *Arath*;SKIP1 in *Arabidopsis*, however this resulted in the creation of *Arath*;SKIP1 sense knockdown lines (Section 5.3.1). A T-DNA insertion was expected to provide an *Arath*;SKIP1 knockout mutant for comparison with the sense knockdown lines, however *Arath*;SKIP1 expression was not reduced in this line (Section 5.3.2), and it behaved like wild type (Section 5.3.3). The root phenotype of the *Arath*;SKIP1 sense knockdown lines was compared with wild type and *Arath*;WEE1 over-expressors (Section 5.3.3). The primary root growth rate of the *Arath*;SKIP1 knockdown lines was intermediate between wild type and the *Arath*;WEE1 over-expressors (Section 5.3.3). The number of lateral roots of one of the *Arath*;SKIP1 sense knockdown lines (5b) was reduced compared to wild type, similar to the *Arath*;WEE1 over-expressors, after seven days (Section 5.3.3). However the number of lateral roots after fourteen days, and in the second *Arath*;SKIP1 knockdown line (1b) at both time points, was similar to wild type (Section 5.3.3).

In light of the results described above I will discuss the stability of the *Arath*;WEE1 protein and also raise the question of the role of WEE1 in higher plants, before describing what further work may be useful and necessary to further characterise plant WEE1.

6.1 *ARATH*;WEE1 PROTEIN IS NUCLEAR AT INTERPHASE, BUT ABSENT DURING METAPHASE

The proximity of WEE1 protein to Cdc2 is an important level of regulation. In fission yeast, cyclinB-Cdc2 is localised to the cytoplasm at interphase, while Wee1 is nuclear, until the Cdc2 complex transfers to the nucleus at mitosis (Masuda et al., 2011). During interphase in mammalian cells, WEE1 is localised to the nucleus, transferring to the mictotubules at mitosis (Baldin and Ducommun, 1995). It has been demonstrated recently that *Arath*;WEE1 is also nuclear at interphase, however its subcellular localisation during mitosis was not recorded (Boruc et al., 2010). Here, *Arath*;WEE1 was confirmed to be nuclear at interphase in both tobacco BY-2 cells and *Arabidopsis* roots using a GFP construct under the 35S promoter (Sections 3.3.1 and 3.3.4).

In budding yeast, *Xenopus* and humans it has been demonstrated that WEE1 degradation is necessary for the onset of mitosis (Kaiser et al., 1998; Simpson-Lavy and Brandeis, 2010; Michael and Newport, 1998; Watanabe et al., 2004). In tobacco BY-2 cells, protein levels of *Nicta*;WEE1 peak early in G2, while kinase activity is highest early in S-phase, dropping consistently during S and G2 to its lowest level in mitosis (Lentz Grønlund, 2007), suggesting that the removal of WEE1 may also be important for the onset of mitosis in higher plants. The expression of the GFP-*Arath*;WEE1 construct in synchronised tobacco BY-2 cells allowed the visualisation of *Arath*;WEE1 subcellular localisation in different cell cycle phases. It was discovered that *Arath*;WEE1 protein is removed prior to metaphase (Section 3.3.1). This was supported by the observation of this construct in *Arabidopsis* roots also expressing the nuclear envelope marker RFP-*Arath*;SUN1 (Section 3.3.2). Additionally, there was no evidence of interactions between *Arath*;WEE1 and other proteins of interest during metaphase using the BiFC technique (Section 4.3.3). Taken together, these results suggest that the removal of WEE1 protein may be important for the progression of mitosis beyond prophase in plants.

An interesting discovery during the course of this work was the observation that the level of WEE1 degradation seemed to vary in the different tissues of *Arabidopsis* roots (Section 3.3.4). The relatively higher levels of GFP signal in the cell lineages destined to become the stelar tissue of the GFP-*Arath*;WEE1 meristems compared to

the fluorescence signal in the H2B-YFP line implied a reduction of WEE1 degradation in this tissue. In the elongation zone the tissue-specific pattern of *Arath*;WEE1 degradation was different, with a relatively increased level of removal in the cortical tissue. In the differentiation zone, however, *Arath*;WEE1 was found to be stable (Section 3.3.4). These observations were supported by the results of treatment of the GFP-*Arath*;WEE1 lines with the proteasome inhibitor MG132 (Section 3.3.5). *Arath*;WEE1 degradation was decreased in the cortex in the elongation/differentiation zones of MG132-treated roots, implying that there is usually a relatively higher degradation of *Arath*;WEE1 in the cortex. In the meristem/elongation zone, *Arath*;WEE1 protein was highly stabilised in the stele by MG132-treatment, implying that *Arath*;WEE1 degradation is usually high in this tissue (Section 3.3.5). Although the pattern of degradation in the cell lineages destined to become the stele of the meristem is contradictory between the untreated and MG132-treated roots, both support the idea that the regulation of *Arath*;WEE1 degradation may be important in this tissue, as well as in the cortex in the elongation zone. This observation is supported by WEE1-promoter-GUS analysis and *in situ* hybridisation studies, which both reported high *Arath*;WEE1 expression in the vascular tissue of roots (De Schutter et al., 2007; Engler et al., 2009), which originates from the stelar tissue. Additionally, *Arath*;WEE1 is required for the protection against premature vascular differentiation in the stelar tissue (Cools et al., 2011).

It is thought that a lack of WEE1 is necessary for the initiation of lateral roots, as demonstrated by the down-regulation of *Arath*;WEE1 observed in roots stimulated to produce laterals by NAA treatment (Engler et al., 2009). The over-expression of *Arath*;WEE1 can have an effect on root phenotype, particularly causing the production of fewer lateral roots compared to wild type (Spadafora, 2008). Conversely, the *wee1* knockout mutants of *Arabidopsis* produce more lateral roots compared to wild type (Lentz Grønlund, 2007). In the GFP-*Arath*;WEE1 lines, a lack of fluorescence in the lateral root primordia compared to the H2B-YFP line supports a requirement for *Arath*;WEE1 degradation prior to the initiation of lateral roots (Section 3.3.4).

From these results it can be concluded that WEE1 degradation may be central to the G2/M transition in plants. Additionally, the levels of WEE1 removal vary in a tissue-

specific manner in the *Arabidopsis* root, with the regulation of WEE1 degradation being particularly important in the stele and lateral root primordia. Another interesting aspect of *Arath*;WEE1 degradation is the mechanism by which this occurs, which could in turn provide further information about the role of WEE1 in plants.

6.2 *ARATH*;SKIP1 PROVIDES A POSSIBLE MECHANISM FOR THE DEGRADATION OF *ARATH*;WEE1 VIA THE 26S PROTEASOME

In budding yeast and vertebrates, the degradation of WEE1 is implemented via the 26S proteasome degradation pathway (Kaiser et al., 1998; Simpson-Lavy and Brandeis, 2010; Michael and Newport, 1998; Watanabe et al., 2004). This pathway can be blocked by the application of the proteasome inhibitor MG132 (Rock et al., 1994). GFP-*Arath*;WEE1 seedlings treated with MG132 exhibited a doubling in GFP signal compared to mock-treated seedlings, clearly demonstrating that *Arath*;WEE1 is degraded via the 26S proteasome pathway (Section 3.3.5).

It has been shown that *Arath*;WEE1 only interacts with one core cell cycle protein, CDKA;1, which occurs in the nucleus (Boruc et al., 2010b). A yeast two-hybrid assay showed that *Arath*;WEE1 is able to interact with over 90 additional cellular proteins (Lentz Grønlund, 2007). The interactions of *Arath*;WEE1 with *Arath;*GCN5, a histone-acetylating protein; *Arath;*GSTF9, a glutathione S-transferase involved in the cell's response to stress; *Arath;*TFCB, an α-tubulin folding cofactor; and *Arath*;14-3-3ω, which may inhibit dephosphorylation of *Arath*;WEE1 have been confirmed *in vivo* using bimolecular fluorescence complementation (BiFC; G. Cook, unpublished data, see Appendix IV; Lentz Grønlund et al., 2009). The interaction of *Arath*;WEE1 with the F-box protein *Arath*;SKIP1 has also been confirmed *in vivo* by BiFC (Section 4.3.1). This interaction suggests that *Arath*;SKIP1 is responsible for targeting *Arath*;WEE1 for degradation via the 26S proteasome degradation pathway.

Arath;SKIP1 is also able to interact with the *Arabidopsis* SKP1 homologue, *Arath*;ASK1 (Farras et al., 2001), meaning it is able to form an SCF complex

capable of targeting proteins for degradation via the 26S proteasome degradation pathway. F-box proteins have been implicated in the degradation of WEE1 in other organisms, for example MET30 in budding yeast (Kaiser et al., 1998) and TOME-1 in *Xenopus* (Ayad et al., 2003). In *Arabidopsis*, *Arath*;*WEE1* and *Arath*;*SKIP1* are co-expressed in some tissues such as roots, stems and cotyledons, however, neither gene is ever highly expressed at the same time (Schmid et al., 2005). This lack of *Arath*;*SKIP1* expression where *Arath;WEE1* is highly expressed could be due to an underlying mechanism ensuring that *Arath;*WEE1 is not degraded when its activity is required.

It was hypothesised that by decreasing *Arath*;*SKIP1* expression, the levels of the appropriate SCF complex would be reduced, in turn reducing the ubiquitination and degradation of *Arath*;WEE1 and increasing levels of *Arath*;WEE1 protein. In turn, this could lead to a delay in mitosis via G2 arrest, leading to a large cell size phenotype. Thus, a root phenotype similar to that of the previously described *Arath*;WEE1 over-expressor lines, WEE1-58 and WEE1-61, might be expected, with a reduced primary root growth rate and reduced numbers of lateral roots compared to wild type (Spadafora, 2008). The root growth phenotype of the *Arath*;SKIP1 sense knockdown lines was reduced compared to wild type, but not to the same extent as the *Arath*;WEE1 over-expressors. One *Arath*;SKIP1 sense knockdown line (5b) had developed fewer lateral roots than wild type after seven days, similar to the *Arath*;WEE1 over-expressors, but had a similar number of lateral roots compared to wild type after fourteen days (Section 5.3.3). This could indicate that *Arath*;SKIP1 has a greater influence on *Arath*;WEE1 degradation early in development, supported by high *Arath*;*SKIP1* expression in seeds and the seed coat of the embryo (Schmid et al., 2005). A semi-redundant mechanism for *Arath*;WEE1 regulation may exist, with its activity also being controlled by phosphorylation at different stages of development (Dunphy, 1994). However, the number of lateral roots in the second *Arath*;SKIP1 sense knockdown line (1b) was similar to wild type at both time points (Section 5.3.3), so the phenotype of fewer lateral roots after seven days would still need to be confirmed in at least one additional line.

To identify the localisation of the interaction of *Arath*;WEE1 with *Arath*;SKIP1 and other proteins of interest in different cell cycle stages, stable tobacco BY-2 cell cultures carrying both SPYNE and SPYCE constructs were created (Section 4.3.2).

When transformed with the SPYCE-*Arath*;WEE1 construct alone, the BY-2 culture displayed effects similar to previously described lines transformed with inducible or stable *Arath*;WEE1 constructs, including premature mitosis compared to wild type (Section 4.3.3; Siciliano, 2006; Spadafora, 2008). However, when co-transformed with the SPYNE-*Arath*;SKIP1 or SPYNE-*Arath*;GSTF9 constructs, both timing of mitosis and cell size were similar to wild type, implying that the BiFC interaction was able to rescue the abnormal effects of *Arath*;WEE1 expression in BY-2 cells (Section 4.3.3). This was probably due to the stabilisation of *Arath*;WEE1 protein via the BiFC complex, which may have physically sequestered *Arath*;WEE1 from the endogenous tobacco cell cycle machinery, preventing the interference of the non-native protein.

Several results from the co-transformed SPYCE-*Arath*;WEE1/SPYNE-*Arath*;SKIP1 BY-2 line support the hypothesis that *Arath*;SKIP1 may target *Arath*;WEE1 for degradation. The high peaks of mitosis in these lines compared to other transgenic lines could be an indication of a decrease in the inhibition of cell cycle progression by *Arath*;WEE1, due to it being targeted for proteolysis by *Arath*;SKIP1 (Section 4.3.3). Additionally, there was a higher drop in the proportion of cells positive for a interaction between *Arath*;WEE1 and *Arath*;SKIP1 between interphase and prophase in this line compared to the SPYCE-*Arath*;WEE1/SPYNE-*Arath*;GSTF9 line. This could be due to the over-expression of *Arath*;SKIP1 leading to an increase in *Arath*;WEE1 degradation, leaving less *Arath*;WEE1 protein available to form a complex with *Arath*;SKIP1 (Section 4.3.3).

It has been previously demonstrated that the over-expression of *Arath*;WEE1 in *Arabidopsis* leads to shorter primary roots and less lateral roots and primordia (Spadafora, 2009). It is hypothesised that an increase in *Arath*;WEE1 expression would also lead to mitotic delay and G2 arrest, increasing cell size as seen in fission yeast (Russell and Nurse, 1987). The expression of human, maize and *Arabidopsis* WEE1 in fission yeast each leads to long cells (Igarashi et al., 1991; Sun et al., 1999; Sorrell et al., 2002). This was seen in the BY-2 cultures described in Chapter 4, where expression of SPYCE-*Arath*;WEE1 led to an increase in cell size. The co-transformation of this line with SPYNE-*Arath*;SKIP1 reduced the cell size back to wild type levels (Section 4.3.1.3), which could be due to the removal of excess *Arath*;WEE1 via *Arath*;SKIP1. However, it is also important to remember that this is

based on an assumption of wild type BY-2 cell size in a 29 mL culture, as used during this investigation, being equal to wild type cell size in a 95 mL culture, as measured previously. This remains to be investigated.

6.3 DOES WEE1 KINASE HAVE A ROLE TO PLAY IN AN UNPERTURBED CELL CYCLE IN HIGHER PLANTS?

The role of WEE1 in higher plants is still a controversial topic. The function of the protein in the *Arabidopsis* DNA replication checkpoint has been clearly illustrated (De Schutter et al., 2007, Cools et al., 2011), however it remains to be seen whether or not there is a role for WEE1 in the unperturbed cell cycle in plants. The lack of a distinct phenotype in *wee1* knockout mutant plants suggests there may not be (De Schutter et al., 2007). However, homologues to the Mik1 and MYT1 proteins, to which WEE1 is functionally redundant in fission yeast and mammalian cells respectively (Den Haese et al., 1995; Mueller et al., 1995), have not been identified in plants. It is of course possible that plant WEE1 is functionally redundant to an as yet undiscovered protein unique to plants.

However, several of the results described in this thesis support a role for WEE1 in the unperturbed cell cycle in plants. Firstly, the clear removal of GFP-*Arath*;WEE1 prior to metaphase, and the lack of BiFC interactions at metaphase, in the tobacco BY-2 lines implies the existence of a strong mechanism for the complete removal of all WEE1 protein before the progression of mitosis beyond prophase. It is already known that *Nicta*;WEE1 protein levels peak early in G2, dropping to their lowest level in mitosis (Lentz Grønlund, 2007). These results suggest that the inhibition of CDK by WEE1 protein must be removed prior to mitosis in plants. The return of the interactions at anaphase and telophase may imply a role for WEE1 in cytokinesis in plants. A similar role was proposed for mammalian WEE1 when it was observed that the protein localises to the microtubules at mitosis in human cells (Baldin and Ducommun, 1995). However, in tobacco BY-2 cells, WEE1 was observed to localise to the chromosomes at anaphase and telophase, rather than the microtubules (Sections 3.3.1, 3.3.2 and 4.4.3). This difference may be due to the highly dissimilar, complex mechanism for cytokinesis which exists in plants, where a new cell wall

must be constructed, compared to the relatively simple division in animal cells (reviewed by Staehelin and Hepler, 1996).

Similarly, it appears that the inhibition of CDK by WEE1 protein must be overcome for the initiation of cell division in the pericycle, which leads to lateral root formation. Pericycle cells are arrested in G2, primed to respond to signals which initiate the production of lateral roots via the resumption of cell division (Beeckman et al., 2001). The onset of lateral root production may be controlled by auxin-regulated degradation via the ubiquitin/26S proteasome pathway (Hellmann and Estelle, 2002). GFP-*Arath*;WEE1 degradation was high in the lateral root primordia (Section 3.3.4). Roots stimulated to produce laterals by NAA treatment had reduced *Arath*;WEE1 expression (Engler et al., 2009). This is supported by the observation that more lateral roots are produced by *wee1* insertion mutants of *Arabidopsis* compared to wild type, while *Arath*;WEE1 over-expression reduces the number of laterals (Lentz Grønlund, 2007; Spadafora, 2008).

Recently WEE1 has been implicated in the protection against premature vascular differentiation in *Arabidopsis* roots under conditions of replication stress (Cools et al., 2011). Dead cells in the stele of the elongation and differentiation zones, characteristic of those seen by Cools et al. (2011) in a *wee1* knockout mutant line treated with hydroxyurea, were also seen in the GFP-*Arath*;WEE1 lines during the course of the work described in this thesis, but these plants were not treated with any kind of replication stress (Section 3.3.4). This could indicate that *Arath*;WEE1 also has an important role in preventing premature vascular differentiation under normal conditions.

In summary, WEE1 could be important for the correct timing of the G2/M transition, the prevention of premature lateral root initiation and the protection against premature vascular differentiation in roots, even under normal conditions, in plants. This is in contrast to various claims made which suggest that the role of the WEE1 protein in plants is exclusively as part of the DNA damage and replication checkpoints (De Schutter et al., 2007, Cools et al., 2011). However, recently attention has been drawn to the fact that “normal” conditions for plants may involve high levels of DNA damage and stress, due to the environmental conditions which they are constantly exposed to, due to their sedentary lifestyle (Francis, 2011). This

should be considered when interpreting any results regarding WEE1 in plants grown under relatively unstressed laboratory conditions.

Another possibility is that WEE1 activity is species-specific. In tomato, for example, the down-regulation of *Solly*;*WEE1* dramatically reduced fruit size in a dose-dependent manner (Gonzalez et al., 2007). This is related to the role of *Solly*;WEE1 in the endocycle, with a reduction in *Solly*;*WEE1* expression leading to reduced endoreduplication and consequently reduced cell size (Gonzalez et al., 2007). Additionally, in apple (*Malus x domestica* Borkh.), WEE1 was important in the promotion of cell production during fruit growth, although the mechanism by which this occurs is yet to be defined (Malladi and Johnson, 2011). It may be, therefore, that while *Arabidopsis* generally provides a useful model for the molecular analysis of cell cycle genes, the study of WEE1 in different systems, especially fruit-bearing plants, might provide a clearer understanding of the protein's role in higher plants.

6.4 FUTURE WORK

The characterisation of higher plant WEE1 is slowly being revealed, however the precise role of the WEE1 kinase in plants is far from clear, and will require much further study. The work presented in this thesis describes, to my knowledge, the first investigation into the stability of *Arath*;WEE1. Several lines of investigation could be taken both to confirm the degradation of the *Arath*;WEE1 protein via the 26S proteasome pathway and to confirm that *Arath*;SKIP1 is the F-box protein responsible for targeting *Arath*;WEE1 for proteolysis.

The proteasome inhibitor MG132 proved to be a useful tool in demonstrating that *Arath*;WEE1 is degraded via the 26S proteasome pathway. Its use could be extended to other transgenic lines and systems to answer further questions regarding the mechanism of *Arath*;WEE1 degradation. If applied to the tobacco BY-2 cell line containing the GFP-*Arath*;WEE1 construct, MG132 could be used to confirm that the disappearance of the fluorescence signal in prophase and metaphase was due to the degradation of the protein. This could be extended to the BiFC lines, to see if the interactions are stabilised and appear in metaphase when the cells are treated with MG132.

The treatment of *Arabidopsis* lines with MG132 would also be interesting. MG132 treatment could be used to confirm that the lack of GFP signal in the lateral root primordia of the GFP-*Arath*;WEE1 lines was due to the degradation of *Arath*;WEE1. The P_{WEE1}:*Arath*;WEE1-GFP plants used by Cools et al. (2011) could also be treated with MG132 to investigate whether the lack of GFP signal observed in these lines under normal growth conditions was due to a low *Arath*;*WEE1* expression or due to a high level of *Arath*;WEE1 turnover.

The study of *Arath*;WEE1 protein levels would be the best test for the effect of the various transgenes and treatments on *Arath*;WEE1 degradation. If the technique for the western blotting of WEE1 could be perfected, the levels of *Arath*;WEE1 protein could be compared in the MG132-treated and mock-treated lines GFP-*Arath*;WEE1 lines, or even in wild type. The levels of WEE1 protein in the SPYCE-*Arath*;WEE1/SPYNE-*Arath*;SKIP1 BY-2 line would also be interesting. If the level of WEE1 protein is reduced in this line compared to the other BiFC lines it could be due to the expression of *Arath*;SKIP1. Similarly, the levels of *Arath*;WEE1 protein could be increased in the *Arath*;SKIP1 sense knockdown *Arabidopsis* lines compared to wild type, if *Arath*;SKIP1 does target *Arath*;WEE1 for degradation.

The further characterisation of *Arath*;SKIP1 will be important for confirming its role as the F-box protein responsible for the targeting of *Arath*;WEE1 for degradation. The characteristics of a true loss-of-function *Arath*;SKIP1 T-DNA insertion line, and those of a line over-expressing *Arath*;SKIP1 in *Arabidopsis* could confirm the function of *Arath*;SKIP1. Knowledge regarding the levels of *Arath*;WEE1 protein in such lines would be especially useful in the confirmation of the role of the *Arath*;SKIP1 protein. Additionally, a line over-expressing *Arath*;SKIP1 should be hypersensitive to hydroxyurea treatment due to the expected reduction in *Arath*;WEE1 protein.

Confirmation that the interaction between *Arath*;WEE1 and *Arath*;SKIP1 is cell cycle regulated could also confirm the role of *Arath*;WEE1 during an unperturbed cell cycle. Firstly mutations could be introduced into the binding sites of one or both proteins to see if the interaction is abolished. A construct in which *Arath*;SKIP1 is connected to a fluorescent marker such as RFP could be produced and tested for co-localisation with GFP-*Arath*;WEE1. Co-immunoprecipitation could be used as a tool

to further confirm the interaction of the two proteins, and could even confirm the occurrence of the interaction in different cell cycle phases if the cells were pre-sorted.

The results described in this thesis focussed on the roots of *Arabidopsis* as a simple model for the study of cell division in plants. However WEE1 may also have a role to play in the above-ground elements of the plant, so the study of *Arath*;WEE1 stability in shoots and leaves would be interesting. Additionally, as described above, WEE1 has a role to play in fruit development in both tomato and apple, probably through the role of the protein in endoreduplication. This may indicate that the extension of the investigation of WEE1 to other fruit-bearing plants could even provide commercially relevant results with the potential for controlling fruit size.

REFERENCES

ACH, R. A., DURFEE, T., MILLER, A. B., TARANTO, P., HANLEY-BOWDOIN, L., ZAMBRYSKI, P. C. & GRUISSEM, W. 1997. RRB1 and RRB2 encode maize retinoblastoma-related proteins that interact with a plant D-type cyclin and geminivirus replication protein. *Mol Cell Biol,* 17**,** 5077-86.

AGUILAR, R. C. & WENDLAND, B. 2003. Ubiquitin: not just for proteasomes anymore. *Curr Opin Cell Biol,* 15**,** 184-90.

AN, G. 1985. High efficiency transformation of cultured tobacco cells. *Plant Physiol,* 79**,** 568-70.

ASCENCIO-IBANEZ, J. T., SOZZANI, R., LEE, T. J., CHU, T. M., WOLFINGER, R. D., CELLA, R. & HANLEY-BOWDOIN, L. 2008. Global analysis of Arabidopsis gene expression uncovers a complex array of changes impacting pathogen response and cell cycle during geminivirus infection. *Plant Physiol,* 148**,** 436-54.

ATHERTON-FESSLER, S., PARKER, L. L., GEAHLEN, R. L. & PIWNICA-WORMS, H. 1993. Mechanisms of p34cdc2 regulation. *Mol Cell Biol,* 13**,** 1675-85.

AYAD, N. G., RANKIN, S., MURAKAMI, M., JEBANATHIRAJAH, J., GYGI, S. & KIRSCHNER, M. W. 2003. Tome-1, a trigger of mitotic entry, is degraded during G1 via the APC. *Cell,* 113**,** 101-13.

AZPIROZ-LEEHAN, R. & FELDMANN, K. A. 1997. T-DNA insertion mutagenesis in Arabidopsis: going back and forth. *Trends Genet,* 13**,** 152-6.

BAI, C., SEN, P., HOFMANN, K., MA, L., GOEBL, M., HARPER, J. W. & ELLEDGE, S. J. 1996. SKP1 connects cell cycle regulators to the ubiquitin proteolysis machinery through a novel motif, the F-box. *Cell,* 86**,** 263-74.

BAILLY, E., DOREE, M., NURSE, P. & BORNENS, M. 1989. p34cdc2 is located in both nucleus and cytoplasm; part is centrosomally associated at G2/M and enters vesicles at anaphase. *EMBO J,* 8**,** 3985-95.

BALDIN, V. & DUCOMMUN, B. 1995. Subcellular localisation of human wee1 kinase is regulated during the cell cycle. *J Cell Sci,* 108 (Pt 6)**,** 2425-32.

BASHIR, T., DORRELLO, N. V., AMADOR, V., GUARDAVACCARO, D. & PAGANO, M. 2004. Control of the SCF(Skp2-Cks1) ubiquitin ligase by the APC/C(Cdh1) ubiquitin ligase. *Nature,* 428**,** 190-3.

BEECKMAN, T., BURSSENS, S. & INZE, D. 2001. The peri-cell-cycle in Arabidopsis. *J Exp Bot,* 52**,** 403-11.

BESSON, A., DOWDY, S. F. & ROBERTS, J. M. 2008. CDK inhibitors: cell cycle regulators and beyond. *Dev Cell,* 14**,** 159-69.

BISCHOFF, J. R. & PLOWMAN, G. D. 1999. The Aurora/Ipl1p kinase family: regulators of chromosome segregation and cytokinesis. *Trends Cell Biol,* 9**,** 454-9.

BLOMBERG, I. & HOFFMANN, I. 1999. Ectopic expression of Cdc25A accelerates the G(1)/S transition and leads to premature activation of cyclin E- and cyclin A-dependent kinases. *Mol Cell Biol,* 19**,** 6183-94.

BOISNARD-LORIG, C., COLON-CARMONA, A., BAUCH, M., HODGE, S., DOERNER, P., BANCHAREL, E., DUMAS, C., HASELOFF, J. & BERGER, F. 2001. Dynamic analyses of the expression of the HISTONE::YFP fusion protein in arabidopsis show that syncytial endosperm is divided in mitotic domains. *Plant Cell,* 13**,** 495-509.

BONIOTTI, M. B. & GUTIERREZ, C. 2001. A cell-cycle-regulated kinase activity phosphorylates plant retinoblastoma protein and contains, in Arabidopsis, a CDKA/cyclin D complex. *Plant J,* 28**,** 341-50.

BOOHER, R. N., DESHAIES, R. J. & KIRSCHNER, M. W. 1993. Properties of Saccharomyces cerevisiae wee1 and its differential regulation of p34CDC28 in response to G1 and G2 cyclins. *EMBO J,* 12**,** 3417-26.

BORUC, J., MYLLE, E., DUDA, M., DE CLERCQ, R., ROMBAUTS, S., GEELEN, D., HILSON, P., INZE, D., VAN DAMME, D. & RUSSINOVA, E. 2010a. Systematic localization of the Arabidopsis core cell cycle proteins reveals novel cell division complexes. *Plant Physiol,* 152**,** 553-65.

BORUC, J., VAN DEN DAELE, H., HOLLUNDER, J., ROMBAUTS, S., MYLLE, E., HILSON, P., INZE, D., DE VEYLDER, L. & RUSSINOVA, E. 2010b. Functional modules in the Arabidopsis core cell cycle binary protein-protein interaction network. *Plant Cell,* 22**,** 1264-80.

BORUC, J., INZE, D. & RUSSINOVA, E. 2010c. A high-throughput bimolecular fluorescence complementation protein-protein interaction screen identifies functional Arabidopsis CDKA/B-CYCD4/5 complexes. *Plant Signal Behav,* 5**,** 1276-81.

BOUDOLF, V., INZE, D. & DE VEYLDER, L. 2006. What if higher plants lack a CDC25 phosphatase? *Trends Plant Sci,* 11**,** 474-9.

BRANDEIS, M. & HUNT, T. 1996. The proteolysis of mitotic cyclins in mammalian cells persists from the end of mitosis until the onset of S phase. *EMBO J,* 15**,** 5280-9.

CAM, H. & DYNLACHT, B. D. 2003. Emerging roles for E2F: beyond the G1/S transition and DNA replication. *Cancer Cell,* 3**,** 311-6.

CAPRON, A., SERRALBO, O., FULOP, K., FRUGIER, F., PARMENTIER, Y., DONG, A., LECUREUIL, A., GUERCHE, P., KONDOROSI, E., SCHERES, B. & GENSCHIK, P. 2003. The Arabidopsis anaphase-promoting complex or cyclosome: molecular and genetic characterization of the APC2 subunit. *Plant Cell,* 15**,** 2370-82.

CARRANO, A. C., EYTAN, E., HERSHKO, A. & PAGANO, M. 1999. SKP2 is required for ubiquitin-mediated degradation of the CDK inhibitor p27. *Nat Cell Biol,* 1**,** 193-9.

CASTRO, A., BERNIS, C., VIGNERON, S., LABBE, J. C. & LORCA, T. 2005. The anaphase-promoting complex: a key factor in the regulation of cell cycle. *Oncogene,* 24**,** 314-25.

CHABOUTE, M. E., CLEMENT, B. & PHILIPPS, G. 2002. S phase and meristem-specific expression of the tobacco RNR1b gene is mediated by an E2F element located in the 5' leader sequence. *J Biol Chem,* 277**,** 17845-51.

CHAN, F. K., ZHANG, J., CHENG, L., SHAPIRO, D. N. & WINOTO, A. 1995. Identification of human and mouse p19, a novel CDK4 and CDK6 inhibitor with homology to p16ink4. *Mol Cell Biol,* 15**,** 2682-8.

CHAUBET-GIGOT, N. 2000. Plant A-type cyclins. *Plant Mol Biol,* 43**,** 659-75.

CHEHAB, N. H., MALIKZAY, A., STAVRIDI, E. S. & HALAZONETIS, T. D. 1999. Phosphorylation of Ser-20 mediates stabilization of human p53 in response to DNA damage. *Proc Natl Acad Sci U S A,* 96**,** 13777-82.

CHEN, I. P., HAEHNEL, U., ALTSCHMIED, L., SCHUBERT, I. & PUCHTA, H. 2003. The transcriptional response of Arabidopsis to genotoxic stress - a high-density colony array study (HDCA). *Plant J,* 35**,** 771-86.

CHENG, M., OLIVIER, P., DIEHL, J. A., FERO, M., ROUSSEL, M. F., ROBERTS, J. M. & SHERR, C. J. 1999. The p21(Cip1) and p27(Kip1) CDK 'inhibitors' are essential activators of cyclin D-dependent kinases in murine fibroblasts. *EMBO J,* 18**,** 1571-83.

CHURCHMAN, M. L., BROWN, M. L., KATO, N., KIRIK, V., HULSKAMP, M., INZE, D., DE VEYLDER, L., WALKER, J. D., ZHENG, Z., OPPENHEIMER, D. G., GWIN, T., CHURCHMAN, J. & LARKIN, J. C. 2006. SIAMESE, a plant-specific cell cycle regulator, controls endoreduplication onset in Arabidopsis thaliana. *Plant Cell,* 18**,** 3145-57.

CIOSK, R., ZACHARIAE, W., MICHAELIS, C., SHEVCHENKO, A., MANN, M. & NASMYTH, K. 1998. An ESP1/PDS1 complex regulates loss of sister chromatid cohesion at the metaphase to anaphase transition in yeast. *Cell,* 93**,** 1067-76.

CLOUGH, S. J. & BENT, A. F. 1998. Floral dip: a simplified method for Agrobacterium-mediated transformation of Arabidopsis thaliana. *Plant J,* 16**,** 735-43.

CLUTE, P. & PINES, J. 1999. Temporal and spatial control of cyclin B1 destruction in metaphase. *Nat Cell Biol,* 1**,** 82-7.

CONAWAY, R. C., BROWER, C. S. & CONAWAY, J. W. 2002. Emerging roles of ubiquitin in transcription regulation. *Science,* 296**,** 1254-8.

CONNELLY, C. & HIETER, P. 1996. Budding yeast SKP1 encodes an evolutionarily conserved kinetochore protein required for cell cycle progression. *Cell,* 86**,** 275-85.

COOLS, T. & DE VEYLDER, L. 2009. DNA stress checkpoint control and plant development. *Curr Opin Plant Biol,* 12**,** 23-8.

COOLS, T., IANTCHEVA, A., WEIMER, A. K., BOENS, S., TAKAHASHI, N., MAES, S., VAN DEN DAELE, H., VAN ISTERDAEL, G., SCHNITTGER, A. & DE VEYLDER, L. 2011. The Arabidopsis thaliana checkpoint kinase WEE1 protects against premature vascular differentiation during replication stress. *Plant Cell,* 23**,** 1435-48.

CORISH, P. & TYLER-SMITH, C. 1999. Attenuation of green fluorescent protein half-life in mammalian cells. *Protein Eng,* 12**,** 1035-40.

CRANE, R., KLOEPFER, A. & RUDERMAN, J. V. 2004. Requirements for the destruction of human Aurora-A. *J Cell Sci,* 117**,** 5975-83.

CRIQUI, M. C., PARMENTIER, Y., DEREVIER, A., SHEN, W. H., DONG, A. & GENSCHIK, P. 2000. Cell cycle-dependent proteolysis and ectopic overexpression of cyclin B1 in tobacco BY2 cells. *Plant J,* 24**,** 763-73.

CRIQUI, M. C., WEINGARTNER, M., CAPRON, A., PARMENTIER, Y., SHEN, W. H., HEBERLE-BORS, E., BOGRE, L. & GENSCHIK, P. 2001. Sub-cellular localisation of GFP-tagged tobacco mitotic cyclins during the cell cycle and after spindle checkpoint activation. *Plant J,* 28**,** 569-81.

CULLIGAN, K., TISSIER, A. & BRITT, A. 2004. ATR regulates a G2-phase cell-cycle checkpoint in Arabidopsis thaliana. *Plant Cell,* 16**,** 1091-104.

CULLIGAN, K. M., ROBERTSON, C. E., FOREMAN, J., DOERNER, P. & BRITT, A. B. 2006. ATR and ATM play both distinct and additive roles in response to ionizing radiation. *Plant J,* 48**,** 947-61.

DAHL, M., MESKIENE, I., BOGRE, L., HA, D. T., SWOBODA, I., HUBMANN, R., HIRT, H. & HEBERLE-BORS, E. 1995. The D-type alfalfa cyclin gene cycMs4 complements G1 cyclin-deficient yeast and is induced in the G1 phase of the cell cycle. *Plant Cell,* 7**,** 1847-57.

DE JAGER, S. M., MENGES, M., BAUER, U. M. & MURRA, J. A. 2001. Arabidopsis E2F1 binds a sequence present in the promoter of S-phase-regulated gene AtCDC6 and is a member of a multigene family with differential activities. *Plant Mol Biol,* 47**,** 555-68.

DE SCHUTTER, K., JOUBES, J., COOLS, T., VERKEST, A., CORELLOU, F., BABIYCHUK, E., VAN DER SCHUEREN, E., BEECKMAN, T., KUSHNIR, S., INZE, D. & DE VEYLDER, L. 2007. Arabidopsis WEE1 kinase controls cell cycle arrest in response to activation of the DNA integrity checkpoint. *Plant Cell,* 19**,** 211-25.

DE VEYLDER, L., BEECKMAN, T., BEEMSTER, G. T., DE ALMEIDA ENGLER, J., ORMENESE, S., MAES, S., NAUDTS, M., VAN DER SCHUEREN, E., JACQMARD, A., ENGLER, G. & INZE, D. 2002. Control

of proliferation, endoreduplication and differentiation by the Arabidopsis E2Fa-DPa transcription factor. *EMBO J,* 21**,** 1360-8.

DE VEYLDER, L., BEECKMAN, T., BEEMSTER, G. T., KROLS, L., TERRAS, F., LANDRIEU, I., VAN DER SCHUEREN, E., MAES, S., NAUDTS, M. & INZE, D. 2001. Functional analysis of cyclin-dependent kinase inhibitors of Arabidopsis. *Plant Cell,* 13**,** 1653-68.

DEL POZO, J. C., BONIOTTI, M. B. & GUTIERREZ, C. 2002. Arabidopsis E2Fc functions in cell division and is degraded by the ubiquitin-SCF(AtSKP2) pathway in response to light. *Plant Cell,* 14**,** 3057-71.

DEMIDOV, D., VAN DAMME, D., GEELEN, D., BLATTNER, F. R. & HOUBEN, A. 2005. Identification and dynamics of two classes of aurora-like kinases in Arabidopsis and other plants. *Plant Cell,* 17**,** 836-48.

DEN ELZEN, N. & PINES, J. 2001. Cyclin A is destroyed in prometaphase and can delay chromosome alignment and anaphase. *J Cell Biol,* 153**,** 121-36.

DEN HAESE, G. J., WALWORTH, N., CARR, A. M. & GOULD, K. L. 1995. The Wee1 protein kinase regulates T14 phosphorylation of fission yeast Cdc2. *Mol Biol Cell,* 6**,** 371-385.

DENG, C., ZHANG, P., HARPER, J. W., ELLEDGE, S. J. & LEDER, P. 1995. Mice lacking p21CIP1/WAF1 undergo normal development, but are defective in G1 checkpoint control. *Cell,* 82**,** 675-84.

DEPHOURE, N., ZHOU, C., VILLEN, J., BEAUSOLEIL, S. A., BAKALARSKI, C. E., ELLEDGE, S. J. & GYGI, S. P. 2008. A quantitative atlas of mitotic phosphorylation. *Proc Natl Acad Sci U S A,* 105**,** 10762-7.

DESHAIES, R. J. 1999. SCF and Cullin/Ring H2-based ubiquitin ligases. *Annu Rev Cell Dev Biol,* 15**,** 435-67.

DEVAULT, A., MARTINEZ, A. M., FESQUET, D., LABBE, J. C., MORIN, N., TASSAN, J. P., NIGG, E. A., CAVADORE, J. C. & DOREE, M. 1995. MAT1 ('menage a trois') a new RING finger protein subunit stabilizing cyclin H-cdk7 complexes in starfish and Xenopus CAK. *EMBO J,* 14**,** 5027-36.

DEWITTE, W. & MURRAY, J. A. 2003. The plant cell cycle. *Annu Rev Plant Biol,* 54**,** 235-64.

DISSMEYER, N., WEIMER, A. K., PUSCH, S., DE SCHUTTER, K., ALVIM KAMEI, C. L., NOWACK, M. K., NOVAK, B., DUAN, G. L., ZHU, Y. G.,

DE VEYLDER, L. & SCHNITTGER, A. 2009. Control of cell proliferation, organ growth, and DNA damage response operate independently of dephosphorylation of the Arabidopsis Cdk1 homolog CDKA;1. *Plant Cell,* 21**,** 3641-54.

DONZELLI, M., SQUATRITO, M., GANOTH, D., HERSHKO, A., PAGANO, M. & DRAETTA, G. F. 2002. Dual mode of degradation of Cdc25 A phosphatase. *EMBO J,* 21**,** 4875-84.

DOUGHERTY, W. G. & PARKS, T. D. 1995. Transgenes and gene suppression: telling us something new? *Curr Opin Cell Biol,* 7**,** 399-405.

DOWIL, R. T., LU, X., SARACCO, S. A., VIERSTRA, R. D. & DOWNES, B. P. 2011. Arabidopsis membrane-anchored ubiquitin-fold (MUB) proteins localize a specific subset of ubiquitin-conjugating (E2) enzymes to the plasma membrane. *J Biol Chem,* 286**,** 14913-21.

DRAETTA, G. 1993. Cdc2 activation: the interplay of cyclin binding and Thr161 phosphorylation. *Trends Cell Biol,* 3**,** 287-9.

DRAETTA, G. F. 1997. Cell cycle: will the real Cdk-activating kinase please stand up. *Curr Biol,* 7**,** R50-2.

DREBOT, M. A., JOHNSTON, G. C. & SINGER, R. A. 1987. A yeast mutant conditionally defective only for reentry into the mitotic cell cycle from stationary phase. *Proc Natl Acad Sci U S A,* 84**,** 7948-52.

DUDITS, D., CSERHÁTI, M., MISKOLCZI, P. & HORVÁTH, G. V. 2007. The Growing Family of Plant Cyclin-Dependent Kinases with Multiple Functions in Cellular and Developmental Regulation. *Annual Plant Reviews Volume 32: Cell Cycle Control and Plant Development.* Blackwell Publishing Ltd.

DULIC, V., STEIN, G. H., FAR, D. F. & REED, S. I. 1998. Nuclear accumulation of p21Cip1 at the onset of mitosis: a role at the G2/M-phase transition. *Mol Cell Biol,* 18**,** 546-57.

DUNPHY, W. G. 1994. The decision to enter mitosis. *Trends Cell Biol,* 4**,** 202-7.

DUNPHY, W. G., BRIZUELA, L., BEACH, D. & NEWPORT, J. 1988. The Xenopus cdc2 protein is a component of MPF, a cytoplasmic regulator of mitosis. *Cell,* 54**,** 423-31.

EDWARDS, K., JOHNSTONE, C. & THOMPSON, C. 1991. A simple and rapid method for the preparation of plant genomic DNA for PCR analysis. *Nucleic Acids Res,* 19**,** 1349.

ELLEDGE, S. J. 1996. Cell cycle checkpoints: preventing an identity crisis. *Science,* 274**,** 1664-72.

ELLIS, R. J. 1979. The most abundant protein in the world. *Trends Biochem Sci,* 4**,** 241-244.

ENDICOTT, J. A., NURSE, P. & JOHNSON, L. N. 1994. Mutational analysis supports a structural model for the cell cycle protein kinase p34. *Protein Eng,* 7**,** 243-53.

ENGLER JDE, A., DE VEYLDER, L., DE GROODT, R., ROMBAUTS, S., BOUDOLF, V., DE MEYER, B., HEMERLY, A., FERREIRA, P., BEECKMAN, T., KARIMI, M., HILSON, P., INZE, D. & ENGLER, G. 2009. Systematic analysis of cell-cycle gene expression during Arabidopsis development. *Plant J,* 59**,** 645-60.

ENGLISH, J. J., MUELLER, E. & BAULCOMBE, D. C. 1996. Suppression of Virus Accumulation in Transgenic Plants Exhibiting Silencing of Nuclear Genes. *Plant Cell,* 8**,** 179-188.

ERRICO, A., DESHMUKH, K., TANAKA, Y., POZNIAKOVSKY, A. & HUNT, T. 2010. Identification of substrates for cyclin dependent kinases. *Adv Enzyme Regul,* 50**,** 375-99.

EVANS, T., ROSENTHAL, E. T., YOUNGBLOM, J., DISTEL, D. & HUNT, T. 1983. Cyclin: a protein specified by maternal mRNA in sea urchin eggs that is destroyed at each cleavage division. *Cell,* 33**,** 389-96.

FAGARD, M. & VAUCHERET, H. 2000. (TRANS)GENE SILENCING IN PLANTS: How Many Mechanisms? *Annu Rev Plant Physiol Plant Mol Biol,* 51**,** 167-194.

FARRAS, R., FERRANDO, A., JASIK, J., KLEINOW, T., OKRESZ, L., TIBURCIO, A., SALCHERT, K., DEL POZO, C., SCHELL, J. & KONCZ, C. 2001. SKP1-SnRK protein kinase interactions mediate proteasomal binding of a plant SCF ubiquitin ligase. *EMBO J,* 20**,** 2742-56.

FEATHERSTONE, C. & RUSSELL, P. 1991. Fission yeast p107wee1 mitotic inhibitor is a tyrosine/serine kinase. *Nature,* 349**,** 808-11.

FELDMAN, R. M., CORRELL, C. C., KAPLAN, K. B. & DESHAIES, R. J. 1997. A complex of Cdc4p, Skp1p, and Cdc53p/cullin catalyzes ubiquitination of the phosphorylated CDK inhibitor Sic1p. *Cell,* 91**,** 221-30.

FERREIRA, P. C., HEMERLY, A. S., VILLARROEL, R., VAN MONTAGU, M. & INZE, D. 1991. The Arabidopsis functional homolog of the p34cdc2 protein kinase. *Plant Cell,* 3**,** 531-40.

FERRELL, K., WILKINSON, C. R., DUBIEL, W. & GORDON, C. 2000. Regulatory subunit interactions of the 26S proteasome, a complex problem. *Trends Biochem Sci,* 25**,** 83-8.

FIELDS, S. & SONG, O. 1989. A novel genetic system to detect protein-protein interactions. *Nature,* 340**,** 245-6.

FISHER, R. P., JIN, P., CHAMBERLIN, H. M. & MORGAN, D. O. 1995. Alternative mechanisms of CAK assembly require an assembly factor or an activating kinase. *Cell,* 83**,** 47-57.

FISHER, R. P. & MORGAN, D. O. 1994. A novel cyclin associates with MO15/CDK7 to form the CDK-activating kinase. *Cell,* 78**,** 713-24.

FRANCIS, D. 2007. The plant cell cycle--15 years on. *New Phytol,* 174**,** 261-78.

FRANCIS, D. 2009. What's New in the Plant Cell Cycle. *In:* LÜTTGE, U. B., W.; BÜDEL, B.; FRANCIS, D. (ed.) *Progress in Botany.*

FRANCIS, D. 2011. A commentary on the G/M transition of the plant cell cycle. *Ann Bot,* 107**,** 1065-70.

FROLOV, M. V. & DYSON, N. J. 2004. Molecular mechanisms of E2F-dependent activation and pRB-mediated repression. *J Cell Sci,* 117**,** 2173-81.

FU, H., GIROD, P. A., DOELLING, J. H., VAN NOCKER, S., HOCHSTRASSER, M., FINLEY, D. & VIERSTRA, R. D. 1999. Structure and functional analysis of the 26S proteasome subunits from plants. *Mol Biol Rep,* 26**,** 137-46.

FUERST, R. A., SONI, R., MURRAY, J. A. & LINDSEY, K. 1996. Modulation of cyclin transcript levels in cultured cells of Arabidopsis thaliana. *Plant Physiol,* 112**,** 1023-33.

FUNABIKI, H., YAMANO, H., KUMADA, K., NAGAO, K., HUNT, T. & YANAGIDA, M. 1996. Cut2 proteolysis required for sister-chromatid seperation in fission yeast. *Nature,* 381**,** 438-41.

GABRIELLI, B. G., DE SOUZA, C. P., TONKS, I. D., CLARK, J. M., HAYWARD, N. K. & ELLEM, K. A. 1996. Cytoplasmic accumulation of cdc25B phosphatase in mitosis triggers centrosomal microtubule nucleation in HeLa cells. *J Cell Sci,* 109 (Pt 5)**,** 1081-93.

GAGNE, J. M., DOWNES, B. P., SHIU, S. H., DURSKI, A. M. & VIERSTRA, R. D. 2002. The F-box subunit of the SCF E3 complex is encoded by a diverse superfamily of genes in Arabidopsis. *Proc Natl Acad Sci U S A,* 99**,** 11519-24.

GALLANT, P. & NIGG, E. A. 1992. Cyclin B2 undergoes cell cycle-dependent nuclear translocation and, when expressed as a non-destructible mutant, causes mitotic arrest in HeLa cells. *J Cell Biol,* 117**,** 213-24.

GARCIA, V., BRUCHET, H., CAMESCASSE, D., GRANIER, F., BOUCHEZ, D. & TISSIER, A. 2003. AtATM is essential for meiosis and the somatic response to DNA damage in plants. *Plant Cell,* 15**,** 119-32.

GAUTIER, J., NORBURY, C., LOHKA, M., NURSE, P. & MALLER, J. 1988. Purified maturation-promoting factor contains the product of a Xenopus homolog of the fission yeast cell cycle control gene cdc2+. *Cell,* 54**,** 433-9.

GAUTIER, J., SOLOMON, M. J., BOOHER, R. N., BAZAN, J. F. & KIRSCHNER, M. W. 1991. cdc25 is a specific tyrosine phosphatase that directly activates p34cdc2. *Cell,* 67**,** 197-211.

GELEY, S., KRAMER, E., GIEFFERS, C., GANNON, J., PETERS, J. M. & HUNT, T. 2001. Anaphase-promoting complex/cyclosome-dependent proteolysis of human cyclin A starts at the beginning of mitosis and is not subject to the spindle assembly checkpoint. *J Cell Biol,* 153**,** 137-48.

GENSCHIK, P. & CRIQUI, M. C. 2007. The UPS: An Engine That Drives the Cell Cycle. *Annual Plant Reviews Volume 32: Cell Cycle Control and Plant Development.* Blackwell Publishing Ltd.

GENSCHIK, P., CRIQUI, M. C., PARMENTIER, Y., DEREVIER, A. & FLECK, J. 1998. Cell cycle -dependent proteolysis in plants. Identification Of the destruction box pathway and metaphase arrest produced by the proteasome inhibitor mg132. *Plant Cell,* 10**,** 2063-76.

GIBSON, S. I. 2005. Control of plant development and gene expression by sugar signaling. *Curr Opin Plant Biol,* 8**,** 93-102.

GIRARD, F., STRAUSFELD, U., CAVADORE, J. C., RUSSELL, P., FERNANDEZ, A. & LAMB, N. J. 1992. cdc25 is a nuclear protein expressed constitutively throughout the cell cycle in nontransformed mammalian cells. *J Cell Biol,* 118**,** 785-94.

GLICKMAN, M. H. 2000. Getting in and out of the proteasome. *Semin Cell Dev Biol,* 11**,** 149-58.

GLOTZER, M., MURRAY, A. W. & KIRSCHNER, M. W. 1991. Cyclin is degraded by the ubiquitin pathway. *Nature,* 349**,** 132-8.

GONZALEZ, N., GEVAUDANT, F., HERNOULD, M., CHEVALIER, C. & MOURAS, A. 2007. The cell cycle-associated protein kinase WEE1 regulates cell size in relation to endoreduplication in developing tomato fruit. *Plant J,* 51**,** 642-55.

GONZALEZ, N., HERNOULD, M., DELMAS, F., GEVAUDANT, F., DUFFE, P., CAUSSE, M., MOURAS, A. & CHEVALIER, C. 2004. Molecular characterization of a WEE1 gene homologue in tomato (Lycopersicon esculentum Mill.). *Plant Mol Biol,* 56**,** 849-61.

GOULD, K. L., MORENO, S., OWEN, D. J., SAZER, S. & NURSE, P. 1991. Phosphorylation at Thr167 is required for Schizosaccharomyces pombe p34cdc2 function. *EMBO J,* 10**,** 3297-309.

GOULD, K. L. & NURSE, P. 1989. Tyrosine phosphorylation of the fission yeast cdc2+ protein kinase regulates entry into mitosis. *Nature,* 342**,** 39-45.

GRAFI, G., BURNETT, R. J., HELENTJARIS, T., LARKINS, B. A., DECAPRIO, J. A., SELLERS, W. R. & KAELIN, W. G., JR. 1996. A maize cDNA encoding a member of the retinoblastoma protein family: involvement in endoreduplication. *Proc Natl Acad Sci U S A,* 93**,** 8962-7.

GRAUMANN, K., RUNIONS, J. & EVANS, D. E. 2010. Characterization of SUN-domain proteins at the higher plant nuclear envelope. *Plant J,* 61**,** 134-44.

GRAY, W. M., KEPINSKI, S., ROUSE, D., LEYSER, O. & ESTELLE, M. 2001. Auxin regulates SCF(TIR1)-dependent degradation of AUX/IAA proteins. *Nature,* 414**,** 271-6.

GUAN, K. L., JENKINS, C. W., LI, Y., NICHOLS, M. A., WU, X., O'KEEFE, C. L., MATERA, A. G. & XIONG, Y. 1994. Growth suppression by p18, a

p16INK4/MTS1- and p14INK4B/MTS2-related CDK6 inhibitor, correlates with wild-type pRb function. *Genes Dev,* 8**,** 2939-52.

GUO, J., SONG, J., WANG, F. & ZHANG, X. S. 2007. Genome-wide identification and expression analysis of rice cell cycle genes. *Plant Mol Biol,* 64**,** 349-60.

GUSTI, A., BAUMBERGER, N., NOWACK, M., PUSCH, S., EISLER, H., POTUSCHAK, T., DE VEYLDER, L., SCHNITTGER, A. & GENSCHIK, P. 2009. The Arabidopsis thaliana F-box protein FBL17 is essential for progression through the second mitosis during pollen development. *PLoS One,* 4**,** e4780.

GYURIS, J., GOLEMIS, E., CHERTKOV, H. & BRENT, R. 1993. Cdi1, a human G1 and S phase protein phosphatase that associates with Cdk2. *Cell,* 75**,** 791-803.

HALIMI, Y., DESSAU, M., POLLAK, S., AST, T., EREZ, T., LIVNAT-LEVANON, N., KARNIOL, B., HIRSCH, J. A. & CHAMOVITZ, D. A. 2011. COP9 signalosome subunit 7 from Arabidopsis interacts with and regulates the small subunit of ribonucleotide reductase (RNR2). *Plant Mol Biol,* 77**,** 77-89.

HANNON, G. J. & BEACH, D. 1994. p15INK4B is a potential effector of TGF-beta-induced cell cycle arrest. *Nature,* 371**,** 257-61.

HARASHIMA, H., SHINMYO, A. & SEKINE, M. 2007. Phosphorylation of threonine 161 in plant cyclin-dependent kinase A is required for cell division by activation of its associated kinase. *Plant J,* 52**,** 435-48.

HARPER, J. W., ADAMI, G. R., WEI, N., KEYOMARSI, K. & ELLEDGE, S. J. 1993. The p21 Cdk-interacting protein Cip1 is a potent inhibitor of G1 cyclin-dependent kinases. *Cell,* 75**,** 805-16.

HARTWELL, L. H. & WEINERT, T. A. 1989. Checkpoints: controls that ensure the order of cell cycle events. *Science,* 246**,** 629-34.

HASS, C., LOHRMANN, J., ALBRECHT, V., SWEERE, U., HUMMEL, F., YOO, S. D., HWANG, I., ZHU, T., SCHAFER, E., KUDLA, J. & HARTER, K. 2004. The response regulator 2 mediates ethylene signalling and hormone signal integration in Arabidopsis. *EMBO J,* 23**,** 3290-302.

HEALD, R., MCLOUGHLIN, M. & MCKEON, F. 1993. Human wee1 maintains mitotic timing by protecting the nucleus from cytoplasmically activated Cdc2 kinase. *Cell,* 74**,** 463-74.

HEALY, J. M., MENGES, M., DOONAN, J. H. & MURRAY, J. A. 2001. The Arabidopsis D-type cyclins CycD2 and CycD3 both interact in vivo with the PSTAIRE cyclin-dependent kinase Cdc2a but are differentially controlled. *J Biol Chem,* 276**,** 7041-7.

HELLMANN, H. & ESTELLE, M. 2002. Plant development: regulation by protein degradation. *Science,* 297**,** 793-7.

HERBERT, R. J., VILHAR, B., EVETT, C., ORCHARD, C. B., ROGERS, H. J., DAVIES, M. S. & FRANCIS, D. 2001. Ethylene induces cell death at particular phases of the cell cycle in the tobacco TBY-2 cell line. *J Exp Bot,* 52**,** 1615-23.

HERMAND, D., PIHLAK, A., WESTERLING, T., DAMAGNEZ, V., VANDENHAUTE, J., COTTAREL, G. & MAKELA, T. P. 1998. Fission yeast Csk1 is a CAK-activating kinase (CAKAK). *EMBO J,* 17**,** 7230-8.

HERMAND, D., WESTERLING, T., PIHLAK, A., THURET, J. Y., VALLENIUS, T., TIAINEN, M., VANDENHAUTE, J., COTTAREL, G., MANN, C. & MAKELA, T. P. 2001. Specificity of Cdk activation in vivo by the two Caks Mcs6 and Csk1 in fission yeast. *EMBO J,* 20**,** 82-90.

HERSHKO, A. & CIECHANOVER, A. 1998. The ubiquitin system. *Annu Rev Biochem,* 67**,** 425-79.

HERSHKO, A., GANOTH, D., PEHRSON, J., PALAZZO, R. E. & COHEN, L. H. 1991. Methylated ubiquitin inhibits cyclin degradation in clam embryo extracts. *J Biol Chem,* 266**,** 16376-9.

HIRAI, H., ROUSSEL, M. F., KATO, J. Y., ASHMUN, R. A. & SHERR, C. J. 1995. Novel INK4 proteins, p19 and p18, are specific inhibitors of the cyclin D-dependent kinases CDK4 and CDK6. *Mol Cell Biol,* 15**,** 2672-81.

HIRAO, A., KONG, Y. Y., MATSUOKA, S., WAKEHAM, A., RULAND, J., YOSHIDA, H., LIU, D., ELLEDGE, S. J. & MAK, T. W. 2000. DNA damage-induced activation of p53 by the checkpoint kinase Chk2. *Science,* 287**,** 1824-7.

HIRT, H., MINK, M., PFOSSER, M., BOGRE, L., GYORGYEY, J., JONAK, C., GARTNER, A., DUDITS, D. & HEBERLE-BORS, E. 1992. Alfalfa cyclins: differential expression during the cell cycle and in plant organs. *Plant Cell,* 4**,** 1531-8.

HOEKSTRA, M. F. 1997. Responses to DNA damage and regulation of cell cycle checkpoints by the ATM protein kinase family. *Curr Opin Genet Dev,* 7**,** 170-5.

HOFFMANN, I., CLARKE, P. R., MARCOTE, M. J., KARSENTI, E. & DRAETTA, G. 1993. Phosphorylation and activation of human cdc25-C by cdc2--cyclin B and its involvement in the self-amplification of MPF at mitosis. *EMBO J,* 12**,** 53-63.

HOLLOWAY, S. L., GLOTZER, M., KING, R. W. & MURRAY, A. W. 1993. Anaphase is initiated by proteolysis rather than by the inactivation of maturation-promoting factor. *Cell,* 73**,** 1393-402.

HOLT, L. J., TUCH, B. B., VILLEN, J., JOHNSON, A. D., GYGI, S. P. & MORGAN, D. O. 2009. Global analysis of Cdk1 substrate phosphorylation sites provides insights into evolution. *Science,* 325**,** 1682-6.

HU, C. D., CHINENOV, Y. & KERPPOLA, T. K. 2002. Visualization of interactions among bZIP and Rel family proteins in living cells using bimolecular fluorescence complementation. *Mol Cell,* 9**,** 789-98.

HUNTLEY, R., HEALY, S., FREEMAN, D., LAVENDER, P., DE JAGER, S., GREENWOOD, J., MAKKER, J., WALKER, E., JACKMAN, M., XIE, Q., BANNISTER, A. J., KOUZARIDES, T., GUTIERREZ, C., DOONAN, J. H. & MURRAY, J. A. 1998. The maize retinoblastoma protein homologue ZmRb-1 is regulated during leaf development and displays conserved interactions with G1/S regulators and plant cyclin D (CycD) proteins. *Plant Mol Biol,* 37**,** 155-69.

IGARASHI, M., NAGATA, A., JINNO, S., SUTO, K. & OKAYAMA, H. 1991. Wee1(+)-like gene in human cells. *Nature,* 353**,** 80-3.

IMAJUKU, Y., HIRAYAMA, T., ENDOH, H. & OKA, A. 1992. Exon-intron organization of the Arabidopsis thaliana protein kinase genes CDC2a and CDC2b. *FEBS Lett,* 304**,** 73-7.

ITO, M., MARIE-CLAIRE, C., SAKABE, M., OHNO, T., HATA, S., KOUCHI, H., HASHIMOTO, J., FUKUDA, H., KOMAMINE, A. & WATANABE, A. 1997. Cell-cycle-regulated transcription of A- and B-type plant cyclin genes in synchronous cultures. *Plant J,* 11**,** 983-92.

IZUMI, T. & MALLER, J. L. 1993. Elimination of cdc2 phosphorylation sites in the cdc25 phosphatase blocks initiation of M-phase. *Mol Biol Cell,* 4**,** 1337-50.

JACKSON, P. K., ELDRIDGE, A. G., FREED, E., FURSTENTHAL, L., HSU, J. Y., KAISER, B. K. & REIMANN, J. D. 2000. The lore of the RINGs: substrate recognition and catalysis by ubiquitin ligases. *Trends Cell Biol,* 10**,** 429-39.

JASINSKI, S., RIOU-KHAMLICHI, C., ROCHE, O., PERENNES, C., BERGOUNIOUX, C. & GLAB, N. 2002. The CDK inhibitor NtKIS1a is involved in plant development, endoreduplication and restores normal development of cyclin D3; 1-overexpressing plants. *J Cell Sci,* 115**,** 973-82.

JIMENEZ, J., ALPHEY, L., NURSE, P. & GLOVER, D. M. 1990. Complementation of fission yeast cdc2ts and cdc25ts mutants identifies two cell cycle genes from Drosophila: a cdc2 homologue and string. *EMBO J,* 9**,** 3565-71.

JINNO, S., SUTO, K., NAGATA, A., IGARASHI, M., KANAOKA, Y., NOJIMA, H. & OKAYAMA, H. 1994. Cdc25A is a novel phosphatase functioning early in the cell cycle. *EMBO J,* 13**,** 1549-56.

JOHN, P. C. L., ZHANG, K., DONG, C., DIEDERICH, L. & WIGHTMAN, F. 1993. p34cdc2 related proteins in control of cell cycle progression, the switch between division and differentiation in tissue development, and stimulation of division by auxin and cytokinin. *Australian Journal of Plant Physiology,* 20**,** 503-526.

JOUBES, J., CHEVALIER, C., DUDITS, D., HEBERLE-BORS, E., INZE, D., UMEDA, M. & RENAUDIN, J. P. 2000. CDK-related protein kinases in plants. *Plant Mol Biol,* 43**,** 607-20.

KAISER, P., SIA, R. A., BARDES, E. G., LEW, D. J. & REED, S. I. 1998. Cdc34 and the F-box protein Met30 are required for degradation of the Cdk-inhibitory kinase Swe1. *Genes Dev,* 12**,** 2587-97.

KERPPOLA, T. K. 2009. Visualization of molecular interactions using bimolecular fluorescence complementation analysis: characteristics of protein fragment complementation. *Chem Soc Rev,* 38**,** 2876-86.

KHARBANDA, S., SALEEM, A., DATTA, R., YUAN, Z. M., WEICHSELBAUM, R. & KUFE, D. 1994. Ionizing radiation induces rapid tyrosine phosphorylation of p34cdc2. *Cancer Res,* 54**,** 1412-4.

KING, R. W., PETERS, J. M., TUGENDREICH, S., ROLFE, M., HIETER, P. & KIRSCHNER, M. W. 1995. A 20S complex containing CDC27 and CDC16 catalyzes the mitosis-specific conjugation of ubiquitin to cyclin B. *Cell,* 81**,** 279-88.

KOBAYASHI, H., STEWART, E., POON, R., ADAMCZEWSKI, J. P., GANNON, J. & HUNT, T. 1992. Identification of the domains in cyclin A required for binding to, and activation of, p34cdc2 and p32cdk2 protein kinase subunits. *Mol Biol Cell,* 3**,** 1279-94.

KONO, A., UMEDA-HARA, C., LEE, J., ITO, M., UCHIMIYA, H. & UMEDA, M. 2003. Arabidopsis D-type cyclin CYCD4;1 is a novel cyclin partner of B2-type cyclin-dependent kinase. *Plant Physiol,* 132**,** 1315-21.

KOUCHI, H., SEKINE, M. & HATA, S. 1995. Distinct classes of mitotic cyclins are differentially expressed in the soybean shoot apex during the cell cycle. *Plant Cell,* 7**,** 1143-55.

KRISHNAN, H. B. & NATARAJAN, S. S. 2009. A rapid method for depletion of Rubisco from soybean (Glycine max) leaf for proteomic analysis of lower abundance proteins. *Phytochemistry,* 70**,** 1958-64.

KUMAGAI, A. & DUNPHY, W. G. 1991. The cdc25 protein controls tyrosine dephosphorylation of the cdc2 protein in a cell-free system. *Cell,* 64**,** 903-14.

LANDRIEU, I., DA COSTA, M., DE VEYLDER, L., DEWITTE, F., VANDEPOELE, K., HASSAN, S., WIERUSZESKI, J. M., CORELLOU, F., FAURE, J. D., VAN MONTAGU, M., INZE, D. & LIPPENS, G. 2004. A small CDC25 dual-specificity tyrosine-phosphatase isoform in Arabidopsis thaliana. *Proc Natl Acad Sci U S A,* 101**,** 13380-5.

LEE, J., DAS, A., YAMAGUCHI, M., HASHIMOTO, J., TSUTSUMI, N., UCHIMIYA, H. & UMEDA, M. 2003. Cell cycle function of a rice B2-type cyclin interacting with a B-type cyclin-dependent kinase. *Plant J,* 34**,** 417-25.

LEE, J., KUMAGAI, A. & DUNPHY, W. G. 2001. Positive regulation of Wee1 by Chk1 and 14-3-3 proteins. *Mol Biol Cell,* 12**,** 551-63.

LEE, L. Y., FANG, M. J., KUANG, L. Y. & GELVIN, S. B. 2008. Vectors for multi-color bimolecular fluorescence complementation to investigate protein-protein interactions in living plant cells. *Plant Methods,* 4**,** 24.

LEE, M. G. & NURSE, P. 1987. Complementation used to clone a human homologue of the fission yeast cell cycle control gene cdc2. *Nature,* 327**,** 31-5.

LEE, M. S., OGG, S., XU, M., PARKER, L. L., DONOGHUE, D. J., MALLER, J. L. & PIWNICA-WORMS, H. 1992. cdc25+ encodes a protein phosphatase that dephosphorylates p34cdc2. *Mol Biol Cell,* 3**,** 73-84.

LEES, E. M. & HARLOW, E. 1993. Sequences within the conserved cyclin box of human cyclin A are sufficient for binding to and activation of cdc2 kinase. *Mol Cell Biol,* 13**,** 1194-201.

LENTZ GRØNLUND, A. 2007. *Regulatory mechanisms of the plant G2/M transition.* PhD thesis, Cardiff University.

LENTZ GRØNLUND, A., DICKINSON, J. R., KILLE, P., HERBERT, R. J., FRANCIS, D. & ROGERS, H. J. 2009. Plant WEE1 kinase interacts with a 14-3-3 protein but a mutation of WEE1 at S485 alters their spatial interaction. *The Open Plant Science Journal,* 3**,** 40-48.

LI, M., TANG, D., WANG, K., WU, X., LU, L., YU, H., GU, M., YAN, C. & CHENG, Z. 2011. Mutations in the F-box gene LARGER PANICLE improve the panicle architecture and enhance the grain yield in rice. *Plant Biotechnol J,* 9**,** 1002-13.

LIU, C., MENG, C., XIE, L., HONG, J. & ZHOU, X. 2009. Cell-to-cell trafficking, subcellular distribution, and binding to coat protein of Broad bean wilt virus 2 VP37 protein. *Virus Res,* 143**,** 86-93.

LIU, F., STANTON, J. J., WU, Z. & PIWNICA-WORMS, H. 1997. The human Myt1 kinase preferentially phosphorylates Cdc2 on threonine 14 and localizes to the endoplasmic reticulum and Golgi complex. *Mol Cell Biol,* 17**,** 571-83.

LUCA, F. C., SHIBUYA, E. K., DOHRMANN, C. E. & RUDERMAN, J. V. 1991. Both cyclin A delta 60 and B delta 97 are stable and arrest cells in M-phase, but only cyclin B delta 97 turns on cyclin destruction. *EMBO J,* 10**,** 4311-20.

LUI, H., WANG, H., DELONG, C., FOWKE, L. C., CROSBY, W. L. & FOBERT, P. R. 2000. The Arabidopsis Cdc2a-interacting protein ICK2 is structurally related to ICK1 and is a potent inhibitor of cyclin-dependent kinase activity in vitro. *Plant J,* 21**,** 379-85.

LUNDGREN, K., WALWORTH, N., BOOHER, R., DEMBSKI, M., KIRSCHNER, M. & BEACH, D. 1991. mik1 and wee1 cooperate in the inhibitory tyrosine phosphorylation of cdc2. *Cell,* 64**,** 1111-22.

MAGYAR, Z., ATANASSOVA, A., DE VEYLDER, L., ROMBAUTS, S. & INZE, D. 2000. Characterization of two distinct DP-related genes from Arabidopsis thaliana. *FEBS Lett,* 486**,** 79-87.

MAKELA, T. P., TASSAN, J. P., NIGG, E. A., FRUTIGER, S., HUGHES, G. J. & WEINBERG, R. A. 1994. A cyclin associated with the CDK-activating kinase MO15. *Nature,* 371**,** 254-7.

MALLADI, A. & JOHNSON, L. K. 2011. Expression profiling of cell cycle genes reveals key facilitators of cell production during carpel development, fruit set, and fruit growth in apple (Malusxdomestica Borkh.). *J Exp Bot,* 62**,** 205-19.

MARROCCO, K., THOMANN, A., PARMENTIER, Y., GENSCHIK, P. & CRIQUI, M. C. 2009. The APC/C E3 ligase remains active in most post-mitotic Arabidopsis cells and is required for proper vasculature development and organization. *Development,* 136**,** 1475-85.

MARTI, A., WIRBELAUER, C., SCHEFFNER, M. & KREK, W. 1999. Interaction between ubiquitin-protein ligase SCFSKP2 and E2F-1 underlies the regulation of E2F-1 degradation. *Nat Cell Biol,* 1**,** 14-9.

MASUDA, H., FONG, C. S., OHTSUKI, C., HARAGUCHI, T. & HIRAOKA, Y. 2011. Spatiotemporal regulations of Wee1 at the G2/M transition. *Mol Biol Cell,* 22**,** 555-69.

MASUI, Y. & MARKERT, C. L. 1971. Cytoplasmic control of nuclear behavior during meiotic maturation of frog oocytes. *J Exp Zool,* 177**,** 129-45.

MATSUOKA, S., EDWARDS, M. C., BAI, C., PARKER, S., ZHANG, P., BALDINI, A., HARPER, J. W. & ELLEDGE, S. J. 1995. p57KIP2, a structurally distinct member of the p21CIP1 Cdk inhibitor family, is a candidate tumor suppressor gene. *Genes Dev,* 9**,** 650-62.

MCGOWAN, C. H. & RUSSELL, P. 1995. Cell cycle regulation of human WEE1. *EMBO J,* 14**,** 2166-75.

MEDEMA, R. H., KLOMPMAKER, R., SMITS, V. A. & RIJKSEN, G. 1998. p21waf1 can block cells at two points in the cell cycle, but does not interfere with processive DNA-replication or stress-activated kinases. *Oncogene,* 16**,** 431-41.

MENDENHALL, M. D. 1993. An inhibitor of p34CDC28 protein kinase activity from Saccharomyces cerevisiae. *Science,* 259**,** 216-9.

MENGES, M., DE JAGER, S. M., GRUISSEM, W. & MURRAY, J. A. 2005. Global analysis of the core cell cycle regulators of Arabidopsis identifies novel genes, reveals multiple and highly specific profiles of expression and provides a coherent model for plant cell cycle control. *Plant J,* 41**,** 546-66.

MENGES, M., HENNIG, L., GRUISSEM, W. & MURRAY, J. A. 2003. Genome-wide gene expression in an Arabidopsis cell suspension. *Plant Mol Biol,* 53**,** 423-42.

MENGES, M. & MURRAY, J. A. 2002. Synchronous Arabidopsis suspension cultures for analysis of cell-cycle gene activity. *Plant J,* 30**,** 203-12.

MESKIENE, I., BOGRE, L., DAHL, M., PIRCK, M., HA, D. T., SWOBODA, I., HEBERLE-BORS, E., AMMERER, G. & HIRT, H. 1995. cycMs3, a novel B-type alfalfa cyclin gene, is induced in the G0-to-G1 transition of the cell cycle. *Plant Cell,* 7**,** 759-71.

MEWS, M., SEK, F. J., MOORE, R., VOLKMANN, D., GUNNING, B. E. S. & JOHN, P. C. L. 1997. Mitotic cyclin distribution during maize cell division: Implications for the sequence diversity and function of cyclins in plants. *Protoplasma,* 200**,** 128-145.

MICHAEL, W. M. & NEWPORT, J. 1998. Coupling of mitosis to the completion of S phase through Cdc34-mediated degradation of Wee1. *Science,* 282**,** 1886-9.

MILLAR, J. B., BLEVITT, J., GERACE, L., SADHU, K., FEATHERSTONE, C. & RUSSELL, P. 1991. p55CDC25 is a nuclear protein required for the initiation of mitosis in human cells. *Proc Natl Acad Sci U S A,* 88**,** 10500-4.

MONTAGNOLI, A., FIORE, F., EYTAN, E., CARRANO, A. C., DRAETTA, G. F., HERSHKO, A. & PAGANO, M. 1999. Ubiquitination of p27 is regulated by Cdk-dependent phosphorylation and trimeric complex formation. *Genes Dev,* 13**,** 1181-9.

MOON, J., PARRY, G. & ESTELLE, M. 2004. The ubiquitin-proteasome pathway and plant development. *Plant Cell,* 16**,** 3181-95.

MORELL, M., ESPARGARO, A., AVILES, F. X. & VENTURA, S. 2008. Study and selection of in vivo protein interactions by coupling bimolecular fluorescence complementation and flow cytometry. *Nat Protoc,* 3**,** 22-33.

MORGAN, D. O. 1997. Cyclin-dependent kinases: engines, clocks, and microprocessors. *Annu Rev Cell Dev Biol,* 13**,** 261-91.

MUELLER, P. R., COLEMAN, T. R., KUMAGAI, A. & DUNPHY, W. G. 1995. Myt1: a membrane-associated inhibitory kinase that phosphorylates Cdc2 on both threonine-14 and tyrosine-15. *Science,* 270**,** 86-90.

MURRAY, A. W., SOLOMON, M. J. & KIRSCHNER, M. W. 1989. The role of cyclin synthesis and degradation in the control of maturation promoting factor activity. *Nature,* 339**,** 280-6.

NACHTWEY, D. S. & CAMERON, I. L. 1968. Cell cycle analysis. *In:* PRESCOTT, D. M. (ed.) *Methods in cell physiology.* New York and London: Academic Press.

NAGATA, T., OKADA, K., KAWAZU, T. & TAKEBE, I. 1987. Cauliflower mosaic virus 35 S promoter directs S phase specific expression in plant cells. *Molecular and General Genetics,* 207**,** 242-244.

NASH, P., TANG, X., ORLICKY, S., CHEN, Q., GERTLER, F. B., MENDENHALL, M. D., SICHERI, F., PAWSON, T. & TYERS, M. 2001. Multisite phosphorylation of a CDK inhibitor sets a threshold for the onset of DNA replication. *Nature,* 414**,** 514-21.

NASMYTH, K. 2001. Disseminating the genome: joining, resolving, and separating sister chromatids during mitosis and meiosis. *Annu Rev Genet,* 35**,** 673-745.

NASMYTH, K. A. & REED, S. I. 1980. Isolation of genes by complementation in yeast: molecular cloning of a cell-cycle gene. *Proc Natl Acad Sci U S A,* 77**,** 2119-23.

NEGANOVA, I. & LAKO, M. 2008. G1 to S phase cell cycle transition in somatic and embryonic stem cells. *J Anat,* 213**,** 30-44.

NICULESCU, A. B., 3RD, CHEN, X., SMEETS, M., HENGST, L., PRIVES, C. & REED, S. I. 1998. Effects of p21(Cip1/Waf1) at both the G1/S and the G2/M cell cycle transitions: pRb is a critical determinant in blocking DNA replication and in preventing endoreduplication. *Mol Cell Biol,* 18**,** 629-43.

NIEUWLAND, J., MENGES, M. & MURRAY, J. A. H. 2007. The Plant Cyclins. *Annual Plant Reviews Volume 32: Cell Cycle Control and Plant Development.* Blackwell Publishing Ltd.

NIGG, E. A. 1996. Cyclin-dependent kinase 7: at the cross-roads of transcription, DNA repair and cell cycle control? *Curr Opin Cell Biol,* 8**,** 312-7.

NOCAROVA, E. & FISCHER, L. 2009. Cloning of transgenic tobacco BY-2 cells; an efficient method to analyse and reduce high natural heterogeneity of transgene expression. *BMC Plant Biol,* 9**,** 44.

NURSE, P. 1990. Universal control mechanism regulating onset of M-phase. *Nature,* 344**,** 503-8.

O'CONNELL, M. J., RALEIGH, J. M., VERKADE, H. M. & NURSE, P. 1997. Chk1 is a wee1 kinase in the G2 DNA damage checkpoint inhibiting cdc2 by Y15 phosphorylation. *EMBO J,* 16**,** 545-54.

OONO, Y., SEKI, M., SATOU, M., IIDA, K., AKIYAMA, K., SAKURAI, T., FUJITA, M., YAMAGUCHI-SHINOZAKI, K. & SHINOZAKI, K. 2006. Monitoring expression profiles of Arabidopsis genes during cold acclimation and deacclimation using DNA microarrays. *Funct Integr Genomics,* 6**,** 212-34.

ORCHARD, C. B., SICILIANO, I., SORRELL, D. A., MARCHBANK, A., ROGERS, H. J., FRANCIS, D., HERBERT, R. J., SUCHOMELOVA, P., LIPAVSKA, H., AZMI, A. & VAN ONCKELEN, H. 2005. Tobacco BY-2 cells expressing fission yeast cdc25 bypass a G2/M block on the cell cycle. *Plant J,* 44**,** 290-9.

ORMENESE, S., DE ALMEIDA ENGLER, J., DE GROODT, R., DE VEYLDER, L., INZE, D. & JACQMARD, A. 2004. Analysis of the spatial expression pattern of seven Kip related proteins (KRPs) in the shoot apex of Arabidopsis thaliana. *Ann Bot,* 93**,** 575-80.

PARDEE, A. B. 1974. A restriction point for control of normal animal cell proliferation. *Proc Natl Acad Sci U S A,* 71**,** 1286-90.

PARKER, L. L. & PIWNICA-WORMS, H. 1992. Inactivation of the p34cdc2-cyclin B complex by the human WEE1 tyrosine kinase. *Science,* 257**,** 1955-7.

PARKER, L. L., WALTER, S. A., YOUNG, P. G. & PIWNICA-WORMS, H. 1993. Phosphorylation and inactivation of the mitotic inhibitor Wee1 by the nim1/cdr1 kinase. *Nature,* 363**,** 736-8.

PERES, A., CHURCHMAN, M. L., HARIHARAN, S., HIMANEN, K., VERKEST, A., VANDEPOELE, K., MAGYAR, Z., HATZFELD, Y., VAN DER SCHUEREN, E., BEEMSTER, G. T., FRANKARD, V., LARKIN, J. C., INZE, D. & DE VEYLDER, L. 2007. Novel plant-specific cyclin-dependent kinase inhibitors induced by biotic and abiotic stresses. *J Biol Chem,* 282**,** 25588-96.

PETER, M. & HERSKOWITZ, I. 1994. Direct inhibition of the yeast cyclin-dependent kinase Cdc28-Cln by Far1. *Science,* 265**,** 1228-31.

PETERS, J. M. 2002. The anaphase-promoting complex: proteolysis in mitosis and beyond. *Mol Cell,* 9**,** 931-43.

PIAGGIO, G., FARINA, A., PERROTTI, D., MANNI, I., FUSCHI, P., SACCHI, A. & GAETANO, C. 1995. Structure and growth-dependent regulation of the human cyclin B1 promoter. *Exp Cell Res,* 216**,** 396-402.

PINES, J. 1995. Cyclins and cyclin-dependent kinases: a biochemical view. *Biochem J,* 308 (Pt 3)**,** 697-711.

PINES, J. & HUNTER, T. 1989. Isolation of a human cyclin cDNA: evidence for cyclin mRNA and protein regulation in the cell cycle and for interaction with p34cdc2. *Cell,* 58**,** 833-46.

PINES, J. & HUNTER, T. 1991. Human cyclins A and B1 are differentially located in the cell and undergo cell cycle-dependent nuclear transport. *J Cell Biol,* 115**,** 1-17.

POLYAK, K., KATO, J. Y., SOLOMON, M. J., SHERR, C. J., MASSAGUE, J., ROBERTS, J. M. & KOFF, A. 1994a. p27Kip1, a cyclin-Cdk inhibitor, links transforming growth factor-beta and contact inhibition to cell cycle arrest. *Genes Dev,* 8**,** 9-22.

POLYAK, K., LEE, M. H., ERDJUMENT-BROMAGE, H., KOFF, A., ROBERTS, J. M., TEMPST, P. & MASSAGUE, J. 1994b. Cloning of p27Kip1, a cyclin-dependent kinase inhibitor and a potential mediator of extracellular antimitogenic signals. *Cell,* 78**,** 59-66.

PORCEDDU, A., STALS, H., REICHHELD, J. P., SEGERS, G., DE VEYLDER, L., BARROCO, R. P., CASTEELS, P., VAN MONTAGU, M., INZE, D. & MIRONOV, V. 2001. A plant-specific cyclin-dependent kinase is involved in the control of G2/M progression in plants. *J Biol Chem,* 276**,** 36354-60.

PRICE, A. M., AROS ORELLANA, D. F., SALLEH, F. M., STEVENS, R., ACOCK, R., BUCHANAN-WOLLASTON, V., STEAD, A. D. & ROGERS, H. J. 2008. A comparison of leaf and petal senescence in wallflower reveals common and distinct patterns of gene expression and physiology. *Plant Physiol,* 147**,** 1898-912.

QIN, L. X., PERENNES, C., RICHARD, L., BOUVIER-DURAND, M., TREHIN, C., INZE, D. & BERGOUNIOUX, C. 1996. G2-and early-M-specific expression of the NTCYC1 cyclin gene in Nicotiana tabacum cells. *Plant Mol Biol,* 32**,** 1093-101.

RAMIREZ-PARRA, E., DEL POZO, J. C., DESVOYES, B., DE LA PAZ SANCHEZ, M. & GUTIERREZ, C. 2007. E2F–DP Transcription Factors. *Annual Plant Reviews Volume 32: Cell Cycle Control and Plant Development.* Blackwell Publishing Ltd.

RAMIREZ-PARRA, E., FRUNDT, C. & GUTIERREZ, C. 2003. A genome-wide identification of E2F-regulated genes in Arabidopsis. *Plant J,* 33**,** 801-11.

RAMIREZ-PARRA, E. & GUTIERREZ, C. 2000. Characterization of wheat DP, a heterodimerization partner of the plant E2F transcription factor which stimulates E2F-DNA binding. *FEBS Lett,* 486**,** 73-8.

RAMIREZ-PARRA, E., XIE, Q., BONIOTTI, M. B. & GUTIERREZ, C. 1999. The cloning of plant E2F, a retinoblastoma-binding protein, reveals unique and

conserved features with animal G(1)/S regulators. *Nucleic Acids Res,* 27**,** 3527-33.

REICHHELD, J. P., CHAUBET, N., SHEN, W. H., RENAUDIN, J. P. & GIGOT, C. 1996. Multiple A-type cyclins express sequentially during the cell cycle in Nicotiana tabacum BY2 cells. *Proc Natl Acad Sci U S A,* 93**,** 13819-24.

REN, H., SANTNER, A., DEL POZO, J. C., MURRAY, J. A. & ESTELLE, M. 2008. Degradation of the cyclin-dependent kinase inhibitor KRP1 is regulated by two different ubiquitin E3 ligases. *Plant J,* 53**,** 705-16.

RENAUDIN, J. P., DOONAN, J. H., FREEMAN, D., HASHIMOTO, J., HIRT, H., INZE, D., JACOBS, T., KOUCHI, H., ROUZE, P., SAUTER, M., SAVOURE, A., SORRELL, D. A., SUNDARESAN, V. & MURRAY, J. A. 1996. Plant cyclins: a unified nomenclature for plant A-, B- and D-type cyclins based on sequence organization. *Plant Mol Biol,* 32**,** 1003-18.

RHIND, N., FURNARI, B. & RUSSELL, P. 1997. Cdc2 tyrosine phosphorylation is required for the DNA damage checkpoint in fission yeast. *Genes Dev,* 11**,** 504-11.

RHIND, N. & RUSSELL, P. 2000. Chk1 and Cds1: linchpins of the DNA damage and replication checkpoint pathways. *J Cell Sci,* 113 (Pt 22)**,** 3889-96.

RIABOWOL, K., DRAETTA, G., BRIZUELA, L., VANDRE, D. & BEACH, D. 1989. The cdc2 kinase is a nuclear protein that is essential for mitosis in mammalian cells. *Cell,* 57**,** 393-401.

RICAUD, L., PROUX, C., RENOU, J. P., PICHON, O., FOCHESATO, S., ORTET, P. & MONTANE, M. H. 2007. ATM-mediated transcriptional and developmental responses to gamma-rays in Arabidopsis. *PLoS One,* 2**,** e430.

RIMMINGTON, G., DALBY, B. & GLOVER, D. M. 1994. Expression of N-terminally truncated cyclin B in the Drosophila larval brain leads to mitotic delay at late anaphase. *J Cell Sci,* 107 (Pt 10)**,** 2729-38.

RIOU-KHAMLICHI, C., HUNTLEY, R., JACQMARD, A. & MURRAY, J. A. 1999. Cytokinin activation of Arabidopsis cell division through a D-type cyclin. *Science,* 283**,** 1541-4.

RIOU-KHAMLICHI, C., MENGES, M., HEALY, J. M. & MURRAY, J. A. 2000. Sugar control of the plant cell cycle: differential regulation of Arabidopsis D-type cyclin gene expression. *Mol Cell Biol,* 20**,** 4513-21.

RIZHSKY, L., LIANG, H., SHUMAN, J., SHULAEV, V., DAVLETOVA, S. & MITTLER, R. 2004. When defense pathways collide. The response of Arabidopsis to a combination of drought and heat stress. *Plant Physiol,* 134**,** 1683-96.

ROCK, K. L., GRAMM, C., ROTHSTEIN, L., CLARK, K., STEIN, R., DICK, L., HWANG, D. & GOLDBERG, A. L. 1994. Inhibitors of the proteasome block the degradation of most cell proteins and the generation of peptides presented on MHC class I molecules. *Cell,* 78**,** 761-71.

ROGNONI, S., TENG, S., ARRU, L., SMEEKENS, S. C. M. & PERATA, P. 2007. Sugar effects on early seedling development in Arabidopsis. *Plant Growth Regulation,* 52**,** 217-228.

ROUDIER, F., FEDOROVA, E., GYORGYEY, J., FEHER, A., BROWN, S., KONDOROSI, A. & KONDOROSI, E. 2000. Cell cycle function of a Medicago sativa A2-type cyclin interacting with a PSTAIRE-type cyclin-dependent kinase and a retinoblastoma protein. *Plant J,* 23**,** 73-83.

RUSSELL, P. & NURSE, P. 1986. cdc25+ functions as an inducer in the mitotic control of fission yeast. *Cell,* 45**,** 145-53.

RUSSELL, P. & NURSE, P. 1987. Negative regulation of mitosis by wee1+, a gene encoding a protein kinase homolog. *Cell,* 49**,** 559-67.

SANCHEZ, Y., WONG, C., THOMA, R. S., RICHMAN, R., WU, Z., PIWNICA-WORMS, H. & ELLEDGE, S. J. 1997. Conservation of the Chk1 checkpoint pathway in mammals: linkage of DNA damage to Cdk regulation through Cdc25. *Science,* 277**,** 1497-501.

SCHMID, M., DAVISON, T. S., HENZ, S. R., PAPE, U. J., DEMAR, M., VINGRON, M., SCHOLKOPF, B., WEIGEL, D. & LOHMANN, J. U. 2005. A gene expression map of Arabidopsis thaliana development. *Nat Genet,* 37**,** 501-6.

SCHNITTGER, A., SCHOBINGER, U., STIERHOF, Y. D. & HULSKAMP, M. 2002. Ectopic B-type cyclin expression induces mitotic cycles in endoreduplicating Arabidopsis trichomes. *Curr Biol,* 12**,** 415-20.

SCHWOB, E., BOHM, T., MENDENHALL, M. D. & NASMYTH, K. 1994. The B-type cyclin kinase inhibitor p40SIC1 controls the G1 to S transition in S. cerevisiae. *Cell,* 79**,** 233-44.

SDEK, P., YING, H., CHANG, D. L., QIU, W., ZHENG, H., TOUITOU, R., ALLDAY, M. J. & XIAO, Z. X. 2005. MDM2 promotes proteasome-dependent ubiquitin-independent degradation of retinoblastoma protein. *Mol Cell,* 20**,** 699-708.

SEBASTIAN, B., KAKIZUKA, A. & HUNTER, T. 1993. Cdc25M2 activation of cyclin-dependent kinases by dephosphorylation of threonine-14 and tyrosine-15. *Proc Natl Acad Sci U S A,* 90**,** 3521-4.

SEKINE, M., ITO, M., UEMUKAI, K., MAEDA, Y., NAKAGAMI, H. & SHINMYO, A. 1999. Isolation and characterization of the E2F-like gene in plants. *FEBS Lett,* 460**,** 117-22.

SERRANO, M., HANNON, G. J. & BEACH, D. 1993. A new regulatory motif in cell-cycle control causing specific inhibition of cyclin D/CDK4. *Nature,* 366**,** 704-7.

SETIADY, Y. Y., SEKINE, M., HARIGUCHI, N., YAMAMOTO, T., KOUCHI, H. & SHINMYO, A. 1995. Tobacco mitotic cyclins: cloning, characterization, gene expression and functional assay. *Plant J,* 8**,** 949-57.

SHEAFF, R. J., GROUDINE, M., GORDON, M., ROBERTS, J. M. & CLURMAN, B. E. 1997. Cyclin E-CDK2 is a regulator of p27Kip1. *Genes Dev,* 11**,** 1464-78.

SHEN, W. H., PARMENTIER, Y., HELLMANN, H., LECHNER, E., DONG, A., MASSON, J., GRANIER, F., LEPINIEC, L., ESTELLE, M. & GENSCHIK, P. 2002. Null mutation of AtCUL1 causes arrest in early embryogenesis in Arabidopsis. *Mol Biol Cell,* 13**,** 1916-28.

SHERR, C. J. & ROBERTS, J. M. 1995. Inhibitors of mammalian G1 cyclin-dependent kinases. *Genes Dev,* 9**,** 1149-63.

SHERR, C. J. & ROBERTS, J. M. 1999. CDK inhibitors: positive and negative regulators of G1-phase progression. *Genes Dev,* 13**,** 1501-12.

SHIEH, S. Y., AHN, J., TAMAI, K., TAYA, Y. & PRIVES, C. 2000. The human homologs of checkpoint kinases Chk1 and Cds1 (Chk2) phosphorylate p53 at multiple DNA damage-inducible sites. *Genes Dev,* 14**,** 289-300.

SHIMOTOHNO, A., MATSUBAYASHI, S., YAMAGUCHI, M., UCHIMIYA, H. & UMEDA, M. 2003. Differential phosphorylation activities of CDK-activating kinases in Arabidopsis thaliana. *FEBS Lett,* 534**,** 69-74.

SHIMOTOHNO, A., OHNO, R., BISOVA, K., SAKAGUCHI, N., HUANG, J., KONCZ, C., UCHIMIYA, H. & UMEDA, M. 2006. Diverse phosphoregulatory mechanisms controlling cyclin-dependent kinase-activating kinases in Arabidopsis. *Plant J,* 47**,** 701-10.

SHIMOTOHNO, A. & UMEDA, M. 2007. CDK Phosphorylation. *Annual Plant Reviews Volume 32: Cell Cycle Control and Plant Development.* Blackwell Publishing Ltd.

SHIMOTOHNO, A., UMEDA-HARA, C., BISOVA, K., UCHIMIYA, H. & UMEDA, M. 2004. The plant-specific kinase CDKF;1 is involved in activating phosphorylation of cyclin-dependent kinase-activating kinases in Arabidopsis. *Plant Cell,* 16**,** 2954-66.

SIA, R. A., HERALD, H. A. & LEW, D. J. 1996. Cdc28 tyrosine phosphorylation and the morphogenesis checkpoint in budding yeast. *Mol Biol Cell,* 7**,** 1657-66.

SICILIANO, I. 2006. *Effect of plant WEE1 on the cell cycle and development in Arabidopsis thaliana and Nicotiana tabacum.* PhD thesis, Cardiff University.

SIGRIST, S., JACOBS, H., STRATMANN, R. & LEHNER, C. F. 1995. Exit from mitosis is regulated by Drosophila fizzy and the sequential destruction of cyclins A, B and B3. *EMBO J,* 14**,** 4827-38.

SIMPSON-LAVY, K. J. & BRANDEIS, M. 2010. Cdk1 and SUMO regulate Swe1 stability. *PLoS One,* 5**,** e15089.

SKOWYRA, D., CRAIG, K. L., TYERS, M., ELLEDGE, S. J. & HARPER, J. W. 1997. F-box proteins are receptors that recruit phosphorylated substrates to the SCF ubiquitin-ligase complex. *Cell,* 91**,** 209-19.

SMALLE, J., KUREPA, J., YANG, P., BABIYCHUK, E., KUSHNIR, S., DURSKI, A. & VIERSTRA, R. D. 2002. Cytokinin growth responses in Arabidopsis involve the 26S proteasome subunit RPN12. *Plant Cell,* 14**,** 17-32.

SMITS, V. A., KLOMPMAKER, R., VALLENIUS, T., RIJKSEN, G., MAKELA, T. P. & MEDEMA, R. H. 2000. p21 inhibits Thr161 phosphorylation of Cdc2 to enforce the G2 DNA damage checkpoint. *J Biol Chem,* 275**,** 30638-43.

SMITS, V. A. & MEDEMA, R. H. 2001. Checking out the G(2)/M transition. *Biochim Biophys Acta,* 1519**,** 1-12.

SOLOMON, M. J., LEE, T. & KIRSCHNER, M. W. 1992. Role of phosphorylation in p34cdc2 activation: identification of an activating kinase. *Mol Biol Cell,* 3**,** 13-27.

SONI, R., CARMICHAEL, J. P., SHAH, Z. H. & MURRAY, J. A. 1995. A family of cyclin D homologs from plants differentially controlled by growth regulators and containing the conserved retinoblastoma protein interaction motif. *Plant Cell,* 7**,** 85-103.

SORRELL, D. A., CHRIMES, D., DICKINSON, J. R., ROGERS, H. J. & FRANCIS, D. 2005. The Arabidopsis CDC25 induces a short cell length when overexpressed in fission yeast: evidence for cell cycle function. *New Phytol,* 165**,** 425-8.

SORRELL, D. A., COMBETTES, B., CHAUBET-GIGOT, N., GIGOT, C. & MURRAY, J. A. 1999. Distinct cyclin D genes show mitotic accumulation or constant levels of transcripts in tobacco bright yellow-2 cells. *Plant Physiol,* 119**,** 343-52.

SORRELL, D. A., MARCHBANK, A., MCMAHON, K., DICKINSON, J. R., ROGERS, H. J. & FRANCIS, D. 2002. A WEE1 homologue from Arabidopsis thaliana. *Planta,* 215**,** 518-22.

SORRELL, D. A., MENGES, M., HEALY, J. M., DEVEAUX, Y., AMANO, C., SU, Y., NAKAGAMI, H., SHINMYO, A., DOONAN, J. H., SEKINE, M. & MURRAY, J. A. 2001. Cell cycle regulation of cyclin-dependent kinases in tobacco cultivar Bright Yellow-2 cells. *Plant Physiol,* 126**,** 1214-23.

SOZZANI, R., CUI, H., MORENO-RISUENO, M. A., BUSCH, W., VAN NORMAN, J. M., VERNOUX, T., BRADY, S. M., DEWITTE, W., MURRAY, J. A. & BENFEY, P. N. 2010. Spatiotemporal regulation of cell-cycle genes by SHORTROOT links patterning and growth. *Nature,* 466**,** 128-32.

SPADAFORA, N. D. 2008. *Effect of CDC25 and WEE1 on plant cell cycle and morphogenesis.* PhD thesis, Cardiff University.

SPREITZER, R. J. & SALVUCCI, M. E. 2002. Rubisco: structure, regulatory interactions, and possibilities for a better enzyme. *Annu Rev Plant Biol,* 53**,** 449-75.

SRILUNCHANG, K. O., KROHN, N. G. & DRESSELHAUS, T. 2010. DiSUMO-like DSUL is required for nuclei positioning, cell specification and viability during female gametophyte maturation in maize. *Development,* 137**,** 333-45.

STAEHELIN, L. A. & HEPLER, P. K. 1996. Cytokinesis in higher plants. *Cell,* 84**,** 821-4.

STAM, M., MOL, J. N. M. & KOOTER, J. M. 1997. The silence of genes in transgenic plants. *Ann Bot,* 79**,** 3-12.

STEPHENS, D. J. & BANTING, G. 2000. The use of yeast two-hybrid screens in studies of protein:protein interactions involved in trafficking. *Traffic,* 1**,** 763-8.

STEVENS, R., MARICONTI, L., ROSSIGNOL, P., PERENNES, C., CELLA, R. & BERGOUNIOUX, C. 2002. Two E2F sites in the Arabidopsis MCM3 promoter have different roles in cell cycle activation and meristematic expression. *J Biol Chem,* 277**,** 32978-84.

STRAUSFELD, U., LABBE, J. C., FESQUET, D., CAVADORE, J. C., PICARD, A., SADHU, K., RUSSELL, P. & DOREE, M. 1991. Dephosphorylation and activation of a p34cdc2/cyclin B complex in vitro by human CDC25 protein. *Nature,* 351**,** 242-5.

SULLIVAN, J. A., SHIRASU, K. & DENG, X. W. 2003. The diverse roles of ubiquitin and the 26S proteasome in the life of plants. *Nat Rev Genet,* 4**,** 948-58.

SUN, Y., DILKES, B. P., ZHANG, C., DANTE, R. A., CARNEIRO, N. P., LOWE, K. S., JUNG, R., GORDON-KAMM, W. J. & LARKINS, B. A. 1999. Characterization of maize (Zea mays L.) Wee1 and its activity in developing endosperm. *Proc Natl Acad Sci U S A,* 96**,** 4180-5.

SURANA, U., AMON, A., DOWZER, C., MCGREW, J., BYERS, B. & NASMYTH, K. 1993. Destruction of the CDC28/CLB mitotic kinase is not required for the metaphase to anaphase transition in budding yeast. *EMBO J,* 12**,** 1969-78.

SUTTERLUTY, H., CHATELAIN, E., MARTI, A., WIRBELAUER, C., SENFTEN, M., MULLER, U. & KREK, W. 1999. p45SKP2 promotes p27Kip1 degradation and induces S phase in quiescent cells. *Nat Cell Biol,* 1**,** 207-14.

TAKATSUKA, H., OHNO, R. & UMEDA, M. 2009. The Arabidopsis cyclin-dependent kinase-activating kinase CDKF;1 is a major regulator of cell proliferation and cell expansion but is dispensable for CDKA activation. *Plant J,* 59**,** 475-87.

TANG, Z., COLEMAN, T. R. & DUNPHY, W. G. 1993. Two distinct mechanisms for negative regulation of the Wee1 protein kinase. *EMBO J,* 12**,** 3427-36.

TASSAN, J. P., JAQUENOUD, M., FRY, A. M., FRUTIGER, S., HUGHES, G. J. & NIGG, E. A. 1995. In vitro assembly of a functional human CDK7-cyclin H complex requires MAT1, a novel 36 kDa RING finger protein. *EMBO J,* 14**,** 5608-17.

TEDESCO, D., LUKAS, J. & REED, S. I. 2002. The pRb-related protein p130 is regulated by phosphorylation-dependent proteolysis via the protein-ubiquitin ligase SCF(Skp2). *Genes Dev,* 16**,** 2946-57.

THORNER, J., EMR, S. D. & ABELSON, J. N. 2000. Applications of chimeric genes and hybrid proteins. Part A: Gene expression and protein purification: Preface.

TOYOSHIMA, H. & HUNTER, T. 1994. p27, a novel inhibitor of G1 cyclin-Cdk protein kinase activity, is related to p21. *Cell,* 78**,** 67-74.

TREHIN, C., AHN, I. O., PERENNES, C., COUTEAU, F., LALANNE, E. & BERGOUNIOUX, C. 1997. Cloning of upstream sequences responsible for cell cycle regulation of the Nicotiana sylvestris CycB1;1 gene. *Plant Mol Biol,* 35**,** 667-72.

TRIMARCHI, J. M., FAIRCHILD, B., VERONA, R., MOBERG, K., ANDON, N. & LEES, J. A. 1998. E2F-6, a member of the E2F family that can behave as a transcriptional repressor. *Proc Natl Acad Sci U S A,* 95**,** 2850-5.

TSVETKOV, L. M., YEH, K. H., LEE, S. J., SUN, H. & ZHANG, H. 1999. p27(Kip1) ubiquitination and degradation is regulated by the SCF(Skp2) complex through phosphorylated Thr187 in p27. *Curr Biol,* 9**,** 661-4.

TYERS, M., TOKIWA, G., NASH, R. & FUTCHER, B. 1992. The Cln3-Cdc28 kinase complex of S. cerevisiae is regulated by proteolysis and phosphorylation. *EMBO J,* 11**,** 1773-84.

UHLMANN, F., WERNIC, D., POUPART, M. A., KOONIN, E. V. & NASMYTH, K. 2000. Cleavage of cohesin by the CD clan protease separin triggers anaphase in yeast. *Cell,* 103**,** 375-86.

UMEDA, M., BHALERAO, R. P., SCHELL, J., UCHIMIYA, H. & KONCZ, C. 1998. A distinct cyclin-dependent kinase-activating kinase of Arabidopsis thaliana. *Proc Natl Acad Sci U S A,* 95**,** 5021-6.

VAN DAMME, D., GADEYNE, A., VANSTRAELEN, M., INZE, D., VAN MONTAGU, M. C., DE JAEGER, G., RUSSINOVA, E. & GEELEN, D. 2011. Adaptin-like protein TPLATE and clathrin recruitment during plant somatic cytokinesis occurs via two distinct pathways. *Proc Natl Acad Sci U S A,* 108**,** 615-20.

VAN LEENE, J., BORUC, J., DE JAEGER, G., RUSSINOVA, E. & DE VEYLDER, L. 2011. A kaleidoscopic view of the Arabidopsis core cell cycle interactome. *Trends Plant Sci,* 16**,** 141-50.

VANDEPOELE, K., RAES, J., DE VEYLDER, L., ROUZE, P., ROMBAUTS, S. & INZE, D. 2002. Genome-wide analysis of core cell cycle genes in Arabidopsis. *Plant Cell,* 14**,** 903-16.

VANDERAUWERA, S., SUZUKI, N., MILLER, G., VAN DE COTTE, B., MORSA, S., RAVANAT, J. L., HEGIE, A., TRIANTAPHYLIDES, C., SHULAEV, V., VAN MONTAGU, M. C., VAN BREUSEGEM, F. & MITTLER, R. 2011. Extranuclear protection of chromosomal DNA from oxidative stress. *Proc Natl Acad Sci U S A,* 108**,** 1711-6.

VERKEST, A., MANES, C. L., VERCRUYSSE, S., MAES, S., VAN DER SCHUEREN, E., BEECKMAN, T., GENSCHIK, P., KUIPER, M., INZE, D. & DE VEYLDER, L. 2005. The cyclin-dependent kinase inhibitor KRP2 controls the onset of the endoreduplication cycle during Arabidopsis leaf development through inhibition of mitotic CDKA;1 kinase complexes. *Plant Cell,* 17**,** 1723-36.

VIERSTRA, R. D. 1996. Proteolysis in plants: mechanisms and functions. *Plant Mol Biol,* 32**,** 275-302.

VIERSTRA, R. D. 2003. The ubiquitin/26S proteasome pathway, the complex last chapter in the life of many plant proteins. *Trends Plant Sci,* 8**,** 135-42.

VOGES, D., ZWICKL, P. & BAUMEISTER, W. 1999. The 26S proteasome: a molecular machine designed for controlled proteolysis. *Annu Rev Biochem,* 68**,** 1015-68.

WAADT, R., SCHMIDT, L. K., LOHSE, M., HASHIMOTO, K., BOCK, R. & KUDLA, J. 2008. Multicolor bimolecular fluorescence complementation reveals simultaneous formation of alternative CBL/CIPK complexes in planta. *Plant J,* 56**,** 505-16.

WALTER, M., CHABAN, C., SCHUTZE, K., BATISTIC, O., WECKERMANN, K., NAKE, C., BLAZEVIC, D., GREFEN, C., SCHUMACHER, K., OECKING, C., HARTER, K. & KUDLA, J. 2004. Visualization of protein interactions in living plant cells using bimolecular fluorescence complementation. *Plant J,* 40**,** 428-38.

WALWORTH, N., DAVEY, S. & BEACH, D. 1993. Fission yeast chk1 protein kinase links the rad checkpoint pathway to cdc2. *Nature,* 363**,** 368-71.

WANG, H., FOWKE, L. C. & CROSBY, W. L. 1997. A plant cyclin-dependent kinase inhibitor gene. *Nature,* 386**,** 451-2.

WANG, H., QI, Q., SCHORR, P., CUTLER, A. J., CROSBY, W. L. & FOWKE, L. C. 1998. ICK1, a cyclin-dependent protein kinase inhibitor from Arabidopsis thaliana interacts with both Cdc2a and CycD3, and its expression is induced by abscisic acid. *Plant J,* 15**,** 501-10.

WANG, H. Y. 2008. How effective is T-DNA insertional mutagenesis in Arabidopsis? *J Biochem Tech,* 1**,** 11-20.

WANG, L., DONG, L., ZHANG, Y., ZHANG, Y., WU, W., DENG, X. & XUE, Y. 2004. Genome-wide analysis of S-Locus F-box-like genes in Arabidopsis thaliana. *Plant Mol Biol,* 56**,** 929-45.

WATANABE, N., ARAI, H., IWASAKI, J., SHIINA, M., OGATA, K., HUNTER, T. & OSADA, H. 2005. Cyclin-dependent kinase (CDK) phosphorylation destabilizes somatic Wee1 via multiple pathways. *Proc Natl Acad Sci U S A,* 102**,** 11663-8.

WATANABE, N., ARAI, H., NISHIHARA, Y., TANIGUCHI, M., WATANABE, N., HUNTER, T. & OSADA, H. 2004. M-phase kinases induce phospho-dependent ubiquitination of somatic Wee1 by SCFbeta-TrCP. *Proc Natl Acad Sci U S A,* 101**,** 4419-24.

WATERHOUSE, P. M., SMITH, N. A. & WANG, M. B. 1999. Virus resistance and gene silencing: killing the messenger. *Trends Plant Sci,* 4**,** 452-457.

WEI, W., AYAD, N. G., WAN, Y., ZHANG, G. J., KIRSCHNER, M. W. & KAELIN, W. G., JR. 2004. Degradation of the SCF component Skp2 in cell-cycle phase G1 by the anaphase-promoting complex. *Nature,* 428**,** 194-8.

WEINERT, T. 1998. DNA damage checkpoints update: getting molecular. *Curr Opin Genet Dev,* 8**,** 185-93.

WEINGARTNER, M., CRIQUI, M. C., MESZAROS, T., BINAROVA, P., SCHMIT, A. C., HELFER, A., DEREVIER, A., ERHARDT, M., BOGRE, L. & GENSCHIK, P. 2004. Expression of a nondegradable cyclin B1 affects plant development and leads to endomitosis by inhibiting the formation of a phragmoplast. *Plant Cell,* 16**,** 643-57.

WEINL, C., MARQUARDT, S., KUIJT, S. J., NOWACK, M. K., JAKOBY, M. J., HULSKAMP, M. & SCHNITTGER, A. 2005. Novel functions of plant cyclin-dependent kinase inhibitors, ICK1/KRP1, can act non-cell-autonomously and inhibit entry into mitosis. *Plant Cell,* 17**,** 1704-22.

WEISSMAN, A. M. 2001. Themes and variations on ubiquitylation. *Nat Rev Mol Cell Biol,* 2**,** 169-78.

WHITFIELD, W. G., GONZALEZ, C., MALDONADO-CODINA, G. & GLOVER, D. M. 1990. The A- and B-type cyclins of Drosophila are accumulated and destroyed in temporally distinct events that define separable phases of the G2-M transition. *EMBO J,* 9**,** 2563-72.

WILKINSON, K. D. 2000. Ubiquitination and deubiquitination: targeting of proteins for degradation by the proteasome. *Semin Cell Dev Biol,* 11**,** 141-8.

WINTER, D., VINEGAR, B., NAHAL, H., AMMAR, R., WILSON, G. V. & PROVART, N. J. 2007. An "Electronic Fluorescent Pictograph" browser for exploring and analyzing large-scale biological data sets. *PLoS One,* 2**,** e718.

WU, L. & RUSSELL, P. 1993. Nim1 kinase promotes mitosis by inactivating Wee1 tyrosine kinase. *Nature,* 363**,** 738-41.

XIE, Q., SANZ-BURGOS, A. P., HANNON, G. J. & GUTIERREZ, C. 1996. Plant cells contain a novel member of the retinoblastoma family of growth regulatory proteins. *EMBO J,* 15**,** 4900-8.

XIONG, Y., HANNON, G. J., ZHANG, H., CASSO, D., KOBAYASHI, R. & BEACH, D. 1993. p21 is a universal inhibitor of cyclin kinases. *Nature,* 366**,** 701-4.

YADAV, R. K., GIRKE, T., PASALA, S., XIE, M. & REDDY, G. V. 2009. Gene expression map of the Arabidopsis shoot apical meristem stem cell niche. *Proc Natl Acad Sci U S A,* 106**,** 4941-6.

YAMANO, H., GANNON, J. & HUNT, T. 1996. The role of proteolysis in cell cycle progression in Schizosaccharomyces pombe. *EMBO J,* 15**,** 5268-79.

YAMANO, H., TSURUMI, C., GANNON, J. & HUNT, T. 1998. The role of the destruction box and its neighbouring lysine residues in cyclin B for anaphase ubiquitin-dependent proteolysis in fission yeast: defining the D-box receptor. *EMBO J,* 17**,** 5670-8.

YAN, N., DOELLING, J. H., FALBEL, T. G., DURSKI, A. M. & VIERSTRA, R. D. 2000. The ubiquitin-specific protease family from Arabidopsis. AtUBP1 and 2 are required for the resistance to the amino acid analog canavanine. *Plant Physiol,* 124**,** 1828-43.

YANAGIDA, M. 2000. Cell cycle mechanisms of sister chromatid separation; roles of Cut1/separin and Cut2/securin. *Genes Cells,* 5**,** 1-8.

YANKULOV, K. Y. & BENTLEY, D. L. 1997. Regulation of CDK7 substrate specificity by MAT1 and TFIIH. *EMBO J,* 16**,** 1638-46.

YANO, A., KODAMA, Y., KOIKE, A., SHINYA, T., KIM, H. J., MATSUMOTO, M., OGITA, S., WADA, Y., OHAD, N. & SANO, H. 2006. Interaction between methyl CpG-binding protein and ran GTPase during cell division in tobacco cultured cells. *Ann Bot,* 98**,** 1179-87.

YOON, H. J., FEOKTISTOVA, A., WOLFE, B. A., JENNINGS, J. L., LINK, A. J. & GOULD, K. L. 2002. Proteomics analysis identifies new components of the fission and budding yeast anaphase-promoting complexes. *Curr Biol,* 12**,** 2048-54.

ZENG, Y. & PIWNICA-WORMS, H. 1999. DNA damage and replication checkpoints in fission yeast require nuclear exclusion of the Cdc25 phosphatase via 14-3-3 binding. *Mol Cell Biol,* 19**,** 7410-9.

ZHANG, K., DIEDERICH, L. & JOHN, P. C. 2005. The cytokinin requirement for cell division in cultured Nicotiana plumbaginifolia cells can be satisfied by

yeast Cdc25 protein tyrosine phosphatase: implications for mechanisms of cytokinin response and plant development. *Plant Physiol,* 137**,** 308-16.

ZHANG, K., LETHAM, D. S. & JOHN, P. C. 1996. Cytokinin controls the cell cycle at mitosis by stimulating the tyrosine dephosphorylation and activation of p34cdc2-like H1 histone kinase. *Planta,* 200**,** 2-12.

ZHANG, Y., GAO, P. & YUAN, J. S. 2010. Plant protein-protein interaction network and interactome. *Curr Genomics,* 11**,** 40-6.

ZHENG, N., SCHULMAN, B. A., SONG, L., MILLER, J. J., JEFFREY, P. D., WANG, P., CHU, C., KOEPP, D. M., ELLEDGE, S. J., PAGANO, M., CONAWAY, R. C., CONAWAY, J. W., HARPER, J. W. & PAVLETICH, N. P. 2002. Structure of the Cul1-Rbx1-Skp1-F boxSkp2 SCF ubiquitin ligase complex. *Nature,* 416**,** 703-9.

ZHOU, Y., FOWKE, L. & WANG, H. 2002. Plant CDK inhibitors: Studies of interactions with cell cycle regulators in the yeast two-hybrid system and functional comparisons in transgenic Arabidopsis plants. *Plant Cell Reports,* 20**,** 967-975.

ZUR, A. & BRANDEIS, M. 2001. Securin degradation is mediated by fzy and fzr, and is required for complete chromatid separation but not for cytokinesis. *EMBO J,* 20**,** 792-801.

APPENDICES

APPENDIX I CELL CYCLE PHASES

LINE	C	S	G2	M	G1
WT	13.0	4.5	4.0	1.3	3.2
GFP-*Arath*;WEE1-4	14.5	5.0	2.0	1.0	6.5
35S-GFP	14.0	5.0	5.0	1.0	3.0
SPYCE-*Arath*;WEE1	15.0	5.5	4.0	2.0	3.5
SPYCE-*Arath*;WEE1/SPYNE-*Arath*;SKIP1-6	13.0	4.0	6.0	1.7	1.3
SPYCE-*Arath*;WEE1/SPYNE-*Arath*;SKIP1-2	15.0	4.0	7.0	2.1	1.9
SPYCE-*Arath*;WEE1/SPYNE-*Arath*;GSTF9-3			8.0		

- C is the cell cycle duration, calculated from the interval between peaks.
- S-phase duration is calculated from the distance between midpoints of the ascending and descending lines of the first peak.
- G2 duration is calculated as the distance from zero to where the curve begins to rise, ie. the first value above 1%. This is on the basis that any mitotic indices of less than one per cent would indicate a MI of less than 1 mitosis in 100 cells, hence those values of less than 1% are seen as random noise following the induction of synchrony.
- M is calculated using the following formula: Duration of M = C/ln2 x ln(P+1), where

  P = The average mitotic index for all points on the graph, including zeros (Nachtwey + Cameron 1968).

APPENDIX II DIC IMAGES OF ROOTS USED TO CALCULATE CELL SIZE

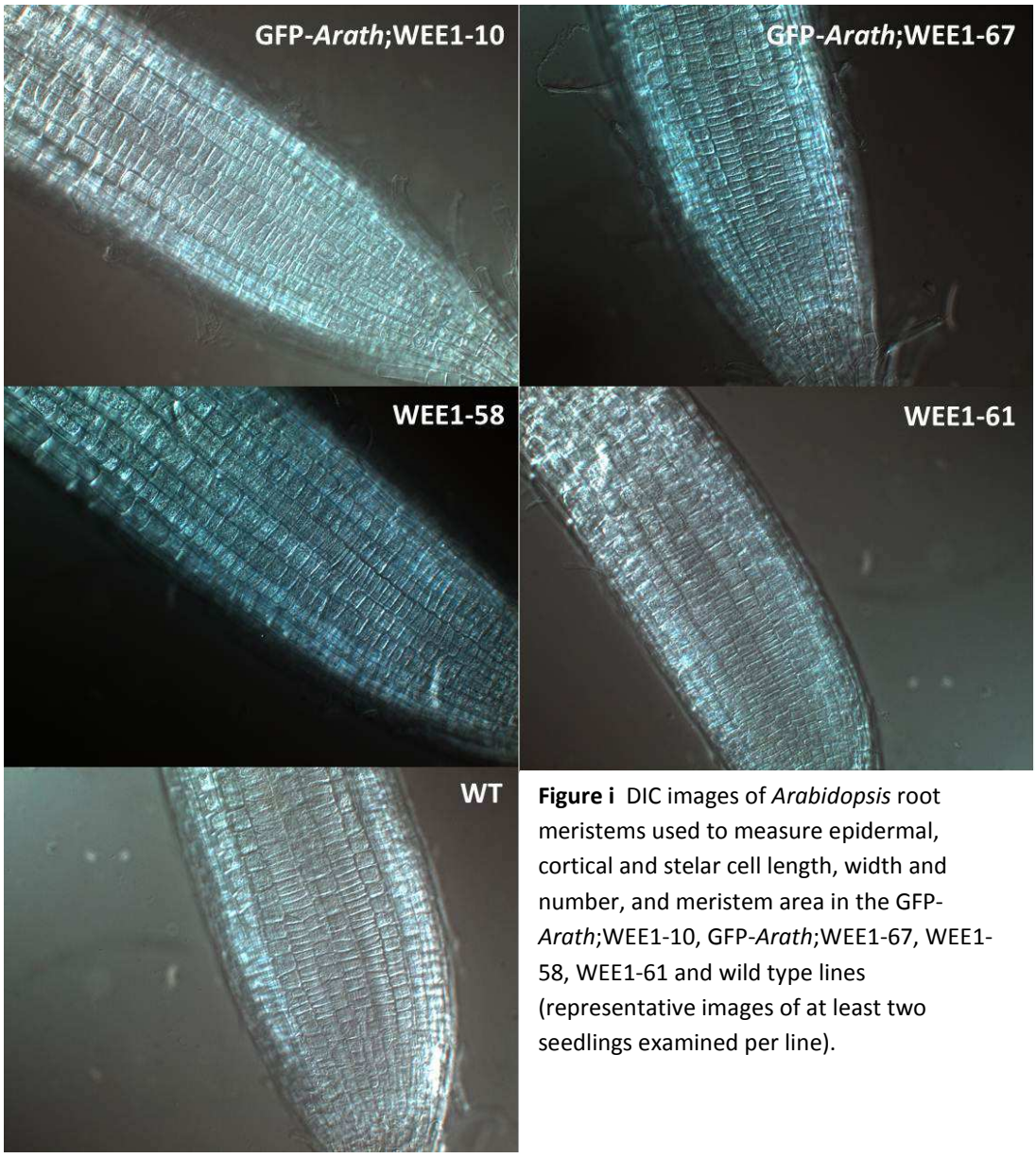

Figure i DIC images of *Arabidopsis* root meristems used to measure epidermal, cortical and stelar cell length, width and number, and meristem area in the GFP-*Arath*;WEE1-10, GFP-*Arath*;WEE1-67, WEE1-58, WEE1-61 and wild type lines (representative images of at least two seedlings examined per line).

APPENDIX III *ARATH*;WEE1 WESTERN BLOTS

Western blotting was used in an attempt to confirm the increase in *Arath*;WEE1 protein levels in MG132-seedlings compared to the mock-treated seedlings. This technique was also used in an attempt to analyse *Arath*;WEE1 protein levels in the *Arath*;SKIP1 sense knock-down lines 1b and 5b compared to wild type and the *Arath*;WEE1 over-expressing line WEE1-58, and in the GFP-*Arath*;WEE1 x SPYNE-*Arath*;SKIP1 F2 lines 11 and 28 compared to the original GFP-*Arath*;WEE1-12 line. Total protein was extracted from 10-day old seedlings treated with MG132 or mock-treated and the protein concentration measured by Bradford assay. Twenty μg of each protein was separated by SDS-PAGE, western blotted and probed using a WEE1 antibody (Section 2.6). However, several problems prevented the quantification of *Arath*;WEE1 protein, including the non-specific detection of RUBISCO (Figures ii and iii) and the aggregation of WEE1 protein (Figure iii).

A strong, non-specific band of RUBISCO was consistently detected on the western blots of the *Arath*;SKIP1 knock-down lines (Figures ii and iii). This was a problem because the molecular weight of *Arabidopsis* WEE1 protein is 57 kDa (Lentz et al, 2009; Lentz Gronlund, 2007), which is very similar in size to the 55 kDa large subunit of RUBISCO (Spreitzer + Silvucci, 2002), rendering the two signals inseparable on this gel system. Although the WEE1 antibody is able to recognise both *Arabidopsis* and tobacco WEE1 (Lentz Gronlund, 2007), in previous work the antibody has been routinely used on protein extracted from tobacco BY-2 cell cultures, which does not contain RUBISCO. Protein extracted from seedlings germinated and grown in darkness, which are known to contain little or no RUBISCO, was used as a control and confirmed that the clear bands were RUBISCO (Figures ii and iii). The slightly larger, uneven bands seen in Figure iii correspond in size to *Arath*;WEE1 protein.

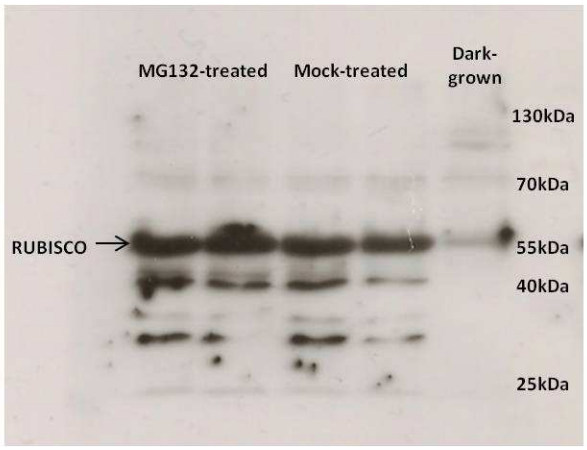

Figure ii WEE1 western blot of protein from MG132- and mock-treated GFP-*Arath*;WEE1-67 seedlings. Dark-grown seedlings were used as a negative control for RUBISCO.

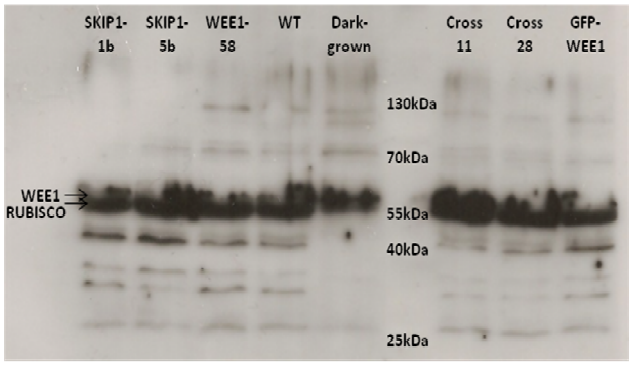

Figure iii Representative WEE1 western blot of *Arath*;SKIP1 knock-down lines (SKIP1-1b and SKIP1-5b) compared to the *Arath*;WEE1 over-expresser, WEE1-58, and wild type (WT), and SPYNE-*Arath*;SKIP1xGFP-*Arath*;WEE1 crossed lines 11 and 28 (Cross 11 and Cross 28) compared to the original GFP-*Arath*;WEE1 line. Dark-grown seedlings were used as a negative control for RUBISCO.

A protocol for the removal of RUBISCO from *Arabidopsis* protein extract was adapted from the method described in Krishnan and Natarajan (2009). Protein was extracted from *Arabidopsis* seedlings as described in Section 2.6.1. Calcium chloride dihydrate and sodium phytate were added to a final concentration of 10 µM each (from 100 mM stock solutions) and mixed gently. The samples were incubated at 42°C for 10 minutes, followed by centrifugation at 16,100g for 10 minutes at 4°C. The supernatant was transferred to a fresh tube and stored at -80°C.

However, this method proved unsuccessful as RUBISCO protein could still be detected on a coomassie-stained gel (Figure iv). When western-blotted and probed with the WEE1 antibody no bands of RUBISCO were visible, but the *Arath*;WEE1 signal remained highly inconsistent and did not form clear enough bands for quantification (Figure v). Several attempts were made to resolve the *Arath*;WEE1 signal, including gel electrophoresis at a lower voltage, decreasing the percentage of acrylamide in the gel, and unfolding the protein prior to loading by treatment at 50°C

for 10 minutes instead of the usual 100°C for five minutes, but all methods attempted proved ineffective.

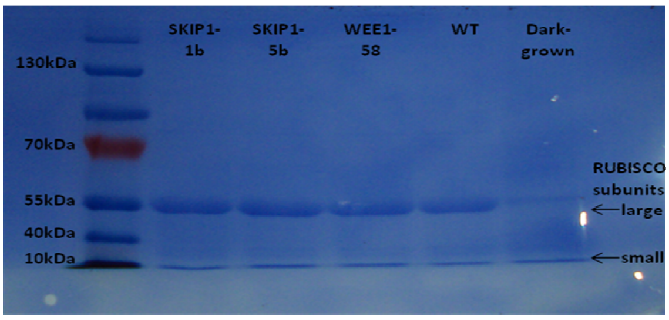

Figure iv Coomassie-stained gel of phytate and calcium chloride treated protein samples: *Arath*;SKIP1 knock-down lines (SKIP1-1b and SKIP1-5b), WEE1-58, and wild type (WT). Dark-grown seedlings were used as a negative control for RUBISCO.

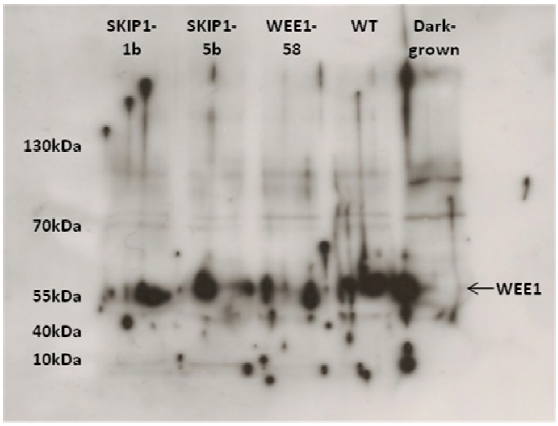

Figure v WEE1-probed western blot of phytate and calcium chloride treated protein samples: *Arath*;SKIP1 knock-down lines (SKIP1-1b and SKIP1-5b), WEE1-58, and wild type (WT). Dark-grown seedlings were used as a negative control for RUBISCO. No non-specific RUBISCO bands were visible, but the WEE1 signal was still too inconsistent to be quantified.

APPENDIX IV RESULTS OF TRANSIENT BiFC AND CONTROLS

Examples of results from controls for transient BiFC (Figure vi):

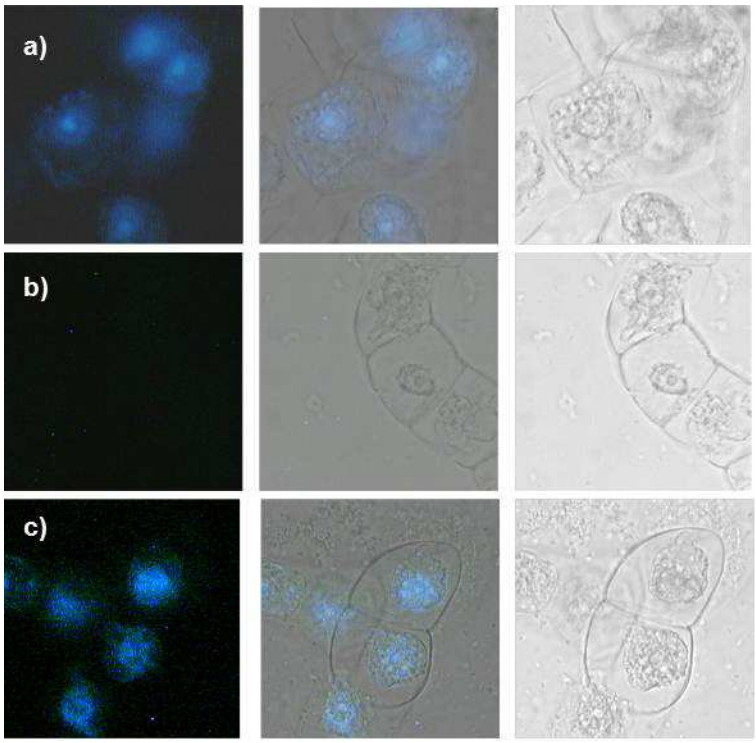

Figure vi Tobacco BY-2 cells cotransformed with a) BZIP63 fused to the split-YFP vector pSPYCE in *Agrobacterium* and BZIP63 fused to pSPYNE in *Agrobacterium*; b) *Arath*;WEE1 fused to pSPYCE and BZIP63 fused to pSPYNE; and c) BZIP63 fused to pSPYCE and *Arath*;GSTF9 fused to pSPYNE; under UV light (left), white light (right) and the two merged (centre). a) is a positive control – clear blue colouring indicating an interaction between the two BZIP63 proteins. b) is a negative control. c) is an experimental negative control, where auto-fluorescence is indicated by grainy blue colouring.

Examples of results of transient BiFC with *Arath*;GSTF9, *Arath*;GCN5 and *Arath*;TFCB (Figure vii):

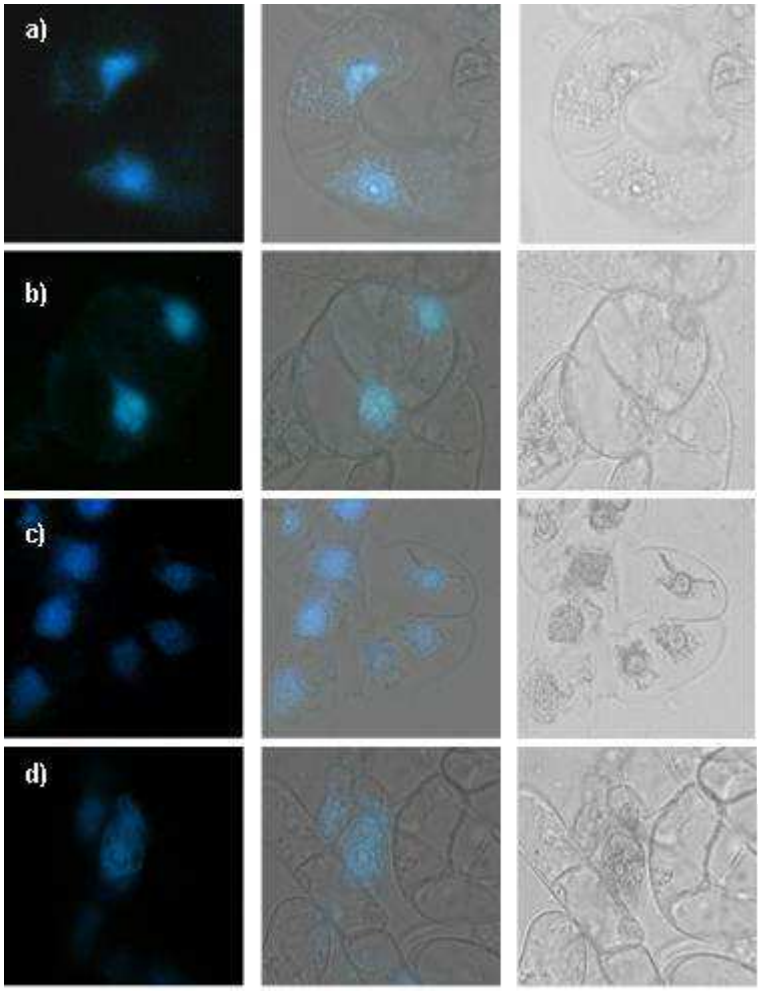

Figure vii Tobacco BY-2 cells cotransformed with *Arath*;WEE1 fused to the split-YFP vector pSPYCE in *Agrobacterium* and a) *Arath*;GCN5, b) and c) *Arath*;GSTF9, and d) *Arath;*TFCB fused to the split-YFP vector pSPYNE in *Agrobacterium*, under UV light (left), white light (right) and the two merged (centre). Blue colouring indicates a positive interaction between *Arath*;WEE1 and the protein of interest.

APPENDIX V FURTHER RESULTS OF TRANSIENT BiFC BETWEEN SPYCE-*ARATH*;WEE1 AND SPYNE-*ARATH*;SKIP1 AND POSITIVE CONTROL

Positive control: SPYCE-*Arath*;BZIP63/SPYNE-*Arath*;BZIP63 (Figure viii):

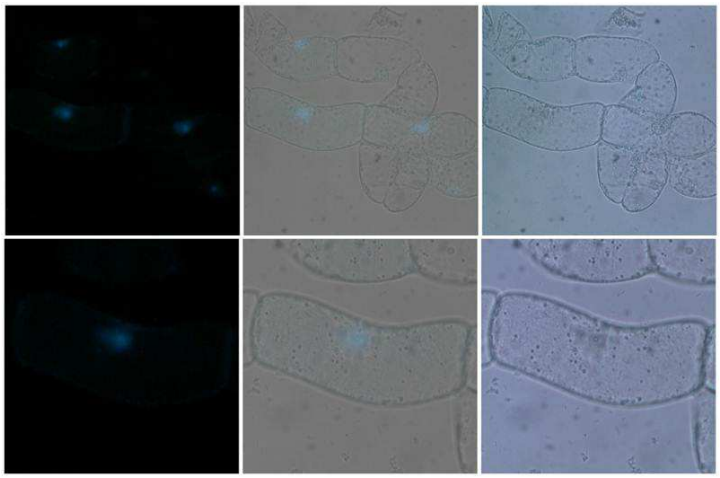

Figure viii Tobacco BY-2 cells co-transformed with *Arath*;BZIP63 fused to both pSPYCE and pSPYNE (positive control); under UV light (left), white light (right) and the two merged (centre). Blue colouring indicates a positive interaction between the two proteins (representative images).

Experiment: SPYCE-*Arath*;WEE1/SPYNE-*Arath*;SKIP1 (Figure ix):

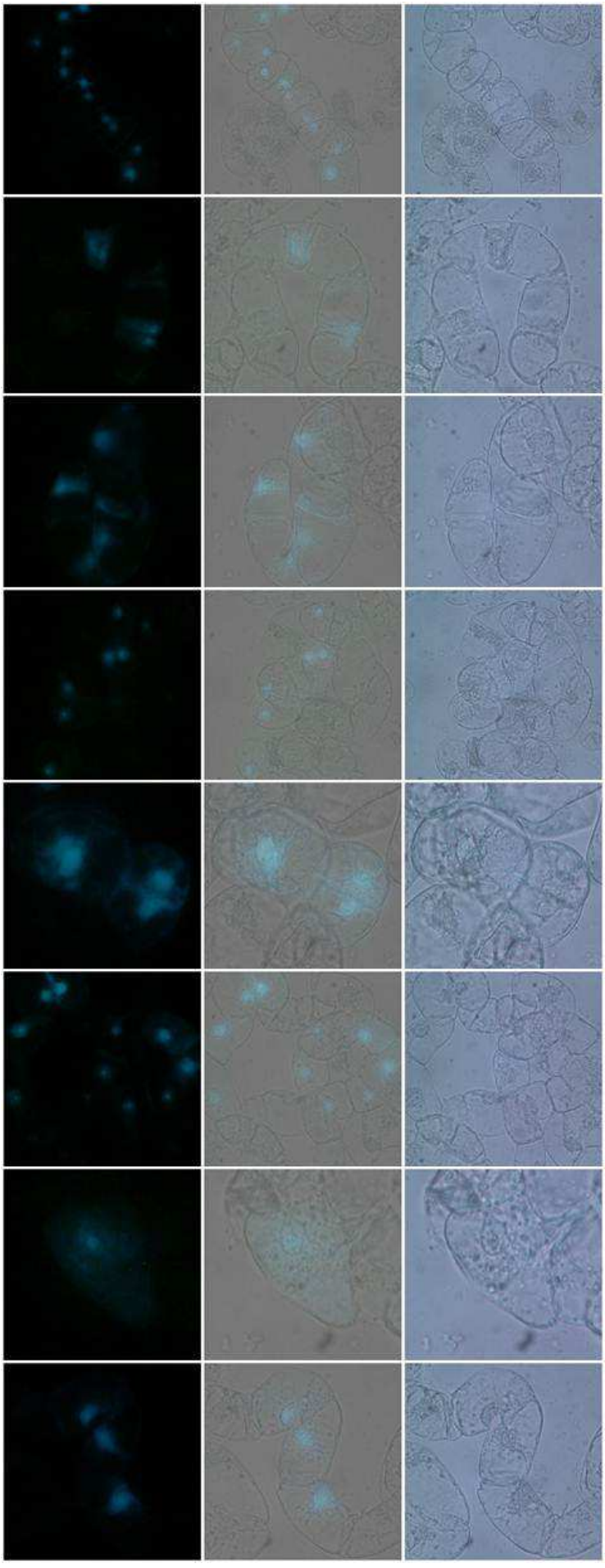

Figure ix Tobacco BY-2 cells co-transformed with *Arath*;WEE1 fused to the split-YFP vector pSPYCE and *Arath*;SKIP1 fused to pSPYNE; under UV light (left), white light (right) and the two merged (centre). Blue colouring indicates a positive interaction between the two proteins (representative images)

APPENDIX VI FURTHER RESULTS OF SEMI-TRANSIENT BiFC TO TEST FOR EXPRESSION OF SPYCE-*ARATH*;WEE1 IN STABLE TRANSFORMED BY-2 CULTURE

Table i Controls for transient BiFC in stable pKanSPYCE-*Arath*;WEE1 BY-2 line

Control/Experiment	BY-2 Cell Line	SPYCE	SPYNE	OUTCOME
1. Experiment	pSPYCE-*Arath*;WEE1	-	*Arath*;SKIP1	Positive
2. Positive control	WT	*Arath*;WEE1	*Arath*;SKIP1	Negative
3. Positive control	pSPYCE-*Arath*;WEE1	BZIP63	BZIP63	Positive
4. Positive control	WT	BZIP63	BZIP63	Positive
5. Negative control	pSPYCE-*Arath*;WEE1	-	BZIP63	Negative
6. Negative control	WT	*Arath*;WEE1	BZIP63	Negative
7. Negative control	WT	BZIP63	*Arath*;SKIP1	Negative

Figure x Results of experiment to test for expression of pkanSPYCE-*Arath*;WEE1 in stably transformed tobacco BY-2 cells by semi-transient BiFC, under white light (left), UV light (right) and the two merged (centre). Clear blue colouring indicates a positive interaction, whereas grainy unclear blue colouring indicates background, or false positive, fluorescence. See Table i for key to numbering.

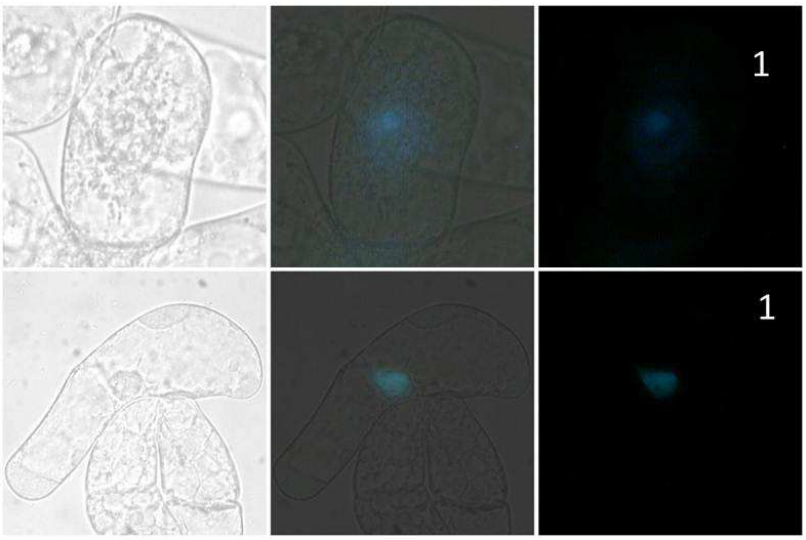

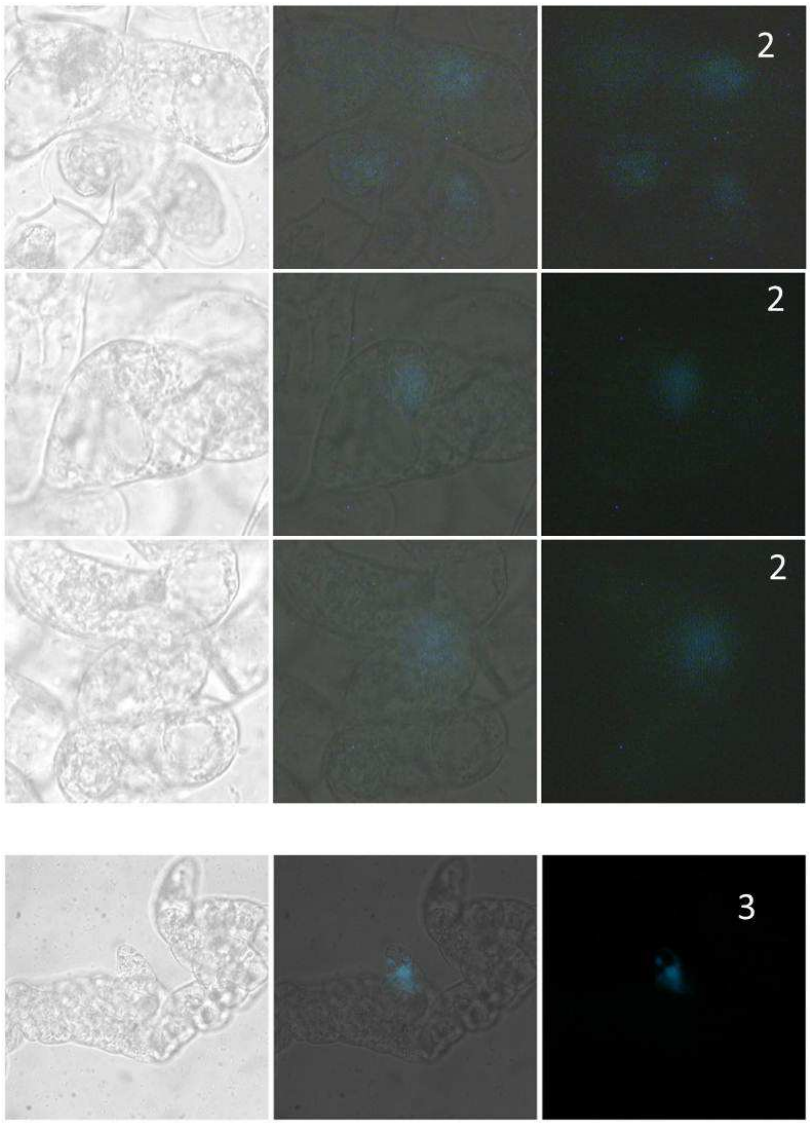
2
2
2
3

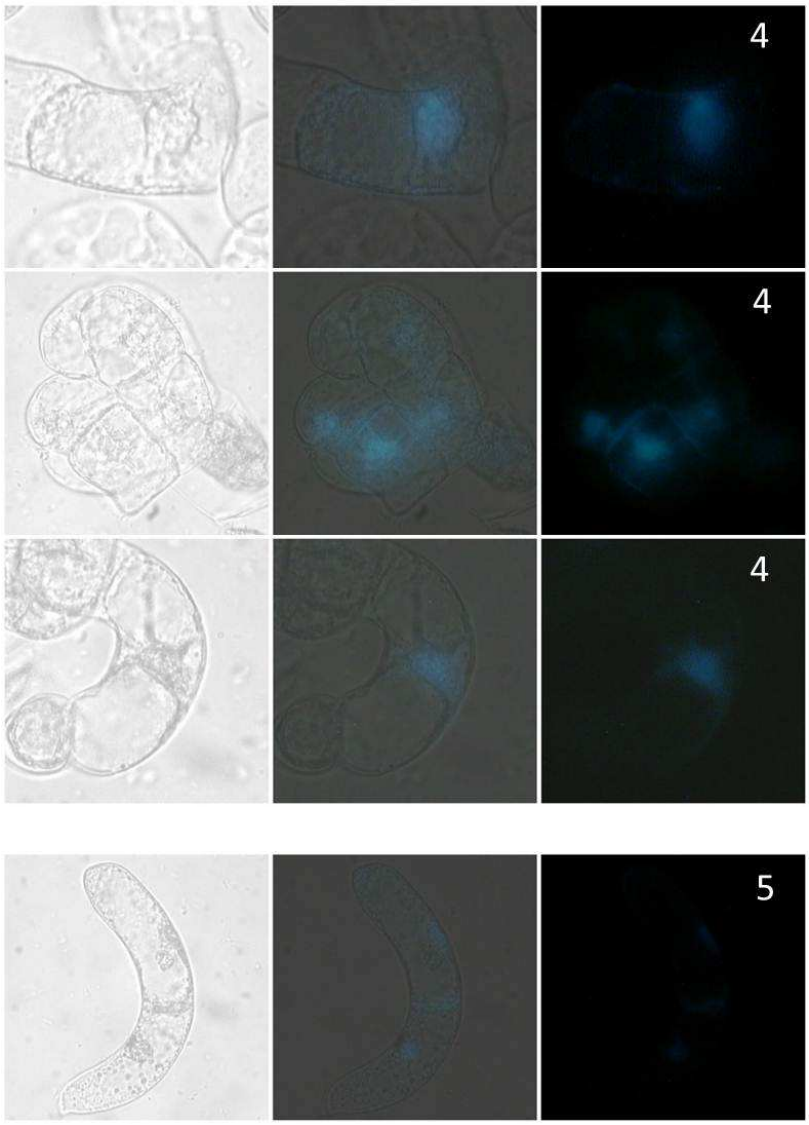
4
4
4
5

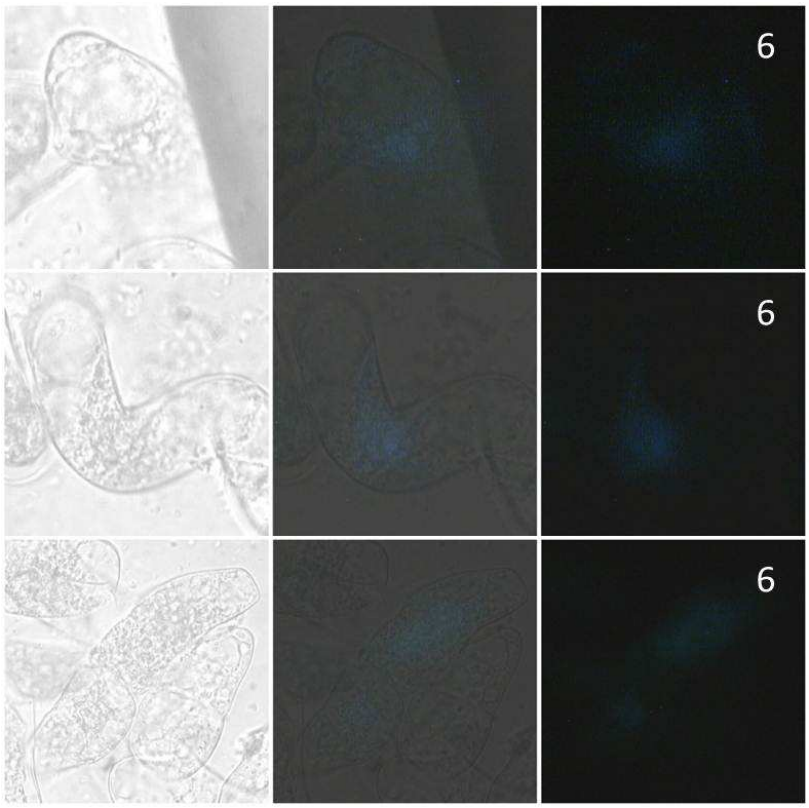
6
6
6